Essential and virulence genes in *Coxiella burnetii*

Submitted by Georgina Metters, to the University of Exeter as a thesis for the degree of:

Doctor of Philosophy in Biological Sciences

January 2022

This thesis is available for Library use on the understanding that it is copyright material and that no quotation from the thesis may be published without proper acknowledgement.

I certify that all material in this thesis which is not my own work has been identified and that any material that has previously been submitted and approved for the award of a degree by this or any other University has been acknowledged.

…………………………………………………

Abstract

Coxiella burnetii is an intracellular pathogen responsible for causing Q fever in humans, which has been classified as a potential category B bioterrorism agent by the CDC. There is a requirement for the identification of possible drug and vaccine targets for *C. burnetii* due to the lack of a licenced vaccine in the UK, and lengthy drug regimens with undesirable side effects. Until the recent development of axenic media for *C. burnetii,* its obligate intracellular lifestyle has meant there is a paucity of information on the virulence mechanisms of *C. burnetii*.

In this project the *Galleria mellonella* insect model was further characterised to aid its use in the identification of *C. burnetii* virulence determinants. It was found that in *G. mellonella, C. burnetii* proliferates quicker than in axenic media, and forms a vacuole comparable to that seen in mammalian cells. To identify essential and virulence determinants in a high-throughput manner, a transposon library containing > 10,000 unique transposon mutants was created. Axenic media was used to identify essential genes, and significant steps were taken in the use of *G. mellonella* as a screen for the high-throughput identification of virulence determinants. Finally, a transposon mutant in *CBU_1468*, a gene which confers a hypothetical protein of unknown function, was discovered to be attenuated in the *G. mellonella* model. Potentially identifying a further virulence factor and giving scope for further investigation.

Contents

List of figures

List of tables

Table 5.8. Fifty-five genes potentially important for *C. burnetii* virulence in *G. mellonella* as determined by the Whiteley lab pipeline.

Table 6.1. Average scores of larvae assessed by the larvae scoring system proposed by Loh *et al*

Table.6.2 Forty genes identified as significantly downregulated in *C. burnetii* NMII::Tn-*CBU_1468*

List of Appendices

Authors declaration

Unless otherwise stated, the work presented in this thesis is solely the work of Georgina Metters, under the guidance and supervision of Professor Rick Titball

- Dr Andrea Kovacs-Simon helped with RNA extractions, sequencing and data analysis in Chapter 4.
- Dr Debbie Salmon helped with experimental design and provided technical support with the operation of the HPLC machine in Chapter 4.
- Dr Christian Hacker performed the transmission electron microscopy in Chapters 4 and 6.
- Dr Claudia Hemsley provided some of the total pool of transposon mutants which were analysed in Chapter 5.
- Paul O'Neil helped with RNA-Seq data analysis reported in Chapter 6.

Acknowledgements

First and foremost I would like to thank my supervisors Professor Rick Titball, Professor Izzy Norville and Dr Claudia Hemsley. Over the last few years you have provided me with an immeasurable amount of guidance, and I am very grateful to have had a supervisory team that is so supportive.

I have thanks to Karen and her team from the Exeter Sequencing Service for teaching me all things TraDIS and giving advice on library preparation. Christian and his team from Exeter bio-imaging for performing electron microscopy and teaching me the ways of the confocal. Dr Debbie Salmon for her help with HPLC analysis and interpretation, and Dr Andrea Kovacs-Simon for her help and advice with working with RNA.

To Dr Vanessa Francis, there aren't quite the words to explain how thankful I am to you, for the coffees, the cakes, the lunchtime walks and the endless conversations about *Galleria*. Who would have thought on that first day of being in the office that we would become the best of friends. The boys, Cam, Josh, Jack, Matt and Jake. For endless banter, amusing coffee breaks and silly office games, and to the other members of the BPRG lab past and present, you've put up with my chatter, ramblings and occasional grumps. I feel very thankful to have been part of a lab with such a friendly and cohesive community.

To my family: Mum, Dad, Tandi, Dan and the boys for providing a much needed distraction from the PhD rollercoaster. The dogs: Bailey, Bentley and Luna for providing much needed cuddles and woodland walks.

Finally, to Katie. There are no words I could write here that can portray how lucky I am to be supported by you. You have carried our household over these past few years, listened to my science rants and supported me in times of wavering confidence. I will be forever grateful.

List of abbreviations

%	Percent
μ	micro
aa	Amino acid
ACCM-2	Acidified citrate cysteine medium
BGM	Buffalo green monkey
BlastP	basic local alignment search tool (protein)
bp	base pairs
CCM	Complex *Coxiella* medium
CCV	*Coxiella*-containing vacuole
CDC	Centre for disease control and prevention
CDS	Coding sequences
CFU	colony forming units
COG	Clusters of orthologous groups
DEG	Database of essential genes
Dex	Dexamethasone
Dex.A	Dexamethasone acetate
Dex.P	Dexamethasone 21- phosphate
DMSO	Dimethyl sulfoxide
DNA	Deoxyribonucleic acid
E-value	Expected value
FE-S	Iron-sulphur
g	Gram
gDNA	Genomic DNA
GE	Genome equivalents
$GPID_{50}$	Guinea pig 50% infectious dose
HITS	High-throughput insertion tracking by deep sequencing
HPLC	High performance liquid chromatography
I.P	Intra-peritoneal
IFA	Immunofluorescence assay

In-Seq	Insertion sequencing
ITRs	Inverted terminal repeat sequences
LB	Luria broth
LCV	Large colony variant
LD50	50% lethal dose
LFD	Lateral flow device
LOD	Limit of detection
LOQ	Limit of quantification
LPS	Lipopolysaccharide
Mbp	Mega base piars
MIC	Minimum inhibitory concentration
mRNA	Messenger RNA
NGS	Next generation sequencing
NHP	Non-human primate
NMI	*Coxiella burnetii* Nine Mile RSA493 Phase I
NMII	*Coxiella burnetii* Nine Mile RSA439 Phase II
Padj	Adjusted P value
PBS	Phosphate buffered saline
PCA	Principle component analysis
PCR	Polymerase chain reaction
Pred	Prednisolone
PRRs	Pathogen recognition receptors
qPCR	Quantitative PCR
RIN	RNA integrity number
RNA	Ribonucleic acid
RPMI	Roswell park memorial institute
rt-PCR	Real-time quantitative PCR
SCV	Small colony variant
STM	Signature tagged mutagenesis
T4SS	Type four secretion system

TEM	Transmission electron microscopy
TIS	Transposon insertion sequencing
TLR	Toll-like receptors
Tn	Transposon
Tn-Seq	Transposon insertion sequencing
TraDIS	Transposon directed insertion site sequencing
TraSH	Transposon site hybridisation
Δ	Delta

Chapter 1: Introduction

1.1.   The discovering of Q fever and *C. burnetii*

Q fever was first discovered in 1935 in Queensland, Australia. Edward Derrick, an Australian researcher, observed a febrile illness in abattoir workers[1]. Upon investigation, known diseases of the time were gradually excluded. When Derrick used patient blood to infect guinea pigs, he observed a similar disease with a characteristic fever. He designated the disease "Q" or query fever, due to the inability to identify the causative agent. Upon collaboration with Frank Macfarlane Burnet, who used tissue from the infected guinea pig tissue to infect mice, an organism of 'rickettsial nature' was identified in the liver[2].

At the same time, in Hamilton, Montana, USA, Davis and Cox identified a febrile illness in a guinea pig that had been used to feed a *Dermacentor andersoni* tick during a field study on Rocky Mountain spotted fever[3]. They described a pathogen which displayed both bacterial and viral characteristics which they named the Nine Mile Agent. It was only after a laboratory worker became infected with the Nine Mile agent, that the remarkable similarities to 'Q' fever were seen.

Later, cross protection studies showed that the Nine Mile and Q fever agents were indeed the same pathogen[4]. Placed in the *Rickettsiaceae* family the organism was named *Coxiella burnetii* in honour of Cox and Burnet, the scientists who first identified the disease. This classification remained until 1989, when16s rRNA-encoding gene sequencing carried out by Weisburg *et al* revealed that *C. burnetii* "bears no relationship whatever to the other members of its tribe" and subsequently reclassified *C. burnetii to the Coxiellaceae* family of the order *Legionellales* [5].

1.2.   The bacterium – *C. burnetii*

C. burnetii is zoonotic Gram-negative pathogen with a small genome (~ 2 Mbp)[6] that has been classified as a potential bioterrorism agent by the CDC[7]. During infection, *C. burnetii* is an obligate intracellular pathogen. *C. burnetii* exists in both a large cell variant (LCV), and a small cell variant (SCV), resulting in size variation from 0.2 - > 1 µm in length[8].

1.2.1. Phase variation

C. burnetii undergoes irreversible phase variation after multiple passages of laboratory culture in embryonated eggs, cell lines, or axenic medium[9–11]. Shifting from a virulent phase I pathogen to a phase II pathogen that is avirulent in humans[12]. This shift occurs as a result of a large chromosomal deletion of 18 genes (*CBU_0679-CBU_0697*) resulting in truncation of the lipopolysaccharide (LPS) (Figure 1.1). Phase I variants have a full length LPS containing *C. burnetii* specific O-antigen sugars L-virenose and dihydrohydroxystreptose[13–16], whereas phase II variants have a truncated LPS, missing the outer core and O-antigen sugars.
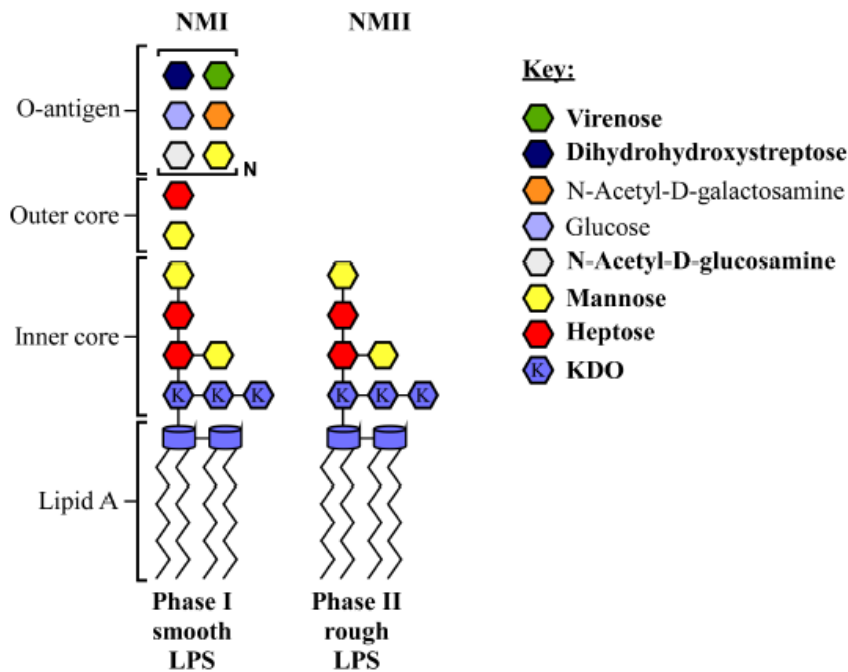
Figure 1.1. LPS profiles of *C. burnetii* phase I and phase II forms. Phase I strains have a full length LPS containing *C. burnetii* specific sugars L-virenose and dihydrohydroxystreptose. Phase II strains have a truncated LPS missing the O-antigen sugars and outer core. Figure adapted from[17]

1.2.2. Morphological variation

The *C. burnetii* SCVs are small (0.2 - 0.5 μm in length), metabolically dormant and have a characteristic condensed chromatin[8,18]. SCVs have been shown to be highly resistant to external stress such as heat, osmotic shock, UV light and chemical

disinfectants[8], these properties probably arise from an unusually high level of peptidoglycan cross-linking[18]. The SCV is typically considered the form allowing *C. burnetii* to persist in the environment.

Upon internalisation in acidic vacuoles within host cells, *C. burnetii* undergoes a reversible SCV-to-LCV switch, to form the larger (>1 µm), metabolically active and replicative LCV[8]. A switch back to SCV form can occur during stationary phase growth and can be seen after prolonged culture (> 21 days)[19].

1.2.3. Intracellular lifestyle of *C. burnetii*

C. burnetii is an obligate intracellular pathogen that can infect both phagocytic and non-phagocytic cells[20] and a tropism for alveolar macrophages[21–23]. Both phase I and phase II strains have been shown to replicate in human and bovine monocyte-derived macrophages with alike kinetics[24,25]. Although the different LPS profiles of the two phases do result in different mechanisms of internalisation. Both phase types infect alveolar macrophages through passive actin-dependent phagocytosis[26,27]. Phase I strains are internalised via binding to $\alpha_v\beta_3$ integrin, whereas phase II strains are internalised more efficiently via binding to the CR3 receptor[28].
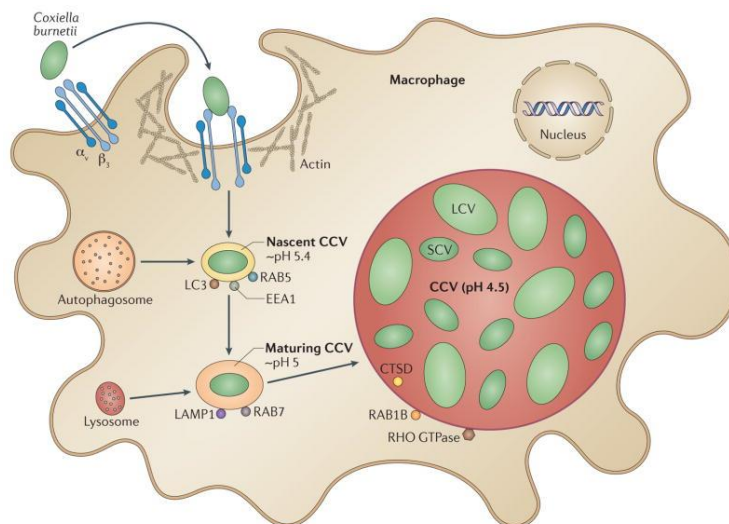
Figure 1.2. Intracellular uptake of *C. burnetii.* Figure from[29]. *C. burnetii* binds to macrophages and is internalised by actin-dependent phagocytosis and is contained within a *Coxiella* containing vacuole (CCV) The early (or nascent) CCV is characteristic of normal phagosomal development and follows a pathway characteristic of the normal endocytic pathway to form an acidic CCV with a pH of ~ 4.5.

After uptake, *C. burnetii* resides in an acid vacuole known as the '*Coxiella* containing vacuole' (CCV), which is formed through a pathway characteristic of the normal endocytic pathway (Figure 1.2). Acidification of the phagolysosome causes the switch of *C. burnetii* from SCV to LCV form and the activation of the Type 4 Secretion system (T4BSS), which begins to secrete effector proteins[30]. The LCV form replicates, causing the mature CCV to expand, filling the majority of host cell cytoplasm. It has been suggested that *C. burnetii* acquires membranes from different cellular compartments to facilitate this expansion.

1.2.4. *C. burnetii* as a potential bioterrorism agent

C. burnetii has been classified as a category B potential bioterrorism agent by the Centre for Disease Classification (CDC) due its low infectious dose, airborne spread and ability to persist for a long duration in the environment[7]. Although extremely debilitating, survivability from Q fever infection is high. For this reason it is considered an incapacitating agent, as opposed to a lethal agent.

Investigations into the utility of *C. burnetii* to be used as a biological weapon are the reason we can state with almost certain confidence the low infectious dose of 1 – 10 organisms. In 1955, at Fort Detrick (USA) a medical countermeasures program termed 'Operation Whitecoat' took place. Operation Whitecoat involved performing experiments on conscientious objectors from the Seventh-day Adventist Church. The volunteers were exposed to aerosolised *C. burnetii* at a range of concentrations in an exposure chamber known as the 'Giant 8 ball' (Figure 1.3).

After exposure they were monitored for the development of a fever, a typical symptom of Q fever[31]. This study also found that treatment with oxytetracycline, before the development of symptoms, protected against the development of symptoms. The same volunteers took place in a biological attack simulation later that year, side by side with guinea pigs and non-human primates at the Dugway Proving Ground, in the Utah desert[31]. Aerosolised *C. burnetii* contained in an egg slurry was released ~ 900 metres from the subjects at a dose where each subject would theoretically receive 150 infectious units, where one infectious unit is the quantity of *C. burnetii* required to produce a serological response in 50% of guinea pigs (GPID$_{50}$). As before, individuals were treated with oxytetracyline at the end of the study. It should be noted that all

human volunteers survived these studies, and long term follow up care was provided during which no adverse effects such as Q fever fatigue syndrome were identified.

Figure 1.3 Operation whitecoat volunteers in the Q fever group pictured (right) at a reunion in 1989. These volunteers were exposed to *C. burnetii* using an exposure chamber known as the 'giant eight ball' (left) after which they were monitored for the development of Q fever symptoms. Images supplied by volunteer Ken Jones (pictured) and shown with permission.

1.2.5. The *C. burnetii* genome

The first sequenced *C. burnetii* genome was of the Nine Mile Phase I RSA493 strain first isolated from a tick in 1935 and was published in 2003[18]. This revealed a 1,995,275 bp chromosome and a 37,393 bp QpH1 plasmid. The genome contains a total of 2,134 predicted coding sequences (CDSs). A large percentage (33.7%) of the CDSs are annotated as encoding hypothetical proteins, i.e. proteins without significant matches to previously identified proteins. In addition, the genome contains 83 pseudogenes, indicating ongoing genome reduction and 29 transposable elements, suggesting a high degree of genome plasticity. The genome contains a high number of genes encoding transport systems, which are to be expected due to the obligate intracellular lifestyle of *C. burnetii,* which relies on nutrient scavenging from the host cell. There are also a surprisingly high number of genes which are similar to eukaryotic genes.

At the time of writing, there are 63 reported *C. burnetii* genomes in the NCBI database. Fourteen of these have a full assembly. Genome size ranges from 1.95 – 2.21 Mbp with GC content from 42.3 – 42.9%. All sequenced isolates contain one of four autonomously replicating plasmids: QpH1, QpRS, QpDV or QpDG or have a plasmid sequence integrated into their chromosome[32–35]. There is a ~16 kb region that is found in all plasmid types[35,36]. It is possible that this could be an essential region of the genome.

C. burnetii genomes can be separated into six distinct genomic groups based on analysis of restriction fragment length polymorphism patterns [34]. These groups were later confirmed by Multispacer Sequence Typing[37] and Multiple-Locus Variable number tandem repeat Analysis[38]

1.3. Virulence mechanisms of *C. burnetii*

1.3.1. *C. burnetii* lipopolysaccharide

Lipopolysaccharide (LPS) is a macromolecule found in the cell wall of Gram-negative bacteria. LPS consist of three domains: cell wall bound lipid A with endotoxin properties, a polysaccharide core, and O-antigen [39]. The LPS of phase I *C. burnetii* is commonly described as a virulence factor that provides *C. burnetii* resistance to host defence mechanisms. The LPS acts as a shielding molecule, preventing ligand binding and therefore protecting *C. burnetii* from innate immune recognition and preventing cytokine production[41].

In the late 1980's, Moos and Hackstadt performed an experiment in guinea pigs comparing LPS variants in different strains. It was found that phase I isolates, with full length LPS resulted in symptomatic infection and viable *C. burnetii* could be isolated from the spleens of infected animals at 30 days post infection. Conversely, phase II isolates with truncated LPS did not result in the development of symptoms and viable *C. burnetii* could not be isolated from the spleens of infected animals in the same timeframe. To date, the *C. burnetii* phase I LPS remains the only virulence factor that has been experimentally verified in immunocompetent animal model[40].

Interestingly, *C. burnetii* LPS - unlike the LPS of other bacterial pathogens such as *Escherichia coli* and *Salmonella typhimurium* – is not considered to have potent endotoxin activity. Showing 1,000-fold less endotoxin activity than the aforementioned

species[42]. This has been deemed as a direct result of conformational differences in the lipid A.

1.3.2. The type four secretion system and effector proteins

Type 4 secretion systems (T4SS) are a structurally diverse group of secretion systems found in many bacteria. T4SSs are involved in horizontal gene transfer (and therefore the spread of antibiotic resistance) [43] and are responsible for the translocation of effector proteins from the bacterial cytosol to the cytosol of a host cell. This latter function makes them important virulence determinants that are involved in the pathogenesis of many bacteria such as *Legionella pneumophilia*[44]*, Helicobacter pylori*[45]*, Bordetella pertussis*[46]

C. burnetii possesses a T4BSS consisting of proteins encoded by ~30 chromosomal *dot/icm* genes (**d**efect in **o**rganelle **t**rafficking/**i**ntra**c**ellular **m**ultiplication), that has been identified as a further virulence determinant that plays a role in disease[47] through the secretion of over 130 effector proteins[48,49].

Many of these effector proteins do not yet have an assigned function. However, some have been recently elucidated. Cig57 has been identified as playing a role in CCV formation and maturation[50]. CypB plays a role in CCV homotypic fusion[51]. EirA is essential for intracellular replication[52]. AnkF is involved in the establishment of a CCV that permits replication[53]. AnkG acts to prevent host cell apoptosis[54]. CaeB inhibits host cell endoplasmic reticulum stress signalling, preventing host cell apoptosis[55]. And NopA manipulates host cell transcription factors resulting in reduced levels of cytokines involved in innate immune sensing of pathogens, promoting *C. burnetii* intracellular survival [56].

1.4.   Q fever in humans

1.4.1. Transmission, symptoms and prognosis

C. burnetii is a zoonotic pathogen and can be carried by both domestic and wild animals. Although the majority of human infections result from inhalation or through direct contact with farmed ruminants such as goats, sheep and cattle[57,58]. there are many vectors such as ticks, rodents, rabbits and dogs[59–62]. Although direct contact is the most common route of infections, animals and their by-products can shed *C.*

burnetii into the environment. For example, greater than 1×10^9 bacteria per gram of placenta can be released during parturition in domestic ruminants[63,64]. C. burnetii released in ths way can persist for a long time, and can be aerosolised and spread by wind[65], therefore Q fever should not be ruled due to an absence of contact with ruminants. Although rare, some incidents of sexual transmission between humans have also been documented[66,67]. Transmission as a result of the ingestion of infected dairy produce has long been debated[68].

Up to 60% of individuals infected with C. burnetii will remain asymptomatic[69]. The remaining 40% develop acute Q fever after an incubation period of one to three weeks, depending on dose recieved[70]. Acute Q fever is often a self-limiting flu like illness, with symptoms of a high fever and characteristic retro-orbital headache persisting for two to six weeks. Approximately 2% of acute Q fever cases progress into an atypical pneumonia or granulomatous hepatitis[70], other rarer clinical manifestations have also been reported such as acute endocarditis[71], myocarditis[72] and spelinic and hepatic abbesses[73]. There is little information available on the cellular pathology of acute or chronic Q fever in humans. It is known that C. burnetii infection persists through the modulation of the host cell metabolism by downregulating the activation of pro-inflammatory cytokines, preventing host cell apoptosis and modulating autophagy[55,138]. Arguably the most debilitating outcome of acute Q fever in around 15% of individuals is the manifestation of post-Q fever fatigue syndrome caused by cytokine dysregulation in response to persistent C. burnetii antigens (as opposed latent C. burnetii whole cells)[74]. In addition to fatigue, individuals with post-Q fever fatigue syndrome have reported addition problems such as blurred vision, cognitive dysfunction, respiratory problems and mood swings [75]. Post-Q fever fatigue syndrome can persist for up to 10 years and often leaves patients requiring unable to work and requiring care[76].

Approximately 1 - 5% of individuals will go onto to develop chronic Q fever[77,78], a long-term debilitating condition that can persist for years after acute infection. The predominant complication of chronic Q fever is culture negative endocarditis[79] or hepatitis. It has been shown that instances of chronic Q fever usually occur in immunocompromised individuals, suggesting that an insufficient T-cell response prevents clearance of the infection. In addition, other parts of the immune system may

play a role in chronic Q fever such as antibody/cytokine response and cellular responses from other cell types [80,81].

1.4.2. Epidemiology of Q fever in humans

It is frequently reported that Q fever has a worldwide distribution[82,83], with the exception of New Zealand. In England and Wales, 904 cases of acute Q fever were reported in 2000 - 2015[84]. The largest number of cases occurring in South-West England (Figure 1.4), which may reflect the large proportion of pastoral farming this this region. Since 2015, between 16 and 33 cases have been reported annually (source – Public Heath England). It should be noted that due to the flu-like nature of acute Q fever these figures are likely underestimated, as many cases go undiagnosed.
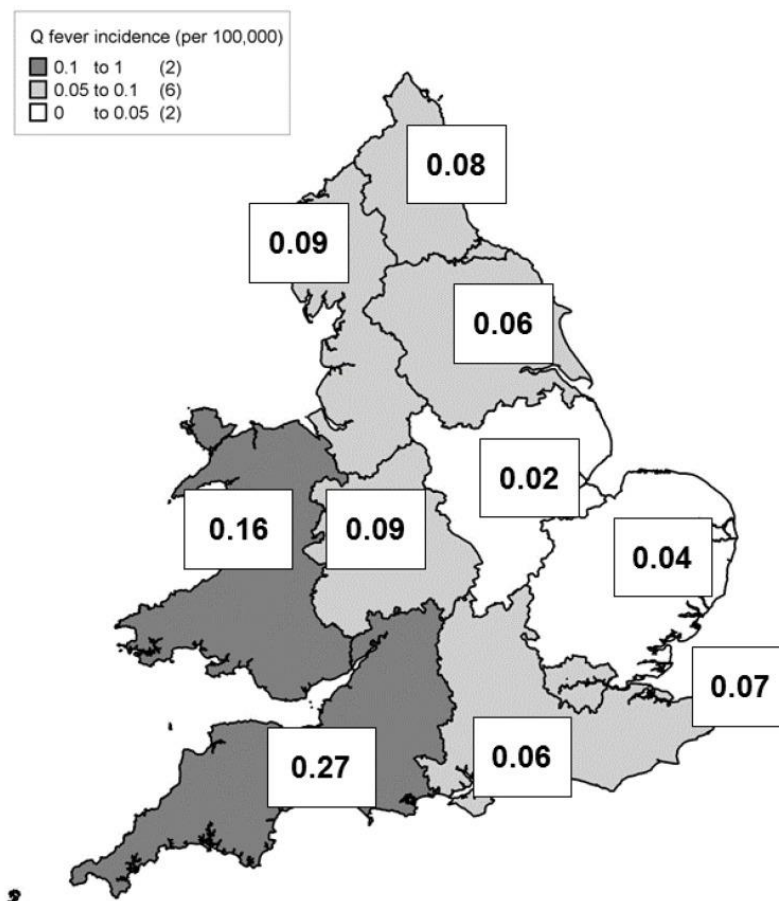
Figure 1.4 Incidence rate per 100,000 persons of acute Q fever in England and Wales from 2000-2015. Figure from Halsby *et* al.[84].

There are many documented outbreaks of human Q fever. The largest of which took place in the Netherlands from 2007 – 2010, more than 4,000 cases of Q fever were reported in this timeframe, although due to the likelihood of an absence of suitable

27

diagnostics it is estimated that actual incidences could exceed 40,000. Prior to the outbreak, The Netherlands had few cases of Q fever. In fact, more than three times as many incidences were reported in the first month of the outbreak than had been reported in the entire six years prior[85,86]. The outbreak was associated with a sudden increase in intense dairy farming using goats. After a failure of more conservative efforts to contain the outbreak, it was ultimately contained by culling more than 50,000 goats across 88 farms, costing more than 300 million euros[87,88]

In the UK, many Q fever outbreaks have been recorded. The largest took place in the West Midlands in 1989 where 147 cases were reported. The cause of this outbreak was determined to be due to airborne spread of *C. burnetii* from farms engaged in outdoor lambing and calving during a day of unusually high winds[89]. Since then, further outbreaks have occurred. In 2002, 95 workers from a cardboard factory in Wales were diagnosed with Q fever. This outbreak was found to have been caused during renovation work in the factory where contaminated straw board was used[90]. The most recent UK outbreak took place in a Scottish slaughterhouse in 2006, 110 cases were identified among staff members who had walked past a holding pen containing infected sheep[91]

Although Q fever outbreaks do not appear to have been reported in the UK since this time, it remains a concern. Most recently, an outbreak of 138 cases has occurred from 2018 – 2019 in Zhuhai City, China[92].

1.4.3. Diagnosis of human Q fever

The "gold-standard" diagnostic test for Q fever diagnosis uses an immunofluorescence assay (IFA) to detect antibodies against phase I and phase II *C. burnetii* , in two samples taken 2-3 weeks apart[93,94]. A diagnosis of acute Q fever occurs when IgM and IgG antibodies are detected against phase II *C. burnetii,* with some IgM phase I antibodies. A diagnosis of chronic Q fever occurs when IgG and IgA antibodies against both phase I and phase II are present[95]. This method of diagnosis has the advantage of being able to differentiate between acute and chronic infection and has high sensitivity (98%) and specificity (100%)[96]. However there remains a need for improved diagnostics. Firstly, treatment for Q fever is most successful if administered within a few days of infection[97], therefore diagnosis using IFA tends to be retrospective. Secondly, IFA does not have the ability to differentiate between actively infected

persons and those that have recovered from the disease. Finally, cut-off levels for antibody titres are not standardised between laboratories[98], which results in varying results across different laboratories[99].

Recently, lateral flow device (LFD) tests for the detection of antibodies have been developed[100]. Like IFA testing, LFD tests still have the disadvantage of being unable to differentiate between actively infected and recovered individuals, they are comparatively cheaper than IFA tests and have good sensitivity and specificity, and do not require specialist laboratories. These tests have not yet reached large scale production.

An alternative diagnostic test utilises the molecular method real-time polymerase chain reaction (qPCR), rather than serology for diagnosis. Common qPCR targets for *C. burnetii* are the transposable element *IS1111* which has multiple genomic copies, making it a good target for assay sensitivity[101] or the *com1* housekeeping gene, which encodes a 27 kDa outer membrane protein[102]. PCR based diagnostics have the advantage of being able to detect *C. burnetii* during the first 11 days of infection, rather than the average of 17 days for IFA testings[103].

1.4.4. Treatment

The main treatment for Q fever is the antibiotic doxycycline, selected due to its ability to readily enter cells, preventing intracellular growth[104]. Many cases of acute Q fever self-resolve without the need for medical intervention. However, in the instance of diagnosis, patients are often prescribed doxycycline for two weeks.

Treatment of chronic Q fever is more difficult, and requires lengthy antibiotic treatment, using a combination of doxycycline and hydrochloroquine for 18 months to 3 years. Hydrochloroquine is used as an alkalising agent, as it was found that the acid conditions within the CCV inhibit antibiotic activity[105]. This combination therapy allows a shortened duration of treatment (18 months – 3 years vs > 4 years) and a reduced risk of relapse[106]

Although doxycycline is an effective treatment for Q fever, and has a low minimum inhibitory concentration (MIC) of less than 2 µg/mL[107–109]. *C. burnetii* resistance to doxycycline has been reported[110,111]. It is therefore important that new treatments are found.

1.4.5. Prevention

The only current vaccine to protect against Q fever, Q-Vax, is only licenced for use in Australia. Q-Vax is a formalin inactivated whole cell vaccine using the Phase I Henzerling strain of *C. burnetii* [112]. Where the intact LPS of the phase I strain acts as a protective immunogen. Q-Vax is a highly protective vaccine (98% efficacy for up to 5 years post inoculation) and is given to individuals aged 15 years and over in occupation risk groups (farmers, abattoir staff and veterinarians). Q-vax was also used in the 2011 Q fever outbreak in the Netherlands[113].

However, the risk of severe adverse local and systemic reactions in individuals that have been previously seroconverted has been deemed too high for licencing in other countries. In Australia, this is overcome (to a degree) with vaccination pre-screening consisting of both intra-dermal skin testing and serology testing. Even with this pre-screening, severe adverse reactions are still reported[114]

The current absence of a *C. burnetii* vaccine in the UK presents a concerning situation should an outbreak occur and there is a requirement for the development of a safe and effective vaccine that does not require pre-vaccination screening.

1.5.   Animal models of Q fever [1]

Experimental animal models of infection play a crucial role in microbiological research, allowing scientists to understand disease pathogenesis, develop and test diagnostics, and create/ improve prophylaxes and treatments for disease. Infection models have a variety of applications including genotype – phenotype studies to identify virulence determinants[115–118] and pathogenic variability between different *C. burnetii* strains[119,120], antibiotic efficacy testing to evaluate treatment options[115,121] and vaccine reactogenicity studies to identify adverse effects[122,123]. Both drug and vaccine development pipelines require pre-clinical testing in animal models prior to clinical trials with human subjects. A good understanding of the advantages and limitations of infection models allows them to be matched to the experimental needs. The pathology

---

associated with bacterial disease is often complex and influenced by both intrinsic and extrinsic factors, some of which are specific to the species in hand. This must be considered when extrapolating findings to human disease, to prevent drawing incorrect conclusions and wasting animal life. Animal models for Q fever can be assigned to one of three groups: invertebrate models[115,124,125], small mammal models[23,120,122], or non-human primate models[126,127].

1.5.1. Invertebrate models of Q fever

Insects, such as *Drosophila melanogaster*, *Caenorhabditis elegans* and *Galleria mellonella* are commonly used as bacterial infection models. They are not subject to the same ethical concerns as compared to mammals, meaning that they are not protected under most animal research legislation. Further to this, the lack of housing requirements and necessary specialist training, along with low cost and small size, makes their use desirable, particularly in the case of high-throughput screening. Insect models are valuable when working with *C. burnetii* because they are susceptible to infection with either phase I or phase II strains[115,124,125], with the latter enabling experimentation in BSL-2 laboratories. Although *D. melanogaster* and *G. mellonella* possess innate immune systems with similarities to the innate system in mammals[128,129], insect models lack an adaptive immune response and can therefore only be considered a preliminary screen for virulence. Due to the lack of adaptive immunity, insect models are less well suited to vaccine research and development. However, insect models could be used to identify live attenuated mutants as vaccine candidates. Finally, any studies involving phase II strains should be validated through infection of an immunocompetent animal with a virulent phase I counterpart.

1.5.1.1. *Caenorhabditis elegans*

C. elegans, a soil-living nematode, is often used as a bacterial infection model due to its small size, low cost, transparent body and natural diet of microorganisms. The innate immune response consists of three main components. Firstly, *C. elegans* displays avoidance behaviour using olfactory mechanisms to detect and avoid the ingestion of harmful pathogens[130]. A pharyngeal grinder then permits mechanical

digestion[131]. Finally, there is production of antimicrobial effectors, such as cationic peptides, in response to infection[132]. When provided with an alternative to their natural nutrient source (e.g. *Escherichia coli* OP50), *C. elegans* demonstrates avoidance behaviour towards *C. burnetii* [125]. After ingestion, *C. burnetii* remains intact, avoiding destruction by the pharyngeal grinder, and initially accumulates in the anterior midgut and posterior pharyngeal–intestinal valve – regions of *C. elegans* that are maintained at ~pH 4.5 – before dissemination throughout the entire intestinal lumen. Nematodes display symptoms including reduced movement, a deformed anal region that grows larger over time and extra luminal blebs off the intestinal lumen[125]. It is possible that extra luminal blebs arise as a consequence of *C. burnetii* entering, and beginning to form a CCV, in enterocytes lining the intestinal lumen given that such pathology has been observed for *L. pneumophila* infection in *C. elegans*[133], a pathogen for which *C. burnetii* shows high similarity[134]. *C. elegans* survival is significantly reduced post infection with *C. burnetii* , with a median time to death of 8 days, compared to 15 days for an *E. coli* control[125]. Toll-like receptors (TLRs) are involved in the innate immune response of many species, acting as pathogen recognition receptors (PRRs) to detect pathogen-associated molecular patterns and initiate an innate immune response. *C. elegans* possesses a single TLR homologue, TOL-1, which appears to play little role in *C. burnetii* infection in this model as a tol-1 mutant of *C. elegans* showed a similar pattern of symptoms and survival to wild-type nematodes[125]. However, TOL-1 is required for the olfactory mechanisms used by *C. elegans* for avoidance behaviour[135], and therefore the role of TOL-1 in avoidance of *C. burnetii* still requires investigation. Additional TLRs have been shown to play important roles in *C. burnetii* infection in humans[136,137], suggesting that the nematode model may not be translational to human disease due to the lack of these TLR homologues in *C. elegans*. In mammals, mitogen-activated protein kinase (MAPK) signalling pathways respond to pro-inflammatory cytokines such as TNF-α and IL-1 to determine cell-fate decisions such as inflammation and apoptosis[138]. Although the PRRs for MAPK signalling in *C. elegans* remain unknown, SEK-1 has been identified as an MAPK in *C. elegans* for which mutation results in increased susceptibility to *Pseudomonas aeruginosa*[139]. Exposure of *C. elegans* with mutated SEK-1 to *C. burnetii* resulted in a significant increase in mortality compared to wild-type nematodes, reducing the median time to death to 5days, with a greater abundance of *C. burnetii* detected in the intestinal lumen, suggesting that MAPK signalling is associated with the *C. elegans* immune response

to *C. burnetii* [125]. In addition to TOL-1 and MAPK signalling pathways, DAF-2/DAF-16 signalling pathways have been associated with the immune response of *C. elegans* through the production of an array of antimicrobial effectors including lysozyme. In the absence of infection, DAF-16 is retained in the cytoplasm as a result of a phosphorylation cascade initiated by the binding of an agonist to DAF-2. When DAF-2 is mutated, non-phosphorylated DAF-16 translocates to the nucleus resulting in the increased expression of antimicrobial effectors[140]. When DAF-2 mutants are infected with *C. burnetii*, the bacteria appear to accumulate to a lesser degree and a significant decrease in mortality is observed[140]. Together, these findings show that *C. elegans* mounts an innate immune response to *C. burnetii* infection.

1.5.1.2. *Drosophila melanogaster*

D. melanogaster makes a desirable insect model of infection for many bacteria as this species is genetically tractable using a number of methods: transposon mutagenesis for gene disruption, gene expression knockdown utilizing RNAi and gain of function through targeted gene activation[141]. Like *G. mellonella* and *C. elegans*[115,125], *D. melanogaster* is susceptible to infection with phase II strains of *C. burnetii*, and females exhibit dose-dependent mortality[124]. However, at a dose of 10^5 genome equivalents (GE) of *C. burnetii* NMII and after 30 days of incubation, mortality of the entire population does not occur. The IMD pathway controls the expression of many antimicrobial peptides in *D. melanogaster* and it is reported to be representative of the TNF pathway in humans[142]. Significant upregulation of the antimicrobial peptide drosocin 12 days after infection with *C. burnetii* suggests that the IMD pathway has been activated. Conversely, defensin – an antimicrobial peptide associated with activation on the Toll pathway – was not differentially regulated after infection[124]. These findings were corroborated by investigating the response of mutants of *D. melanogaster* in the peptidoglycan-recognition protein LC (a recognition receptor) and Relish (a transcription factor) in the IMD pathway. Both mutants showed increased susceptibility to infection compared with wild-type flies[124]. *D. melanogaster* Eiger is the only known invertebrate TNF superfamily ligand. Due to the finding that infection with *C. burnetii* induced the expression of pro-inflammatory cytokines, including TNF-α[143], the effect of an Eiger mutation in *D. melanogaster* was evaluated. Compared to the wildtype, the Eiger mutant showed increased survival after challenge with *C. burnetii,* but no difference in bacterial load was observed. This suggests that the Eiger mutant

was better able to tolerate infection than wild-type *D. melanogaster*[124]. Similar results have been reported after challenge of an Eiger mutant with *S. typhimurium*[144]. In addition to investigating the innate immune response, Bastos et al. identified that, like mammalian cells and *G. mellonella* haemocytes, the T4SS is essential for productive infection of *D. melanogaster* haemocytes. Flies challenged with a Δ*dotA* (T4SS) mutant did not display significant mortality[124]. This indicates that this model may be useful for identifying virulence determinants of *C. burnetii,* in addition to investigating host–pathogen interactions with human gene homologues.

1.5.1.3. *Galleria mellonella*

Larvae of the greater wax moth (*G. mellonella*) have an advantage over the aforementioned insect models for bacteria in that they can be kept at 37 °C (the physiological temperature of mammals), and their large body size compared to *D. melanogaster* and *C. elegans* permits inoculation with a precise dose through injection into pro-legs on the underside of the larval body. In addition, macroscopic changes such as melanization of the cuticle, a drop in activity level and an inability to form a full cocoon can be observed over the course of infection, and a health index scoring system for monitoring these macroscopic changes has been proposed by Loh et al.[145]. The main limitation of the *G. mellonella* model is that although a draft genome sequence recently became available[146], the larvae are not yet genetically tractable. Many research groups utilize larvae purchased from bait-shops. This can lead to inconsistent results because of batch-to-batch differences in the origin and rearing conditions of the larvae. This limitation has been resolved with the development of standardized research-grade larvae[147]. The *G. mellonella* model of *C. burnetii* infection shows dose dependent mortality with no significant difference in susceptibility to infection with phase I or phase II isolates (LD50 values of 4.2×10^2 and 9.1×10^2 GE ml , respectively[115]). This is desirable because it allows studies to be carried out with phase II isolates at BSL2. Using the *G. mellonella* model, Norville *et al.* showed that larvae dosed with doxycycline – the recommended treatment for Q fever – 24h post-challenge with *C. burnetii* showed a significant delay in mortality[115].

This finding suggests that this model could be used to develop and test therapies for Q fever infection. Furthermore, *dotA* and *dotB* (T4SS) mutants did not cause

significant mortality in *G. mellonella*[115], suggesting that the T4SS is essential for infection. This model has since been used to show that the *Coxiella* vacuolar protein B (CvpB) – a T4SS effector – is essential for correct CCV biogenesis[117] and to investigate genotype-specific virulence[119].

Although little is known on the cellular pathology of Q fever in humans, the *G. mellonella* model could be applied to identify genes or proteins involved in *C. burnetii*'s ability to prevent host cell apoptosis and modulate autophagy. Developments in genetic tractabilitily of *G. mellonella* could permit further investigation of host-pathogen interactions and therefore increase our understanding of the cellular pathology of Q fever.

1.5.2. Small animal models of Q fever

Guinea pigs were one of the first animal species to be used as infection models of Q fever[1], and this model is suggested to be the most physically relevant model of Q fever due to its close similarity to most aspects of human disease[31]. Tigertt and Benenson were able to directly compare data from guinea pigs (inhalation vs intraperitoneal (I.P.) challenge) and human subjects by inhalational challenge, and demonstrated a similar dose effect in the serological response between guinea pigs and humans when data were adjusted for differences in respiration rates, as well as similar, linear relationships between infectious dose and incubation periods before the onset of fever[31]. However, incubation periods were longest in humans by inhalational challenge and shortest in guinea pigs infected via the I.P. route[31]. A more recent study comparing guinea pigs infected by the I.P. route or intranasally also revealed differences in the pathological changes between the two groups, thereby indicating that the route of infection does influence the clinical outcome[148]. After inhalational challenge (the preferred infection route), animals display dose-dependent pathologies[22] and at a challenge dose of 2×10^6 *C. burnetii* , a fever develops within 5 days with an 8-day duration. During this period, lethargy and loss of appetite correlate with weight loss. Respiratory changes occur from 5 days post-infection (PI.), with necroscopy indicating the presence of severe pneumonia and hepatitis. This model shows a pneumonia progression closely matching that seen in cases of acute Q fever in humans[149,150]. Overall there is 70% mortality at this dose. Despite this difference in lethality between guinea pigs and humans, where Q fever usually only presents as a mild illness, guinea pigs still remain

the best small animal model of Q fever, and are considered to be the gold-standard for vaccine reactogenicity studies[122]. However, a lack of genetic tractability limits their use as a model. In addition, they are more costly and require more housing space than mice. Immunocompetent mice are not susceptible to phase II strains of *C. burnetii* , and A/J mice show the highest susceptibility to phase I strains when infected intraperitoneally[151]. Immunocompetent mice, including A/J and CB-17 strains, are not usually reported to show signs of disease such as weight loss and inactivity that are seen after the challenge of SCID (severely compromised immunodeficient) mice[120,152], even though ruffled coats, arched backs and weight loss have been shown in A/J mice infected via aerosol challenge[121]. Gross pathology is limited to mild hepatitis and splenomegaly in A/J mice and splenomegaly only in CB-17 mice. These models have been used in vaccine research studies[153–155] and to test antibiotic efficacy[121]. However, the lack of consistent overt signs of disease indicates the need for alternative models. Severely compromised immunodeficient (SCID) mice are susceptible to a lethal infection with either phase I or phase II strains of *C. burnetii* when dosed intraperitoneally[120,152]. Both phase I and phase II strains cause splenomegaly and the dissemination of *C. burnetii* to the lung, liver and spleen[120,152]. In a NMI model, mice exhibit signs of infection including ruffled fur from 7 days post-infection. By day 9, a hunchback appearance ensues and reduced activity is observed, correlating with a loss of body weight, until death typically on day 33[152]. At necroscopy, severe hepatitis is evident in addition to endocarditis with the presence of focal calcification, matching findings seen in patients with chronic Q fever endocarditis[156,157]. When infected by the aerosol or intra-tracheal route with NMII, SCID mice show slight splenomegaly, with bacterial loads in the liver and lungs increasing to a lesser degree than that seen after I.P. challenge[120,158], and infection is not lethal 14 days after exposure[158]. Aerosol exposure to the NMI strain has been shown to result in a pattern of tissue dissemination and degree of splenomegaly similar to that seen after I.P. challenge with NMII[159]. As both aerosol studies using the NMII strain were terminated by day 14 post-infection, it would be interesting to see whether a longer time-frame of infection would allow more efficient systemic infection with this strain to develop. A NMII aerosol challenge model for preliminary studies would be preferable over an I.P. model as it better mimics the natural route of Q fever infection combined with the advantage of fewer biological safety concerns compared to a NMI model, even though not all of the findings may be transferrable to infections with a virulent strain.

1.5.3. Non-human primate models of Q fever

Infection of non-human primates (NHPs) with *C. burnetii* results in disease which closely mirrors disease in humans. However, the ethical considerations, housing costs and specialist training needs which are associated with NHP studies mean that they are used minimally in research, and are often reserved for the final stages of studies prior to a human clinical trial. The first reported use of primates was alongside human volunteers during Operation Whitecoat by the US military in 1955, where both humans and animals were exposed to an indoor aerosol of *C. burnetii* [160]. Later in 1979, a fully characterized NHP model of Q fever was reported by Gonder *et al.*[127]. Monkeys were challenged by the aerosol route with either a low or a high dose of *C. burnetii* phase I Henzerling strain. The low-dose group did not show any signs of Q fever. Sign of disease in the high-dose group were similar to the symptoms of acute Q fever in humans and began to emerge 5 days post-infection. Fever, anorexia and depression were evident with a 4 – 6 day duration. Dyspnoea, cough and increased respiration persisted from days 5 to 14 and radiographic images showed pneumonia with increasing severity over time. Haematological examination showed an increase in serum aspartate transaminase, alkaline phosphatase and total bilirubin, with subacute hepatitis seen at necroscopy. These findings were reproduced by Waag *et al.*[126] in a study comparing cynomolgus and rhesus macaques as models of acute Q fever and, considering the pronounced radiographic changes seen in cynomolgus macaques, the authors suggested this was the superior model. Waag *et al.* subsequently used this model to compare a chloroform/methanol extract and a formalin inactivated whole cell formulation (Q-vax) as vaccines and were able to demonstrate that both immunogens provided similar levels of protection against experimental Q fever[123].

Most recently, a NHP model using *Callithrix jacchus* (the common marmoset) was developed[161]. As with the previously stated NHP models, the marmosets displayed many features of acute Q fever infection that align with what is seen in humans (fever onset, fever duration, weight loss and bacteraemia). Serology testing of the marmosets using the human criteria for diagnosis (Phase II IgG > Phase I IgG) confirmed that they were exhibiting acute Q fever. Haematological examination showed an increase in liver enzymes aspartate transaminase and alanine transaminase. The finding that marmosets are a suitable model of acute Q fever may allow the assessment of potential novel treatments and vaccines. The common

marmoset has the advantage over previously discussed NHP models in that it is not as expensive, and its small size makes it easier to work with in high-containment laboratory environments required for work with phase I *C. burnetii* strains.

1.5.4. Dexamethasone is an immune modulator

Dexamethasone is a glucocorticoid drug that is widely used in human medicine. Dexamethasone has potent anti-inflammatory and immunosuppressive effects making it a good drug of choice when inflammation is present, for example during an allergic response, or during an asthma attack or when an inappropriate or undesirable immune response occurs for example for individuals with autoimmune disorders such as Lupus. Dexamethasone has an intracellular effect. The drug enters the cell membrane passively and binds to glucocorticoid receptors. The dexamethasone-receptor complex enters the nucleus, and binds to glucocorticoid response elements[162]. As a result, transcription of inflammation associated genes is modified in a way that anti-inflammatory mediator production is stimulated, concurrently with the suppression of inflammatory mediators such as the synthesis of macrophages and phospholipase A2[163]

Dexamethasone is often used in animal studies to increase susceptibility to infection. For example, *Mycobacteroides abscessus* is a pathogen associated with incurable disease in individuals with lung damaging conditions such as cystic fibrosis, and yet there was no suitable animal model for this disease. Pre-treatment of mice with dexamethasone permitted the development of a model of *M. abscessus* disease, permitting pre-clinical antibiotic efficacy study[164]. In addition, dexamethasone can be used to model disease outcomes. For example, dexamethasone is often used as a treatment for individuals with chronic pulmonary diseases, and *P. aeruginosa* pneumonia is frequently associated with immunocompromised hosts. It was shown that treatment of mice with dexamethasone significantly increased the levels of bacteria in the lungs when compared to untreated mice in which the levels of bacteria decreased over time[165].
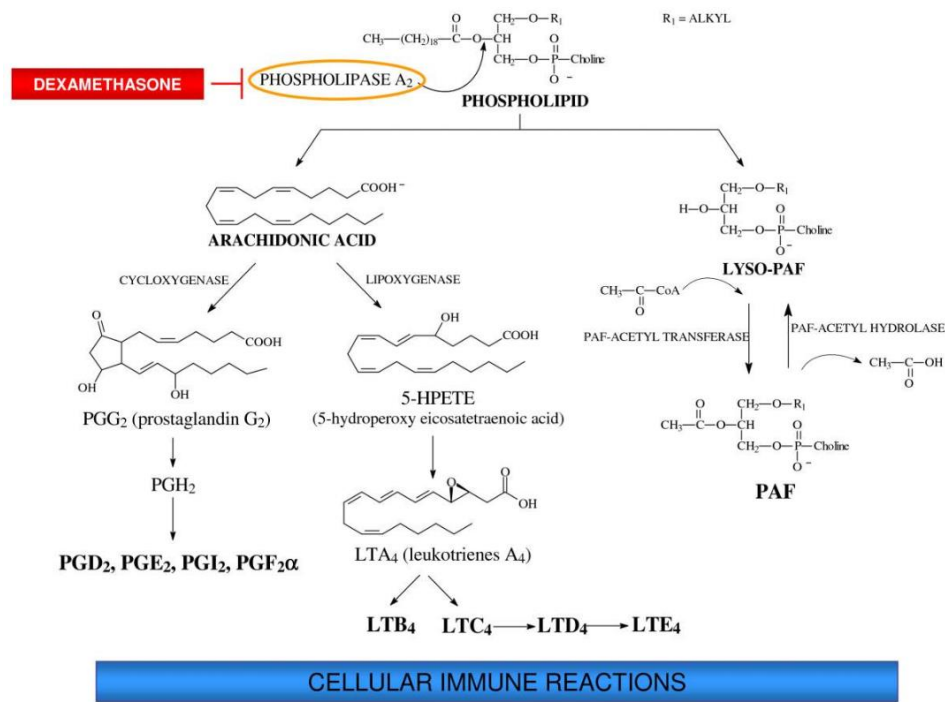
Figure 1.5 Eicosanoid biosynthesis in insects. Arachidonic acid is liberated from phospholipids by phospholipase A_2 (PLA$_2$) to produce various prostaglandins associated with downstream haemocytic response. Dexamethasone inhibits phospholipase A_2 activity, resulting in a reduced immune response. Figure adapted from Garcia *et al.*[166]

Insects do not have an adaptive immune response. Possessing exclusively innate immunity consisting of three main components: the insect cuticle; haemocytic defences; and humoral responses[129]. Haemocytic defences such as microaggregation, nodulation and cell spreading occur as a result of exposure of haemocytes to bacteria, viruses and parasites and are known to be mediated by eicosanoids, oxygenated metabolites of arachidonic acid[167]. Upon infection pattern recognition receptors identify pathogen-associated molecular patterns, resulting in the activation of phospholipase A_2, catalysing the hydrolysis of arachidonic acid from cellular phospholipids. Subsequent downstream reactions result in the formation of prostaglandins, which have been associated with the aforementioned haemocytic responses (Figure 1.5). In insects, dexamethasone can inhibit eicosanoid biosynthesis, resulting in a reduced immune response to infection (Figure 1.5). Pre-treatment of *G. mellonella* with dexamethasone has been shown in increase susceptibility to *E. coli* and *Klebsiella pneumoniae*[168]. In this project the potential to

utilise dexamethasone to increase *G. mellonella* susceptibility to *C. burnetii* has been studied.

1.6. Transposon mutagenesis and its applications in the identification of essential and virulence-associated genes

Essential genes are defined as genes, without which an organism or cell cannot survive. An insight into gene essentiality in pathogens has been of interest to molecular and synthetic biologists for many years, for two main reasons. Firstly, essential genes can be exploited to allow the development of new antibiotics[203-206]; this is imperative in the current antibiotic resistance crisis. Additionally, defining a universal 'minimal genome' required for bacterial survival will aid in the understanding of the universal principles of life[209]. It is important to note that gene essentiality is not binary, and different genes are considered essential in different environments. For this reason, essential gene sets are generally determined *in vivo* on a rich media, in which almost all nutrients are available in the absence of environmental stress. As pathogenic gene expression varies during infection to mediate cell survival at different stages of disease progression, this approach can be used to determine genes essential for simple viability[196].

1.6.1. Transposon mutagenesis

Early geneticists considered a genome to be a stationary entity. The discovery of transposons, or "jumping genes" by scientist Barbara McClintock in the 1950s showed that they are dynamic[169]. Transposons have subsequently been found within the genomes of all kingdoms of life[170].

Transposons can be classified as either Class I or Class II dependent on the mechanism by which they transpose (Figure 1.6). Class I, or replicative transposons utilise a 'copy and paste' mechanism. Using reverse transcription of RNA intermediates for transposition. Class II, or conservative transposons are identifiable by the presence of short inverted terminal repeat sequences (ITRs). Between the ITRs they contain a gene encoding a transposon-specific transposase which allows transposons to move around the genome using a cut and paste method whereby the transposon is excised from the genome and reintegrated at a new location [170,171]. Both

classes of transposons result in genetic rearrangement and alteration. These rearrangements can have a variety of implications of the genome, such as gene inactivation, recombination and modulation of gene expression[170].
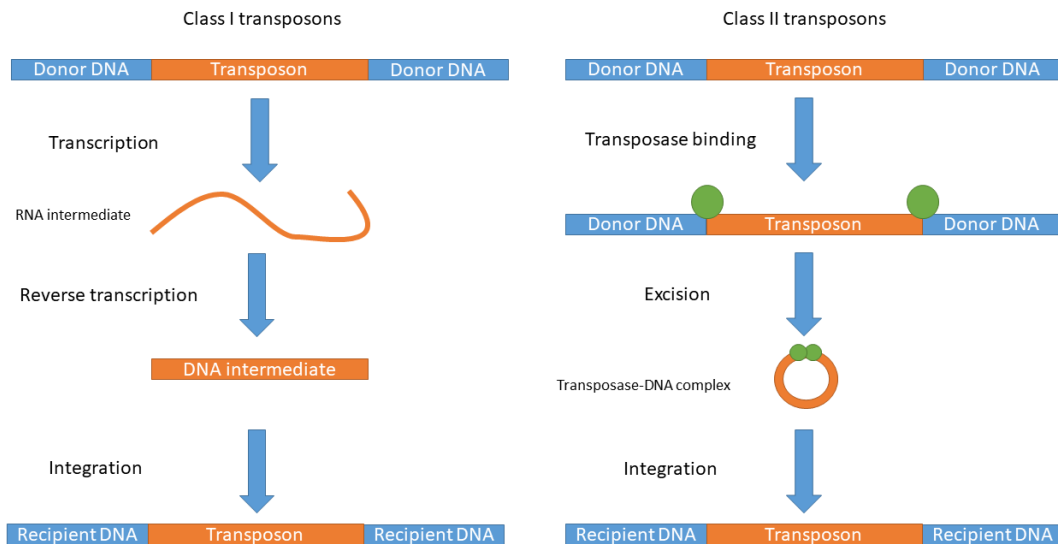
Figure 1.6. Class I and Class II transposon mechanisms of transposition. Class I transposons (left) utilise a 'copy and paste' mechanism. Using reverse transcription of RNA intermediates for transposition. Class II, or conservative transposons use a cut and paste method where the transposon is excised from the genome by a transposase enzyme (green circles) and reintegrated at a new location.

In the 1970s, researchers found that they could modify Class II transposons and use them for genetic manipulation[172]. Modification of transposons by replacing the transposase encoding gene with a gene encoding a selective marker (such as an antimicrobial resistance cassette) and providing the transposase elsewhere on a vector that cannot replicate in the organism of interest results in the loss of the transposase post-transposition, producing a stable mutant with a single transposon insertion.

Theoretically, the utilisation of hundreds of natural transposons for genetic analysis is possible. However the most commonly used transposons in research are derivatives of Tn5 or *Mariner/Himar1* transposons due to the confidence that these transposons meet the set of requirements necessary for successful mutagenesis.

Tn5 is a transposon of prokaryotic origin first discovered in *E. coli*[173]. Tn5 inserts randomly into the genome. Due to this random insertion, Tn5 is a good transposon of choice in GC rich genomes, and its low target specificity allows the construction of a high number of transposon mutants. On the other hand, *Himar1* is a transposon of eukaryotic origin isolated from the Horn Fly *Haematobia irritans*[174]. *Himar1* inserts only at TA dinucleotide sites. The specificity of TA insertion makes *Himar1* an excellent candidate for the identification of essential genes as every potential insertion site is known[175].

1.6.2. Transposon mutant screening approaches

1.6.2.1. Screening transposon mutants in the 'pre-genomics era.

The first methods utilising transposon mutagenesis occurred before the development of DNA sequencing. These methods relied on individually screening mutants for attenuated phenotypes associated with virulence[176] prior to investigation of protein products through the utilisation of techniques such as SDS-PAGE and southern blotting[177]. Hoover *et al.* utilised this screening approach to investigate the cell envelope of Gram-negative oral pathogen *Porphyromonas gingivalis.* They constructed a transposon mutant library and screened mutants for their ability to produce black colonies on blood agar, an observation associated with virulence and the pathogen's requirement for heme-containing compounds. They isolated four mutants with attenuated phenotypes, and by protein analysis identified that these mutants were lacking putative hemagglutinin and hemagglutinin/protease cell envelope proteins present in the wild-type, concluding that these proteins must be associated with the virulence of *P. gingivalis*[178]. Similar approaches have been taken to identify proteins associated with intracellular replication of *S. typhimurium* in a murine model, disproving previous reports that *S. typhimurium* did not grow in phagocytic cells[179], as well as to identify proteins associated with intestinal colonisation of *Vibrio cholerae*[180].

Although these studies were successful in identifying virulence factors and their associated proteins, there were some severe limitations. Firstly, without the ability to sequence the genome, and thus identify specific genes, it was not possible to form genotype-phenotype associations. Additionally, the one-by-one approach of

investigating mutants is time-consuming and impractical for a full, comprehensive screen of an entire bacterial genome.

1.6.2.2. Screening transposon mutants in the 'post-genomic era.'

The development of Sanger sequencing in 1977 resulted in the first DNA sequences of bacterial genomes[181], and the identification of many genes with unknown functions. Thus began the development of the first methods utilising transposon mutagenesis screens in combination with DNA sequencing to determine gene function. This technology, for the first time, allowed researchers to link an observed phenotype with its associated genotype.

The first development combining these technologies was genetic foot printing[182]. Genetic foot printing can be applied to any bacteria for which the DNA sequence is known. Initially, transposon mutagenesis is used to produce an array of mutants, which are pooled together and exposed to a biologically relevant selective condition. Genomic DNA isolated from pre and post exposure pools is amplified by PCR, using primer pairs in which one is primed for the transposon end and the other for a gene of interest (determined from the known DNA sequence). Mutants detected in the pre-exposure pool but absent in the post-exposure pool can be considered essential genes for survival in the selective condition chosen[183–185]. Genetic footprinting has been applied to identify candidate conditionally essential genes in *Streptococcus pneumoniae* and *Haemophilus influenzae,* including those involved in translation initiation and ribosome binding, as well as genes of unknown function with importance in infection[186].

In 1995 Hensel *et al.* developed signature-tagged mutagenesis (STM), a screen for simultaneously analysing pools of transposon mutants using an animal model. By incorporating unique DNA tags into the transposon, each transposon mutant created had its own signature, flanked by a 20 bp 'arm' common to all mutants that was separated from the unique barcode with a restriction endonuclease site. This tagging of mutants facilitated amplification and radiolabelling of the barcode sequences by PCR using primers to match the arm sequences. Removal of the common arms by restriction digest permitted colony blot analysis using tag-specific probes to analyse mutant pools pre and post selection in the model of choice. By comparing these input and output pools mutants with attenuated virulence could be identified. Mutants which

are present in the original inoculum but absent upon recovery from the host likely contain transposon insertions within genes important for infection in the given condition, and are subjected to DNA sequencing of the regions flanking the transposon insertion site. A DNA database search can then be used to identify the gene in which the insertion has occurred, allowing an association between phenotype and genotype. This method was validated via the identification of thirteen previously known virulence genes in *S. typhimurium*, during the same validation experiment, a new pathogenicity island containing genes encoding a type III secretion system was identified[187]. This approach negated the considerable limitations of simple phenotypic screens previously mentioned by allowing a mixed population of transposon mutants to be pooled together and analysed in parallel, while using negative selection to identify attenuated genes in the screened conditions. However, signature tagged mutagenesis is both costly and time-consuming. In addition, colony blot recovery of mutants requires that mutants be present in sufficient numbers for hybridisation, and an increase in complexity of the mutant pool to greater than 96 mutants significantly increases the likelihood that mutants will not be present in sufficient numbers[187,188]. This makes screening every gene within a genome implausible.

STM has been adapted to reduce the experimental load of screening a large number of mutants. One of these adaptations is the development of Transposon site hybridisation (TraSH). TraSH utilises DNA microarrays for mass detection of mutants as opposed to colony blot analysis. This, in principle, allows screening of large numbers of mutants from organisms for which a DNA microarray can be produced, with the only restrictions being those instilled by the animal model of choice[189]. To utilise TraSH, mutant DNA pre and post-selection is isolated and fragmented by restriction digest before the addition of adapters to facilitate PCR amplification. PCR products are then size selected to reduce the likelihood that amplified fragments span multiple open reading frames[190]. Amplified fragments are *in vitro* transcribed to produce cDNA fragments, which are differentially labelled with fluorescent tags to allow comparison of input and output pools. Upon microarray analysis, genes attenuated in the model of choice are identified by a reduced fluorescent signal in the post-selection pool compared to that of the pre-selection pool[191]. Although an improvement on previously discussed screening methods, TraSH is not without its

limitations. Microarray signal resolution can make it difficult to distinguish between positive and negative results[192].

1.6.3. Next-generation transposon screening approaches

The advent of next-generation sequencing (NGS) has allowed a combination of transposon mutagenesis and NGS to make a robust tool for investigating pathogens in a high throughput manner. A large population of transposon mutants can be pooled together, put under selective conditions and simultaneously assayed at a much higher rate than the previously discussed approaches.

Four research groups simultaneously published similar methods utilising this combination in 2009, named Insertion sequencing (IN-seq)[193], transposon sequencing (Tn-Seq)[194], high-throughput insertion tracking by deep sequencing (HITS)[195], and transposon-directed insertion-site sequencing (TraDIS)[192]. The mass scale of these studies, which will be referred to collectively as transposon insertion sequencing (TIS) studies, allows the construction of extensive lists of essential and virulence-associated genes allowing the identification of many potential drug targets.

To carry out transposon insertion sequencing accurately, a highly complex, fully saturated library of transposon mutants must first be created, in which all genes undergo insertion at multiple positions. Like the previously described screens, the mutant pool is analysed pre and post-exposure to a particular condition to identify essential and conditionally essential genes. Genomic DNA is extracted from bacteria pre and post selection as is either enzymatically[193,194] or mechanically fragmented[192,195] prior to the addition of adapters to facilitate PCR amplification of transposon/DNA junctions. Addition of adapters to cleaved fragments is generally undertaken by ligation or PCR amplification with the aim to add adapters at each transposon/chromosome junction, generating a library representative of the mutant pool[196]. Purified and amplified transposon/chromosome junctions are sequenced by NGS and mapped to the wild-type genome to locate the insertion site, as well as determine the abundance of each mutant in the pooled population[192–195] (for an overview of TIS workflow see Figure 1.7).
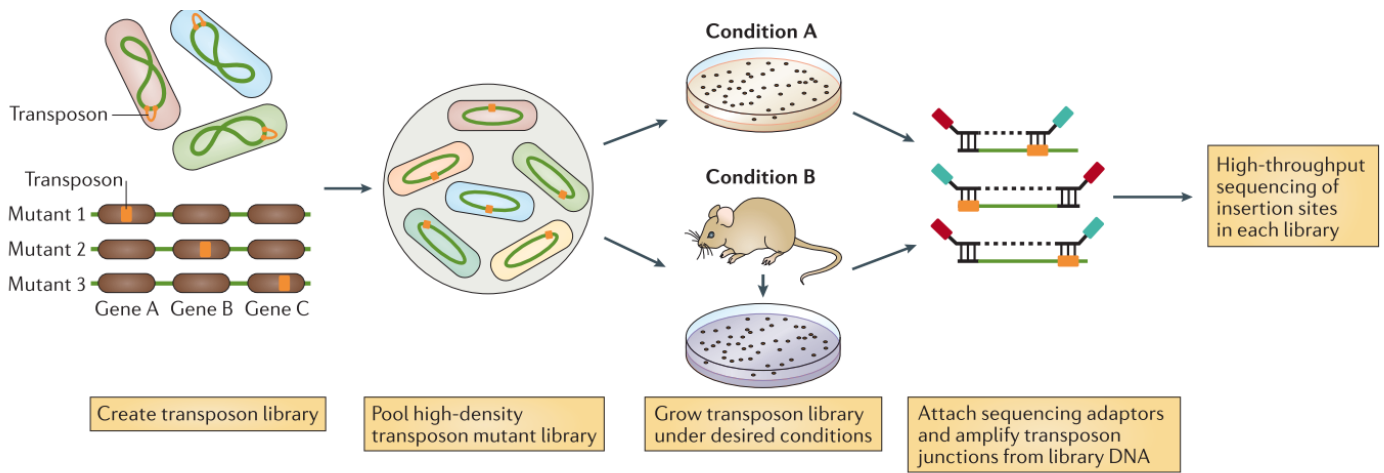
Figure 1.7. Workflow for TIS studies. A high density transposon library is created and pooled together. The library is subjected to one or more conditions and DNA is prepared to enrich for transposon-chromosome junctions prior to NGS. Figure adapted from[196].

By analysing sequencing data both prior to input and post-exposure to a biologically relevant condition in this way, digital counting can be used to determine the number of sequence reads for a particular insertion, and therefore its abundance in the population. After exposure to a particular condition, the change in frequency directly correlates to the contribution of each gene to the fitness of the organism and thus its essentiality for growth, survival or virulence, i.e. a mutant that disappears from the population is essential to the organism under the selected condition. In TIS studies, gene essentiality can be determined by analysing different insertions within a gene, which act as independent indicators. It is therefore necessary to not just have a highly saturated library, but also a library with high complexity whereby all genes have experienced multiple insertions. Essential genes can be identified from TIS data by first obtaining an insertion index by normalising the data, i.e. dividing the number of unique insertions in a gene by gene length and then graphically representing the data where genes are separated by the percentage of potential insertion sites disrupted[192,195]. Where adequate saturation of the genome has been achieved, this representation gives a clear bimodal distribution, where the leftmost peak represents genes which have undergone few insertions and are likely to be essential (as insertion impedes on the organisms growth and survival abilities) and the rightmost peak

represents genes which have undergone multiple insertions and are likely to be non-essential (as insertion does not have an adverse effect on growth and survival) (Figure 1.8).
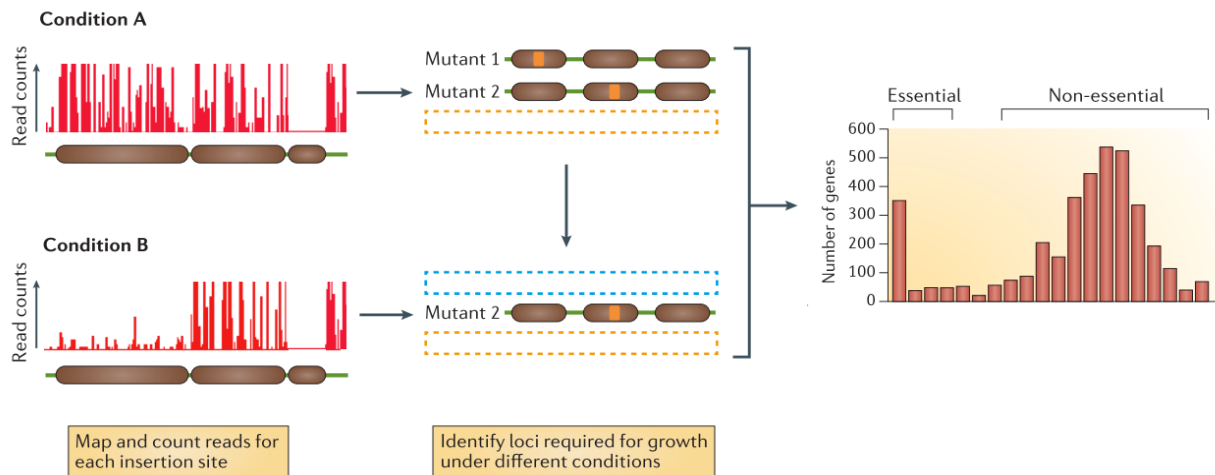
Figure 1.8. Analysis of transposon insertion sequencing data. Sequencing data is mapped to a reference genome to identify insertion sites. By dividing the number of unique insertions in a gene by gene length to generate an insertion index, and then using a histogram to plot the frequency of insertion indexes in the whole genome. Where adequate saturation of the genome has been achieved, this representation gives a clear bimodal distribution, where the leftmost peak represents genes which have undergone few insertions and are likely to be essential (as insertion impedes on the organisms growth and survival abilities) and the rightmost peak represents genes which have undergone multiple insertions and are likely to be non-essential (as insertion does not have an adverse effect on growth and survival). Figure adapted from[196].

With this approach, in the original TraDIS study, Langridge *et al.* were able to identify that 356 *Salmonella typhi* genes are essential for growth on rich media, approximately 8% of the genome[192]. In the instance where sufficient complexity has not been obtained, these peaks can overlap due to non-essential genes avoiding insertion entirely by chance or as a result of short gene length or fewer potential insertion sites, which can lead to false identification of essential genes[196].

As a result of the increasing popularity of TIS methods, an array of software has become available for improved data analysis. These include, but are not limited to: ESSENTIALS, Tn-Seq explorer, Bio-TraDIS and ARTIST[197–200]. In addition to this, databases of essential genes have been compiled and are readily available, including the database of essential genes (DEG)[201] and the online gene essentiality database[202]. Together, these developments make TIS methods more accessible to the broader scientific community and lessen the requirement for computational experience for analysis.

Theoretically, mutants in genes essential for growth and survival of the organism in the given condition will not tolerate transposon insertions, and can be identified by negative selection. In practice, some essential genes may tolerate insertions at the ends of the gene, as this can result in the formation of a functional protein. Exclusion of mutants with transposon insertions neighbouring the 3' and 5' ends of a gene is generally applied when carrying out TIS studies, as these insertions may still allow expression of a functioning protein. The cutoff point of exclusion for the four methods varies. HITs researchers report that insertions are most likely to abrogate gene function when they occur in the first 5-80% of the gene[195] whereas the IN-seq developers excluded insertions within 10% of the 3' end only[193]. The Tn-seq research group appear to be the only team to investigate this positional bias quantitatively, during which they determined that removing insertions in the first and last 10% of the gene had no effect and negligible effect respectively, concluding that adverse effects due to insertion position are a rarity[194].

When exposing a TIS library to an animal model on infection, population bottlenecks must be considered. Population bottlenecks are a confounding variable that leads to the false identification of essential genes, they arise when factors such as host immune defences cause the stochastic loss of mutants in an animal model. As a result, only a percentage of the input pool successfully colonises the model. The severity of a population bottleneck can be assessed by either carrying out colony forming unit enumeration to determine the dose of bacteria that pass host defences, or by inputting a selection of uniquely tagged bacteria with neutral fitness, where a reduction in the identified tags results solely from genetic drift[196]. The input TIS pool can then be adjusted accordingly, I.e. in the instance in which the population bottleneck is 10^6 (10^6

cells colonise regardless of the size of the input pool) an input pool containing less than 10^6 unique mutants, and 10-100 cells per mutant[194].

The application of TIS has been successful in the identification of essential genes across over 60 bacterial species[201], however it has not been performed for *C. burnetii.* It is vital to note that the identified genes can only be considered putatively essential, and only in the conditions tested. Due to the negative selection nature of the screen, there is always a chance that a given mutant is merely underrepresented in the pool, and is not truly essential. For this reason, all current TIS methods have the potential of incorrect annotation of essential genes. To categorically determine that a gene is essential, and to meet the requirements of Molecular Kochs Postulates, experimental verification must be performed.

The data that arrises from TIS studies has many applications, and has been used to (for example) identify potential targets for future antibiotic development, understand virulence mechanisms, identify candidates for live attenuated vaccines and increase understanding of how bacterial survive and resposond to stress.

Due to the computational nature of the analysis, previously constructed transposon mutant libraries can be screened with these new methods. Such an approach has been applied to data obtained from a STM screen of *Burkholderia pseudomallei* in mice. Moule *et al.* applied TraDIS to one million previously obtained transposon mutants and were able to identify many essential genes and potential drug targets without the need for further animal studies[203]. This has obvious benefits as animal studies are associated with ethical constraints, specialist housing, training requirements and high costs. TIS for drug target identification has also been applied to *Campylobacter jejuni:* by investigating three highly related strains in a variety of *in vitro* and *in* vivo growth conditions, de Vries *et al.* were able to identify 331 essential genes homologous between all three strains. Of particular interest in this study are essential genes encoding products for recognised potential drug targets, namely genes associated with flagella and fatty acid synthesis[204]. An example approach targeting the former is a combination of currently available antibiotics with single-stranded DNA, or RNA molecules termed aptamers which have been shown to have synergistic antibiotic effects against the formation of biofilms in flagella mediated motile bacteria[205]. Disruption of the fatty acid synthesis pathway is a well-established

but underutilised approach to antibiotic development. Such approach was taken to produce isoniazid, an antibiotic proven to be effective against *Mycobacterium tuberculosis* [206]. The de Vries *et al.* study[204] gives scope for further exploitation of this pathway.

Attempts to identify the minimal genome required for bacterial survival began as early as the 1950s, when Harold Morowitz began searching for the ''smallest autonomous self-replicating entity''. As DNA sequencing has developed this search has continued, and attempts have been made to determine the minimal genome with the goal to reconstruct the genome of the earliest primordial ancestral cell[207]. With the development of TIS, further contributions to this knowledge can be made. Many recent studies have contributed to the understanding of a minimal genome of different species by comparing different strains of the same organism. In addition, lists of genes essential to all strains of a given species allow the identification of potential drug targets that would allow the treatment of infection regardless of the infecting strain. For example, in a study that identified 352 essential *P. aeruginosa* genes and compared their finding to three other strains from previous studies, 141 of these essential genes were determined to be homologous within all four strains, suggesting that progress had been made towards defining the minimal genome of this pathogen. However, the small number of genes identified, coupled with the fact that the list lacks presumed essential genes including those encoding RNA polymerase and genes required for bacterial replication such as *dnaB* suggests that this list is not comprehensive[208]. A similar approach was taken by Capel *et al.*[209] who determined that 383 genes (19% of the genome) in the *Neissera meningitidis* genome are essential. Further to this, they used the DEG database[201] to compare this essential gene profile with other Gram-negative pathogens. Their findings identified 77 core essential genes shared across Gram-negative pathogens including *E.coli, H. influenzae* and *P. aeruginosa*, providing further insights into the 'minimal genome' of Gram-negative pathogens[209].

When investigating bacterial pathogenicity, it is imperative to identify factors contributing to virulence. This not only provides an insight into the bacteria's role in diseases but, as with essential genes, virulence determining genes can also be exploited to facilitate antibiotic development. TIS can be applied to identify different genes required for specific stages and sites of infection by investigating infection

relevant biological fluids. Many recent studies have adopted this approach. *N. meningitidis* is an opportunistic pathogen, found as a commensal in the epithelial cells of the nasopharynx in 8-20% of healthy individuals. By applying TIS to both human epithelial and endothelial cells, a total of 288 genes essential for colonisation were identified[209]. Of these, 108/288 genes were required for both cell types and 151 and 29 were required for colonisation of epithelial and endothelial cells, respectively. The identification of these niche-specific genes suggests that genetic requirements for *N. meningitidis* colonisation vary between cell types and provides an insight into the genetic requirements for the commensal to pathogen switch when *N. meningitidis* crosses the epithelial barrier to enter the bloodstream[209]. A similar approach was taken by Valentino *et al.*,[210] who investigated the genetic requirements for *S. aureus* infection in an array of different biological conditions. In total, they identified 426 essential genes, of these 31, 30 and 153 were required for infections of whole blood, ocular fluid and abscess formation, respectively. Of note in these finding are essential genes involved in nucleotide biosynthesis in *Staphylococcus aureus* abscesses, suggesting that free nucleotides are not abundant in this environment. Additionally, 32% (136/426) of essential genes identified in this study are previously unreported, many of which do not have a known function. This gives scope for future investigation as to whether these gene products may be potential targets of antibiotic development, as well as providing further information on the already well-studied pathogenesis of *S. aureus*[210].

1.7.   Axenic media development

Up until 2009 the requirement to propagate *C. burnetii* in cell cultures, or in embryonated eggs,[211] made genetic manipulation of the pathogen difficult. The development of an axenic (cell-free) medium was a milestone in *C. burnetii* research. By interrogating the genome sequence, using existing knowledge of the acidic phagolysosome required for intracellular replication, and metabolic profiling, a medium was developed that supports host cell free propagation of *C. burnetii*[212].

The initial media, Complex *Coxiella* Medium (CCM) sustained metabolic activity of *C. burnetii*, albeit without facilitating growth. CCM mimicked the acidic conditions of the CCV using a citrate buffer of pH 4.75 containing complex nutrient sources neopeptone, fetal bovine serum and RPMI cell culture medium, supplemented with chloride (140 mM)[213]. Transcriptome analysis later showed that *C. burnetii* incubated in CCM,

compared to bacteria replicating in Vero cells, showed significantly reduced expression of ribosomal genes suggesting insufficient protein synthesis could be contributing to the observed lack of growth. Supplementation of CCM with the protein precursors L-cysteine and casamino acids, to make acidified citrate cysteine medium (ACCM), resulted in a 13-fold increase in protein synthesis, confirming these findings. The same group investigated the *C. burnetii* genome and found genes encoding cytochrome *o* cytochrome *bd* terminal oxidases associated with aerobic and microaerobic respiration respectively. Suggesting *C. burnetii* adapts to alterations in oxygen levels during intracellular growth. Through the application of phenotype microarrays, it was determined that *C. burnetii* was potentially a microaerophile requiring conditions of 0.5% oxygen, 2.5% carbon dioxide for proliferation. Indeed when *C. burnetii* ACCM cultures were incubated in these conditions a 3-log increase in genome equivalents (GE) was observed over a 6 day period. ACCM mixed with a low concentration of agarose supported the solid culture of *C. burnetii* colonies approx. 0.05-0.1 mm in size. Later, ACCM was further modified to ACCM-2 replacing FBS with methyl-β-cyclodextrin. This development resulted in improved growth (4-5 log increase over 7 days), larger colonies on ACCM-2 agarose plates and increased viability of *C. burnetii* after extended incubations. The use of ACCM-2 media allows higher yields of *C. burnetii* to be obtained, when compared to cell lines[214]. During *in vitro* culture, *C. burnetii* has a doubling between 20 and 45 hours[68]. This discovery facilitated genetic manipulation of *C. burnetii* which was not previously possible.

1.8. Transposon mutagenesis in *Coxiella burnetii*

As an intracellular pathogen, *C. burnetii* is inherently difficult to genetically manipulate. The first successful transposon mutagenesis of an intracellular pathogen occurred in 1994, when Tam *et al.* mutated *Chlamydionis trachomatis* by electroporation[215]. The first genetic manipulation of *C. burnetii* occurred in 1996 when Suhan *et al.* developed a plasmid system to transform *C. burnetii* to ampicillin resistance[216]. However, the lack of axenic culture systems at the time resulting in an incredibly lengthy selection process, during which spontaneous ampicillin resistance emerged[216]. It was not until shortly after the development of axenic media that Beare *et al.* developed a suitable suicide plasmid system to perform transposon mutagenesis in *C. burnetii* [217]. Within the two plasmids employed in the study, one provided a *himar1* transposase. The other provided the *himar1* transposon, selective markers CAT and mCherry, encoding

a chloramphenicol resistance cassette and mCherry fluoresccent protein, respectively, which allow for selection of successful mutants, and ColE1 to allow for rescue cloning of successful *C. burnetii* mutants in *E. coli*[217]. More recently, the suicide vector pkm225 was developed[218], which permits transposon mutagenesis in *C. burnetii* using a single plasmid (Figure 1.9).
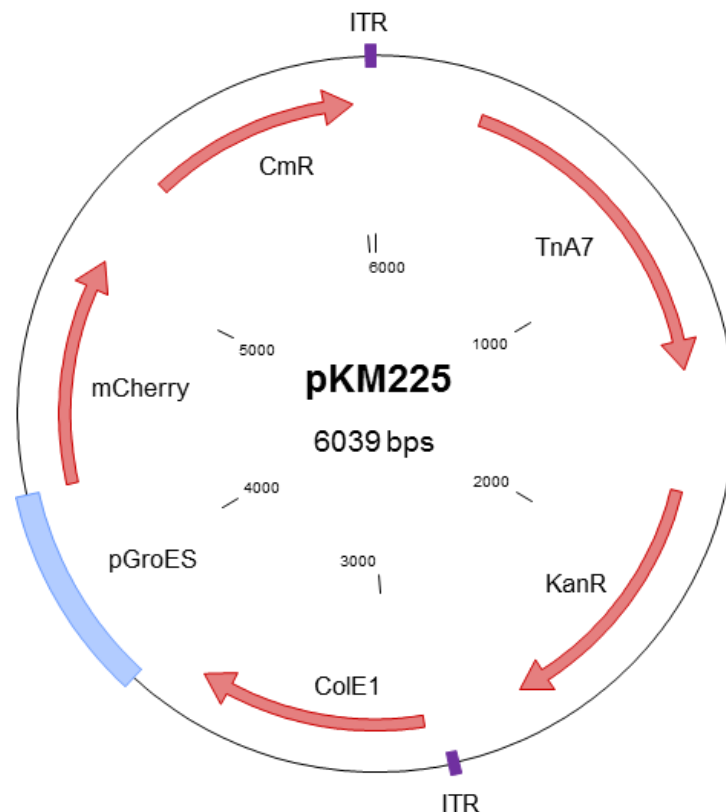
Figure 1.9. Plasmid map of suicide vector *pkm225,* which permits transposon mutagenesis in *C. burnetii.*

Transposon mutagenesis has been used to identify many genes encoding proteins that play important roles in *C. burnetii* infection. For example, transposon insertion in *ftsZ* resulted in incomplete cell division, resulting in a significant growth defect in Vero cells[217] and transposon insertion into *CBU_1260* (OmpA) resulted in a defect in host cell invasion[219]. Additionally, large screens of individual transposon mutants have been undertaken. Newton *et al.* generated a library of 3, 237 transposon mutants[51], subsequently identifying 21 genes in which disruption resulted in the absence of intracellular replication, 27 genes which had reduced intracellular replication, and seven genes which disruption resulting in a filamentous phenotype. Martinez *et al.*

determined the insertion site of 1,082 transposon mutants[219], subsequently identifying 131 genes in which transposon insertion resulting in a severe intracellular replication defect, 84 genes in which transposon insertion resulted in a severe defect in internalisation, and five genes which resulted in severe cytotoxic phenotypes. However, a whole genome transposon mutagenesis study in *C. burnetii* such as the one in this project has not been performed to date.

1.9.   Aims of this project

The main aim of this project was to generate a transposon mutant pool to carry out a TraDIS study in *C. burnetii* to identify essential genes in the axenic media ACCM2, and virulence genes in the *G. mellonella* model of *C. burnetii* infection. In parallel, it was aimed to further characterise the *G. mellonella* model for *C. burnetii* infection and develop the model for the TraDIS screen.

Chapter 2: Materials and Methods

Table 2.1. Bacterial strains and plasmids used in this study

Bacterial Strain	Description	Source
C. burnetii Nine Mile phase II clone 4 (NMII,RSA439)	Wild-type	DSTL
C. burnetii NMII::tn-*relA*	NMII with a transposon insertion in *relA*	DSTL
C. burnetii NMIIΔ*dotA*	NMII with an deletion of *dotA*	Laboratory stock
C. burnetii NMII::tn-*intergenic*	NMII with an intergenic transposon insertion	Laboratory stock
E. coli DH5α	pKMm225 storage	Kind gift from James Samuel, Texas A&M
Plasmid		
pKM225	*pMW1650, com1p-TnA7, groESp-mCherry, com1p-cat, CmR*	Laboratory stock

Table 2.2 Components of media and buffers used in this study

Media	Composition	Sterilisation
ACCM-2	1284 mg citric acid, 2370 mg sodium citrate, 250 mg potassium phosphate, 100 mg magnesium chloride, 6.6 mg calcium chloride, 1.39 mg iron sulphate, 3640 mg sodium chloride, 132 mg L-cysteine,50 mg bacto neopeptone, 1250 mg casamino acids, 500 mg Methyl-b-Cyclodextrin, 62.5 ml RPMI+glutamax, 437.5 ml Milliq water.	Filter sterilise using a 0.2 μm filter
ACCM-2-agarose	**2xACCM-2** 1284 mg citric acid, 2370 mg sodium citrate, 250 mg potassium phosphate, 100 mg magnesium chloride, 6.6 mg calcium chloride, 1.39 mg iron sulphate, 3640 mg sodium chloride, 132 mg L-cysteine,50 mg bacto neopeptone, 1250 mg casamino acids, 500 mg Methyl-b-Cyclodextrin, 62.5 ml RPMI+glutamax, 187.5 ml Milliq water. **0.5% agarose** 1.25 g ultra-pure agarose, 250 ml Milliq water.	**2xACCM-2** Filter sterilise using a vacuum and 0.22 μm filter. **0.5% agarose** Autoclave at 121°C for 15 min. Equilibrate temperature to 55°C in a water bath and combine.

LB broth	5 g peptone, 2.5 g yeast extract, 2.5 g sodium chloride, 500 ml Milliq water	Autoclave at 121°C for 15 min
LB Agar	5 g peptone, 2.5 g yeast extract, 2.5 g sodium chloride,10 g agar, 500 ml Milliq water	Autoclave at 121°C for 15 min
TAE buffer	4.84 g Tris base, 1.14 ml Glacial acetic acid, 2 ml 0.01 M EDTA, 1 litre Milliq water, pH 8.0	
TBE buffer	10.8 g Tris base, 5.5g boric acid, 4 ml 0.5 M EDTA, 1 litre Milliq water, pH 8.0	

Table 2.3. Antibiotics and compounds used in this study

Antibiotic	Diluent	Final Concentration
Chloramphenicol	Ethanol	3 µg/µl or 5 µg/µl
Kanamycin	Water	150 µg/µl or 350 µg/µl
Polymyxin B	Water	800 – 1.56 µg/ml
Hydrogen Peroxide	Water	4 – 0.003 mM
Sodium chloride	Water	16 – 0.06 mM

Table 2.4 Sequences of primers, probes and adapters used in this study

Primer	Sequence	Use
*com*1 F	5'-CGACCGAAGCATAAAAGTCAATG	GE/ml quantification
*com*1 R	5'-ATTTCATCTTGCTCTGCTCTAACAAC	GE/ml quantification
com1 probe	5'-FAM-TTATGCGCGCTTTCGACTACCATTTCA-BHQ1	GE/ml quantification
CAT F	5'-CGCCATATGGAGAAAAAAATCACTGGATATACC	Tn/ml quantification
CAT R	5'-CGCGATATCTTACGCCCCGCCCTGC	Tn/ml quantification
CAT probe	5'-FAM-CTGATGCCGCTGGCGATTCAGG-TAMRA	Tn/ml quantification
Kan F	5'-GTGCCCTGAATGAACTGCAA	NMII*ΔdotA* quantification
Kan R	5'-ATACTTTCTCGGCAGGAGCA	NMII*ΔdotA* quantification
Kan probe	5'-FAM ACGGGCGTTCCTTGCGCAGC TAMRA	NMII*ΔdotA* quantification
Adaptor 1	5'-GATCGGAAGAGCACACGTC*T	Adapter ligation
PCR 1	5'-GTGACTGGAGTTCAGACGTGTGCTCTTCCGATC*T	Adapter ligation
Himar-PCR-3	5'-AATGATACGGCGACCACCGAGATCTACACAGTCAGT TATTGGTACCCTTAAAC*G	

MPX1		
MPX2	5'-CAAGCAGAAGACGGCATACGAGAT<u>CGATGT</u>GTGACTGGAGTT*C	Multiplexing primer
MPX3	5'-CAAGCAGAAGACGGCATACGAGAT<u>TTAGGC</u>GTGACTGGAGTT*C	Multiplexing primer
MPX6	5'-CAAGCAGAAGACGGCATACGAGAT<u>ACTTGA</u>GTGACTGGA GTT*C	Multiplexing primer
MPX7	5'-CAAGCAGAAGACGGCATACGAGAT<u>TAGCTT</u>GTGACTGGA GTtC	Multiplexing primer
MPX8	5'-CAAGCAGAAGACGGCATACGAGAT<u>GATCAG</u>GTGACTGG AGTtC	Multiplexing primer
ARB1	5'- GGCCACGCGTCGACTAGTACNNNNNNNNNNGATAT	Arbitrary PCR
ARB2	5'- GGCCACGCGTCGACTAGTAC	Arbitrary PCR
ARB3	5'- GGCCACGCGTCGACTAGTACNNNNNNNNNNGACG	Arbitrary PCR
ARB4	5'- GGCCACGCGTCGACTAGTACNNNNNNNNNNACGCC	Arbitrary PCR
ARB5	5'- GGCCACGCGTCGACTAGTACNNNNNNNNNNTACNG	Arbitrary PCR
Cat-taq-F	5'- TTATACGCAAGGCGACAAGGT	Arbitrary PCR
Cat-Seq-out-2	5'- TCTGTGATGGCTTCCATGTC	Arbitrary PCR
P3	5'- TGTCGGCAGAATGCTTAATG	Sanger Sequencing
16S F	5'- TTCGGACCTCGTGCTATAAG	Transcriptomics
16S R	5'- ACTACCAGGGTCTCTAATCC	Transcriptomics
rpoB F	5'- TACCAGCTATTCTGGGTACG	Transcriptomics
rpoB R	5'- CAACCACGAACCACGATAAG	Transcriptomics
CBU_1477 F	ATTTGGGCGACTGAATGG	RT-qPCR
CBU_1477 R	AACGCACGATGTGGTTAG	RT-qPCR
CBU_2007 F	TTGGCGCTTTCCTCATTC	RT-qPCR
CBU_2007 R	TCTTGTGCTGTACCTTGAC	RT-qPCR
CBU_0231 F	AGTGCTTGAATACGTAGGTTACAG	RT-qPCR
CBU_0231 R	TTTCGCCCATGTAAACTTCTTG	RT-qPCR
CBU_1289 F	TTGGCGATGAAATACCATCCG	RT-qPCR
CBU_1289 R	TGATCGTAGGAAGCACGTTTG	RT-qPCR
CBU_1584 F	AGTTCTGACGCCACACTTTC	RT-qPCR
CBU_1584 R	ATCAATAAACATCGCGTGGAC	RT-qPCR
CBUA0015 F	AAAGCGGAGTCTCCTCAATG	RT-qPCR
CBUA0015 R	TCAGTTTCCGTTTCGGAATC	RT-qPCR
CBU_0029 F	TCATTAAAGGTGCTTACATCCTC	RT-qPCR
CBU_0029 R	TACGGTCTACCGCAATTAAATTC	RT-qPCR

CBU_1551 F	AACGCGGCTTTCGGTTAG	RT-qPCR
CBU_1551 R	TGCCTCACGCAAGGTTTC	RT-qPCR
CBU_0780 F	TTCGCATCGTTGGTGAAG	RT-qPCR
CBU_0780 R	AAACGCATGGGCAATAGC	RT-qPCR
CBU_1910 F	TATTTAACGACCCTGCATCAC	RT-qPCR
CBU_1910 R	AATGGGCAGTTCTTTGAAGAC	RT-qPCR
CBU_1222 F	AGAGTCACCGACGATCAC	RT-qPCR
CBU_1222 R	AGAATTTGCACCCGTTCCC	RT-qPCR
CBU_0410 F	AGCTATCAACGAACTCCTTAATG	RT-qPCR
CBU_0410 R	TGTTCTAGCCGAATTTACTTCAG	RT-qPCR
CBU_1626 F	TAACGGCGGTTATTGCAG	RT-qPCR
CBU_1626 R	TGCTCATCATCTCAGGATCAG	RT-qPCR
CBU_1375 F	TCCTACCGTTACCCAATCTG	RT-qPCR
CBU_1375 R	TGCGAACATCGTCTACCATC	RT-qPCR
CBU_1648 F	ATAGGCTCAATGAAGGCATTATC	RT-qPCR
CBU_1648 R	ACGTCTTGCAACAAAGAATAACC	RT-qPCR
CBUA0006 F	TTTGCTAGAGGCGATGTAAC	RT-qPCR
CBUA0006 R	AGAAAGGGTGTAAGCAATCC	RT-qPCR
CBU_1891 F	TTATCGCCCTCTACCCAAG	RT-qPCR
CBU_1891 R	AGTCTGCTCCTCACGAATC	RT-qPCR
CBU_0469 F	TACACAGACGCCGTTGATG	RT-qPCR
CBU_0469 R	TTTCGCCCACAGACAACTC	RT-qPCR
CBU_1643 F	AAATGGCTATTCATCCCAAGG	RT-qPCR
CBU_1643 R	TTCCGCAATAAAGGCTCAATC	RT-qPCR
CBU_16S F	AAACCCTGATCCAGCAATG	RT-qPCR
CBU_16S R	TGCTTCTTCTGTGGGTAAC	RT-qPCR

Table 2.5. Immunomodulatory compounds used in this study

Compound	**Solvent**	**Description**	**Final Concentration**
Dexamethasone	DMSO	Active compound	200 µg/ml
Dexamethasone 21-phosphate	Water	Dexamethasone Pro-drug	2 mg/ml

Dexamethasone acetate	Acetone	Dexamethasone Pro-drug	2 mg/ml

2.1. Bacterial strains and culture conditions

2.1.1. *C. burnetii* strains

C. burnetii strains used in this study are listed in Table 2.1. For liquid cultures, bacteria were grown in either pre-formulated (Sunrise Science Products) or homemade ACCM-2 (See Table 2.2. for components) in 1ml, 6ml or 25ml volumes in 12 well plates, T25 tissue culture flasks (Nunc EasyFlask, Thermo Scientific) or 250ml disposable, vented Erlenmeyer flasks (Corning® , Sigma Aldrich), respectively. To obtain colonies, bacteria were plated onto ACCM-2-agarose plates (See Table 2.2 for components). Cultures were incubated statically at 37°C in an anaerobic workstation (Don-Whitley Scientific) fitted with a microaerophilic gas mix (2.5% O_2, 5% CO_2) or in bio boxes containing GENbox microaer sachets (BioMérieux) for 7 days (liquid cultures) or 14 days (agarose plates). Where appropriate, antibiotics were added to media (see Table 2.1.). All manipulations of *C. burnetii* NMII were carried out in a class I microbiological safety cabinet in a Biological Safety Level 2 (BSL2) laboratory.

2.1.2. E. coli strains and plasmids

A glycerol stock of *E. coli* DH5α harbouring transposon plasmid pKMm225 (accession # HQ386859) was grown overnight at 37°C on Luria Bertani (LB) agar plates or in LB broth (See Table 2.2 for components). Liquid cultures were incubated with agitation.

2.2. *C. burnetii* growth curves

100 µl of a standardised NMII glycerol stock (10^6 GE/ml) was used to inoculate 25 ml of ACCM-2 medium and incubated as described. On days 0, 1, 4, 5, 6 and 7, samples were taken to measure optical density (OD_{600nm}), colony forming units (CFU/ml) and genome equivalents (GE/ml).

To obtain ODs, 1 ml of culture was removed and absorbance read using a Jenway 6705 UV/Vis spectrophotometer (Jenway) at 600 nm. For CFU/ml enumeration, 100 µl of culture was serially diluted in ACCM-2 medium, spot plated in 10 µl aliquots onto ACCM-2 agarose plates, and enumerated after 14 days incubation. To quantify GE/mL, 100 µl culture was added to 900 µl instagene matrix (Bio-rad laboratories),

heated (99°C, 15 min, shaking at 750 RPM) and centrifuged (10,000 RPM, 3 min). Supernatant was used as template DNA for quantitative PCR (qPCR) to determine GE/ml.

2.2.1. Quantification of genome equivalents

GE/ml was determined by qPCR targeting the *com1* housekeeping gene (for primer sequences see Table 2.4.). qPCR samples were comprised of 12 μl template DNA, 2.16 μl *com1* forward primer (900 nM), 0.72 μl *com1* reverse primer (300 nM), 0.48 μl *com1* probe (10 μM) and 6 μl master mix (containing 8% glycerol, 50 mM Tris.HCl pH 8.8, 0.05 mM EGTA, 1 μg/μl BSA, 0.2 mM dNTP nucleotides, 4 mM magnesium chloride and 0.04 U/μl JumpStart *Taq* DNA polymerase). Samples were analysed on a qPCR SmartCycler (Cepheid Inc) using the following cycling conditions

$$
\begin{array}{ll}
\text{3min} & \text{95°C} \\
\text{30sec} & \text{60°C} \\
\text{15sec} & \text{95°C} \\
\text{30sec} & \text{60°C}
\end{array} \Big\} \text{x50}
$$

ct values were converted to GE/mL using the following equation

$$\text{GE/12μl sample} = 10^{((Ct-36.051) \div -3.227)}$$

$$\text{GE/ml} = (\text{GE/12μl} \div 12) \times 1000$$

2.2.2. Calculation of mean generation times

Generation times were calculated during the exponential phases of growth in ACCM-2 (day 1 – 4 post inoculation) or in *G. mellonella* (day 1-2 post infection) using the following formula:

$$Generation\ time = duration * \log(2) \div \log(final\ concentration) - \log(initial\ concentration)$$

2.3. Whole genome sequencing of *C. burnetii*

Whole genome sequencing of *C. burnetii* was performed by Exeter Sequencing Service. 3 μg of genomic DNA was submitted for sequencing as 250 bp paired end reads on an Illumina MiSeq platform. Sequence reads in fastq format were mapped to the *C. burnetii* RSA493 reference genome (accession no. NC_002971) or the *C. burnetii* RSA439 NMII genome (accession no. CP020616) using Burrows-Wheeler

Aligner[220]. Samtools[221] rmdup was applied to remove PCR duplicated reads and flagstat to obtain mapping statistics. Bcftools was used to identify Single nucleotide polymorphisms (SNPs) and insertions/deletions (Indels). Quality control on sequencing data was performed using FastQC[222] and qualimap[223].

2.4. *G. mellonella* model of *C. burnetii* infection

2.4.1. *G. mellonella* storage

Standardised sixth- instar larvae of the greater wax moth *G. mellonella* (TruLarv^{TM}) were purchased from Biosystems Technology Ltd and stored on wood shavings in the dark at 15°C to prevent pupation. All larvae were used within 1 week of delivery and excluded if there was evidence of melanisation.

2.4.2. Inoculation of *G. mellonella*

For inoculation of *G. mellonella,* groups of 10 larvae were injected through the upper left pro-leg using a 250 µl (10 µl dose) or 25 µl (1 µl dose) Hamilton syringe fitted with a repeating dispenser. Larvae were secured with forceps to prevent needle-stick injury (see Figure 2.1.). Post inoculation, larvae were kept in petri dished lined with 0.45 mm Whatmann filter paper and incubated at 37°C inside boxes with vented lids. No-stab and PBS inoculated controls were included in all experiments. Larvae were considered dead when no movement occurred after stimulation with a pipette tip. Statistical analysis was performed by the log rank (Mantel-Cox) method using GraphPad Prism version 8.3.1 for Windows.

2.4.3. Infection of *G. mellonella* with *C. burnetii*

C. burnetii was adjusted to OD_{600} 0.2 in PBS, equal to 1×10^8 GE/ml, and the adjusted cell suspension was quantified by qPCR targeting *com1* (see section 2.2). To determine the optimum dose, larvae were injected with 10 µl of *C. burnetii* at variable doses from $10^2 – 10^6$ GE/larvae and survival was monitored daily for 12 days. For all further experiments, larvae were injected at a dose of 10^6 GE/larvae and survival was monitored daily for 8 days.
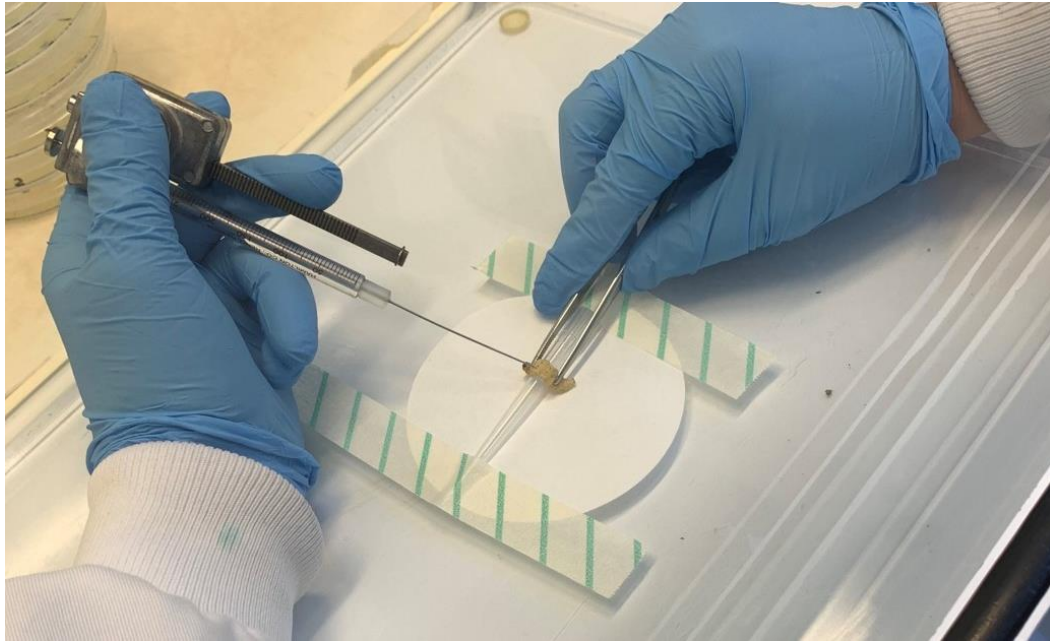
Figure 2.1. Hands free inoculation of *G. mellonella*

2.4.4. *In vivo* colonisation assay - *G. mellonella* haemocytes

At daily time points post infection, haemocytes were extracted from infected larvae. For this, five larvae were placed on ice for 10 minutes to prevent movement. The bottom 2 mm of the larvae was aseptically removed using scissors and the larvae were placed over a micro centrifuge tube to drain. Haemolymph was pooled and 100 µl was centrifuged at 500 xg, 4°C, for 5 minutes to separate haemocytes. The cell pellet was washed and re-suspended in 100 µl sterile PBS. To determine GE/mL of haemocytes, 100 µl of haemocyte suspension was used for qPCR targeting *com1* as described in section 2.2.

2.4.5. Visualisation of *C. burnetii* within haemocytes by confocal microscopy

For visualisation of infected haemocytes by confocal microscopy, haemolymph was extracted from groups of 10 larvae on days 1-3 post infection as described in section 2.3.4. Haemolymph was centrifuged at 500 x G for 5 minutes to pelleted haemocytes, followed by three washes in sterile PBS to remove haemolymph. Haemocytes were re-suspended in 4% paraformaldehyde and allowed to fix for 10 minutes at room temperature, followed by a further three washes followed by re suspension in sterile PBS to remove paraformaldehyde. Haemocytes were placed on glass coverslips cleaned with 70% ethanol and allowed to dry prior to mounting on glass microscope slides using ProLong Gold Antifade with DAPI (Thermofisher). Fixed haemocytes were

visualised as Z-stacks with a Zeiss LSM 880 microscope with Airyscan using a C-Apochromat 40x objective. mCherry images were taken using a He 543 laser, DAPI images were taken using a Blue diode later. Images were processed in Zen Blue software.

2.4.6. Visualisation of *C. burnetii* within haemocytes by transmission electron microscopy

Haemocytes were visualized with a Jeol JEM-1400 transmission electron microscope by the University of Exeter Bioimaging Unit. On day's 1 - 3 post infection, haemolymph was extracted from groups of 10 larvae as described in section 2.3.4. into a sterile micro centrifuge tube containing a couple of granules of phenolphetourea to prevent melanisation. Haemocytes were fixed overnight with 2% glutaraldehyde, 2% paraformaldehyde, and 0.1 M sodium cacodylate pH 7.2 before embedding in 2% agarose. Duplicate 10 minute washes were performed with 0.1 M sodium cacodylate pH 7.2 before post-fixation with 1% osmium tetroxide, reduced with 1.5% potassium ferrocyanide in 0.1 M sodium cacodylate pH7.2. Fixed samples were dehydrated with a crescent gradient of ethanol prior to embedding overnight in a durcupan resin. Samples were polymerized in the oven at 60º C for 24 hours prior to visualisation.

2.4.7. Processing *C. burnetii* and *G. mellonella* for transcriptomics

Bacterial cells from 10 ml of a 7 day culture of *C. burnetii* were collected by centrifugation at 4,000 RPM for 10 minutes, re-suspended in 1 ml TRIzol® Reagent (Invitrogen), frozen at -80°C and used as a reference transcriptome.

Control larvae and three groups of 30 larvae were processed at 1 and 2 days post-infection and three groups of 10 larvae were processed at 3 and 4 days post-infection. At each time point, haemolymph was aseptically removed from larvae as described in section 2.3.4. Haemocytes were re-suspended in 1 ml TRIzol® Reagent and frozen at -80°C.

2.4.8. RNA extraction and RNA sequencing (RNA-Seq) for transcriptional studies.

RNA extraction, sequencing and analysis was performed by Dr Andrea Kovacs-Simon. Samples stored frozen in TRIzol® Reagent were thawed and total RNA (total eukaryotic and total prokaryotic RNA) was extracted using the Direct-zol™ RNA

MiniPrep Kit (Zymo Research). Contaminating DNA was digested by DNAse I treatment (Ambion), which was confirmed by PCR using the 16S-F and 16S-R primer pair (for primer sequences see Table 2.4).

Presence of *C. burnetii* mRNA in the DNA-free total RNA extract was confirmed by reverse transcriptase PCR using the Qiagen OneStep RT-PCR kit and both *com1* and *rpoB* primer pairs (for primer sequences see Table 2.4). RNA integrity number (RIN) score and concentration of the extracted RNA was determined using an Agilent 4200 TapeStation System. Five micrograms of RNA isolated from infected larvae, and 2 µg RNA isolated from bacterial culture (both in triplicate) was further processed. Eukaryotic mRNA was depleted from the samples extracted from infected *G. mellonella* using TruSeq mRNA stranded (oligo-dT) beads (TruSeq RNA Library Preparation Kit v2, Illumina). The depleted RNA (eukaryotic rRNA and total bacterial RNA) as well as the total *C. burnetii* RNA isolated from bacterial culture (bacterial rRNA and bacterial mRNA) was then enriched for bacterial mRNA using the riboPOOL Human:Pan-prokaryote or the riboPOOL Pan-prokaryote kits, respectively (Cambridge Bioscience). RNA-Seq libraries were prepared using the Illumina TruSeq Stranded mRNA Library Prep Kit according to the manufacturer's protocol. The concentration, quality and integrity of the libraries were analysed using the Agilent 4200 TapeStation System.

Sequencing was performed at the University of Exeter Sequencing Facility using an Illumina HiSeq System benchtop sequencing instrument to produce paired end reads 125bp in length. Reads from RNA-Seq were mapped to the *C. burnetii* strain RSA493 genome (GCA_000007765.2_ASM776v2) using Tophat[224]. Cufflinks[225] was used for transcript assembly of individual samples. All assemblies were merged to create a reference transcript, which was used to quantify transcript expression using Salmon[226]. DESeq[227] was then used to find differentially expressed genes. Transcripts with a *p*-value < 0.05 and more than 2-fold differential expression were considered significantly expressed.

To validate the RNA-Seq data, 1 µg of total RNA isolated from *C. burnetii* grown in culture and from *G. mellonella* at 4 days post-infection was reverse transcribed to generate cDNA using random hexamers and the Superscript III Reverse Transcriptase

Synthesis System (Invitrogen) according to the manufacturer's recommendations. qPCR was performed with primers annealing to internal regions of the target genes (See table 2.4 for primer sequences) using SYBR™ Green PCR Master Mix (Applied Biosystems) on a QuantStudio 6 Flex Real-Time PCR System (Applied Biosystems). Data was obtained through QuantStudio Real-Time PCR Software v1.3. Relative mRNA abundances were calculated by the following equation using the 16S rRNA gene to normalize the results:

$$Ratio = \frac{Efficiency\ (target)^{CT(target,untreated)-CT(target,\ treated)}}{Efficiency\ (ref)^{CT(ref,untreated)-CT\ (ref,treated)}}$$

2.4.9. Population bottleneck determination

An inoculum was prepared by spiking *C. burnetii* NMII at 10^8GE/ml with two different mutants, NMII::Tn-intergenic and NMIIΔ*dotA,* at a ratio of 100:1 wildtype: mutants. Larvae were infected as described in section 2.3.2 and the inoculum was quantified by qPCR as described in section 2.2.1 using primer pairs *com1,* CAT and *KanR* for NMII, NMII::Tn-intergenic and NMIIΔ*dotA* respectively (for primer sequences see Table 2.4). At four days post infection, haemocytes were harvested and genome equivalents quantified as described in section 2.3.4.

2.5. Development of an immunosuppressed *G. mellonella* model of *C. burnetii* infection

2.5.1. Solvent toxicity testing in *G. mellonella*

Groups of 10 *G. mellonella* larvae were injected with 10 µl ethanol or acetone, at concentrations of 75%, 50% and 25% (v/v in sterile water) or 1 µl neat dimethyl sulfoxide (DMSO) or acetone as described in section 2.3.2. Survival was monitored daily for a total for four days.

2.5.2. Drug toxicity testing in *G. mellonella*

Groups of 10 *G. mellonella* larvae were injected with 10 µl dexamethasone 21-phosphate or dexamethasone acetate or 1 µl dexamethasone at a dose of 200 µg/larvae (see Table 2.5. for details of stock solutions). Survival was monitored daily for a total for four days.

2.5.3. Pre-treatment of *G. mellonella* with dexamethasone 21-phosphate and dexamethasone prior to NMII infection

Larvae were infected with various concentrations (50 -200 µg/larvae) of drug in a volume of 10 µl for dexamethasone 21-phosphate or 1 µl for dexamethasone into the lower right proleg 10 minutes prior to infection with NMII or NMII::tn-*relA* (200 µg dose only) at 10^6 GE/larvae as described in section 2.3.3. Control groups were PBS + PBS, PBS + NMII and DMSO + NMII. Survival was monitored daily for a total for four days.

2.5.4. HPLC determination of dexamethasone 21-phosphate and dexamethasone in G. mellonella

High performance liquid chromatography (HPLC) was performed with the following settings: C-18 silica ultrasphere 4.6 mm x 4.5 cm column fitted with a C-18 column guard; mobile phase 10 mM potassium phosphate: acetonitrile (50:50, pH 7); isocratic flux; wavelength 240 (UV); flow rate 1.5 ml/min; injection volume 10 µl; run time 6 mins. For standards and samples, haemolymph was harvested as described in section 2.3.4 and diluted 1:5 in 60% acetonitrile (v/v) containing 1.2 µg/ml prednisolone as an internal standard. Standards were spiked with dexamethasone 21-phosphate and dexamethasone at known concentrations ranging from 20 µg/ml – 156 ng/ml. For samples, larvae were injected with dexamethasone 21-phosphate at 200 µg/larvae 10 minutes prior to haemolymph harvest. 3 larvae were pooled for each time point.

2.6.   Transposon mutagenesis of *C. burnetii*

2.6.1. Plasmid Extraction

E. coli DH5α harbouring pKM225 was inoculated into LB broth containing kanamycin at 50µg/ml and incubated overnight at 37°C, shaking at 200 rpm. Purification of pKM225 was performed using the HiSpeed Plasmid Midi Kit (Qiagen) following the manufacturer's instructions. Plasmid DNA was concentrated by ethanol precipitation and DNA concentration was determined using Nanodrop.

2.6.2. Preparation of electrocompetent *C. burnetii*

Electrocompetent *C. burnetii* was also prepared. For this, 25 ml of 7 day old cultures were pelleted by centrifugation at 4°C for 15 minutes at 4,000 rpm. The cell pellet was washed twice in ice-cold, sterile-filtered 10% glycerol before resuspension in 50 µl ice-cold 10% glycerol per 25 ml culture. Electrocompetent cells were used on the day of preparation.

2.6.3. Electroporation

10 µg pKM225 (for details see Table 2.6) or water for mock was added to 50 µl electrocompetent *C. burnetii* and transferred to a precooled 0.1 cm Gene pulser electroporation cuvette (Bio-Rad Laboratories). Electroporation was performed with an ECM630 electroporator (BTX Harvard Apparatus) at 1.8 kV, 500 Ω, 25 uF. Immediately after electroporation, 950 µl RPMI-glutamax was added to cuvettes. 500 µl of sample was used to inoculate 6 ml ACCM-2 medium in duplicate. Cultures were incubated overnight, before the addition of chloramphenicol, followed by a further four days of incubation.

To determine CFU/ml, samples were plated onto ACCM-2 agarose plates containing chloramphenicol and incubated as described. Remaining cultures were stored at -80°C until further use. CFU/ml determinations were used to obtain the dilution factor required to yield approximately 500 colonies per 100 µl and glycerol stocks of electroporations were plated as such. After 14 days incubation, 60 individual colonies were sub-cultured into 1 ml ACCM-2 medium inside 12-well plates with chloramphenicol and incubated for a further 7 days before storage at -80°C until further use. The remaining colonies were washed from the plate and pooled. 100 µl was used to inoculate triplicate 25 ml ACCM-2 cultures for qPCR confirmation of transposon mutants and TraDIS library preparation. The remaining culture was stored at -80°c (for a visual representation of the transposon mutagenesis method see Figure 2.2).
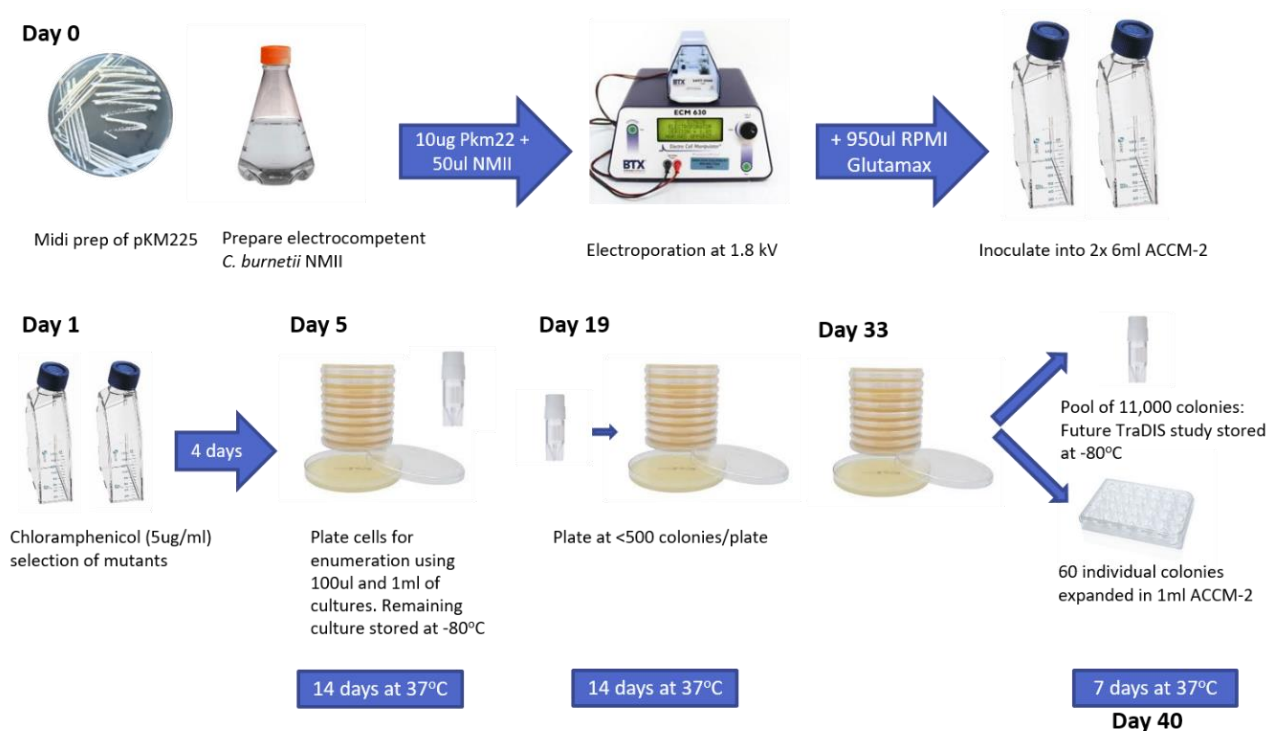
Figure 2.2. Transposon mutagenesis workflow. 10 µg pKM225 was electroporated in 50 µl electrocompetent *C. burnetii* at 1.8 kV. Immediately after electroporation 950 µl RPMI was added to cuvettes to aid recovery. 500µl of electroporated cell suspension was inoculated into duplicate 6 ml ACCM-2 broths and incubated overnight prior to the addition of chloramphenicol at 5 µg/ml. After 4 days of outgrowth electroporated cultures were enumerated by plating out 100 µl neat culture and 100 µl 10x culture, remaining culture was stored at -80°C until further use. CFU/ml determinations were used to obtain the dilution factor required to yield approximately 500 colonies per 100 µl and glycerol stocks of electroporations were plated as such. After 14 days incubation, 60 individual colonies were sub-cultured into 1 ml ACCM-2 medium inside 12-well plates with chloramphenicol and incubated for a further 7 days before storage at -80°C until further use. The remaining colonies were washed from the plate and pooled. 100 µl was used to inoculate triplicate 25 ml ACCM-2 cultures for qPCR confirmation of transposon mutants and TraDIS library preparation. The remaining culture was stored at -80°c.

2.6.4. Input of mutant pools to *G. mellonella*

To create sub-pools of 1,000 colonies for screening of transposon mutant pools in *G. mellonella,* stocks of *C. burnetii* transposon mutants generated in section 2.6.3. were plated and incubated as described. Pools of mutants were created by washing approximately 1,000 colonies from the plate which were stored as glycerol stocks at -80°C. To infect *G. mellonella* stocks were used to inoculate 25 ml ACCM-2, which was incubated as described. After 7 days of incubation the culture was adjusted to 10^8 GE/ml (confirmed by qPCR as described). Three groups of 10 larvae were injected per pool at a dose of 10^6 GE/larvae as described. In addition, three 25 ml ACCM-2 cultures were inoculated and incubated as described, on day 7 gDNA was extracted (input pool). After 3 days of incubation, haemocytes from infected larvae were harvested as described, and subjected to three freeze-thaw cycles to lyse haemocytes. Lysed haemocytes were plated at a concentration to yield < 500 colonies a plate (as determined by *in vivo* colonisation assay). After 14 days of incubation colonies were washed from the plate and used to inoculate 3 x 25 ml ACCM-2 cultures which were incubated as described. The remaining culture was stored at -80°C. After 7 days of incubation gDNA was extracted (output pool).
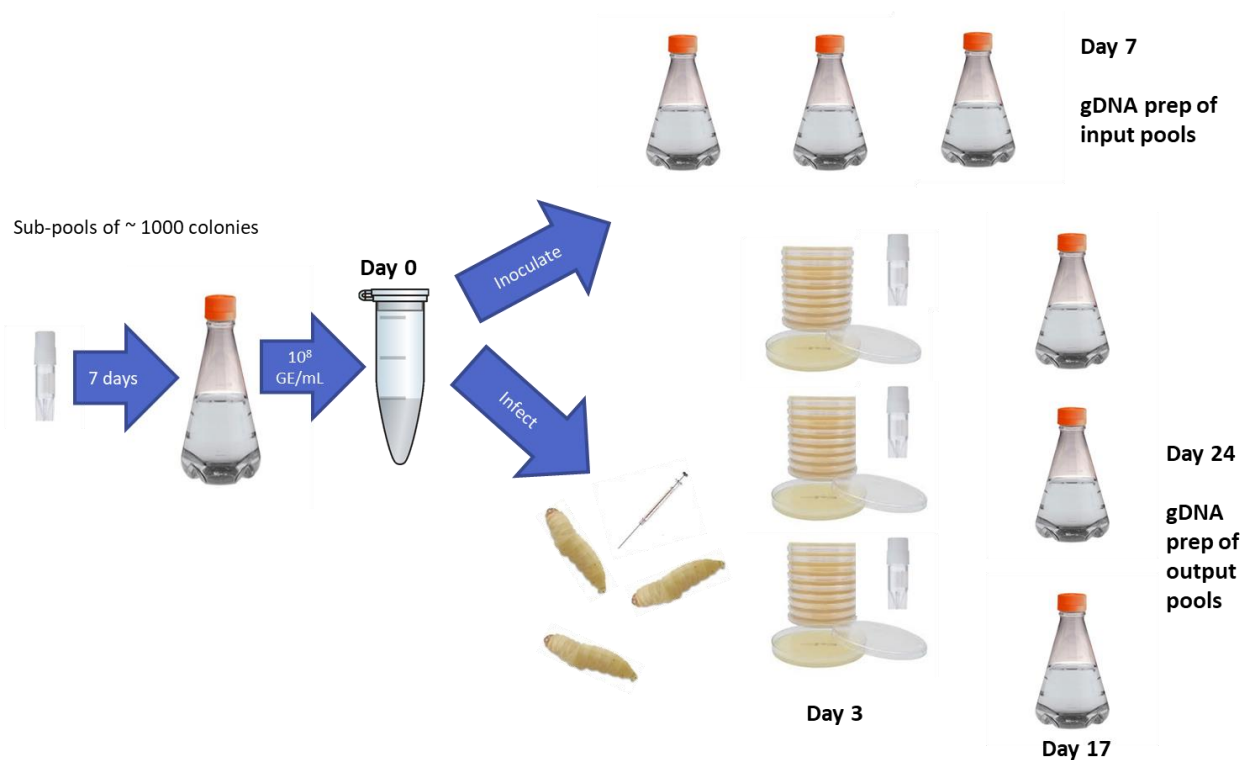
Figure 2.3 Input of sub-pools of *C. burnetii* transposon mutants into *G. mellonella* larvae. Three groups of 10 larvae were injected at a dose of 10^6 GE/larvae with sub-pools of 1,000 colonies. In addition, three 25 ml ACCM-2 cultures were inoculated, on day 7 gDNA was extracted (input pool). After 3 days of incubation, haemocytes from infected larvae were harvested, and subjected to three freeze-thaw cycles to lyse haemocytes. Lysed haemocytes were plated at a concentration to yield < 500 colonies a plate. After 14 days of incubation colonies were washed from the plate and used to inoculate 3 x 25 ml ACCM-2 cultures. After 7 days of incubation gDNA was extracted (output pool).

2.6.5. qPCR confirmation of transposon mutagenesis

To confirm the success of the transposon mutagenesis, qPCR was performed on 16 of 60 individually sub cultured mutants. 100 µl of culture was added to 900 µl instagene matrix and heated in a thermocycler to 99°C shaking at 750 rpm for 15 minutes before centrifugation to pellet cell debris. The resulting supernatant was used for a qPCR targeting *com1* as above, to determine total GE/ml. A further qPCR was performed targeting CAT, a chloramphenicol acetyltransferase encoded on pKM225, to enumerate transposon mutants (for primer sequences, see Table 2.4) using the same components and cycling conditions.

2.7. Characterisation of individual transposon mutants

2.7.1. Arbitrary PCR

Individual transposon mutant stocks were thawed and 100 µl culture was added to 900 µl instagene matrix (Bio-rad laboratories), heated (99°C, 15 min, shaking at 750 RPM) and centrifuged (10,000 RPM, 3 min). Supernatant was used as template DNA for arbitrary PCR to identify the transposon insertion site (see Figure 2.2). Arbitrary PCR was performed by mixing 2.5 µl template DNA with 2.5 µl of 10 µM degenerate primer ARB1, ARB3. ARB4 or ARB5, 2.5 µl 10 µm primer Cat-Taq-F (for primer sequences see table 2.4), 5 µl 5x Phusion HF Buffer, 0.5 µl 10 mM dNTPs, 0.5 µl Phusion High-Fidelity DNA Polymerase (New England Biolabs Inc.) and 11.5 µl nuclease free water. PCR was performed using the following conditions:

10min	98°C	
10sec	98°C	
30sec	30°C	} x 6 cycles
2min	72°C	
10sec	98°C	
30sec	45°C	} x 30 cycles
2min	72°C	
7min	72°C	

A second round of PCR was performed by mixing 2 µl of each PCR product with 5 µl of 10 µM primer ARB2, 5 µl 10 µm primer Cat-Seq-Out-2 (for primer sequences see Table 2.4), 10 µl 5x Phusion HF Buffer, 1 µl 10 mM dNTPs, 1 µl Phusion High-Fidelity DNA Polymerase and 26 µl nuclease free water. PCR was performed using the following conditions:

10min	98°C	
10sec	98°C	
30sec	45°C	} x 35 cycles
2min	72°C	
7min	72°C	

2.7.2. Agarose gel electrophoresis

PCR products were separated on a 1.5% agarose gel (w/v). Agarose gels were prepared by adding 1.5 g of agarose to 100 ml TAE buffer (see table 2.2 for compositions) and heating until dissolved. 5 μl of Midori green advance DNA stain (NIPPON Genetics Europe) was added to aid DNA visualisation. 6 x loading dye (Thermo Fisher Scientific) was added to samples at a final concentration of 1 x prior to loading and DNA was resolved by electrophoresis at 100 V for 30 minutes. Samples were compared to a GeneRuler 1kb plus DNA ladder. Gels were imaged on a ChemiDoc XRS+ system (Bio-Rad Laboratories) and visualised using Quantity One software.

Unique bands were excised with a clean scalpel and a gel extraction was performed using the MinElute Gel Extraction kit (Qiagen) following the manufacturer's instructions.

2.7.3. Sanger sequencing

DNA concentration of gel extracted samples was determined by nanodrop. 5 ng of DNA was submitted for sanger sequencing by Eurofins Genomics using primer P3 (for primer sequences see Table 2.4). Resulting reads were analysed in BioEdit[228], to confirm transposon presence. The transposon sequence was trimmed, and the resulting transposon insertion site was determined by BlastN against the *C. burnetii* NMI RSA439 reference genome. The insertion site was then visualised in Artemis[229].

2.8. TraDIS library preparatin

2.8.1. Genomic DNA extraction

Genomic DNA (gDNA) was extracted from 25 ml 7 day old cultures using the GenElute Bacterial Genomic DNA Extraction kit (Sigma-Aldrich) following the protocol for Gram-positive bacteria with slight modification. Cultures were centrifuged for 15 minutes at 4,000 rpm and resuspended in 760 μl gram positive lysis solution before separating into 4x 190 μl aliquots to process in 4 columns. The protocol was then followed with an extended 16 hour step in lysis solution and proteinase K. DNA was concentrated by ethanol precipitation and pooled for each 25 ml culture.

2.8.2. Fragmentation of gDNA

5 μg of gDNA was fragmented by ultra-sonication in a COVARIS E220 focused-ultrasonicator. Sample volumes were made up to 130 μl with Qiagen EB buffer and placed in AFA fiber crimp-cap microtubes. Sonication was performed at a peak incident power of 140 watts for 55 seconds.

2.8.3. Size selection of fragmented gDNA

Small (<150 nt) fragments of gDNA were removed using the GeneRead Size Selection Kit (Qiagen) following the manufacturer's instructions. gDNA fragments were eluted in 50 μl EB buffer.

2.8.4. End-repair

gDNA fragments were end-repaired using the NEBNext® DNA Library Prep Master Mix Set for Illumina® (New England Biolabs) following the manufacturer's instructions. Clean up steps were performed using the QIAquick PCR purification kit (Qiagen) following the manufacturer's instructions. Samples were eluted in 35 μl EB buffer.

2.8.5. A-tail addition

End-repaired samples were A-tailed using the NEBNext® DNA Library Prep Master Mix Set for Illumina® (New England Biolabs) following the manufacturer's instructions. Clean up steps were performed using the MinElute PCR purification kit (Qiagen) following the manufacturer's instructions. Samples were eluted in 22 μl EB buffer.

1 μl of sample was quantified on a DNA7500 chip (Agilent Technologies) using a BioAnalyser (Agilent Technologies) to get sample concentration and mean fragment size required for adapter ligation.

2.8.6. Adapter annealing

To phosphorylate and anneal adapters, 100 μM each of adapter-1 and PCR-1 (for adapter sequences see Table 2.4) were combined with 5μl T4 polynucleotide kinase (10 U/μl, New England Biolabs) and 5 μl T4 DNA ligase buffer. Adapters were annealed in a thermal cycler heated to 37°C for 30 seconds before ramping up temperature at +0.5°C per second to 97°C. Samples were maintained at 97.5°C for

155 seconds and then cooled at a rate of -0.1ºC every 5 seconds to 20ºC. Phosphorylated annealed adapters were stored in aliquots at -20°C.

2.8.7. Adapter ligation

The volume of adapters required was calculated using the following equation:

$$x = \frac{Adapter\ excess \times A-tailed\ DNA\ concentration\ \times A-tailed\ DNA\ volume \times 25}{650\ \times mean\ fragment\ size}$$

The volume of 2 x ligation buffer was calculated using the following equation:

$$y =\ A-tailed\ DNA\ volume + adapter\ volume + 5\ (ligase\ volume)$$

17.5 µl A-tailed DNA, x µl annealed adapters, y µl 2 x ligation buffer (NEB) and 5 µl ligase were combined and incubated at room temperature for 15 minutes. Adapter ligated samples were cleaned up using the MinElute PCR purification kit (Qiagen) following manufacturer's instructions. Samples were eluted in 30 µl EB buffer and stored at -20ºC.

2.8.8. Parallel PCR

Parallel PCR was performed by mixing 10 µl adapter-ligated DNA with 50 µl NEBNext Q5 Hot Start HiFi PCR Master Mix, 39 µl nuclease-free water and 0.5 µl each of 100 µM primers Himar-PCR-3 and one of three custom Illumina primers MPX1-3 (for primer sequences see Table 2.4). Each sample was separated into 2x 50 µl aliquots and PCR was performed on the following thermal profile:

2 min	98ºc
10 sec	98ºc
30 sec	57ºc
30 sec	65ºc
5 min	65ºc

} x20 cycles

At the end of the reaction, aliquots were re-pooled and PCR contaminants removed with a 2 column clean-up using the Generead Size Selection kit (Qiagen).

2.8.9. Size selection by agarose gel electrophoresis

A 2% agarose gel (w/v) was prepared by adding 1.6 g of agarose to 80 ml TBE buffer (See table 2.2 for composition) and heating until dissolved. 4 µl of Midori green advance DNA stain was added to aid DNA visualisation. 6x loading dye was added to samples at a final concentration of 1 x prior to loading and DNA was resolved by electrophoresis at 60 V for 70 minutes. Samples were compared to a GeneRuler 100 bp plus DNA ladder.

2.8.10.　　Gel extraction

350-500 nt fragments were excised using a clean scalpel and DNA was extracted using the MinElute Gel Extraction kit (Qiagen) following the manufacturer's instructions. Samples were eluted in 17 µl EB buffer. 1 µl of sample was quantified on a DNA7500 chip (Agilent Technologies) using a BioAnalyser (Agilent Technologies) to get sample concentration and mean fragment size required for adapter ligation.

2.9.　Sequencing of TraDIS library

Samples were diluted to 2 nM and submitted for sequencing as 150 bp single end reads on an Illumina MiSeq platform (Exeter Sequencing Service).

2.9.1. TraDIS data analysis – BioTraDIS pipeline

Illumina MiSeq 150 bp reads in fastq format from six individual electroporation reactions were concatenated with fastq files from two electroporations previously generated by Dr Claudia Hemsley and analysed using the Bio-TraDIS pipeline[230] with smalt_y adjusted to .99 to reduce the false positive rate. Firstly, the bacteria_tradis pipeline identified reads beginning with the transposon tag 'TGTTA' with 0 mismatches allowed. The transposon tag was subsequently trimmed. bacteria_tradis then implements the SMALT short read mapping tool to map reads to the reference genome. Secondly, generated plot files were analysed with tradis_gene_insert_sites generating a document containing information of unique insertions and read counts for each gene. These files were used as an input for tradis_essentiality.R. In brief, this script calculates a normalised insertion index for each gene (insertion sites per gene/gene length) producing tables of essential, non-essential and ambiguous genes.

2.9.2. TraDIS data analysis – Whiteley Lab pipeline

Illumina MiSeq 150 bp reads in fastq format from six individual electroporation reactions were concatenated with fastq files from two electroporations previously generated by Dr Claudia Hemsley and analysed using a custom pipeline generated by the Whiteley Lab (https://github.com/glew8/Tn-seq_co-infection_analyses). Firstly, reads were screened to identify the TGTTA transposon tag, allowing 0 mismatches. The transposon tag was trimmed, and resulting reads mapped to the *C. burnetii* RSA493 reference genome with bowtie2 by implementing the TnSeq2.sh script. A correction for polymerase slippage was performed by taking reads that map within 1bp of each other and collapsing them to the local maxima using slippage.sh script. Next, the TnSeqDESeq2Essential_mariner.R script was executed, generating 1,000 pseudodatasets. This analysis uses estimateSizeFactors() from DESeq2 to normalise samples for sequencing depth before generating pseudodatasets, these pseudodatasets contain the same number of insertion sites, and total reads mapping to those insertion sites than the inputted experimental dataset, randomly distributed across the genome at TA sites. 1,000 pseudodatasets were created. A custom .gff file was created in Microsoft Excel to trim 10% of the 3' end of each gene, before insertion sites were binned to obtain gene-level insertion counts. DESeq2 was used to compare expected insertions per gene (from the pseudodatasets) to observed insertions per gene (from the experimental datasets). Genes were classified as essential based if they had a P_{adj} value of <0.05, were classified as 'reduced', and had an uncertainty of <0.05.

2.10. Bioinformatic analysis of essential and virulence genes

2.10.1. Investigating conservation of essential genes in different genomic groups

Essential genes were compared to the core genome of *C. burnetii,* as well as the core genomes of different *C. burnetii* genomic groups using the pan-genome analysis pipeline BPGA (https://sourceforge.net/projects/bpgatool/)

2.10.2. BlastP database searches of essential genes

C. burnetii essential genes were investigated by BlastP similarity (https://blast.ncbi.nlm.nih.gov/Blast.cgi) against the Database of Essential genes (DEG)[201] , and known drug targets stored in DrugBank[231]. Further investigation of

essential genes encoding hypothetical proteins was performed by BlastP similarity against the human genome and the human gut microbial gene catalogue[232].

2.10.3.   Assignment of clusters of orthologous groups

Clusters of orthologous groups (COGs) were assigned to essential genes using Eggnog Mapper v2 (http://eggnog-mapper.embl.de/)

2.10.4.   Prediction of cellular location

Cellular location of proteins encoded by essential genes were predicted using pSortB version 3.0.2[233]

2.10.5   Prediction of transmembrane domains

The presence of transmembrane domains was predicted by TMHMM version 2.0[234]

2.10.6   Prediction of signal peptides

The presence of a Sec signal peptide on proteins was predicted with SignalP version 5.0[235]

2.10.7   Protein sequence alignment

Alignment of protein sequences was performed using Clustal Omega [236]

Chapter 3: Growth and characterisation of the laboratory strain *C. burnetii* Nine Mile Phase II

3.1. Introduction

Historically, the only way to culture *C. burnetii* in the laboratory was through multiple passages in cell culture or embryonated eggs[237,238], imposing experimental constraints. In 2009[212], the development of an axenic media, ACCM-2, permitted the development of experiments that were not previously possible.

The whole genome sequence of *C. burnetii* Nine Mile Phase I RSA493 was published in 2003[6], revealing a 1,995,275 bp chromosome, with a 37,393 bp QpH1 plasmid. Conferring 2094 and 40 protein coding genes respectively. A significant proportion of which are designated hypothetical proteins, of which the structure and function is unknown. Later, in 2017, the *C. burnetii* Nine Mile Phase II RSA439 whole genome was sequenced[239].

In this chapter, axenic growth of *C. burnetii* in ACCM-2 was optimised. In addition, the *C. burnetii* Nine Mile Phase II RSA439 strain used in our laboratory was sequenced and compared to the reported gene sequences of *C. burnetii* Nine Mile phase I RSA493 and *C. burnetii* Nine Mile Phase II RSA439

3.2. Results and discussion

3.2.1. Growth of *C. burnetii* in ACCM-2

To underpin the studies in this project, the first requirement was to grow *C. burnetii* in culture to ensure enough bacteria was obtained for a suitable challenge inoculum. Previous work by Norville *et al.*[115] who developed the *G. mellonella* model found that at a dose of 10^6 GE/larvae, 100% of the population succumbed to infection by 9 days post-infection. It was therefore important to achieve a culture density of at least 10^8 GE/ml, so that larvae injected with 10 µl of the inoculum received a dose of 10^6 GE/larvae.

Cultures were incubated in O-ring sealed GENboxes containing GENbox Microaer sachets (Biomerieux). The GENbox Microaer sachets contain activated charcoal, sodium ascorbate and other organic and inorganic compounds which when placed in a GENbox achieve an oxygen concentration from 6.3 - 13.2% after one hour and a carbon dioxide levels of 2.5 – 9.5% after 24 hours (manufacturer's instructions). The first observation of this study was that *C. burnetii* cultures did not grow reliably, often resulting in an OD_{600} of 0 after 7 days of incubation at 37°C in GENboxes. For this reason, optimum culturing conditions were assessed. Duplicate GENboxes containing GENbox Microaer sachets were prepared each containing 12 cultures. Six of each prepared with pre-formulated or in-house prepared ACCM-2 (Table 3.1, Figure 3.1). After 7 days of incubation at 37°C the average OD_{600} for homemade and pre-formulated cultures in box one and box two were 0.075 ± 0.003, 0.034 ± 0.004, 0.078 ± 0.002 and 0.044 ± 0.005 respectively. A significant reduction in growth was observed (p = <0.0001, unpaired T-test) in cultures prepared with pre-formulated ACCM-2, no difference was observed between GENboxes supplied with different Microaer bags (p = 0.3, unpaired T-test).

Table 3.1. A comparison of the components in homemade and pre-formulated ACCM-2. N/A – component is not in formulation.

Name	Pre-formulated ACCM-2 (mg/L)	Homemade ACCM-2 (mg/L)
Bacto neopeptone	N/A	100
Calcium chloride dehydrate	13	13.2
Casamino acids	2500	2500
Casein peptone	100	N/A
Citric acid	2570	2568
Iron sulphate anhydrous	1.5	2.78
L-cysteine	265	264
Magnesium chloride anyhydrous	95	200
Methyl-b-cyclodextrin	1000	1000
Potassium phosphate monobasic	500	500
Sodium chloride	7280	7280
Citric acid trisodium salt anhydrous	4160	4740
RPMI+glutamax	125 ml	125 ml
Deionized H2O	875 ml	875 ml
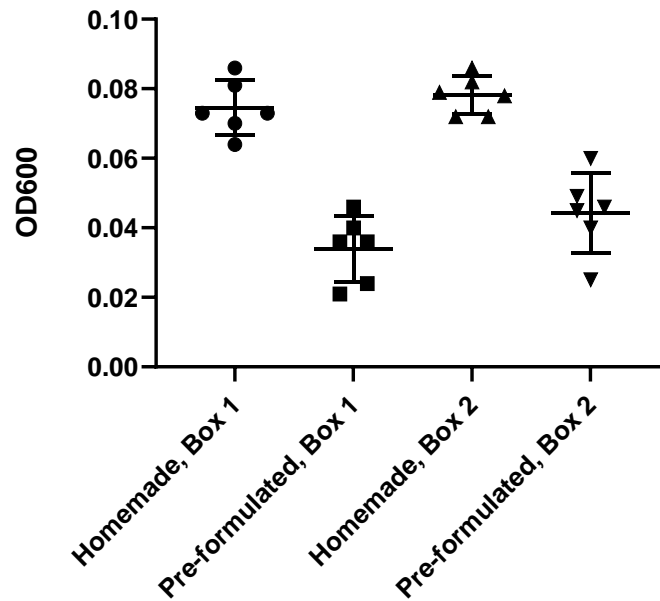
Figure 3.1. *C. burnetii* growth in homemade vs pre-formulated ACCM-2. Duplicate GENboxes (Box 1 and Box 2) were prepared each containing 12 cultures, 6 each using homemade or pre-formulated ACCM-2. After 7 days of incubation at 37°C, O_2 6.3 - 13.2%, CO_2 2.5 – 9.5%, growth was determined by measuring optical density at 600nm. Error bars show standard deviation. No significant difference in the level of growth was observed between box 1 and box 2 samples with the same media type (*p* = 0.03, unpaired T-test). A significant difference was seen between the level of growth in homemade or pre-formulated media (*p* = <0.0001, unpaired T-test). This experiment was performed on a single occasion.

Recently, ACCM-2 became available in commercial sachets, however in this experiment *C. burnetii* culture in pre-formulated ACCM-2 resulted in significantly reduced growth when compared to in-house formulations. *C. burnetii* has been reported to be extremely sensitive to fluctuations in ACCM-2 pH[240]. In addition, increased concentrations of nutrient sources and chloride ions massively reduces axenic growth[212]. Perhaps the slight differences between homemade and pre-formulated ACCM-2 (Table 3.1) are responsible for the growth differences seen. Comparisons between cultures incubated in separate GENboxes revealed no significant difference, indicating that reproducibility between GENbox Microaer sachets was unlikely to be the source of the problem. Nevertheless, a microaerobic gas mix (2.5% O^2, 5% CO^2, N balance) for use in an anaerobic cabinet was also

evaluated, resulting in consistent *C. burnetii* growth in homemade ACCM-2 (Figure 3.2).
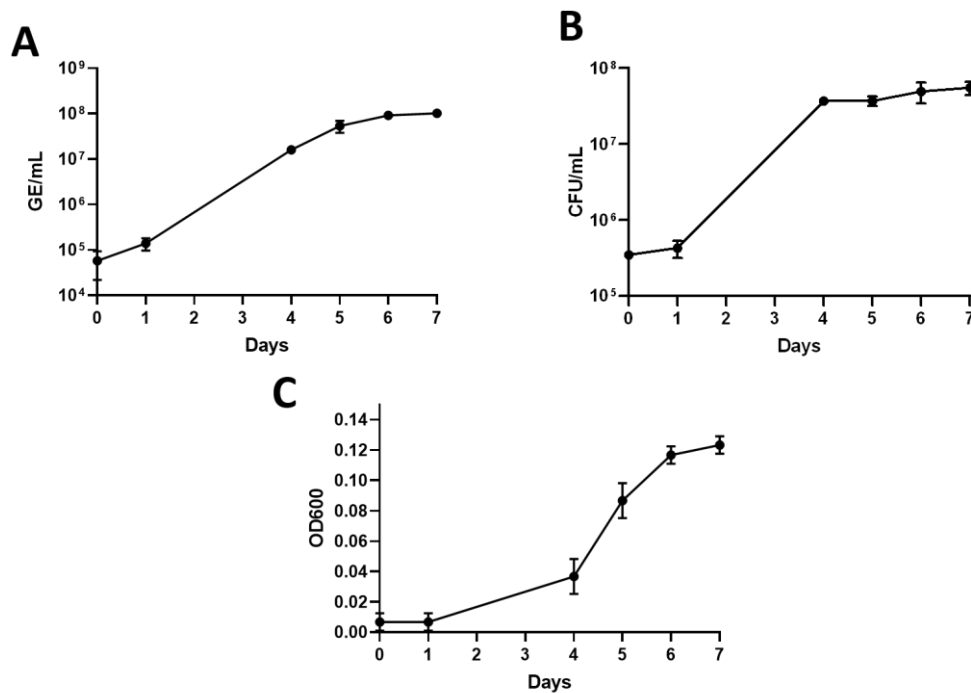
Figure 3.2. *C. burnetii* growth curves in homemade ACCM-2. A) GE/ml B) CFU/ml C) OD_{600}. Data obtained from three independent replicates. Error bars show standard deviation.

C. burnetii NMII was cultured in homemade ACCM-2 and samples were collected on days 0, 1, 4, 5, 6 and 7 post inoculation. Growth was assessed by measuring optical density at 600 nm (OD_{600}), genome equivalents (GE) using a qPCR assay and colony forming units (CFU) after plating onto ACCM-2-agarose plates (Figure 3.2). Under microaerobic conditions, approximately 2 logs of growth occurred during the 7 day culture period with a mean generation time of 10.6 hours, resulting in OD_{600} 0.12, equal to 5.53 x 10^7 CFU/ml and 1.01 x 10^8 GE/ml on day 7. The profile of OD_{600} readings differs from the GE and CFU profiles, with OD_{600} appearing to show a longer exponential phase than GE and CFU. Possibly the change in culture density is not obvious by absorbance at less than 10^7 GE/ml, where it then changes drastically between 10^7 and 10^8 GE/ml. This sudden change in density could be explained by an increase of LCVs, resulting in a higher optical density. Over the course of the project it was found that measuring *C. burnetii* concentration by OD_{600} alone often resulted in

an under-estimation of cell density and therefore GE/ml of the culture was determined by qPCR prior to experiments.

It has previously been reported that supplementation of ACCM-2 with 0.5 mM L-tryptophan can increase *C. burnetii* growth on solid and in liquid media[240]. In order to evaluate this further, liquid cultures with and without L-tryptophan were set up and growth was monitored for 7 days. No significant difference was seen between liquid cultures with and without L-tryptophan supplementation. Liquid cultures incubated in ACCM-2 or ACCM-2 + L-tryptophan resulted in 1.11 x 10^7 GE/ml and 3.96 x 10^7 GE/ml respectively on day 7 (Figure 3.3a, $p = 0.08$, unpaired T-test). Therefore it was decided not to supplement liquid cultures with L-tryptophan. In this experiment, although the GE/ml of the cultures on day 7 was as expected from previous growth experiments, the starting inoculum appears to be much lower. It is possible that the inoculum was under-estimated and therefore less than the limit of quantification for the qPCR.

However, on ACCM-2 agarose plates a significant difference in CFU/ml and colony size was seen. Agarose plates prepared with ACCM-2 and ACCM-2 + L-tryptophan resulted in 1.04 x 10^7 CFU/ml and 3.91 x 10^7 CFU/ml respectively on day 14 (Figure 3.3b, $p = 0.004$, unpaired T-test), and colonies appeared larger than those on ACCM-2 alone, suggesting supplementation is desirable for plating on solid media. ACCM-2 agarose plates were therefore supplemented with L-tryptophan for subsequent experiments going forwards.
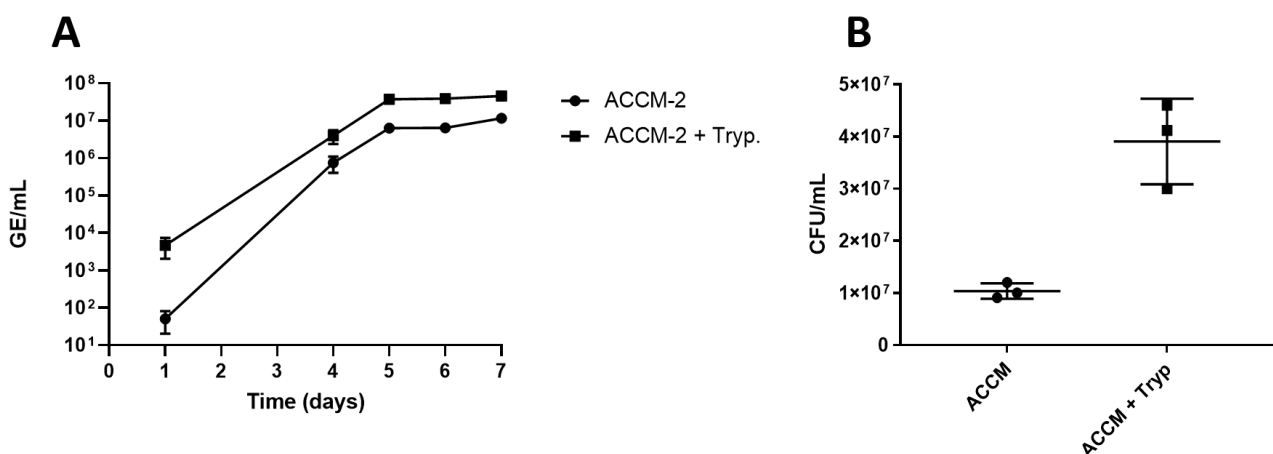
Figure 3.3. ACCM-2 supplementation with L-tryptophan in liquid cultures (A), no significant difference, $p = 0.08$, unpaired t-test or on ACCM-2 agarose plates (B),

significant difference, $p = 0.004$, unpaired t-test. Data obtained from three independent replicates. Error bars show standard deviation.

3.2.2. Quality control of sequencing data

In order to see how the *C. burnetii* NMII stock used in our laboratory compared to the published genome sequences of *C. burnetii* NMII[239] and *C. burnetii* NMI[6], *C. burnetii* NMII was grown in ACCM-2 media and genomic DNA (gDNA) was extracted using the GenElute genomic DNA extraction kit (Sigma-Aldrich) following a modified protocol (see methods 2.8.1) and sequenced by the University of Exeter Sequencing Service as 250 bp paired end reads on the Illumina Miseq platform.

Quality of the sequencing reads was determined using FastQC[222]. FastQC is a quality control tool which applies a number to tests to determine whether the sequencing data obtained is of high quality. The first test applied is per base sequence quality (Figure 3.4. A). A plot is derived that shows the quality scores per base position in the reads. The majority of reads have high quality base calling, this drops for reverse read (Figure 3.4, A2) which is often the case[241]. Next, per sequence quality score was assessed (Figure 3.4 B). The average quality per read was greater than 30 for both forward and reverse reads with a small subset of sequences in the reverse read set of quality 18-28 (Figure 3.4 B2). Finally, per base sequence content was inspected (Figure 3.4 C). As the G + C content of *C. burnetii* is 42.6%[6] parallel lines are expected with A and T at approximately 30% each and G and C at approximately 20% each. Such is the case for the majority of the forward reads, however in the end of the reverse reads these expected proportions are not seen, probably because of the drop in quality towards the end of the reads.
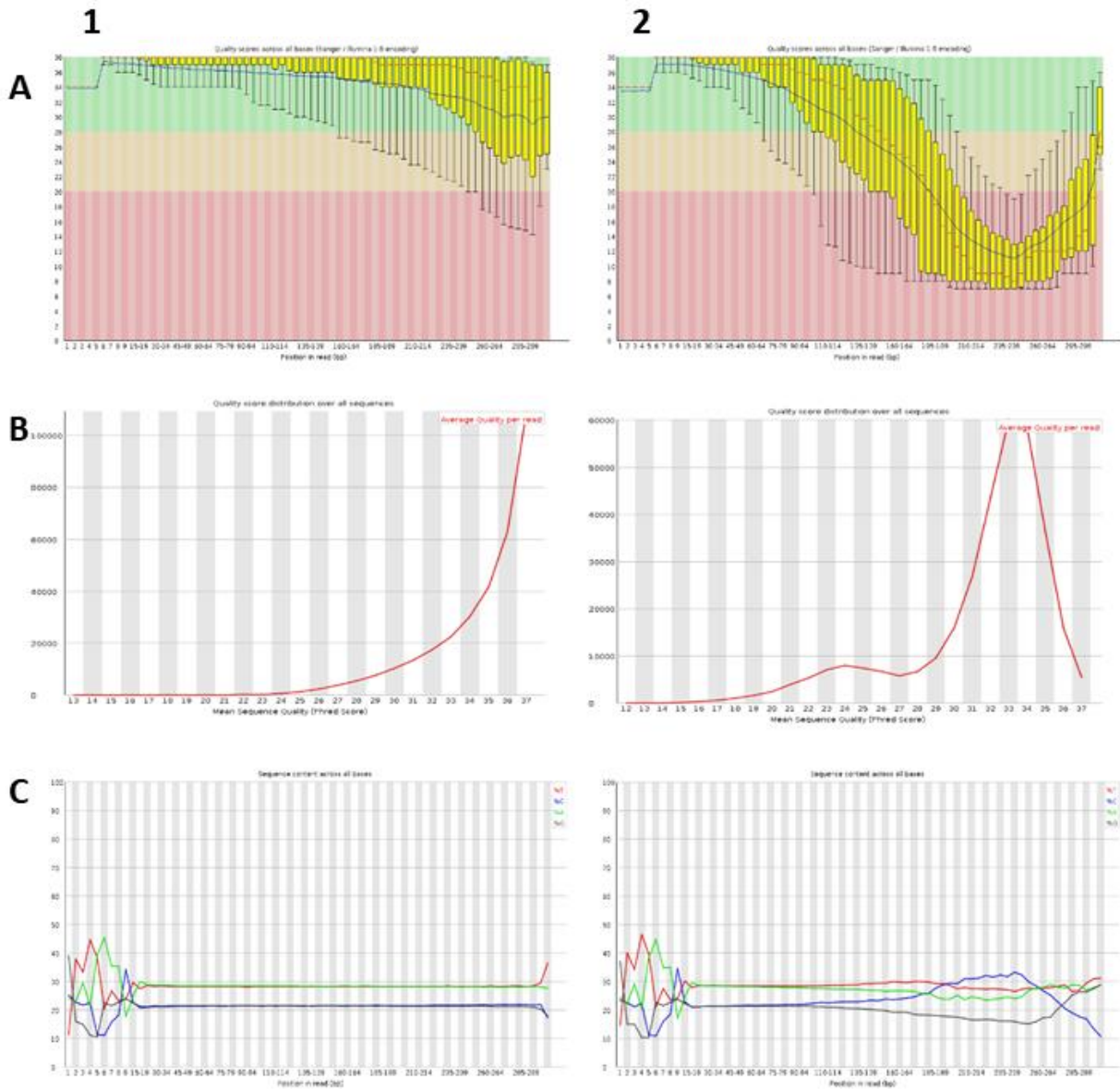
Figure 3.4. Quality control of forward (1) and reverse (2) reads using FastQC. A) Per base sequence quality, Y axis shows quality score X axis shows base position in the read. B) Per sequence quality score, Y axis shows number of reads, X axis shows overall quality score. C) Per base sequence content, Y axis shows proportion of A, T, C or G. X axis shows position in the read.

3.2.3. Mapping of sequencing data to the *C. burnetii* NMII and NMI genome

A total of 657,104 sequencing reads were obtained and mapped to concatenated files of the *C. burnetii* Nine Mile II and the corresponding QpH1 plasmid [239] or the Nine Mile I RSA493 reference genome (NMI) and the corresponding QpH1 plasmid[6] (for detail on read processing and mapping see methods 2.3). For mapping statistics see table 3.2. A total of 99.92% of reads mapped to both genomes, giving coverage of 64.4x and 63.1x for NMII and NMI respectively, mapping quality was assessed using Qualimap[223].

Table 3.2. Mapping statistics. Sequencing reads were mapped to concatenated chromosome and plasmid files for *C. burnetii* NMII and NMI

	C. burnetii NMII RSA439	*C. burnetii* NMI RSA4932
Reference size (chromosome + plasmid)	2,006,543	2,032,807
No. of reads	657,104	657,104
Mapped reads	656,548 (99.92%)	656,625 (98.49%)
Coverage (x)	64.40	63.07

Reads mapped to the *C. burnetii* NMII RSA439 genome with good coverage (Figure 3.5, A) and no insertions, deletions or single nucleotide polymorphisms (SNPs) were identified, giving confidence that the *C. burnetii* strain used in this study has not undergone any spontaneous mutation and is representative of *C. burnetii* used in other studies.

When mapping to the *C. burnetii* NMI genome (Figure 3.5, B), the well elucidated large ~26kb chromosomal deletion found in Nine Mile Phase II (partial deletion of *CBU_0678,* complete deletion of *CBU_0679*– *CBU_0697*) that is associated with the truncated LPS and absence of O antigen was identified as expected[13–16,239,242]. An inframe deletion in *CBU_*0533, which has also been associated with the truncated LPS[17] in *C. burnetii* NMII was also seen. The function of *CBU_0533* remains unknown, the conferred protein shares homology with *E. coli wecA* which confers undecaprenyl-phosphate α-N-acetylglucosamine phosphotransferase, a protein involved in the initiation of O-antigen elongation. However, *CBU_0533* is not complemented by *E. coli*

wecA[243]. It has been suggested that *CBU_0533* catalyses the initial step of LPS outer core biosynthesis, as deletion results in the loss of the outer core and O-antigen[17].

Figure 3.5. Coverage of mapped reads across reference genomes for NMII (A) and NMI (B) as determined by Qualimap[223]. X axis shows base position, Y axis shows coverage (upper traces) or GC% (lower traces). Red lines show coverage distribution, blue shaded areas show coverage deviation. Mapping against NMII shows an average of 64.4x coverage across the whole genome, mapping against NMI shows an average of 63.07x coverage, with the expended region of 0x coverage in the positions corresponding to LPS associated genes *CBU_0679 – CBU_0697*.

In addition, 15 SNPs and three additional deletions that have not been associated with the LPS were seen, all of which have been previously reported[17] (Table 3.3). Of the SNPs identified, 11 are missense and four are synonymous. All three additional deletions are frameshift. No insertions were seen.

Table 3.3. SNPs and deletions identified when mapping *C. burnetii* NMII RSA439 to *C. burnetii* NMI RSA493. Nuc – nucleotide, AA – amino acid, Ref – NMI Reference sequence, Test – NMII strain sequenced in this study.

Locus tag	Gene	Product	Position	Type	Ref Nuc	Test Nuc	Ref, AA	Test AA	Type
CBU_0136	murC	UDP-N-acetylmuramate--alanine ligase	124181	Snp	C	T	Ala	Val	Missense
CBU_0139		carbonic anhydrase	126357	Snp	C	T	Leu	Leu	Synonymous
CBU_0184		membrane-associated protein	173284	Snp	C	T	Arg	Arg	Synonymous
CBU_0311		outer membrane porin P1	277094	Snp	G	A	Gly	Ser	Missense
CBU_0372		Fic family protein	336658	Snp	G	A	Ser	Leu	Missense
CBU_0533	Rfe	undecaprenyl-phosphate alpha-N-acetylglucosaminephosphotransferase	478158	Del	CTAT	C			Inframe
CBU_0547		tetratricopeptide repeat family protein	496565	Snp	G	T	Ala	Asp	Missense
CBU_0596a		hypothetical protein	544353	Del	GC	G			Frameshift
CBU_0766		acetoacetyl-CoA synthetase	710512	Snp	G	T	Ala	Glu	Missense
CBU_0768		multidrug resistance protein B	712654	Snp	G	C	Gly	Ala	Missense
CBU_1043	gacA.4	response regulator	985012	Del	GAT	G			Frameshift
CBU_1084		two component system histidine kinase	1029452	Snp	G	A	Arg	Cys	Missense
CBU_1084		two component system histidine kinase	1029577	Snp	T	C	His	Arg	Missense
CBU_1176	phrB	deoxyribodipyrimidine photolyase	1119416	Del	CA	C			Frameshift
CBU_1634	icmQ	Icm secretion system protein IcmQ	1574754	Snp	C	T	Ser	Asn	Missense
CBU_1716a		IS110 family transposase IS1111A	1646510	Snp	G	A	Lys	Lys	Synonymous
CBU_1772	yihA	GTP-binding protein	1705067	Snp	T	C	Lys	Glu	Missense
CBUA0003	fic	Cell filamentation protein	1030	snp	A	G	Leu	Leu	Synonymous
CBUA0032		3',5'-cyclic-nucleotide phosphodiesterase	29217	snp	G	A	Glu	Lys	Missense

3.3. Conclusion

In this chapter the growth of *C. burnetii* NMII in our laboratory has been optimised. The use of homemade ACCM-2 and the investment of an anaerobic gas mix ensured that reliable growth to an appropriate concentration was achieved. Whole genome sequencing of *C. burnetii* NMII showed results consistent with previous findings on the *C. burnetii* NMI sequence[6], and no obvious differences when compared to the *C. burnetii* NMII sequence[239]. Suggesting that there are not any apparent differences between the strain used in our laboratory to other RSA439 strains, giving confidence to comparisons of the data found in this study to the current literature.

Chapter 4: The *Galleria mellonella* model of *C. burnetii* infection

4.1.   Introduction

The larvae of the greater wax moth, *G. mellonella* are widely used as an infection model for a range of bacterial and fungal pathogens [244–247]. This model has recently been developed for *C. burnetii* [115] . *G. mellonella* has advantages over other insect models of *C. burnetii* infection such as *D. melanogaster* and *C. elegans*[124,125] as they can be incubated at 37ºC (the physiological temperature of mammals), allowing the expression of temperature-regulated virulence genes. Additionally, their large body size permits inoculation with a precise dose through injection into pro-legs on the underside of the larval body, allowing the 50% lethal dose (LD$_{50}$) to be calculated. Together these properties permit comparison studies to evaluate mutant virulence or the efficacy of antimicrobial compounds. The *G. mellonella* model of *C. burnetii* infection has previously been described and the LD$_{50}$ of phase I and phase II strains was calculated[115]. The model has also been used to investigate comparative virulence of naturally occurring *C. burnetii* isolates, T4SS mutants, and transposon mutants[115,119,219]. Bacterial burden of *C. burnetii* in haemocytes has also been described, In addition to antibiotic efficacy [115]. Larvae dosed with doxycycline, the recommended treatment for Q fever, show increased survival[115].

G. mellonella possess haemocytes, specialised phagocytic cells comparable to mammalian neutrophils that exhibit lectin-mediation phagocytosis and subsequent killing of pathogens through respiratory burst. Additionally, haemocytes possess Toll-like receptors, of which binding triggers cell signalling through a NFkB-like pathway[129]. This permits investigation into host-pathogen interactions that cannot be captured through cell culture infection models.

Dexamethasone, an anti-inflammatory glucocorticoid drug, is known to interfere with eicosanoid synthesis in insects, resulting in a reduced haemocyte response. Early studies in insects showed that dexamethasone severely impaired the ability of *Manduca sexta* (tobacco hornworm) to clear the Gram negative pathogen *Serratia marcescens*, resulting in increased mortality[248]. Later, it was shown that dexamethasone inhibits the expression of cecropin B and lysozyme associated genes in *Bombyx mori*, which are usually up-regulated during infection[230].

The aim of this chapter is to further characterise the *G. mellonella* infection model of *C. burnetii.* To do this, *C. burnetii* growth and vacuole formation in haemocytes have been characterised. By mapping the transcriptome of *C. burnetii* during *G. mellonella* infection, genes that may play a role in infection have been identified which can be explored further as potential targets for diagnostics, prophylactics or therapeutics. In addition, the ability of the steroid drug dexamethasone to increase *G. mellonella* susceptibility to *C. burnetii* infection was evaluated.

4.2. Results and discussion

4.2.1. *G. mellonella* larvae are susceptible to *C. burnetii* NMII in a dose-dependent manner

To determine the virulence of *C. burnetii* NMII in *G. mellonella,* larvae were injected with doses at 10^3, 10^4, 10^5 or 10^6 GE/larvae. The survival of larvae was monitored at daily intervals for up to 10 days (Figure 4.1). The highest dose of *C. burnetii* tested (10^6 GE/larvae) was the only dose consistently resulting in 100% larvae death by day 10 post infection, and was therefore used in the following experiments. Eighty seven percent, 27% and 10% of larvae succumbed to infection by 10 days post infection following injection with 10^5, 10^4 or 10^3 GE/larvae at *C. burnetii* doses respectively. No mortality was observed in control larvae injected with sterile PBS. The median lethal dose (MLD) of NMII was calculated as 1.19×10^4 GE/larvae, with 100% of the population succumbing to infection within 8 days when infected with 1×10^6 GE/larvae, this model could be an effective tool for the investigation of attenuated *C. burnetii* mutants.
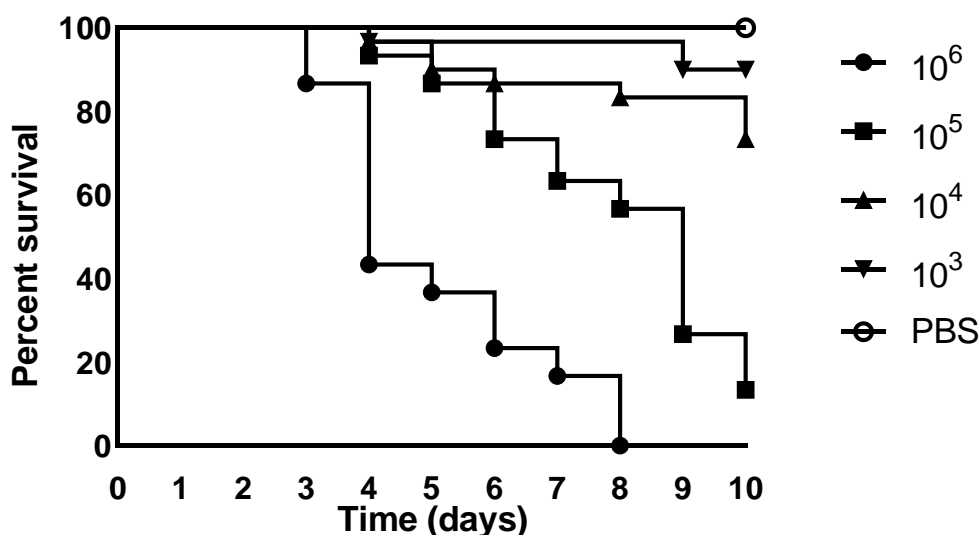
Figure 4.1. *C. burnetii* infection of *G. mellonella* induces dose-dependent mortality. Ten *G. mellonella* larvae were injected with *C. burnetii* NMII at variable doses (10^3 - 10^6 GE/larvae) and survival was monitored over 10 days post infection. No data was recorded on days 1 and 2. Results show the mean of three independent experiments.

4.2.2. *C. burnetii* replication in *G. mellonella* larvae

In order to confirm growth of *C. burnetii* NMII within *G. mellonella,* larvae were injected with 10^6 GE/larvae, and at daily intervals post infection the haemolymph from 3 larvae was extracted and haemocytes were re-suspended in sterile PBS, Resuspended haemocytes were lysed and *C. burnetii* NMII gDNA was enumerated using qPCR to determine bacterial load (Figure 4.2).
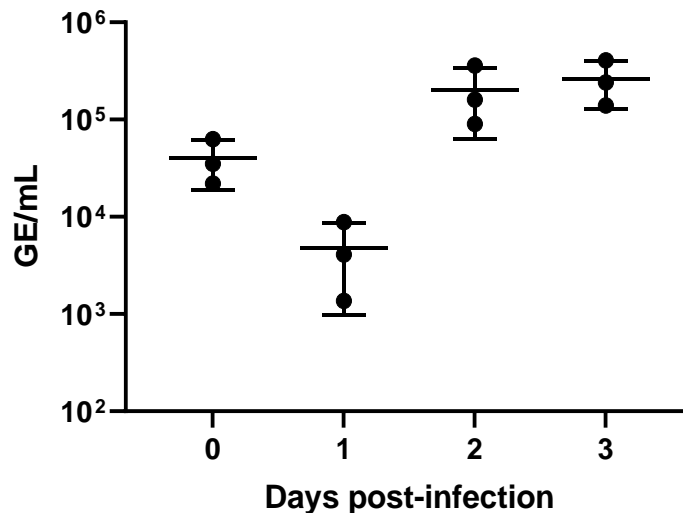
Figure 4.2 Expansion of *C. burnetii* NMII in *G. mellonella* haemocytes. Larvae were injected with 10^6 GE/larvae of *C. burnetii* NMII and bacterial numbers were enumerated by qPCR at daily timepoints. Each point represents one larva, with error bars showing standard deviation.

Haemocytes isolated immediately after infection (T0, Figure 4.2) were found to have a GE/mL of $2.19 - 6.30 \times 10^4$ and, considering the dilution of the inoculum in the larvae, this represents almost all of the recoverable challenge dose, suggesting that the majority of bacteria were haemocyte-associated immediately after infection. There was a subsequent decline in bacteria on day 1 post infection which may be due to uptake and killing of *C. burnetii* within haemocytes, followed by a phase of bacterial growth with a mean generation time of 5 hours. Previous work using the Nine mile phase I strain reported a decline in *C. burnetii* 2 days post infection, followed by an increase[119]. These differences may reflect strain specific differences, or differences in the source of *G. mellonella* larvae used.

4.2.3. *C. burnetii* forms a CCV in *G. mellonella* haemocytes

In order to determine if *C. burnetii* NMII forms a CCV in *G. mellonella* haemocytes, haemocytes from infected *G. mellonella* at 3 days post infection were visualised by transmission electron microscopy (TEM). TEM samples and images were prepared by the University of Exeter Bioimaging Unit. This revealed bacteria in clearly defined vacuoles which had filled the majority of the haemocyte cytoplasm (Figure 4.3). *C. burnetii* exists in two forms, a metabolically inactive small cell variant (SCV), which is typically 0.2 - 0.5 µm in length, and a metabolically active large cell variant (LCV) which can exceed 1 µm in length[249]. These vacuoles observed in *G. mellonella* appeared to contain a mixed population of *C. burnetii* NMII in both SCV forms with a length approximately 0.23 – 0.31 µm (Figure 4.6, white arrows) and large cell variant (LCV) forms with a length of approximately 0.68 – 0.87 µm (Figure 4.6, black arrows). In addition, the vacuole appears to be morphologically similar to *Coxiella* containing vacuoles previously reported in macrophages infected with *C. burnetii.* [250]
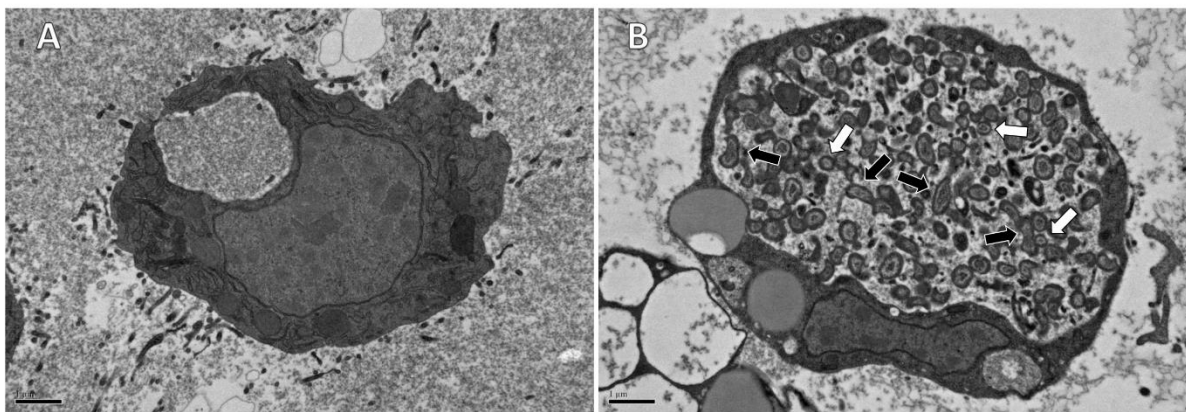
Figure 4.3. Transmission electron microscopy of *G. mellonella* haemocytes post-infection with *C. burnetii*. *G. mellonella* larvae were injected with *C. burnetii* NMII at a dose of 10^6 GE/larvae and 3 days post infection larvae were bled, and haemocytes visualised by a transmission electron microscope. A) Uninfected controls with no bacteria being visible 3 days post sham infection with sterile PBS. B) Haemocytes from infected larvae with a *Coxiella*-containing vacuole clearly visible, which spread to fill the entire cell cytoplasm. Arrows indicate proposed LCVs (black) and SCVs (white). Images shown are representative of 100 total imaged haemocytes. 50 control images, and 50 images of infected haemocytes. Scale bar = 1µm.

4.2.4. Solvent toxicity testing in *G. mellonella*

It was decided to evaluate whether pre-treatment of *G. mellonella* with dexamethasone would increase susceptibility to *C. burnetii* infection, as this would allow the identification of weakly attenuated mutants. To do this, it was first important to determine the toxicity of the diluents of various dexamethasone based drugs. Dexamethasone 21-phosphate (Dex.P), dexamethasone acetate (Dex.A) and dexamethasone (Dex.) are soluble in water, acetone, and ethanol or DMSO respectively. To determine the toxicity of these diluents to *G. mellonella,* larvae were injected with 10 µl ethanol or acetone at concentrations of 25%, 50% or 75% (v/v) in sterile water or with 1 µl neat DMSO or acetone. Ethanol and acetone were toxic at concentrations greater than 50% and 25% respectively (Figure 4.4). *G. mellonella* were able to tolerate 1 µl neat DMSO or acetone without mortality (data not shown). Dex.A solubilised well in 25% acetone, so this was selected as the diluent for following experiments. One microlitre DMSO was selected as the diluent for Dex., as the drug precipitated out of solution at ethanol concentrations <100%, and as previously mentioned, *G. mellonella* were able to tolerate this small volume of DMSO.
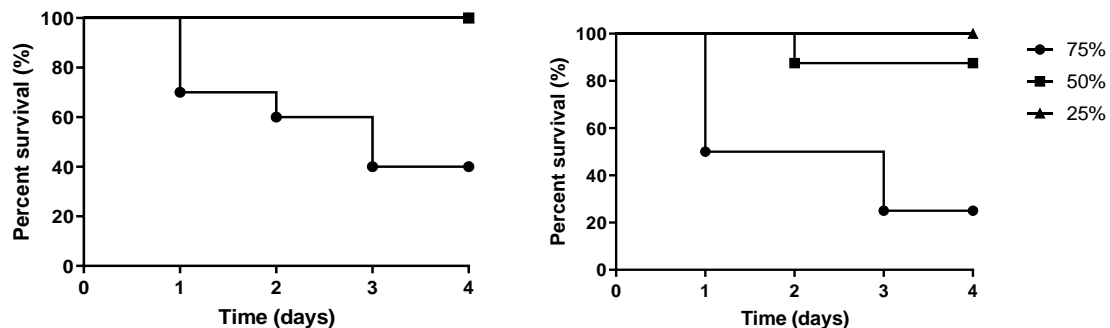
Figure 4.4 Toxicity testing of ethanol (left) or acetone (right) in *G. mellonella*. Larvae were dosed with 10 µl of solvent at concentrations of 75%, 50% and 25%. Ethanol and acetone were toxic at concentrations greater than 50% and 25% respectively. Results show survival of 10 larvae per group.

4.2.5. Drug toxicity in *G. mellonella*

To determine the toxicity of various dexamethasone based drugs, groups of 10 *G. mellonella* larvae were injected with 10 µl Dex.P, Dex.A or 1 µl Dex. at a dose of 200 µg/larvae. Control groups consisted of larvae inoculated with 10 µl PBS, 10 µl of sterile water, 10 µl of 25% acetone, or 1 µl neat DMSO.

Dex.A and Dex. both displayed toxicity in *G. mellonella* showing 90% and 20% mortality respectively (Figure 4.5) at 2 days post inoculation. No deaths occurred in larvae injected with Dex.P or control groups of PBS, sterile water, 25% actetone or DMSO injected larvae.
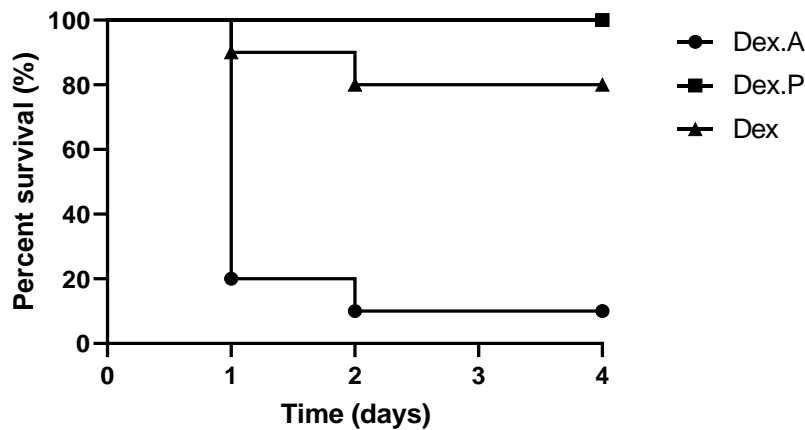
Figure 4.5 Drug toxicity testing in *G. mellonella*. Larvae were injected with 10 µl of Dex.A or Dex.P or 1 µl Dex at a concentration of 200 µg/larvae and survival was recorded daily for a total of four days. No deaths were seen in diluent controls of 10 µl 25% acetone or PBS, or 1 µl DMSO (data not shown). Dex.A and Dex. show toxicity with 90% and 20% mortality respectively. Results show survival of 10 larvae per group.

4.2.6. Pre-treatment of *G. mellonella* with dexamethasone 21-phosphate prior to NMII infection

To determine the effect of pre-treatment with Dex.P on *C. burnetii* NMII infection, groups of 10 *G. mellonella* were dosed with 50, 100 or 200 µg/larvae Dex.P 10 minutes prior to *C. burnetii* NMII infection at 10^6 GE/larvae and survival was monitored at daily intervals for a total of four days (Figure 4.6). At the end of the four day period, the percentage of larval death at doses of 200, 100 and 50 µg/larvae was 100%, 40% or 50% respectively. Untreated NMII larval death was 80%. No deaths were seen in the PBS control group (data not shown). A significant increase in larval death occurred when pre-treated with 200 µg/larvae ($p = 0.0002$, Log-rank test) compared to *C. burnetii* NMII alone. No significant difference was observed at any other concentration. These findings suggested that pre-treatment of *G. mellonella* with 200 µg/larvae Dex.P increased the susceptibility of *G. mellonella* to *C. burnetii* NMII infection.
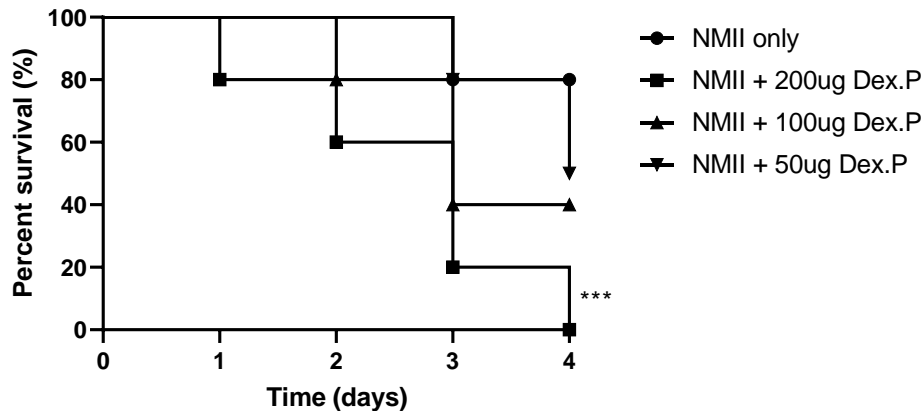
Figure 4.6 The effect of pre-treatment of *G. mellonella* with Dex.P shows a dose dependent increase in larval death. Larvae were injected with 10 µl of Dex.P at various doses 10 minutes prior to infection with 10^6 GE/larvae *C. burnetii* NMII. On day 4 larval death at doses of 200, 100, 50 and 0 µg/larvae was 100%, 40%, 50% and 80% respectively. No deaths were seen in the PBS control group (data not shown). A significant difference between the 200 µg/larvae and NMII only group was seen ($p = 0.0002$, Log-rank test). No significant difference was observed at any other concentration. Results show survival of 10 larvae per group.

To investigate whether this increase in disease severity would allow the identification of attenuated phenotypes, a *C. burnetii* NMII::Tn-*relA* mutant was tested in the model with and without pre-treatment of larvae with 200 µg Dex.P/larvae (Figure 4.7). *relA* (*CBU_1375)* confers a GTP pyrophosphokinase, and transposon insertion in this gene has been shown to have a mild defect in intracellular replication in Vero cell culture during a large scale screen of individual transposon mutants[219].

In the untreated *G. mellonella* model no significant difference was observed between *C. burnetii* NMII and NMII::Tn-*relA*, with total larval death at 8 days post infection of 100% and 90% respectively ($p = 0.6$, log-rank test, Figure 4.7A). When pre-treated with 200 µg/larvae Dex.P there was a significant delay in mortality in the *C. burnetii* NMII::Tn-*relA* challenged group compared to the wild type. ($p = 0.01$, log-rank test, Figure 4.7B), with 100% of the population succumbing the infection by day 7, compared to day 3 for *C. burnetii* NMII.
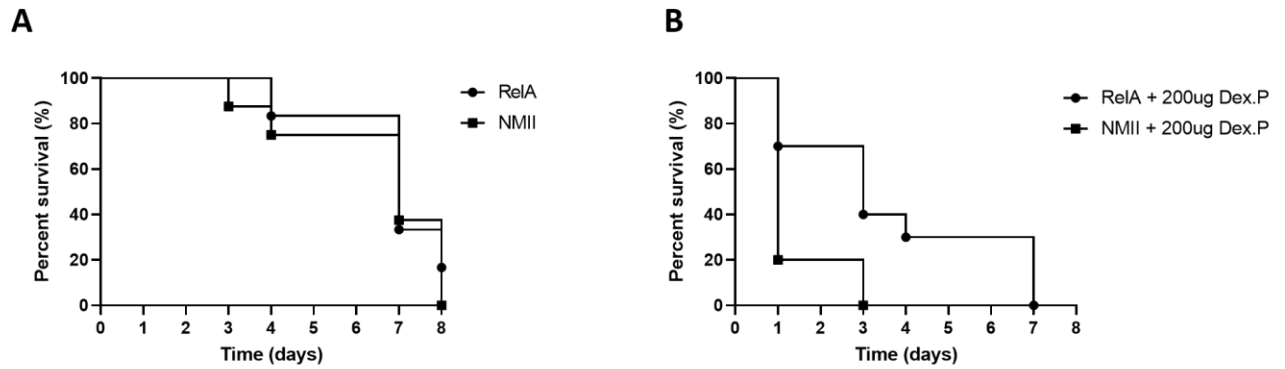
Figure 4.7. Pre-treatment with 200 µg/larvae of Dex.P permits the identification of attenuated phenotypes. Without pre-treatment (A), no significant difference is seen between NMII and NMII::Tn-*relA*, *p* = 0,6 log-rank test. With pre-treatment of 200 ug/larvae Dex.P a significant difference is seen between NMII and NMII::Tn-*relA, p* = 0.01 log-rank test. No deaths were seen in PBS and Dex.P only controls (data not shown). Results show survival of 10 larvae per group.

4.2.7. HPLC determination of dexamethasone 21-phosphate and dexamethasone in *G. mellonella*

Dex.P, the phosphate ester of Dex. is a glucocorticoid steroid pro-drug that is utilised in human medicine. To be biologically active in humans, Dex.P must be converted to *in vivo* in the plasma and liver by phosphatases to form Dex. which binds glucocorticoid receptors resulting in anti-inflammatory responses.

To investigate the ability of *G. mellonella* to utilise Dex.P as the active drug product Dex. High Performance Liquid Chromatography (HPLC) analysis was performed on *G. mellonella* haemolymph extracted from larvae dosed with 200 µg Dex.P. Standard curves generated after analysis of haemolymph spiked with known concentrations of Dex. or Dex.P resulted in R^2 values of 0.99 for both compounds (Figure 4.8). The limit of detection (LOD) for Dex. or Dex.P was 0.15 µg/ml or 2.5 µg/ml respectively. The limit of quantification (LOQ) for Dex. or Dex.P was 1.23 µg/ml or 10 µg/ml respectively.
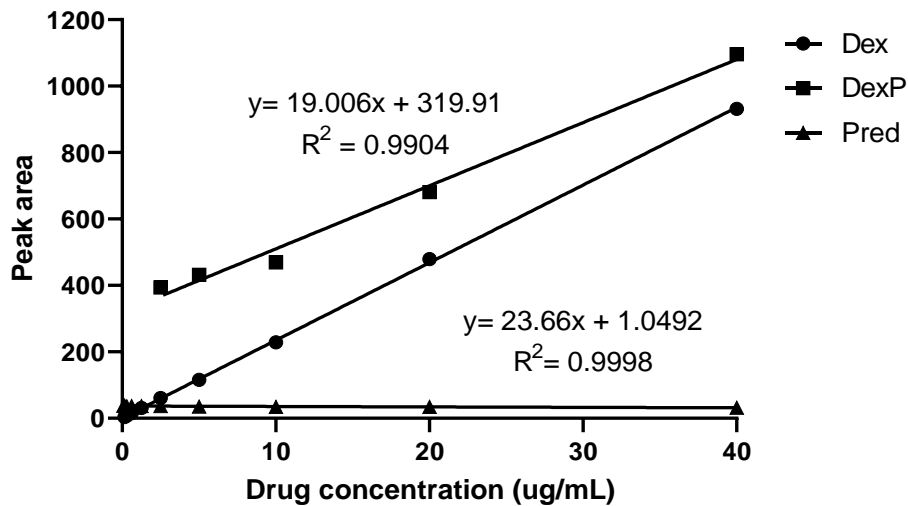
Figure 4.8 Generation of a standard curve for the quantification of Dex. and Dex.P by HPLC. Haemolymph extracted from *G. mellonella* was spiked with various concentrations of the two compounds resulting in R^2 values of 0.99 for both. Prednisolone (Pred.) was used as an internal control.
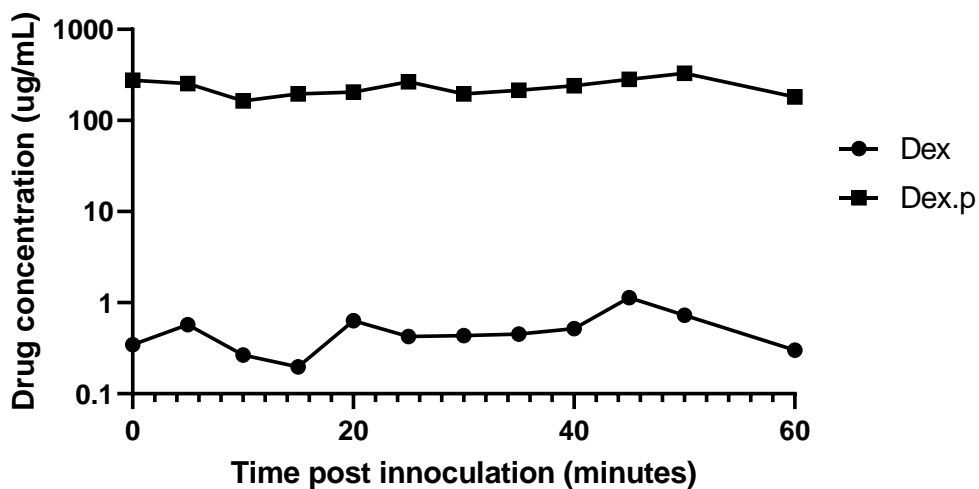
Figure 4.9 Drug concentration measured in *G. mellonella* haemolymph at 5 minute intervals post-injection from T0 to T60. Dexamethasone 21-phosophate (Dex.P) concentration was between 164-281 µg/ml. Dexamethasone concentration was <LOQ 0.19-1.13 µg/ml. Each point shows the drug concentration from the haemolymph of 3 larvae pooled together

The initial findings suggested that Dex.P increased *G. mellonella* susceptibility to infection with *C. burnetii* in a dose dependent manner, with a significant increase in mortality occurring at a drug dose of 200 μg/larvae. This supports the findings reported by Torres *et al* using Dex.P at doses of 80 and 200 μg/larvae pre-infection with various *K. pneumoniae* and *E. coli* strains[168]. However, HPLC analysis of *G. mellonella* haemolymph from larvae injected with 200 μg/larvae of Dex.P showed drug levels staying reasonably level over time (164-281 μg/ml) with the active drug present in levels lower than the LOQ (0.19-1.13 μg/ml) (Figure 4.9), suggesting that Dex.P is not being converted to Dex. As previously mentioned, Dex.P conversion occurs as a result of phosophatase enzymes, it is possible that the increase in mortality is caused by an unknown effect from dexamethasone 21-phosphate, and not as a direct effect of active Dex. It was decided not to continue with this model

4.2.8. Isolation of *C. burnetii* mRNA from *G. mellonella* haemocytes[2]

Bacterial mRNA was isolated from *C. burnetii* NMII grown in ACCM-2 medium and from haemocytes from *G. mellonella* that had been infected with 10^6 GE/larvae of *C. burnetii* NMII by Dr Andrea Kovacs-Simon. The RNA integrity number (RIN) score for isolated samples was at least 9.3 indicating minimal degradation had occurred. The mRNA levels of two *C. burnetii* NMII housekeeping genes, *com1* and *rpoB* were determined by real-time quantitative PCR (RT-qPCR) using total RNA extracted from the haemocytes of infected *G. mellonella* larvae (prokaryotic and eukaryotic RNA) as template, and the resulting PCR product was analysed by electrophoresis on a 1% agarose gel . The levels of *com1* and *rpoB* mRNA increased as the infection progressed (Figure 4.10), this corroborates the earlier finding that the numbers of *C. burnetii* cells within *G. mellonella* haemocytes increase during the course of infection (Fig. 3.2). This increase may be a combination of intracellular growth and increasing uptake of bacteria by haemocytes.

---

2 Parts of sections 4.2.8 – 4.2.12 are published in: Kovacs-Simon A*, Metters G*, Norville I, Hemsley C, Titball RW. *Coxiella burnetii* replicates in *Galleria mellonella* hemocytes and transcriptome mapping reveals *in vivo* regulated genes. *Virulence*. 2020;11(1):1268-1278.
* Joint first authors

Days post-infection
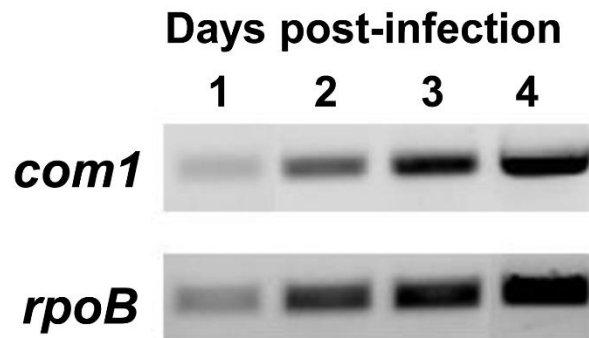
Figure 4.10 Visualisation of *C. burnetii* -specific RNA in total RNA extracted from infected *G. mellonella* haemocytes. RNA was extracted from infected haemocytes from 10 *G. mellonella* larvae at the timepoints indicated, and used to amplify the *com1* and *rpoB* housekeeping genes of *C. burnetii* NMII by RT-PCR. Equal amounts of PCR products were subjected to electrophoresis on a 1% agarose gel and imaged using a Bio-Rad Chemidoc system.

4.2.9. Mapping the transcriptome of *C. burnetii* during *G. mellonella* infection by RNA-Seq

To investigate how *C. burnetii* NMII adapts to infection of *G. mellonella* larvae, the transcriptional landscapes of *C. burnetii* NMII in *G. mellonella* haemocytes were profiled, using RNA-Seq, at 1, 2, 3 and 4 days post-infection. Three groups each of 10-30 larvae were processed for each time point analysed, any deceased larvae were excluded. These profiles were compared to the transcriptional profile of *C. burnetii* NMII grown in ACCM-2 liquid medium for 7 days.

First, a principal component analysis (PCA) was performed to compare the datasets obtained from three biological replicates. This showed that sample replicates clustered together, indicating experimental reproducibility (Figure 4.11). Next, the number of expressed genes was determined. Broadly similar numbers of genes were expressed *in vitro* (n=1780) and in infected *G. mellonella* at the four timepoints (n=1708-1727). The majority these genes (n=1668) were expressed in all samples. However the expression of some genes was only evident during *in vivo* or *in vitro* growth, or at different timepoints post infection (Appendix 4.1).
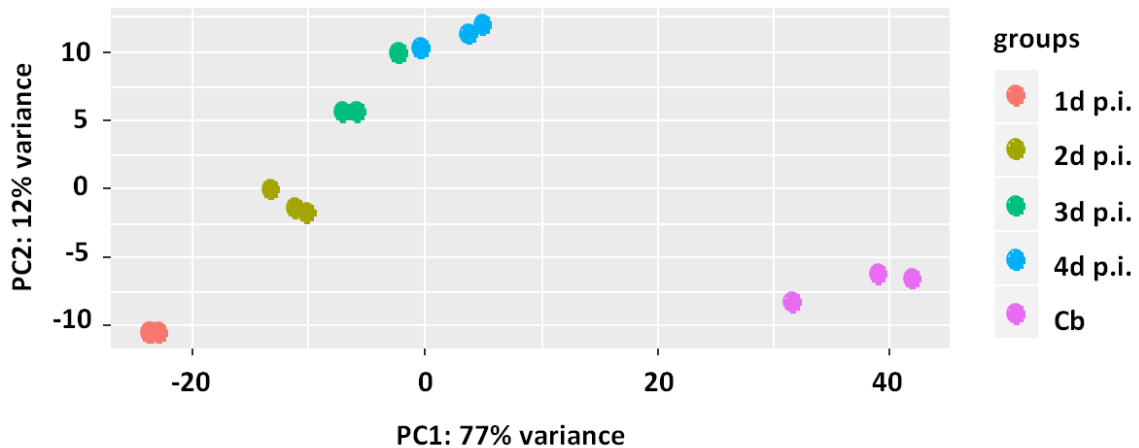
Figure 4.11 Principal component analysis on global expression profiles of *C. burnetii* NMII obtained from bacteria grown *in vitro* ("Cb") and during *G. mellonella* infection (Days 1-4 post infection). Replicates of most of the samples are tightly clustered indicating experimental reproducibility.

The similarity between the global transcriptomes was determined using regression analysis (Figure 4.12). The 1, 2, and 3 days post-infection transcriptomes were most similar to each other (R^2 = 0.7898-0.9527) while the transcriptome of bacteria at 4 days post-infection was more dissimilar (R^2 = 0.2316-0.6953). Conversely, the 4 day post infection transcriptome was more similar to the transcriptome of bacteria grown in ACCM-2 liquid media (R^2 = 0.3402) than other post infection timepoints (R^2 = 0.0118 – 0.1864). In addition to investigating reproducibility and similarity, changes in gene expression were measured. Compared to growth *in vitro*, 467, 386, 370 or 320 genes were significantly upregulated at 1, 2, 3 or 4 days post-infection respectively. On the other hand, 481, 397, 399 or 394 genes were significantly downregulated at 1, 2, 3 or 4 days post-infection respectively (Appendix 4.1). Overall these findings suggest that the transcriptome of *C. burnetii* NMII at 3 and 4 days post-infection are more similar to the conditions in ACCM-2, than to 1 and 2 days post-infection.
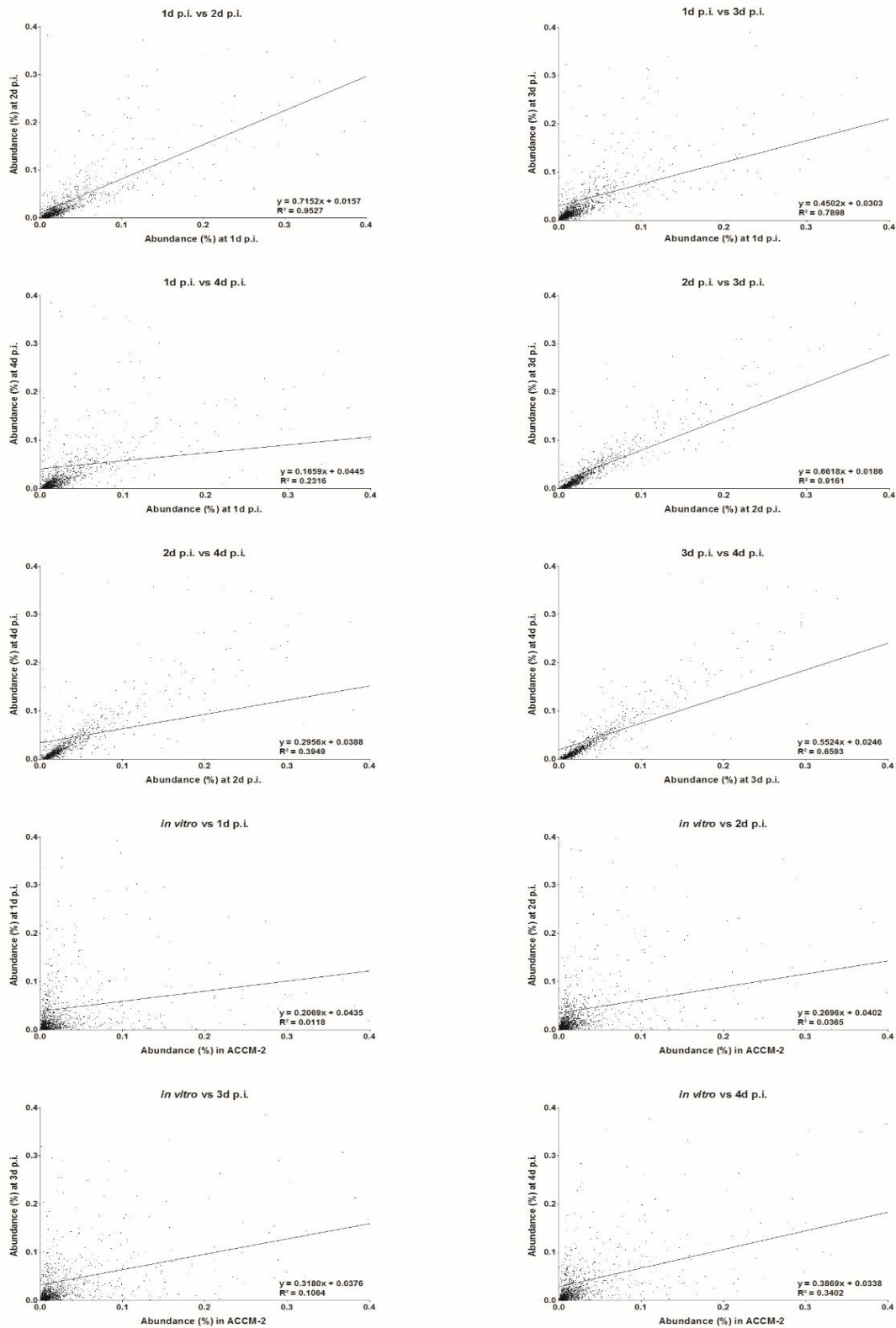
Figure 4.12 Scatter plots of transcript abundances between the transcriptomes of *C. burnetii* grown *in vitro*, and during *G. mellonella* infection. In the panels pairwise plots of normalised abundances of transcripts are shown. The equation and R square (R^2) of the linear regression line (black line) are included in each plot.

To validate the RNA-Seq expression data 19 genes were selected for RT-qPCR, using 16S rRNA as an internal control (Figure 4.13). Similar results for fold change difference in the expression of the selected genes by RT-qPCR and RNA-Seq were seen. Validating that the RNA-Seq data provides a robust picture of the transcriptome of *C. burnetii* NMII.
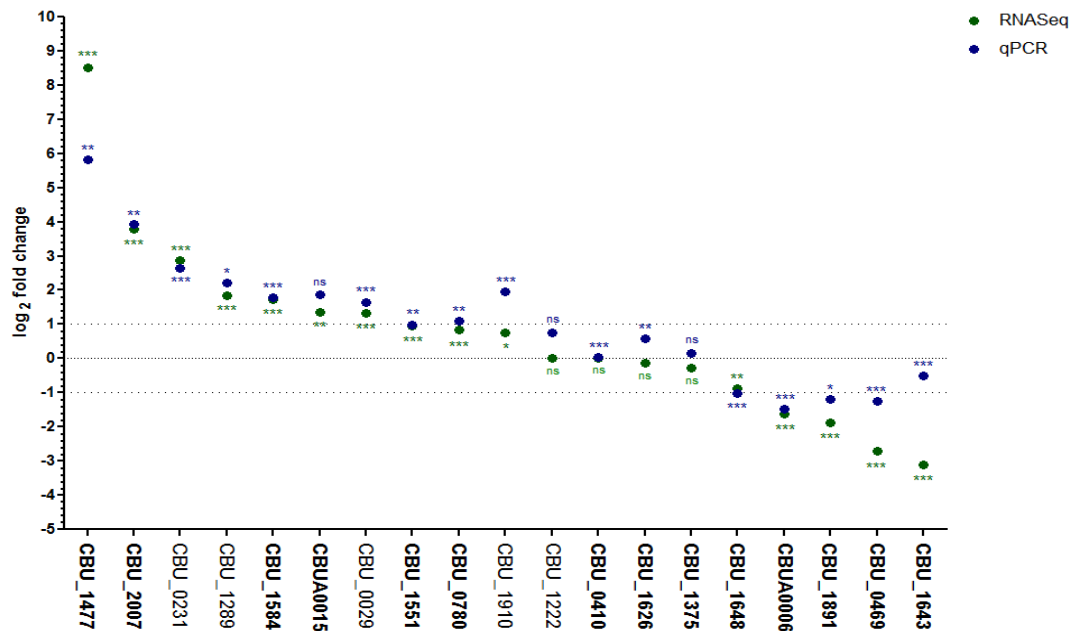
Figure 4.13 Validation of RNA-Seq data by RT-qPCR. RNA-Seq (green) and RT-qPCR (blue) data at 4-day post-infection of *G. mellonella* compared to *in vitro* growth in ACCM-2 medium. Tested genes include putative virulence-related factors (shown in bold fonts), and significantly and non-significantly regulated genes. 16S rRNA was used as internal control in the RT-PCR. Dotted lines show 2-fold change in expression (cut-off for significance). Asterisks on the graph indicate statistical significance (*p<0.05, **p<0.01, ***p<0.001).

4.2.10.   *C. burnetii* cell variants present in *G. mellonella* haemocytes

Previous studies have identified genes which are associated with the LCV or SCV forms of *C. burnetii* [18,251,252]. These genes were identified through transcriptional profiling[18,252] and proteome profiling of LCVs and SCVs separated by equilibirium density centrifugation in cesium chloride[251]. It should be noted that there are some unexpected genes in these lists, such as DNA gyrase and polymerase. Upon inspection of the data some of these genes are on the cusp of significance cutoff, and may therefore be incorrectly classified. In addition, there are some limitations with

density centrifugation, where the separated LCVs and SCVs may not be homogenous for each cell variant.

Nonetheless, based on these data   sets lists of LCV-associated (n= 325) or SCV-associated (n=197) genes were generated (Appendix 4.1) . Compared to *C. burnetii* grown in ACCM-2 liquid medium, 50% (163/325) of the LCV-associated genes were significantly upregulated at one of more timepoints post *G. mellonella* infection (Table 4.1). On the other hand, 72% (141/197) of SCV-associated genes were significantly downregulated at least at one time-point post infection (Table 4.2).

Table 4.1 Fold change in expression of *C. burnetii* NMII LCV associated genes that were significantly upregulated at at least one time-point from 1, 2, 3 and 4 days post infection in *G. mellonella* when compared to *C. burnetii* NMII grown *in vitro* determined by DESeq2. Dark green: significantly upregulated (Fold change > 2, p = < 0.05, light green: upregulated (fold change > 1.05), yellow: un-regulated (fold change 0.95 – 1.05) pink: downregulated (fold change < 0.95) , red: significantly downregulated (fold change < 0.5, p = < 0.05).

Locus tag	Symbol	Name	Fold change in expression (vs *in vitro*)			
			1d	2d	3d	4d
CBU_0024	csrA-1	carbon storage regulator	2.61	1.82	0.94	1.20
CBU_0029		1-acyl-sn-glycerol-3-phosphate acyltransferase	2.35	3.13	3.44	2.51
CBU_0042	hemH	ferrochelatase	3.11	2.06	1.64	1.46
CBU_0049		hypothetical protein	7.36	3.14	2.74	2.68
CBU_0063	kdtA	3-deoxy-D-manno-octulosonic-acid transferase	2.48	1.48	1.74	1.88
CBU_0148	mutT	7 8-dihydro-8-oxoguanine-triphosphatase	2.48	1.82	2.03	1.87
CBU_0155	pilB	type 4 pili biogenesis protein (nuleotide-binding protein)	2.28	0.65	0.79	1.01
CBU_0156a		phage integrase family protein	1.93	2.28	1.94	1.37
CBU_0205	gltX-1	glutamyl-tRNA synthetase	2.67	1.45	1.61	1.55
CBU_0287	folK-2	2-amino-4-hydroxy-6-hydroxymethyldihydropteridine pyrophosphokinase	1.76	1.40	2.10	1.65
CBU_0294		phosphomannomutase	2.01	1.65	1.63	1.92
CBU_0312	folD	methylenetetrahydrofolate dehydrogenase (NADP+)	5.98	5.20	5.13	3.99
CBU_0338	pepN	membrane alanine aminopeptidase	2.83	2.43	2.82	2.82
CBU_0378		hypothetical membrane associated protein	7.14	3.85	3.61	3.78
CBU_0423	panC	pantoate--beta-alanine ligase	4.53	2.21	1.08	1.90
CBU_0424	panB	3-methyl-2-oxobutanoate hydroxymethyltransferase	2.27	1.33	1.29	1.15
CBU_0439		hypothetical protein	1.12	4.42	0.61	1.80
CBU_0441	ogt	O6-methylguanine-DNA methyltransferase	3.63	1.77	1.69	1.32
CBU_0442	rplS	LSU ribosomal protein L19P	5.30	3.05	2.82	3.06
CBU_0450	ffh	signal recognition particle subunit FFH/SRP54	6.74	3.11	2.19	2.47
CBU_0461	pdhA	pyruvate dehydrogenase E1 component	2.09	1.83	1.86	1.87
CBU_0465		hypothetical protein	21.75	8.72	2.44	4.59
CBU_0479	kdsB	3-deoxy-manno-octulosonate cytidylyltransferase	0.84	1.63	2.01	2.03
CBU_0486		ribonuclease E	4.36	3.04	2.08	2.54
CBU_0492	plsX	fatty acid/phospholipid synthesis protein	4.70	2.68	2.23	2.37
CBU_0493	fabH	3-oxoacyl-[acyl-carrier-protein] synthase III	9.49	6.25	5.88	5.13
CBU_0497	fabF	3-oxoacyl-[acyl-carrier-protein] synthase	2.44	2.08	1.80	1.72
CBU_0517	aspB	aspartate aminotransferase	2.53	1.42	1.59	1.55
CBU_0519		DedA family protein	2.23	1.31	1.35	1.46

CBU_0521		chlorohydrolase/deaminase family protein	2.20	1.62	1.33	1.77
CBU_0528	rpsA	SSU ribosomal protein S1P	2.03	1.42	1.65	1.74
CBU_0570		amino acid permease	2.05	1.24	1.00	1.06
CBU_0607	mvaD	diphosphomevalonate decarboxylase	7.76	3.40	3.74	3.31
CBU_0609		mevalonate kinase	6.14	3.56	4.05	3.85
CBU_0611	yaeT	outer membrane protein assembly factor	3.22	1.99	1.88	1.92
CBU_0616		hydrolase family protein	5.40	4.22	4.61	3.03
CBU_0640		pyruvate dehydrogenase E1 component alpha subunit	3.76	3.37	3.95	3.65
CBU_0671	rfbA	mannose-6-phosphate isomerase	2.69	2.47	2.29	2.34
CBU_0673		histidinol-phosphatase	2.15	2.49	2.12	2.53
CBU_0675		transaldolase	3.90	3.35	2.60	2.55
CBU_0676		UDP-glucose 4-epimerase	8.56	8.07	8.59	10.02
CBU_0677		NAD dependent epimerase/dehydratase family	9.28	10.05	12.56	12.69
CBU_0703		O-antigen export system permease protein	2.32	3.57	4.37	3.60
CBU_0720		agmatinase	5.95	3.25	4.67	4.59
CBU_0721		deoxyhypusine synthase	6.72	3.43	5.13	5.42
CBU_0722		ornithine decarboxylase	5.89	4.24	3.04	5.19
CBU_0767		hypothetical protein	7.81	4.88	2.98	2.14
CBU_0796		adenosine 5'-monophosphoramidase	1.86	2.90	2.38	2.89
CBU_0799		hypothetical protein	6.94	3.38	10.58	1.00
CBU_0801	rimI	ribosomal-protein-S18-alanine acetyltransferase	0.71	2.10	1.55	1.54
CBU_0812		Na+ driven multidrug efflux pump	6.85	4.43	1.88	2.31
CBU_0825		nucleotide-sugar aminotransferase	13.04	7.19	5.49	5.80
CBU_0826	rfaH	transcriptional activator	15.33	9.74	10.12	8.67
CBU_0841		alpha-D-QuiNAc alpha-1 3-galactosyltransferase	2.09	2.57	2.14	1.73
CBU_0844		UDP-N-acetylglucosamine 4-epimerase	3.13	2.58	2.93	3.43
CBU_0845		UDP-N-acetyl-D-galactosamine 6-dehydrogenase	2.35	1.57	1.45	2.02
CBU_0847		3-hydroxyacyl CoA dehydrogenase	1.69	1.85	1.90	2.19
CBU_0867	rplI	LSU ribosomal protein L9P	3.73	2.53	3.23	3.48
CBU_0884	typA/bipA	GTP-binding protein	8.08	4.03	3.38	3.59
CBU_0885		hypothetical cytosolic protein	2.52	2.04	1.79	1.97
CBU_0886	coaBC	phosphopantothenoylcysteine decarboxylase	6.18	2.86	3.86	2.75
CBU_0894	folC	folylpolyglutamate synthase	2.81	1.84	1.42	1.54
CBU_0964a		hypothetical protein	2.15	2.15	1.91	1.57
CBU_0970		hypothetical exported membrane spanning protein	6.25	4.00	5.37	5.66
CBU_0993	def	peptide deformylase	5.57	3.51	3.18	4.10
CBU_0999	hflX	GTP-binding protein	2.69	2.67	2.41	1.68
CBU_1039	cyoB	cytochrome c oxidase polypeptide I	3.35	1.80	2.66	2.73
CBU_1067	ttcA	tRNA s2C32 biosynthesis protein	2.91	2.16	1.84	1.91
CBU_1081		hypothetical exported protein	2.77	3.20	2.86	2.82
CBU_1117	etfA	electron transfer flavoprotein alpha-subunit	3.31	2.88	3.27	3.02
CBU_1119		carboxymethylenebutenolidase	2.19	1.33	1.29	1.20
CBU_1124		hypothetical protein	2.64	1.66	1.52	1.13
CBU_1193	trxB	thioredoxin reductase	2.20	1.62	1.51	1.58
CBU_1194		hypothetical membrane spanning protein	2.37	1.52	1.91	2.10
CBU_1200	icd	isocitrate dehydrogenase (NADP)	3.13	1.64	1.65	1.82
CBU_1201	queA	S-adenosylmethionine:tRNA ribosyltransferase-isomerase	2.72	1.61	1.18	1.52
CBU_1206		delta(24(24(1)))-sterol reductase	3.29	2.40	1.62	1.37
CBU_1230		ATP-dependent nuclease subunit A	4.91	2.90	2.19	1.28
CBU_1240	gcp	O-sialoglycoprotein endopeptidase	6.65	5.33	5.74	5.21
CBU_1241	mdh	malate dehydrogenase	4.01	3.11	3.36	3.68
CBU_1258	ndk	nucleoside diphosphate kinase	2.44	2.22	2.12	2.49
CBU_1273		pyrophosphate--fructose 6-phosphate 1-phosphotransferase	4.92	3.07	3.03	3.29
CBU_1276		short chain dehydrogenase	3.10	2.20	1.88	1.76
CBU_1281	carB	carbamoyl-phosphate synthase large chain	5.11	2.41	2.61	2.47
CBU_1282	carA	carbamoyl-phosphate synthase small chain	3.46	2.02	1.46	1.44
CBU_1339	rnhB	ribonuclease HII	3.37	2.14	2.52	1.71
CBU_1341	guaA	GMP synthase (glutamine-hydrolyzing)	3.62	2.86	2.77	2.57
CBU_1342	guaB	inosine-5'-monophosphate dehydrogenase	2.62	1.97	1.72	1.70
CBU_1374		cytidine/deoxycytidylate deaminase family protein	0.86	1.68	2.37	2.69
CBU_1397	sucC	succinyl-CoA synthetase beta chain	3.95	3.13	3.70	3.24
CBU_1399	sucA	2-oxoglutarate dehydrogenase E1 component	5.51	3.80	4.79	3.90
CBU_1400	sdhB	succinate dehydrogenase iron-sulfur protein	2.40	1.91	2.31	2.38
CBU_1401	sdhA	succinate dehydrogenase flavoprotein subunit	5.14	3.26	3.40	3.72
CBU_1417	nusB	N utilization substance protein B	3.01	2.29	3.41	2.31
CBU_1431	rbfA	ribosome-binding factor A	4.91	3.24	3.50	2.40
CBU_1433	nusA	N utilization substance protein A	3.35	2.41	2.00	1.94

CBU_1435	nuoN	NADH-quinone oxidoreductase chain N	4.33	2.60	2.37	2.39
CBU_1436	nuoM	NADH-quinone oxidoreductase chain M	3.23	1.84	1.63	1.61
CBU_1445	nuoD	NADH-quinone oxidoreductase chain D	2.11	1.24	1.71	1.72
CBU_1451		peptidyl-prolyl cis-trans isomerase	3.19	1.87	1.00	1.14
CBU_1473	gatC	aspartyl/glutamyl-tRNA(Asn/Gln) amidotransferase subunit C	3.77	2.45	1.22	1.47
CBU_1556		hypothetical membrane spanning protein	5.76	2.06	1.88	1.81
CBU_1594		GatB/YqeY domain protein	2.72	2.04	1.85	1.89
CBU_1655	rfaE	D-glycero-D-manno-heptose-7-phosphate 1-kinase	2.68	2.18	2.26	2.42
CBU_1675	kdsA	2-dehydro-3-deoxyphosphooctonate aldolase	2.86	1.56	1.18	1.26
CBU_1699		hypothetical protein	2.32	1.61	1.27	1.13
CBU_1704	rnt	ribonuclease T	3.28	2.51	3.74	2.73
CBU_1707		hypothetical protein	2.96	3.63	5.11	4.09
CBU_1710		hypothetical protein	0.80	1.76	3.17	1.67
CBU_1711		hypothetical protein	2.19	2.38	2.39	2.31
CBU_1713		glycine dehydrogenase (decarboxylating)	4.55	2.92	3.42	2.82
CBU_1714		glycine dehydrogenase (decarboxylating)	2.73	2.53	2.52	2.55
CBU_1715	gcvH	glycine cleavage system H protein	2.99	1.76	1.79	1.63
CBU_1716	gcvT	aminomethyltransferase	5.65	2.67	1.68	1.92
CBU_1718	groEL	60 kDa chaperonin GROEL	2.53	1.92	2.50	3.13
CBU_1720	acnA	aconitate hydratase	5.45	3.42	2.61	2.71
CBU_1727	arcB	ornithine cyclodeaminase	3.45	1.81	1.68	1.79
CBU_1728		nicotinamide mononucleotide transporter	2.83	1.24	0.82	1.05
CBU_1732		D-3-phosphoglycerate dehydrogenase	3.56	2.08	0.75	1.77
CBU_1747	sspA	stringent starvation protein A	3.74	2.64	2.12	2.55
CBU_1772	yihA	GTP-binding protein	2.59	1.34	0.78	0.94
CBU_1777		hypothetical protein	4.59	2.92	2.74	2.16
CBU_1778	fbaA	fructose-bisphosphate aldolase	0.86	0.77	0.81	0.83
CBU_1784	tkt	transketolase	4.72	2.80	3.01	3.19
CBU_1787	glmS	glucosamine--fructose-6-phosphate aminotransferase	2.04	1.68	1.16	1.02
CBU_1788		hypothetical cytosolic protein	4.12	3.61	2.30	1.94
CBU_1809		ABC transporter ATP-binding protein	0.66	1.61	2.76	2.27
CBU_1814		outer membrane protein	1.43	1.65	1.81	2.14
CBU_1826	psd	phosphatidylserine decarboxylase	3.92	2.25	1.50	1.35
CBU_1827		tRNA nucleotidyltransferase	3.18	3.03	1.93	2.30
CBU_1828		hypothetical protein	3.17	2.39	2.07	1.59
CBU_1834	rmlA	glucose-1-phosphate thymidylyltransferase	3.49	2.15	2.15	1.77
CBU_1835		protoporphyrinogen oxidase	3.83	3.52	3.51	3.03
CBU_1836		homoserine dehydrogenase	2.48	1.86	2.08	2.01
CBU_1837		UDP-glucose 4-epimerase	2.03	1.58	1.58	1.59
CBU_1838	rfbC	dTDP-4-dehydrorhamnose 3 5-epimerase	2.44	1.40	1.39	1.26
CBU_1839		aminobutyraldehyde dehydrogenase	3.99	2.22	2.03	2.22
CBU_1841	pth	peptidyl-tRNA hydrolase	24.39	13.98	13.86	14.66
CBU_1842		GTP-binding protein probable translation factor	9.93	7.08	8.37	6.95
CBU_1843		hypothetical exported protein	1.18	2.18	2.05	2.23
CBU_1863		hypothetical membrane spanning protein	4.22	3.38	5.36	4.84
CBU_1872	rpe	ribulose-phosphate 3-epimerase	2.06	1.72	2.18	1.65
CBU_1881		rubredoxin	1.68	2.32	1.16	1.21
CBU_1888		hypothetical protein	5.08	1.86	2.18	1.28
CBU_1921		hypothetical protein	15.30	4.09	5.90	8.07
CBU_1929		transporter MFS superfamily	1.86	1.83	2.36	1.84
CBU_1939	atpB	ATP synthase A chain	5.50	3.01	1.73	2.22
CBU_1940	atpE	ATP synthase C chain	9.21	4.68	4.73	5.15
CBU_1943	atpA	ATP synthase alpha chain	7.26	4.93	7.57	6.97
CBU_1944	atpG	ATP synthase gamma chain	7.53	4.76	5.58	4.94
CBU_1955	pntAA	NAD(P) transhydrogenase alpha subunit	4.46	3.27	3.54	3.21
CBU_1956	pntAB	NAD(P) transhydrogenase alpha subunit	8.60	5.70	4.86	3.30
CBU_1960		hypothetical cytosolic protein	2.84	1.41	1.10	1.00
CBU_1966	hemA	glutamyl-tRNA reductase	3.02	1.91	1.47	1.78
CBU_1968	folB	dihydroneopterin aldolase	2.04	1.92	2.16	1.43
CBU_2005	rstB	sensor protein	5.87	3.02	3.67	2.44
CBU_2012	hslU	ATP-dependent endopeptidase hsl ATP-binding subunit	7.19	4.17	3.94	5.12
CBU_2030	metK	S-adenosylmethionine synthetase	2.43	1.85	1.16	1.70
CBU_2031	ahcY	adenosylhomocysteinase	3.48	3.31	4.37	4.31
CBU_2049	trpS	tryptophanyl-tRNA synthetase	2.12	1.02	0.99	1.04
CBU_2054	uvrD	DNA helicase II	3.59	1.88	1.94	2.09
CBU_2055		zinc uptake transporter	7.58	4.31	4.91	4.42

Locus tag	Symbol	Name	1d	2d	3d	4d
CBU_2068		transporter MFS superfamily	2.56	1.92	1.52	1.31
CBU_2083	queC	queuosine biosynthesis protein	1.59	2.03	2.36	1.48

Table 4.2 Fold change in expression of *C. burnetii* NMII SCV associated genes that were significantly downregulated at at least one time-point from 1, 2, 3 and 4 days post infection in *G. mellonella* when compared to *C. burnetii* NMII grown *in vitro* determined by DESeq2. Dark green: significantly upregulated (Fold change > 2, $p = < 0.05$, light green: upregulated (fold change > 1.05), yellow: un-regulated (fold change 0.95 – 1.05) pink: downregulated (fold change < 0.95) , red: significantly downregulated (fold change < 0.5, $p = < 0.05$).

Locus tag	Symbol	Name	Fold change in expression (vs *in vitro*)			
			1d	2d	3d	4d
CBU_0004	gyrB	DNA gyrase subunit B	0.49	0.56	0.52	0.59
CBU_0007		hypothetical protein	0.25	0.74	0.39	0.72
CBU_0007a		hypothetical cytosolic protein	0.42	1.31	0.65	0.79
CBU_0019		hypothetical protein	0.10	0.06	0.07	0.06
CBU_0020		ribosome-associated factor Y	0.01	0.03	0.05	0.20
CBU_0021		hypothetical protein	0.24	0.33	0.37	0.34
CBU_0048		periplasmic component of efflux system	0.40	0.51	0.64	0.64
CBU_0053	enhA.1	enhanced entry protein	0.03	0.06	0.24	0.57
CBU_0066		5-formyltetrahydrofolate cyclo-ligase	0.51	0.46	0.42	0.38
CBU_0087		phosphoglycerol transferase MdoB and related protein-like protein	0.03	0.06	0.13	0.28
CBU_0090	tolB	TolB	0.17	0.20	0.23	0.33
CBU_0115	mraZ	cell division protein	0.47	0.75	0.67	0.75
CBU_0116	mraW	S-adenosyl-methyltransferase	0.21	0.43	0.49	0.63
CBU_0167	pksH	enoyl-CoA hydratase	0.14	0.73	0.14	0.19
CBU_0173		hypothetical membrane spanning protein	0.03	0.09	0.01	0.14
CBU_0176	degP.1	endopeptidase	0.03	0.05	0.14	0.36
CBU_0181a		hypothetical protein	0.01	0.01	0.01	0.02
CBU_0193		hypothetical membrane associated protein	0.04	0.03	0.05	0.10
CBU_0206		hypothetical membrane spanning protein	0.01	0.03	0.14	0.41
CBU_0274	uvrA	excinuclease ABC subunit A	0.22	0.38	0.30	0.28
CBU_0275	hemE	uroporphyrinogen decarboxylase	0.18	0.47	0.44	0.59
CBU_0302	rpoZ	DNA-directed RNA polymerase omega chain	0.20	0.47	0.56	0.64
CBU_0303	spoT	GTP pyrophosphokinase	0.31	0.58	0.58	0.56
CBU_0311		outer membrane porin P1	0.20	0.59	1.09	1.38
CBU_0318	enhA.2	enhanced entry protein	0.01	0.02	0.16	0.47
CBU_0354		amino acid permease	0.40	0.66	0.57	0.55
CBU_0400		hypothetical protein	0.29	0.37	0.47	0.36
CBU_0419		polysaccharide deacetylase family	0.03	0.02	0.08	0.28
CBU_0425		hypothetical protein	0.74	0.39	0.27	0.19
CBU_0456		histone H1 homolog	0.12	0.64	1.30	2.12
CBU_0469		hypothetical protein	0.05	0.03	0.07	0.15
CBU_0470		purine/pyrimidine phosphoribosyl transferase	0.02	0.05	0.06	0.15
CBU_0481	artP	arginine transport ATP-binding protein	0.46	0.50	0.86	1.66
CBU_0482		arginine-binding protein	0.33	0.55	0.88	1.60
CBU_0488		bis(5'-nucleosyl)-tetraphosphatase (symmetrical)	0.12	0.25	0.30	0.44
CBU_0490		DNA Polymerase X family	0.10	0.27	0.30	0.38
CBU_0498		hypothetical exported protein	0.55	0.33	0.34	0.45
CBU_0508		hypothetical membrane spanning protein	0.35	0.35	0.59	0.49

CBU_0515		transporter	0.58	0.76	0.51	0.42
CBU_0536		hypothetical protein	0.07	0.16	0.09	0.24
CBU_0545	*lemA*	LemA	0.01	0.05	0.07	0.15
CBU_0546	*htpX*	endopeptidase	0.03	0.07	0.13	0.25
CBU_0555		hypothetical protein	0.02	0.01	0.05	0.20
CBU_0562a		hypothetical protein	0.06	0.16	0.21	0.32
CBU_0571		hypothetical exported protein	0.01	0.07	0.02	0.07
CBU_0644		plasmid stabilization system toxin protein	0.24	0.01	0.12	0.07
CBU_0645		plasmid stabilization system antitoxin protein	0.15	0.11	0.19	0.27
CBU_0711		hypothetical protein	0.04	0.22	0.18	0.17
CBU_0718		hypothetical membrane associated protein	0.00	0.02	0.08	0.21
CBU_0719		hypothetical protein	0.00	0.03	0.07	0.19
CBU_0731		hypothetical exported protein	0.04	0.06	0.17	0.52
CBU_0743	*ptsH*	phosphocarrier protein HPr	0.40	0.38	0.09	0.07
CBU_0745		ribosome-associated factor Y	0.13	0.33	0.25	0.26
CBU_0751	*murA*	UDP-N-acetylglucosamine 1-carboxyvinyltransferase	0.12	0.12	0.21	0.38
CBU_0774	*pspC*	stress-responsive transcriptional regulator	0.74	1.22	0.66	0.43
CBU_0776		ABC transporter ATP-binding protein	0.20	0.53	0.53	0.39
CBU_0789		two component system histidine kinase	0.25	0.77	0.76	0.78
CBU_0819		glutathione S-transferase	0.12	1.83	0.75	1.20
CBU_0909		sua5/YciO/YrdC/YwlC family protein	0.38	0.61	0.70	0.74
CBU_0914		hypothetical membrane spanning protein	0.13	0.21	0.21	0.26
CBU_0920		acyl-CoA desaturase	0.17	0.22	0.20	0.22
CBU_0921		hypothetical cytosolic protein	0.04	0.08	0.10	0.13
CBU_0924		O-methyltransferase	0.04	0.04	0.08	0.14
CBU_0925		membrane-bound lytic murein transglycosylase B	0.00	0.01	0.05	0.14
CBU_0943		rhodanese-related sulfurtransferase	0.02	0.07	0.15	0.41
CBU_0956		hypothetical membrane associated protein	0.04	0.08	0.23	0.42
CBU_0957		hypothetical protein	0.06	0.04	0.10	0.17
CBU_0960		transcriptional regulator	0.02	0.08	0.05	0.10
CBU_0961		hypothetical protein	0.12	0.18	0.22	0.29
CBU_0979		lipoprotein	0.05	0.15	0.26	0.36
CBU_1031		lysozyme	0.16	0.63	0.46	0.39
CBU_1050	*csrA-2*	carbon storage regulator	0.14	0.23	0.36	0.65
CBU_1089		hypothetical protein	0.83	0.39	0.28	0.18
CBU_1092		hypothetical lipoprotein	0.13	0.14	0.08	0.09
CBU_1095		hypothetical exported protein	0.04	0.08	0.11	0.21
CBU_1096	*fumC*	fumarate hydratase	0.04	0.10	0.18	0.29
CBU_1135		hypothetical exported protein	0.19	0.44	0.38	0.54
CBU_1136	*enhC*	enhanced entry protein tetratricopeptide repeat family	0.00	0.01	0.04	0.10
CBU_1137	*enhB.2*	enhanced entry protein	0.00	0.00	0.05	0.12
CBU_1138	*enhA.4*	enhanced entry protein	0.00	0.01	0.11	0.34
CBU_1154	*trpC*	indole-3-glycerol phosphate synthase	0.36	0.49	0.29	0.45
CBU_1155	*trpBF*	N-(5'-phosphoribosyl)anthranilate isomerase	0.21	0.42	0.65	0.52
CBU_1156	*trpA*	tryptophan synthase alpha chain	0.55	0.25	0.39	0.36
CBU_1169		small heat shock protein	0.11	0.21	0.44	1.14
CBU_1173		hypothetical protein	0.06	0.21	0.29	0.53
CBU_1196	*clpA*	ATP-dependent clp protease ATP-binding subunit	0.02	0.03	0.13	0.30
CBU_1202		hypothetical membrane spanning protein	0.17	0.35	0.26	0.24
CBU_1217		hypothetical membrane spanning protein	0.27	0.18	0.09	0.19
CBU_1233		5'-nucleotidase	0.11	0.24	0.17	0.15
CBU_1234		hypothetical ATPase	0.40	0.47	0.19	0.18
CBU_1252		radical SAM family enzyme	0.15	0.29	0.31	0.39
CBU_1267a	*scvA*	ScvA	0.00	0.01	0.03	0.07
CBU_1272		hypothetical protein	0.02	0.19	0.25	0.42
CBU_1280a		hypothetical protein	0.02	0.06	0.22	0.49
CBU_1294		PIN domain protein	0.22	0.25	0.16	0.22
CBU_1295		hypothetical membrane associated protein	0.09	0.14	0.13	0.12
CBU_1300		hypothetical exported protein	0.17	0.30	0.30	0.43
CBU_1314		hypothetical cytosolic protein	0.38	0.47	0.20	0.19
CBU_1331		CBS domain containing protein	0.00	0.01	0.02	0.05
CBU_1332		hypothetical cytosolic protein	0.02	0.02	0.02	0.07
CBU_1387		hypothetical cytosolic protein	0.22	0.50	0.65	0.59
CBU_1394	*enhA.5*	enhanced entry protein	0.01	0.01	0.14	0.52
CBU_1404		hypothetical exported protein	0.04	0.26	0.26	0.45
CBU_1429a		hypothetical protein	0.08	0.19	0.29	0.59
CBU_1494	*pdxJ*	pyridoxal phosphate biosynthetic protein	0.16	0.16	0.19	0.37

			Day 1	Day 2	Day 3	Day 4
CBU_1502	era	GTP-binding protein	0.75	0.45	0.62	0.34
CBU_1512		rhodanese-related sulfurtransferase	0.25	0.40	0.43	0.46
CBU_1513		short chain dehydrogenase	0.41	0.50	0.40	0.47
CBU_1516		hypothetical protein	0.01	0.10	0.12	0.26
CBU_1517		23S rRNA methyltransferase	0.19	0.14	0.14	0.12
CBU_1530		hypothetical membrane spanning protein	0.48	1.04	1.05	1.08
CBU_1560		hypothetical protein	0.15	0.22	0.21	0.27
CBU_1561		hypothetical membrane spanning protein	0.01	0.01	0.02	0.07
CBU_1596	rpoD	RNA polymerase sigma factor	0.35	0.55	0.63	0.69
CBU_1623	icmJ	IcmJ	0.37	0.53	0.78	0.76
CBU_1632	icmO	IcmO	0.41	0.41	0.78	0.72
CBU_1634	icmQ	IcmQ	0.14	0.16	0.22	0.28
CBU_1644	dotC	DotC	0.18	0.13	0.19	0.20
CBU_1648	dotaA	DotA	0.20	0.26	0.58	0.54
CBU_1649	icmV	IcmV	0.23	0.17	0.32	0.38
CBU_1669	rpoS	RNA polymerase sigma factor	0.18	0.37	0.34	0.40
CBU_1677		hypothetical cytosolic protein	0.02	0.06	0.10	0.29
CBU_1678	speG	spermidine N1-acetyltransferase	0.39	0.85	0.57	0.73
CBU_1681		hypothetical exported protein	0.01	0.07	0.13	0.36
CBU_1724		hypothetical protein	0.09	0.10	0.07	0.09
CBU_1768		hypothetical exported protein	0.04	0.06	0.08	0.11
CBU_1789		gluconolactonase	0.14	0.38	0.35	0.43
CBU_1822	sodC	superoxide dismutase (Cu-Zn)	0.19	0.28	0.27	0.45
CBU_1847b		hypothetical protein	0.04	0.22	0.43	0.56
CBU_1874		glutamate--cysteine ligase	0.38	0.42	0.59	0.60
CBU_1932		hypothetical protein	0.00	0.03	0.20	0.52
CBU_1933		hypothetical DNA-binding protein	0.01	0.03	0.09	0.23
CBU_1934		ATP-dependent DNA ligase	0.06	0.04	0.15	0.21
CBU_1950		hypothetical membrane spanning protein	0.03	0.07	0.16	0.42
CBU_1995		acylphosphatase	0.33	0.73	0.65	0.69
CBU_2016		hypothetical cytosolic protein	0.14	0.42	0.23	0.23
CBU_2023		hypothetical protein	0.23	0.45	0.53	0.67
CBU_2071		hypothetical membrane spanning protein	0.01	0.03	0.07	0.30
CBU_2079		hypothetical protein	0.04	0.12	0.29	0.41
CBUA0007		hypothetical protein	0.19	0.58	0.32	0.42
CBUA0033		hypothetical protein	0.49	1.15	0.17	0.39

The average fold change of LCV associated genes at days 1, 2, 3 or 4 days post infection is 2.78, 1.94, 1.91 or 1.87 respectively (Appendix 4.1. Whereas the average fold change for SCV associated genes at days 1, 2, 3 or 4 days post infection is 1.46, 2.85, 2.42 or 3.15 respectively (Appendix 4.1).

Together, this shows a progressive decrease in the number of LCV associated genes in parallel to a progressive increase in the number of SCV associated genes over 4 days of infection in *G. mellonella*. As the inoculum is prepared from a 7 day stationary phase culture, it is likely that this contained a mixed population of LCVs and SCVs. It is possible that SCVs switch to LCVs post inoculation and before the day 1 timepoint, hence a large number of LCV associated genes with significant upregulation on day 1 when compared to the inoculum. It is interesting that the number of SCV associated genes appears to increase, as this is typically considered to be the environmental 'spore-like' cell variant.

110

Although the data appears to show the number of LCVs decreasing over time, and the number of SCVS increasing, It is important to note that the relative abundance of *C. burnetii* LCVs and SCVs cannot be extrapolated from this data. Nevertheless, imaging of haemocytes by TEM (Figure 4.6) shows clear evidence that both LCVs and SCVs are able to exist in *G. mellonella*.

4.2.11.   Genes potentially important for *G. mellonella* infection

Identification of the most highly upregulated genes during *in vivo* infection can give an insight into genes that may be important for infection[253]. By combining the 25 most highly upregulated *C. burnetii* NMII genes at 1,2,3 and 4 days post infection of *G. mellonella* (Figure 4.14) a list of 46 genes was collated (Table 4.3) that are upregulated at one or more time-points.
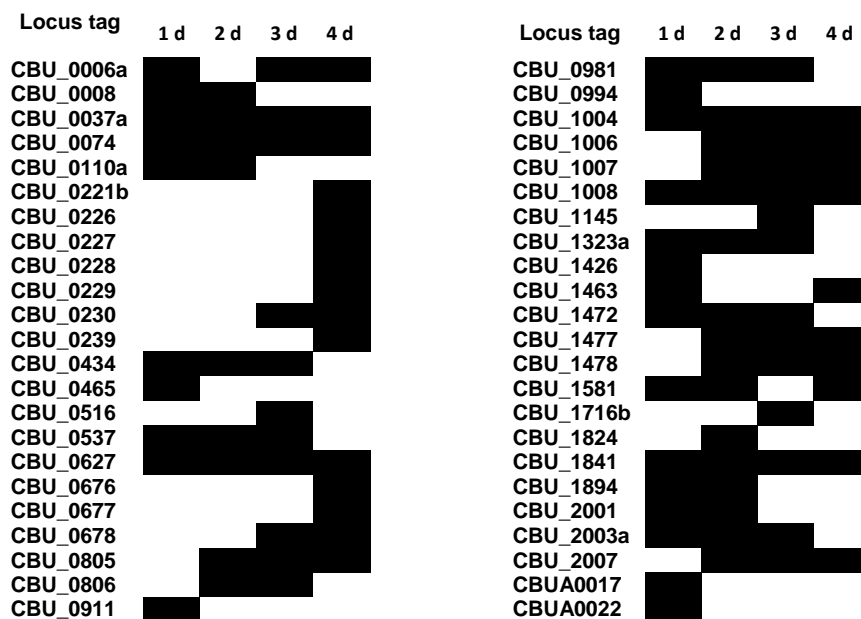
Figure 4.14 The top 25 most highly upregulated genes at days 1,2,3 or 4 days post infection

Of the 46 most highly upregulated genes, 15% (7/46) encode proteins assigned to the COG J- Translation, ribosomal structure and biogenesis, further validating the previous finding that *C. burnetii* exhibits faster growth in *G. mellonella* larvae compared to ACCM-2 medium (Figures 3.1, 3.5). The COG categories for the remaining most highly upregulated genes were 9% (4/46) H – coenzyme transport and metabolism,

4% (2/46), M – cell wall and outer membrane structure and biogenesis, and 2% (1/46) O - post-translational modification, protein turnover and chaperone. For the remaining 32 most highly upregulated genes a COG category could not be assigned.

Table 4.3. Most highly upregulated *C. burnetii* genes at one or more time-points during *G. mellonella* infection

Locus tag	Gene	Name	COG
CBU_0006a		hypothetical protein	
CBU_0008		hypothetical protein	
CBU_0037a		hypothetical protein	
CBU_0074		hypothetical protein	
CBU_0110a		hypothetical protein	
CBU_0221b		protein translation elongation factor Tu (EF-TU)	J
CBU_0226	*rplK*	LSU ribosomal protein L11P	J
CBU_0227	*rplA*	LSU ribosomal protein L1P	J
CBU_0228	*rplJ*	LSU ribosomal protein L10P	J
CBU_0229	*rplL*	LSU ribosomal protein L12P (L7/L12)	J
CBU_0230		hypothetical protein	
CBU_0239	*rplD*	LSU ribosomal protein L1E (= L4P)	J
CBU_0434		hypothetical cytosolic protein	
CBU_0465		hypothetical protein	
CBU_0516		hypothetical protein	
CBU_0537		hypothetical cytosolic protein	
CBU_0627		hypothetical protein	
CBU_0676		UDP-glucose 4-epimerase	MG
CBU_0677		NAD dependent epimerase/dehydratase family	M
CBU_0678		D-glycero-D-manno-heptose-1-phosphate adenylyltransferase	M
CBU_0805		hypothetical protein	
CBU_0806		hypothetical protein	
CBU_0911		hypothetical protein	
CBU_0981		hypothetical protein	
CBU_0994		hypothetical protein	
CBU_1004	*bioC.2*	biotin synthesis protein	H
CBU_1006	*bioF*	8-amino-7-oxononanoate synthase	H
CBU_1007	*bioB*	biotin synthase	H
CBU_1008	*bioA*	adenosylmethionine-8-amino-7-oxononanoate aminotransferase	H
CBU_1145		hypothetical protein	
CBU_1323a		hypothetical cytosolic protein	
CBU_1426		hypothetical protein	
CBU_1463		hypothetical protein	
CBU_1472		hypothetical protein	
CBU_1477	*ahpC*	Peroxiredoxin	O
CBU_1478	*ahpD*	peroxiredoxin reductase (NAD(P)H)	S
CBU_1581		hypothetical protein	
CBU_1716b		hypothetical protein	
CBU_1824		hypothetical protein	
CBU_1841	*pth*	peptidyl-tRNA hydrolase	J
CBU_1894		hypothetical cytosolic protein	
CBU_2001		hypothetical protein	
CBU_2003a		hypothetical protein	
CBU_2007		hypothetical protein	
CBUA0017		hypothetical protein	
CBUA0022		hypothetical protein	

The majority of the most highly upregulated genes are chromosomal, except from *CBUA0017* and *CBUA0023* which are encoded on the QpH1 plasmid. There is a lack of experimental data for *CBUA0017*, which could be a direction for future research into *C. burnetii* virulence. *CBUA0023* is conserved across all four known *C. burnetii* plasmids[15] and has been predicted to be a secreted T4SS effector[254]. Surprisingly transposon insertion in this gene by Martinez *et al*[19] did not show a strong replication, internalisation or cytotoxic phenotype, however this could be a result of both of the *CBUA0023* mutants used in this study having transposon insertion in the extreme ends of the gene.

Biotin has been associated with the virulence of many pathogens[255,256] including *C. burnetii*[257], and has been identified as a potential novel antimicrobial target[258,259]. The majority of the genes involved in biotin synthesis in *C. burnetii (bioA, bioB, bioC.2, bioF, bioH)* were significantly upregulated at all timepoints with the exception of *bioD* which was only significantly upregulated on days 1,2 and 3 post infection and *bioC.1* which was only significantly upregulated on day 1 post infection. Four of these genes (*bioA, bioB, bioC.2* and *bioF*) are contained in the list of the most highly upregulated at one or more timepoints. Together this provides further support of the role of biotin in *C. burnetii* virulence. Three of the most highly upregulated genes (*CBU_0676, CBU_0677* and *CBU_0678*) are predicted to involved in virenose synthesis with *CBU_0676* and *CBU_0677* contained in an operon. Virenose is a sugar unique to the O-antigen of *C. burnetii* LPS. However, as these genes are located directly upstream of a large chromosomal deletion responsible for the truncated LPS in *C. burnetii* NMII, the upregulation of these genes may be a polar effect. Both components of the *ahpCD* operon, encoding a peroxierdoxin, and a peroxieredoxin reductase were also highly upregulated. These genes have previously been identified as virulence-associated in *C. burnetii*[6,260,261] that may play a role in SCV formation[18].

Genes encoding hypothetical proteins are over-represented in the dataset. The *C. burnetii* genome consists of 33.7% hypothetical proteins[6], and 65% (30/46) of the most highly upregulated genes encode hypothetical proteins. Identification of the structure and function of these hypothetical proteins could provide further insights into the virulence mechanisms of *C. burnetii.* Experiments using transposon mutagenesis by other research groups have yielded some information on the hypothetical proteins

identified. Transposon insertion into *CBU_1716b* has been shown to result in a defect in intracellular replication, in the same study, transposon insertion in *CBU_2003a* showed a defect in internalisation[219]. *CBU_2007* encodes a putative T4SS effector. However, transposon insertion in this gene does not show a defect in replication, or CCV formation in cell culture[49,218]. In addition, transposon insertion in *CBU_0006a, CBU_0008* and *CBU_0037a* showed no defects in cell culture[49,51]. The remaining genes encoding hypothetical proteins lack experimental data, but may serve as targets for future *C. burnetii* virulence studies.

4.2.12.   Type IV secretion system

The core components of the T4SS were expressed, but not significantly upregulated at any time post infection in *G. mellonella* compared to bacteria grown in ACCM-2. Previous studies have shown that the T4SS core components were not upregulated during infection of buffalo green money cells or in mice[261]. However, in Vero cells, expression of *icmX, icmW, icmV, icmT, dotA* and *dotB* increased during the first 24 hours of infection, followed by a subsequent decline[262]. Therefore, it's is possible that the upregulation of T4SS core components occurred during the first 24 hours post infection, before the isolation of bacterial mRNA. Also, as ACCM-2 mimics the conditions within a CCV[212], where the T4SS is functional, and transcripts of many core components were abundant during *in vitro* growth. Overall these findings are consistent with previous work showing that the T4SS plays a role in infection of *G. mellonella*[115,117].

4.3. Conclusion

In conclusion, the findings in this chapter have built on the existing knowledge of the *G. mellonella* model of *C. burnetii* infection. It has been found that *C. burnetii* proliferates in *G. mellonella* haemocytes over the course of infection, and that this growth rate in *G. mellonella* haemocytes is faster than what is seen *in vitro* in ACCM-2. Although, it cannot be excluded that *C. burnetii* replicates in other *G. mellonella* cell types. It has also been shown that in *G. mellonella* haemocytes, *C. burnetii* forms a vacuole that is similar to the CCV seen in mammalian cells that appears to contain *C. burnetii* cells of both large and small colony forms. In agreement with this, mapping the transcriptome of *C. burnetii* at different time-points post infection showed a progressive decrease in expression of LCV associated genes in parallel to a progressive increase of SCV associated genes. Additionally, a wide range of *C. burnetii* genes that are upregulated during infection of *G. mellonella* have been identified, many of which encode proteins of unknown function, which should be targets for future studies into *C. burnetii* virulence.

The utility of pre-treatment of *G. mellonella* with Dex.P, a phosphorylated pro-drug of Dex. was also assessed. Whilst survival studies initially showed promising results, increasing the susceptibility of *G. mellonella* to *C. burnetii* infection and permitting the identification of attenuated phenotypes, it cannot be ruled out that these effects were seen as a result of an unknown effect by Dex.P, rather than Dex., as conversion of the pro-drug was not observed during HPLC analysis. It was decided not to continue with this aspect of the study due to the time constraints of the project.

Chapter 5. Essential genes of *C. burnetii*

5.1. Introduction

Transposon directed insertion site sequencing (TraDIS) is a negative selection screen that has be applied to identify essential genes of many bacterial species under a range of biologically relevant conditions[263]. Application of this technique to *C. burnetii* NMII aims to provide information on *C. burnetii* genes fundamental for the growth and survival of this pathogen in ACCM-2 enabling further analysis of essential gene products as prospective drugable targets. Further, conservation of essential genes in the core genome of *C. burnetii* may be determined. Application of this high throughput mutagenesis technique will greatly increase our knowledge and understanding of a pathogen for which genetic manipulation techniques have only recently become available[264].

The major aim of this chapter was to increase the saturation of a mutant pool previously generated by Dr Claudia Hemsley containing 2,415 unique insertion sites (2% of possible insertion sites). A *himar1* transposon was used to generate additional *C. burnetii* transposon mutants to increase library saturation. The library was sequenced after growth in ACCM-2 and the resulting data was concatenated with Dr Hemsley's data resulting in a library of ~ 17,000 - 20,000 unique insertion sites, depending on the analysis used. Analysis with the Bio-TraDIS pipeline revealed 512 essential genes and analysis with the Whiteley lab pipeline revealed 511 essential genes. These genes were further analysed *in silico* to investigate their conservation in the core genome of *C. burnetii* and their potential drugability.

5.2. Results and discussion

5.2.1. Transposon mutagenesis of *C. burnetii*

Transposon insertion libraries were generated in *C. burnetii* NMII using the *Himar1* Mariner transposon which inserts at TA sites in the genome, harboured on the plasmid vector pKM225. As pKM225 cannot replicate in *C. burnetii*, transposition results in the loss of the transposase, resulting in transposon mutants with a single, stable insertion[218]. Transposon mutagenesis yielded approximately 3,000 colonies per electroporation. Mock electroporation reactions using nuclease-free water in place of pKM225 resulted in numbers of colonies 20 times lower. These most likely represent spontaneous chloramphenicol resistant mutants which should not be amplified during subsequent library preparation stages. From six individual electroporation reactions, approximately 20,000 colonies were picked from ACCM-2 agarose plates and pooled to form the TraDIS library. To confirm that the mutants contained transposon insertions, an individual colony was picked at random from each plate (a total of 60 colonies) and expanded in ACCM-2. Separate qPCR reactions were performed on 16 of these randomly picked colonies, using primers targeting *C. burnetii* housekeeping gene *com1* to confirm that colonies were *C. burnetii* (GE/ml, Figure 5.1) and the chloramphenicol acetyltransferase gene *cat* to identify transposon containing mutants (Tn/ml, Figure 5.1).
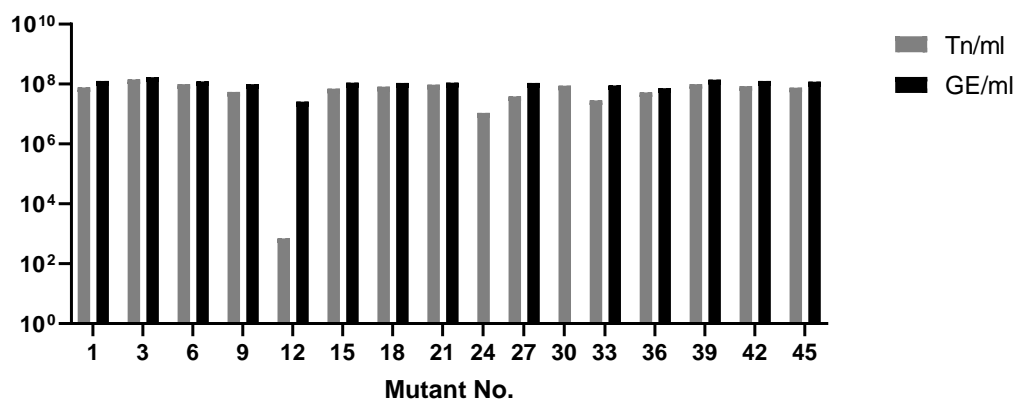
Figure 5.1. qPCR confirmation of transposon mutagenesis. Transposon copies (Tn/ml, grey bars) were determined with transposon specific primer targeting the chloramphenicol acetyltransferase gene present in *himar1*. Genome equivalents (GE/ml, black bars) were determined with *C. burnetii* specific primer targeting the

com1 housekeeping gene. 81% (13/16) of selected colonies are confirmed as transposon mutants with the exception of colonies 12, 24 and 30.

Eighty one percent (13/16) were confirmed to be transposon mutants, indicating generation of a transposon mutant pool. Nineteen percent (3/16) were not confirmed to be transposon mutants, suggesting that of the 20,000 colonies isolated, approximately 3800 may not be transposon mutants.

5.2.2. TraDIS library preparation

To identify the location of transposon insertions, the DNA flanking the transposon was sequenced. Mutant pool genomic DNA (gDNA) was isolated from three technical replicates of the 20,000 colonies isolated (Samples 1, 2 and 3) and fragmented by sonication to obtain a mean fragment size of ~500 bp. The gDNA fragments were end-repaired and A-tailed prior to analysis using an Agilent 2100 Bioanalyzer (Figure 5.2) to determine gDNA concentration and mean fragment size. Samples 1, 2 and 3 had mean fragment size of 562, 448 and 468 bp and concentrations of 16.7, 14.21 and 28.47 ng/µl respectively.

A

B
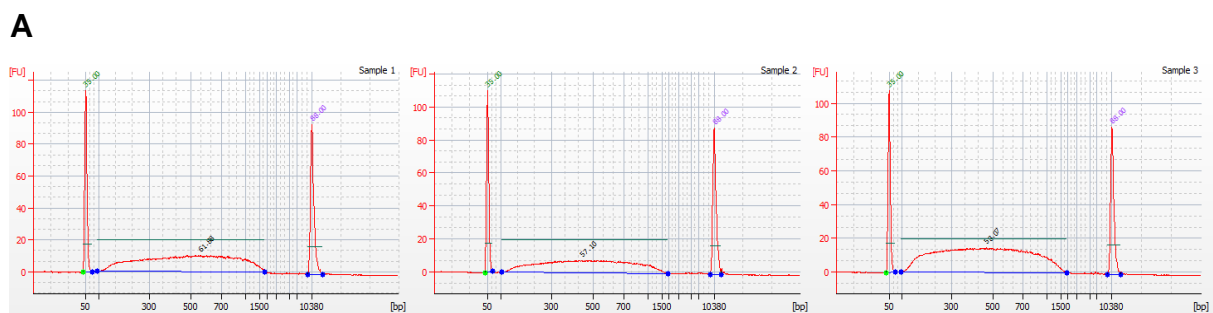
Sample ID	Sample 1	Sample 2	Sample 3
Mean gDNA fragment size (bp)	562	448	468
Concentration of fragmented gDNA (ng/ul)	16.7	14.21	28.47
Molarity of fragmented gDNA (nmol/l)	45.1	48.1	92.3

Figure 5.2. Bioanalyzer results of gDNA from samples 1,2 and 3 after fragmentation by sonication. A) Bioanalyzer traces. B) Sample concentration, molarity and mean fragment size

Samples were adapter ligated, and amplified in parallel using PCR with pKM225 specific primer Himar-seq-2 and one of three multiplexing primers: MPX1, MPX2 or MPX3. PCR products were resolved in a 2% agarose gel and 300-500 bp fragments were excised and gel extracted (Figure 5.3).
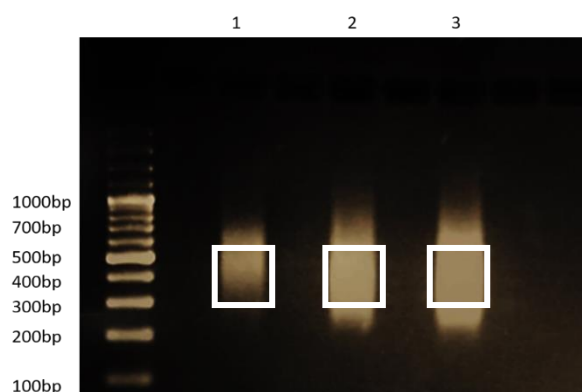
Figure 5.3. Agarose gel electrophoresis of adapter ligated, PCR amplified libraries. From left to right: 100 bp DNA ladder, sample 1, sample 2, and sample 3. PCR products were resolved on a 2% agarose gel, 300-500bp fragments (white boxes) were excised and gel extracted.

The bioanalyzer traces of size selected libraries (Figure 5.4) show mean fragment sizes of 465, 382, and 399 bp and concentrations of 2.11, 5.29 and 4.56 ng/ul for samples 1, 2 and 3 respectively

A

B
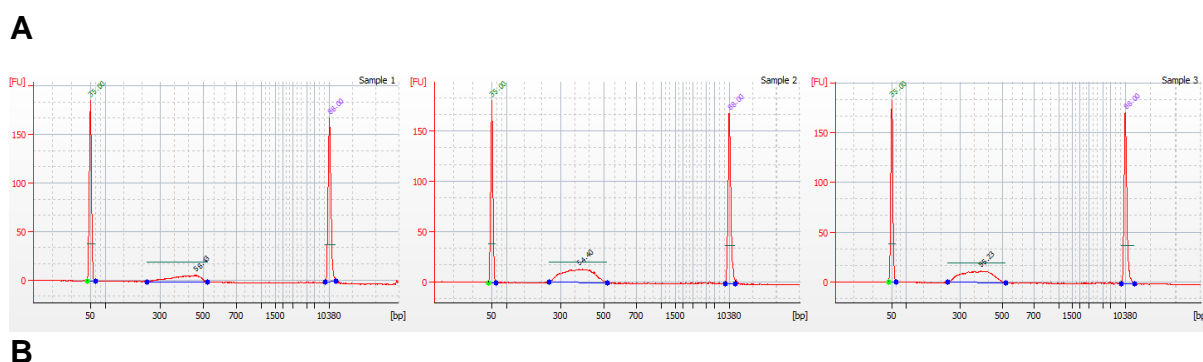
Sample ID	Sample 1	Sample 2	Sample 3
Mean library fragment size (bp)	465	382	399
Library concentration (ng/ul)	2.11	5.29	4.56
Library molarity (nmol/l)	6.9	21	17.3

Figure 5.4. Final bioanalyzer results of size selected libraries A) Bioanalyzer Traces. B) Sample concentration and mean fragment size after gel fractionation of gDNA

5.2.3. Quality control of sequencing data

Samples were sequenced as 150 bp single-end reads using an Illumina Miseq platform. Resulting reads were concatenated with .fastq files of transposon mutant pools previously generated by Dr Claudia Hemsley (for a breakdown of the relative contribution of each dataset see table 5.1). Quality control was performed using FastQC[222]. The FastQC program provides a range of analysis to investigate the quality of sequencing data. Per base sequence quality shows an overview of the range of quality scores (between 0-34) across all bases in each position of a sequencing file, with higher quality scores indicating more accurate base calling. Per base sequence quality of the concatenated fastq file used in this study (Figure 5.5.A) showed all quality scores in the 'very good' category (quality score 28-34), suggesting the data was suitable for further analysis. The per base sequence content analysis can be used to indicate the degree of pool complexity. As the G + C content of *C. burnetii* is 42.6% [6], in a random library (with the exception of the transposon tag at the start of reads) one would expect to see A and T at approximately 30% each and G and C at approximately 20% each. In the current dataset, the presence of the TGTTA transposon tag is obvious (Figure 5.5.B) and a degree of pool complexity apparent. The TGTTA sequence occurs naturally at 1,851 positions in the *C. burnetii* genome, with 1,846 within coding sequences. It is possible that this could result in false identification of up to 1,846 insertion sites.

A

B
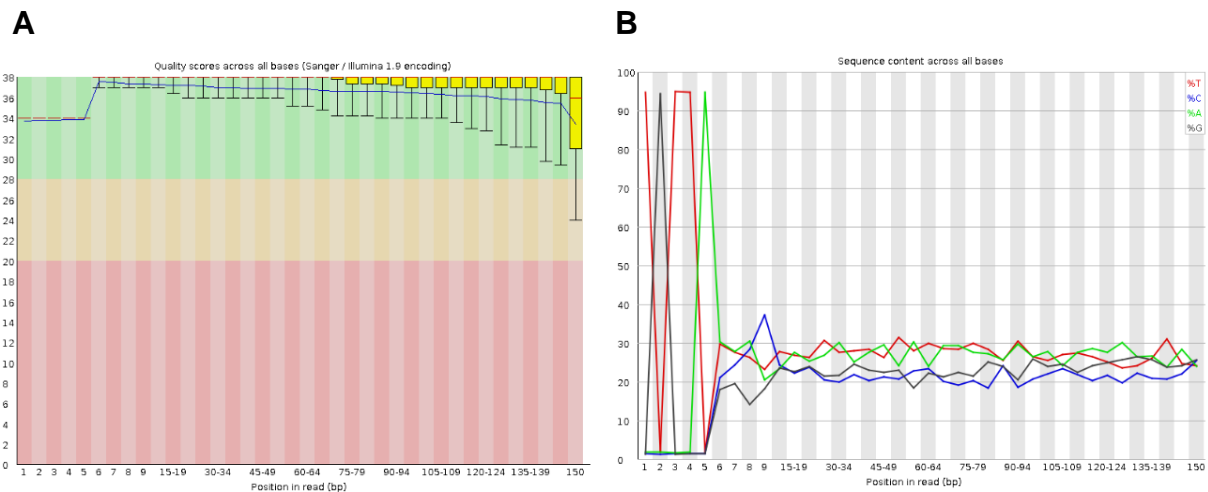
Figure 5.5. FastQC sequencing quality control. A) Per base sequence quality. X axis shows the position of the base in the sequencing read. The Y axis shows the Quality score. Green, yellow and red backgrounds represent good, satisfactory and poor quality respectively. All reads have been determined to be of high quality. B) Per base sequence content. X axis shows the position of the base in the sequencing read. The Y axis shows the percentage of T (red), A (green), C (blue) and G (black). The first 6 bases show the TGTTA transposon tag.

5.2.4. Identification of essential genes, the Bio-TraDIS pipeline

Initial analysis of essential genes was performed using the Bio-TraDIS pipeline[199]. The bacteria_tradis script was applied to the data using adjusted parameters to reduce the false positive rate, therefore increasing specificity. The command line parameters used for this were:

```
$> bactera_tradis -v --smalt_y 0.99 -m 0 -f concat_fastq.fastq -
r RSA439.fasta -t TGTTA
```

The script filters reads for those that begin with the TGTTA transposon tag (-t TGTTA). The tag is subsequently trimmed and the reads mapped to the *C. burnetii* RSA439 NMI reference genome using the SMALT short read mapper with 0 mismatches allowed in the transposon tag (-m 0), and a minimum identity threshold of 0.99 for each mapped read (--smalt_y 0.99). From a total of 22,776,700 sequencing reads, 21,109,567 (92.68%) started with the transposon tag. 17,647,764 (83.60%) reads successfully mapped to the reference genome (Table 5.1). Mapping identified 20,879

unique insertion sites distributed across the genome (Table 5.1, Figure 5.7) amounting to approximately one insertion every 97 bp, disrupting approximately 19% of available TA sites.

Table 5.1 Mapping statistics obtained using BioTraDIS. Original dataset represents the original transposon mutant pool created by Dr Hemsley. The additional dataset represents additional transposon mutants created in this study. The total dataset contains information for both datasets combined, which has been used for all future analysis.

	Original dataset	*Additional dataset*	*Total*
Total reads	7,959,683	14,817,017	22,776,700
Reads matched	7,865,597	13,243,970	21,109,567
% matched	98.81	89.38	92.68
Reads mapped	5,862,564	11,785,200	17,647,764
% mapped	74.53	88.99	83.60
Unique insertion sites	5,456	15,423	20,879

In TraDIS studies using *Himar1*, it is often the case that shorter genes are less likely to undergo insertion, as there are less TA sites in which the transposon can insert[265,266]. Although approximately 13% of *C. burnetii* genes are of length <200 bp, a very weak link between transposon insertion count and gene length is observed (Figure 5.6, $R^2 = 0.1085$ Spearman correlation coefficient, $p = < 0.0001$).
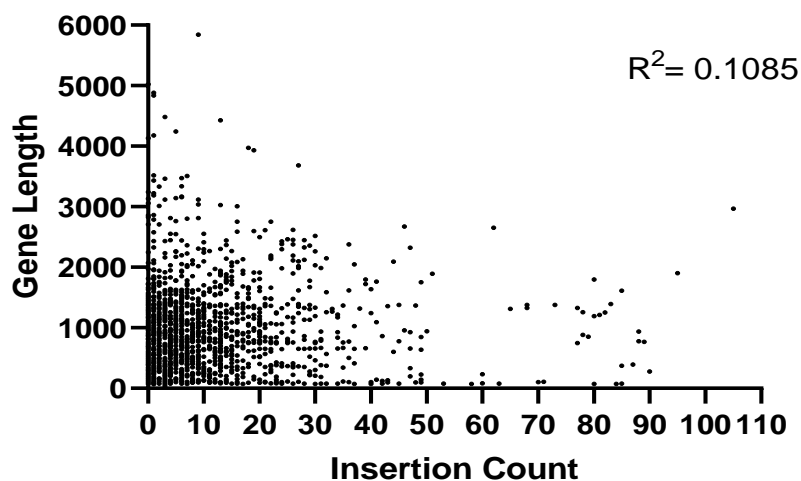
Figure 5.6. Insertion count against gene length. X axis shows the unique insertion count, Y axis shows gene length. $R^2 = 0.1085$, Spearman correlation coefficient P < 0.0001.

Another potential bias arises from the use of *himar1* which has been shown to show reduced insertion into the sequence [CG]GNTANC[CG][266]. As expected, *himar1* insertions into this sequence were not observed.

In addition to mapping statistics, the bacteria_tradis script generates insert site plot files containing insertion counts for each nucleotide position in the genome. These plot files were used to generate gene-level statistics of read counts and unique insertions per gene by applying the tradis_gene_insert_sites script. The command line parameters used for this were:

```
$> tradis_gene_insert_sites -trim3 0.1 RSA439.embl
concat_fastq_RSA439.insert_site_plot.gz
```

Adjustment of the –trim3 parameter commands the software to ignore insertions in the final 10% of the gene (at the 3' end), this has been applied as insertions at the extreme end of the gene are unlikely to have a detrimental effect on protein function, as a functional, albeit truncated protein may be transcribed.

Mapping of read counts per gene against gene position along the chromosome (Figure 5.7) shows a relatively even distribution, with a small number (approximately 10^6 genes) of genes showing an insertion carrying less than 10 reads, which could represent sequencing noise. There is some slight bias towards the origin of replication (gene position 2-5) as seen in other TraDIS studies[192,197,267]. It has previously been suggested that this bias is imparted due to the use of exponentially growing cells for electroporation, as genes close to the origin of replication are encountered in multiple copies and therefore more likely to be mutagenized by the transposon[267,268].
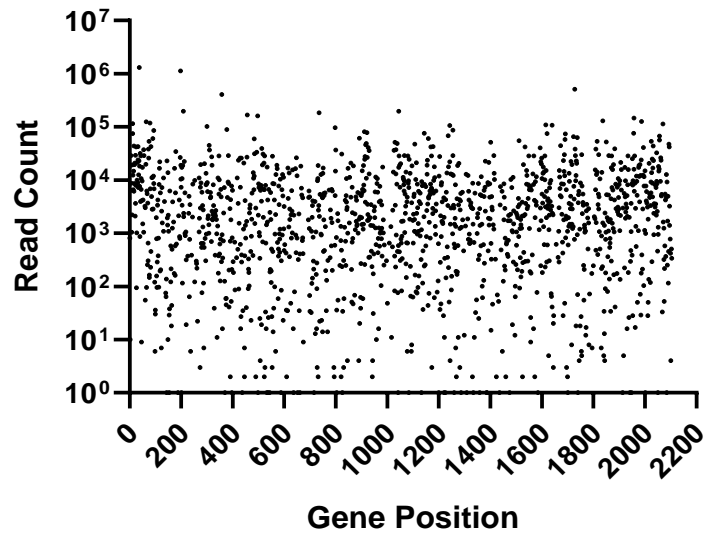
Figure 5.7. Read counts against gene position in the genome. X axis shows gene position in the genome, Y axis shows the read count. The data shows a relatively even distribution with some slight bias towards gene position 2-5, the origin of replication.

Visualisation of the number of unique insertion counts per gene across the genome (Figure 5.8, top panel) indicates that a large proportion of genes have been disrupted, with genes with multiple insertions representing non-essential genes (Figure 5.8, middle panel), and genes lacking insertion representing essential genes (Figure 5.8, bottom panel). The exception to this is the region *CBU_0679 – CBU_0698* which corresponds to the phase I LPS of NMI RSA439 reference genome, this is a region that is absent in the attenuated laboratory strain used in this study.
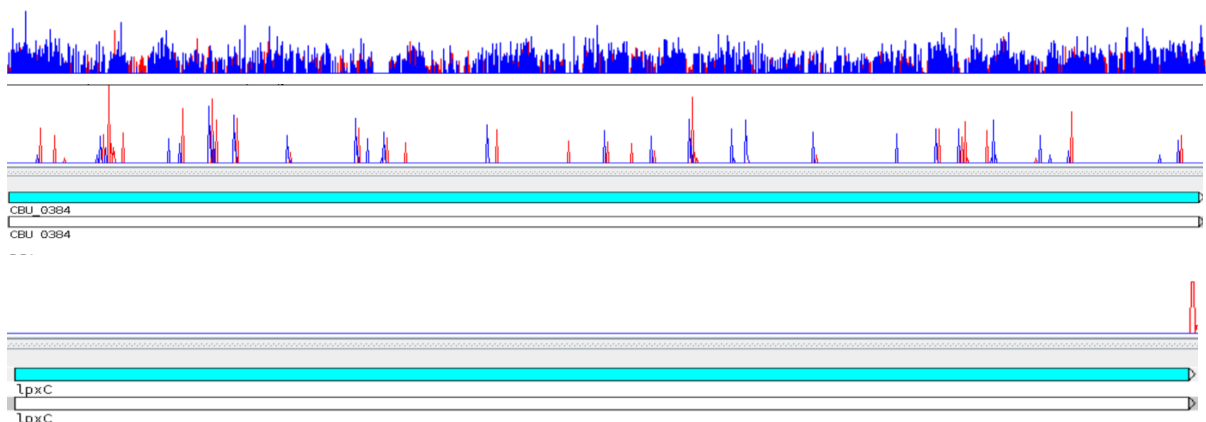
Figure 5.8. Top: Visualisation of unique insertions across the genome as determined by the BioTraDIS pipeline. Middle: *CBU_0384*, a non-essential gene. Bottom: *lpxC*, a predicted essential gene

An insertion index is calculated for each gene by normalising the insertion sites per gene to gene length. Gamma plots are fitted that attempt to fit a bimodal distribution to the data, enabling the identification of cut-off insertion index values to classify genes as essential, or ambiguous (Figure 5.9), In the typical TraDIS study one would expect to see a bimodal distribution, with essential genes forming the leftmost peak and non-essential genes forming a separate right hand peak. The data in the current study shows a power-law distribution indicating that there is still progress to be made with library saturation. Nevertheless the software was able to determine cut-off points for both essential genes (4 x 10^{-4}) and ambiguously classified genes (7 x 10^{-4}).

Gamma fits
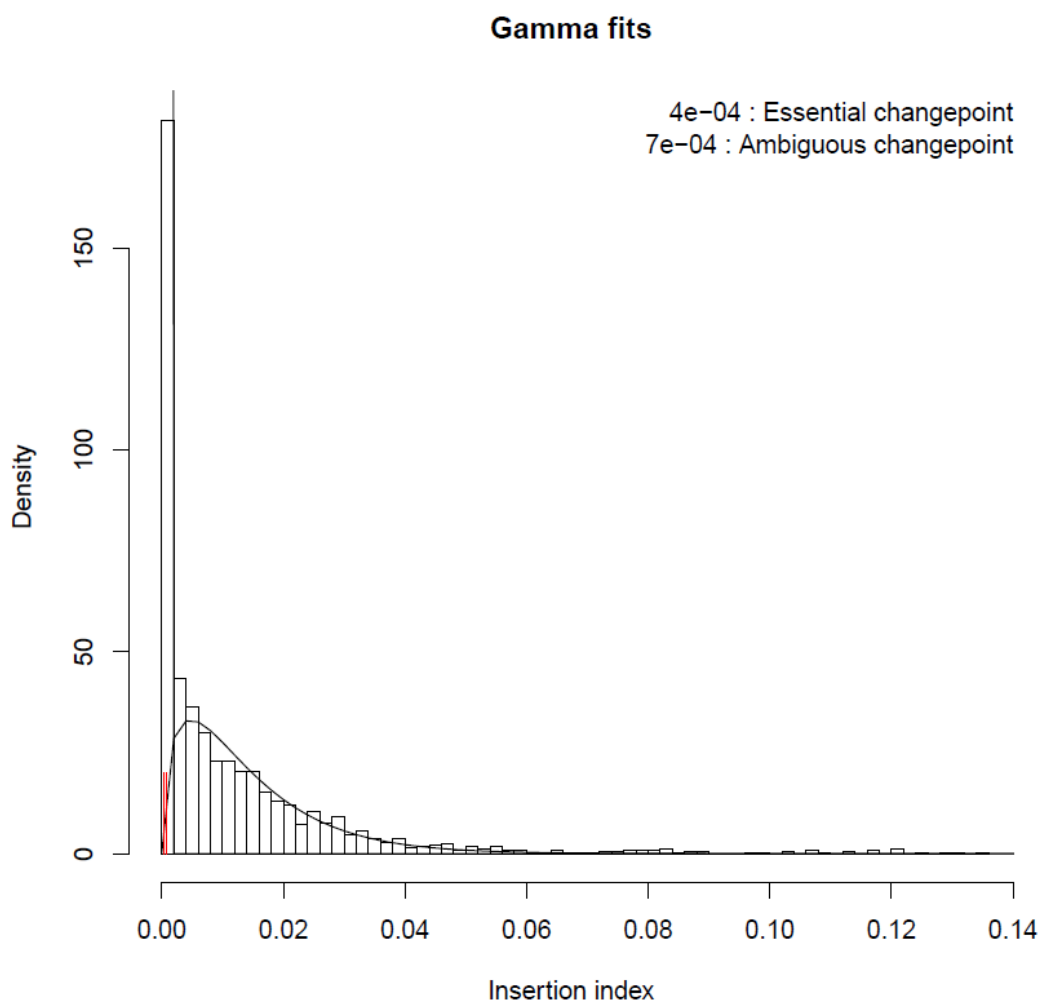
Figure 5.9. Density histogram of insertion index. X axis shows insertion index, Y axis shows density. Red lines indicate cutoff points for genes to be classified as essential (leftmost) or ambiguous (rightmost).

The *C. burnetii* genome contains 2,134 coding sequences[6]. Unique insertion sites per gene were between 0 and 116 with a mean of 8. Only 36 genes had greater than 50 unique insertion sites. After removal of phase I LPS associated genes, pseudogenes and tRNAs, a total of 502 genes on the chromosome and 10 genes on the QpH1 plasmid were identified with an insertion index less than the 4×10^{-4} cut-off for essentiality (For a list of essential genes see appendix 5.1), the vast majority of which did not contain a transposon insertion (Figure 5.8). The predicted *C. burnetii* essential genome contains 24% of the total genes. This is in line with other studies of gene essentiality in different microorganisms, where the essential genome can range from 5-35% of the total genome content[199,267–270].

Included in the list of essential genes are genes which have been shown to be essential for fundamental biological processes in other bacterial species. For example, all components of RNA polymerase (*rpoABC*), and all bar one of the subunits of DNA polymerase III (*dnaENZX, holAB*). The non-essential subunit is DNA polymerase III epsilon chain, encoded by *dnaQ* which has been classified as non-essential in other transposon sequencing studies[266,270]. In addition, 17/22 tRNA sythentases were assigned essential (*alaS, argS, CBU_1817, cysS, gltX.2, glyQS, ileS ,leuS, lysS, metG, pheS, serS, thrS, trpS, tyrS, valS).* Surprisingly, DNA supercoiling associated genes *gyrAB* have been deemed non-essential. Additionally, although *tuf2* is thought to be essential to *C. burnetii* [271], it has been classified as non-essential in this study. However, upstream operon-sharing genes *fusA*, *rpsL* and *rpsG* have been deemed essential. It is possible that the designation of these genes as non-essential are false negatives.

5.2.5. Identification of essential genes, the Whiteley lab pipeline

As the BioTraDIS analysis did not give the classical bimodal distribution expected and a number of probable false positives were identified as essential genes, it was decided to test an alternative analysis. The Whiteley lab pipeline is a custom Unix, Perl and R pipeline that has been implemented in studies with a comparable number of unique insertions to this study[272,273]. As with the previous analysis, the initial step – using the TnSeq2.sh script - was to search reads for the TGTTA transposon tag, with 0 mismatches allowed. The tag is subsequently trimmed and the reads mapped to the *C. burnetii* RSA493 NMI reference genome using bowtie2 with 1 mismatch allowed.

From a total of 22,776,700 sequencing reads, 21,358,299 (93.77%) started with the transposon tag. 17,826,711 (83.60%) reads successfully mapped to the reference genome (Table 5.1). Mapping identified 17,143 unique insertion sites distributed across the genome, which was reduced to 10,129 after correcting for polymerase slippage (Table 5.2, Figure 5.9) amounting to approximately one insertion every 200bp, disrupting approximately 8% of available TA sites.

Table 5.2. Mapping statistics obtained using the Whiteley Lab pipeline

Total reads	22,776,700
Reads Matched	21,358,299
% Matched	93.77
Reads Mapped	17, 826, 711
% Mapped	83.47
Insertion Sites	17, 143
Corrected Insertion Sites	10,129

As before, visualisation of insertion counts across the genome shows that the majority of genes have been disrupted (Figure 5.10), with the expected absent region from *CBU_0679 – CBU_0698*. This data represents the 'observed dataset'.
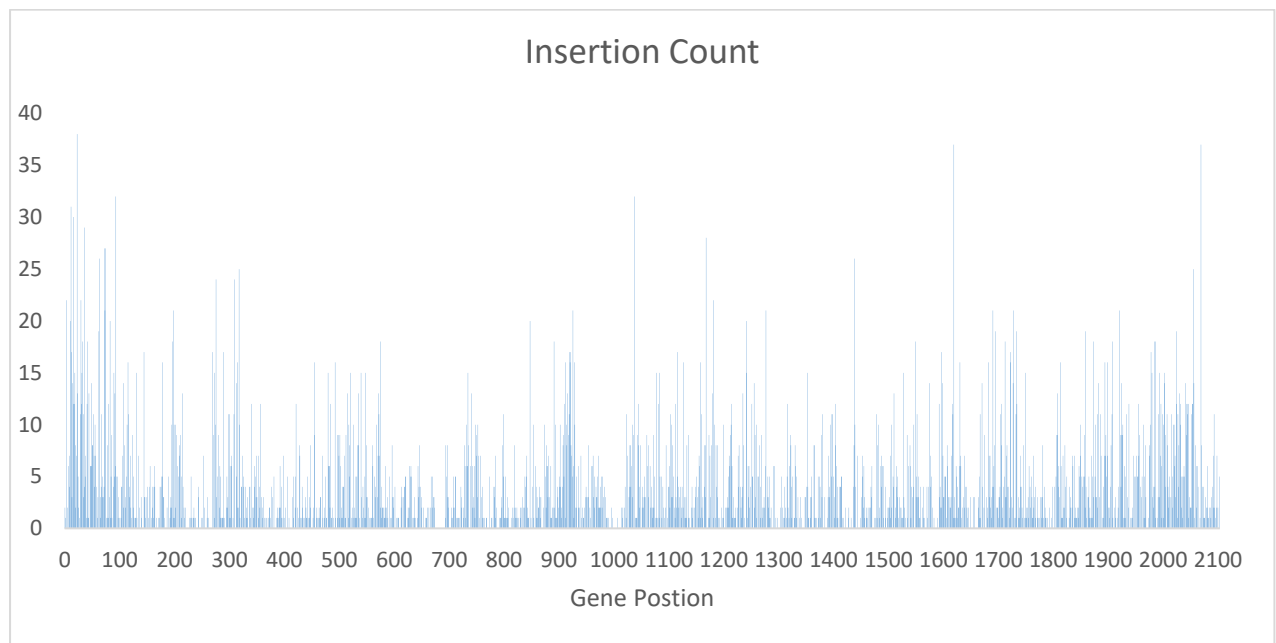
Figure 5.10. Insertion site distribution across the genome as determined by the Whiteley lab pipeline. X axis shows gene position, Y axis shows insertion frequency.

Pseudodatasets were generated by arranging the ~ 10,000 insertions and the corresponding number of reads, randomly at TA sites on the *C. burnetii* RSA493 NMI genome. This simulation was carried out 1,000 times, although no significant difference was seen above 500 pseudodatasets. This represents the 'expected dataset'.

Finally, DESeq2 was used to determine whether insertion site abundance in the observed dataset was significantly different from the expected dataset. When plotting a histogram of the log fold change between observed insertions per gene vs expected insertions per gene (Figure 5.11), a bimodal distribution is observed, with genes with less insertions than expected in the left hand peak, and genes with the same or more insertions than expected in the right hand peak. Genes were classified as essential if they contributed to the left hand side 'reduced' peak (log2 fold change < - 2.3), with an uncertainty of < 0.05 and an adjusted p value (Padj) < 0.05. It should be noted that although a bimodal distribution has been fitted by the mClust algorithm incorporated into the pipeline, the dataset is not strongly bimodal and there is a valley between the two peaks. Unlike the BioTraDIS pipeline, the Whiteley lab pipeline does not classify any genes as ambigious, i.e. falling close to the cutoff. This may result in the incorrect classification of genes with log2 fold changes close to the cutoff.
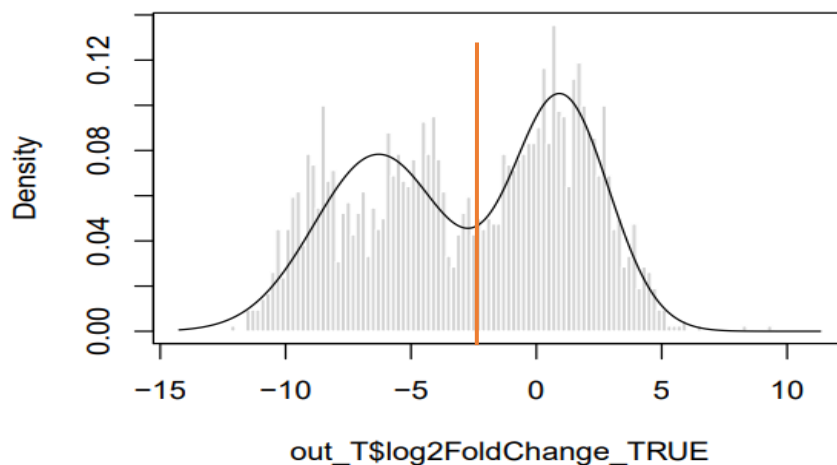
Figure 5.11. Density histogram showing the log fold change of expected vs observed insertion counts. The left hand peak contains genes with fewer insertions than expected, the right hand peak contains genes with an expected, or greater than expected number of insertion sites. The red line indicates the log2 fold change cutoff of -2.3, genes that fall on the left hand side of this line are considered to contribute to the left hand 'reduced' peak.

Based on the above criteria, the Whiteley lab pipeline revealed 506 predicted essential genes on the chromosome, and 6 predicted essential genes on the QpH1 plasmid, after the removal of Phase I LPS associated (*CBU_0679-CBU_0697*) genes and pseudogenes. This is a similar number to the previous BioTraDIS analysis.

Notably, the list of essential genes generated with the Whiteley lab pipeline contains the genes that have been shown to be essential for fundamental biological processes that were missing from the previous analysis, such as DNA supercoiling associated genes *gyrAB* and all 22 tRNA synthetases. Additionally, the predicted *C. burnetii* essential gene *tuf2*[271] was also classified as essential in this screen.

5.2.6. A comparison of BioTraDIS vs Whiteley Lab Pipeline analysis.

A comparison of predicted essential genes from the BioTraDIS and Whiteley lab pipeline revealed that the two datasets share 313 predicted essential genes. To gain an insight into which dataset was most likely to be representative of the *C. burnetii* essential genome, genes unique to each dataset were examined and compared to the database of essential genes[201]. The database of essential gene contains 19,000 entries spanning 48 bacterial strains and is often used to help validate studies of gene essentiality. The protein sequences of genes unique to each dataset were searched against the database by BlastP using a cut-off E value of $\leq 1 \times 10^{-10}$ for hits to be considered matches. The genes unique to the BioTraDIS dataset had hits for 29.6%, whereas the Whiteley lab pipeline dataset had hits for 67.2%.

In addition, the entire essential gene datasets from both pipelines were compared to a list of 20 universally conserved essential COGs determined by Grazziotin *et al.*[274], outlined in table 5.3. The BioTraDIS dataset contains representatives of 80% (16/20) of these COGs, whereas the Whiteley lab pipeline dataset contained representatives of 100% (20/20).

Together, these findings indicate that considering the small dataset obtained, the Whiteley lab analysis provided a more accurate representation of the essential gene set of *C. burnetii,* and will therefore be the data discussed for the remainder of this chapter.

Table 5.3. Identification of representatives of universally conserved essential COGs in the BioTraDIS and Whiteley lab pipeline datasets, adapted from Grazziotin *et al.*[274].

Information storage and processing			BioTraDIS	Whiteley
Translation, ribosomal structure and biogenesis (J)	COG0018	Arginyl-tRNA synthetase	Y	Y
	COG0008	Glutamyl- and glutaminyl-tRNA synthetases	Y	Y
	COG0124	Histidyl-tRNA synthetase	N	Y
	COG0495	Leucyl-tRNA synthetase	Y	Y
	COG0442	Prolyl-tRNA synthetase	N	Y
	COG0172	Seryl-tRNA synthetase	Y	Y
	COG0090	Ribosomal protein L2	N	Y
	COG0087	Ribosomal protein L3	Y	Y
	COG0088	Ribosomal protein L4	Y	Y
	COG0097	Ribosomal protein L6P/L9E	Y	Y
	COG0102	Ribosomal protein L13	Y	Y
	COG0092	Ribosomal protein S3	Y	Y
	COG0522	Ribosomal protein S4 and related proteins	Y	Y
	COG0098	Ribosomal protein S5	N	Y
Transcription (K)	COG0202	DNA-directed RNA polymerase, alpha subunit/40 kDa subunit	Y	Y
Replication, recombination and repair (L)	COG0592	DNA polymerase III sliding clamp (beta) subunit	Y	Y
Cellular processes and signalling				
Cell cycle control, cell division, chromosome partitioning (D)	COG0037	Predicted ATPase of the PP-loop superfamily implicated in cell cycle control	Y	Y
Intracellular trafficking, secretion, and vesicular transport (U)	COG0201	Preprotein translocase subunit SecY	Y	Y
	COG0552	Signal recognition particle GTPase	Y	Y
Metabolism				
Nucleotide transport and metabolism (F)	COG0462	Phosphoribosylpyrophosphate synthetase	Y	Y

5.2.7. Removal of false positive essential genes

There have been numerous studies that isolated large numbers of transposon mutants for individual mutant screening[51,218,219,275] which obtained transposon insertions in 55 of the predicted essential genes identified in this study. It is possible that the classification of these genes as essential could be false positives. This is unsurprising as the reasonably low saturation of the transposon mutant pool in this study will put

limitations on its accurateness. To increase accuracy, these 49 genes have been removed from the predicted essential genes list, with the exception of six genes in which the transposon has inserted at the extreme end of the gene. This left a total of 463 predicted essential genes (appendix 5.2).

5.2.8. Comparison to database of essential genes

Protein sequences of the 463 predicted essential genes identified in this study were searched against the database of essential genes by BlastP using a cut-off E value of 1 x 10⁻¹⁰ (or less) for hits to be considered matches. This resulted in hits for 77% (358/463) of predicted essential proteins against proteins within the database of essential genes. Of those proteins without hits, 47% (51/108) encode hypothetical proteins, explaining their absence in the database. It should be considered for this, and further analysis in this chapter, that where no hits are observed this could arise from errors in the genome annotation.

In the database of essential genes, genes encoding hypothetical proteins make up 0-48% of the essential genome of different species, indicating that some core bacterial cellular processes remain largely uncharacterised. The predicted *C. burnetii* essential genome identified in this study consists of 13% (62/466) genes encoding hypothetical proteins, within the range to be expected. Further elucidation of the structure and function of the proteins encoded by these genes may reveal important aspects related to the physiology of *C. burnetii* that makes it differ so much from other intracellular pathogens.

5.2.9. Comparison to *C. burnetii* core genome

Previous studies comparing different strains of *C. burnetii* have identified a core genome that is conserved between all stains, consisting of 1311 genes[276]. A search of the essential genes identified in this study shows 67% (310/463) of essential genes are conserved across all strains, a further 54 were only absent in one strain and therefore considered part of the core genome bringing to total to 78% (364/463). Although it was initially expected that this value would be higher, the *C. burnetii* core genome is derived from a range of *C. burnetii* strains, including those that grow poorly, or do not grow at all in ACCM-2 [11,277] and the Dugway strains, which appear to be avirulent to humans and in immunocompetent animal models of *C. burnetii* infection [22,278,279].

Next, conservation of predicted essential genes between different genomovars were inspected (Figure 5.12). The core genomes of isolates in genomic groups (GG) I, IIa, IIb, III, IV, V or VI contain 1810, 1781, 1702, 1875, 1573, 1844 or 1978 genes respectively[276]. 92% (430/463) of predicted essential genes were conserved within all available isolates in GGI, for which the ACCM-2 media used in this study was designed. Whereas only 77% (361/463) of predicted essential genes were conserved in all available isolates in GGIV, which contains isolates unable to grow in ACCM-2.

Together, this suggests that strains in different genomic groups are likely to have different repertoires of essential genes. Future work identifying the essential genome of each *C. burnetii* genomic group could reveal novel therapeutic targets. However, this would require knowing the *C. burnetii* strain that is causing infection.

5.2.10. Assignment of essential genes to clusters of orthologous groups

Next, predicted essential genes were assigned to Clusters of Orthologous Groups (COGs)[280] to give an insight into dominant predicted essential gene functions. COG categories most highly enriches among the 463 predicted essential genes were: J-Translation, ribosomal structure and biogenesis (11.3%); H – Coenzyme transport and metabolism (9.0%); C – Energy production and conservation (8.6%). and L – replication, recombination and repair (7.7%); Moderately enriched COG categories were: M – Cell wall and outer membrane structure and biogenesis (6.2%); E – Amino acid transport and metabolism (4.9%) and F- Nucleotide transport and metabolism (4.7%) (Figure 5.12). These findings are in agreement with other essential gene studies, a comparison of essential gene features between 15 bacterial, and 1 archaeal species[281] found that information, storage and processing genes are overrepresented in most species. The COG J – Translation, ribosomal structure and biogenesis were overrepresented in all species, and H –Coenzyme transport and metabolism were over-represented in 87% species. As with other studies, genes that have are poorly characterised, or have no COG annotation account for 22% of the predicted essential gene set, indicating that further trends between bacterial species may emerge, as genome annotations improve.
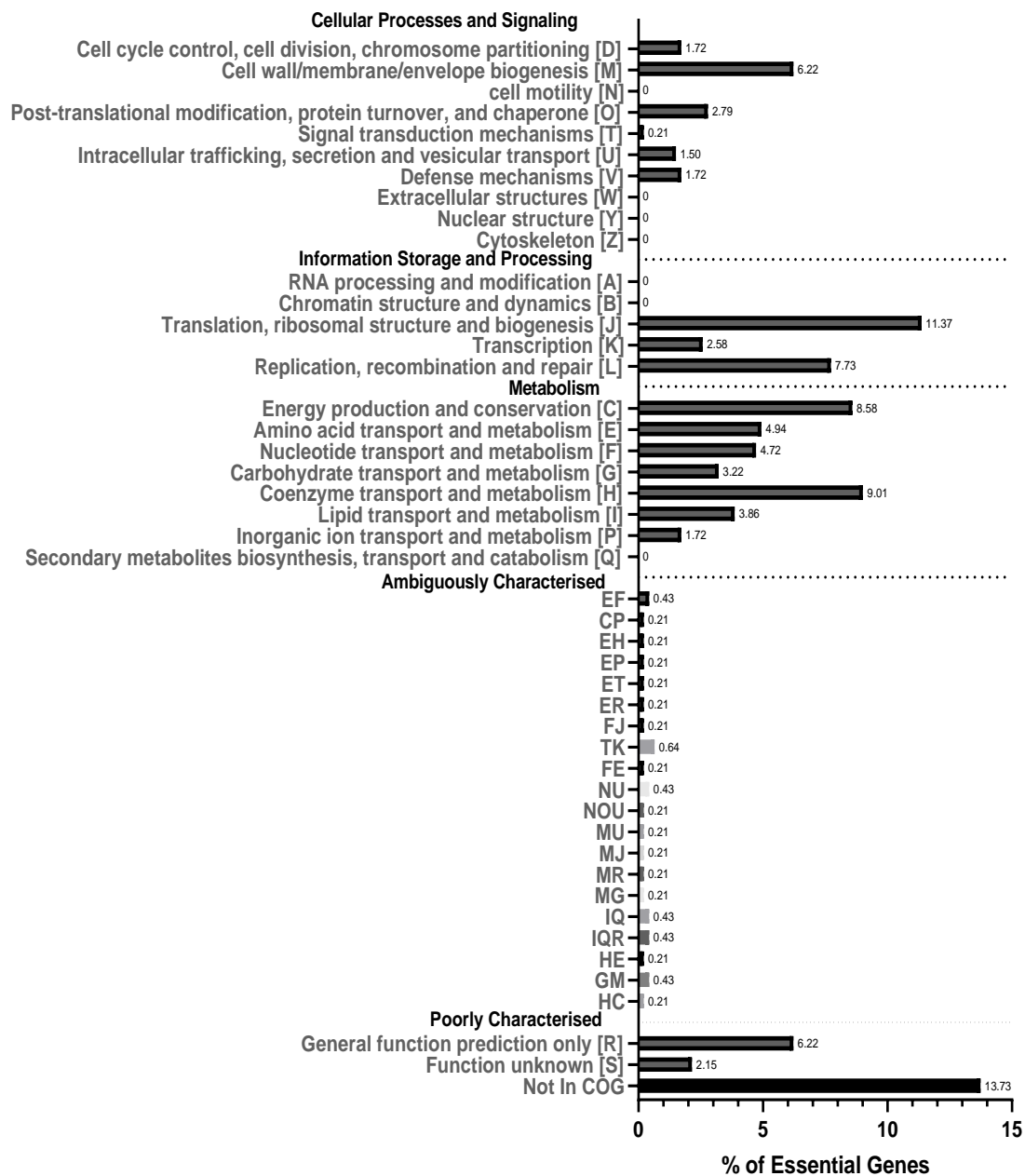
Figure 5.12 COG classification of essential genes. X axis shows the percentage of essential genes, Y axis shows COG categories

5.2.11.   Essential pathways of *C. burnetii*

Due to the structural properties of peptidoglycan, it is not surprising that the majority of the components of the peptidoglycan biosynthesis pathway were deemed essential (Figure 5.13), with an obvious essential route to synthesis. Peptidoglycan is the target for commonly used antibiotics such as the beta-lactams (e.g. penicillin, ampicillin) as well as "last resort" glycopeptide antibiotics (e.g. vancomycin). However, pathogens have developed multiple mechanisms of resistance against these drugs such as the inactivation of the antibiotic by beta-lactamases[282,283], the modification of penicillin binding proteins[284], or removal of the drug through efflux pumps[285].

Beta-lactam antibiotics have been shown to have very little effect on *C. burnetii* infection, both *in vitro* and *in vivo*[286–289], taking almost three times longer to subside a fever when compared to the current 'gold standard' doxycycline[286]. This is not surprising as beta-lactam antibiotics do not accumulate in host cells, and as a result are not appropriate for treatment against intracellular pathogens[290]. This shows that, although essential for *C. burnetii* growth and survival, these genes would not be appropriate drug targets.
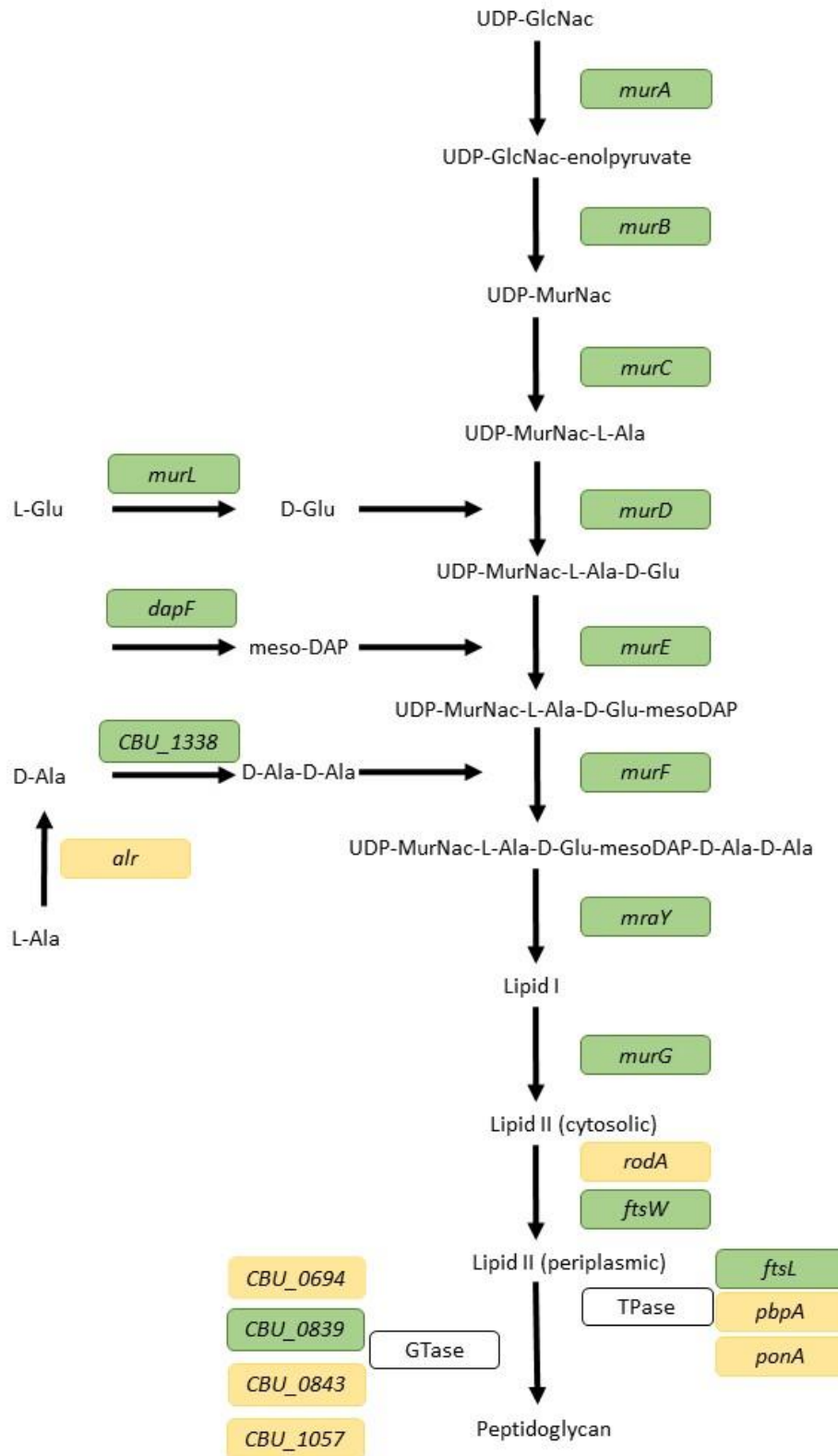
Figure 5.13 Peptidoglycan synthesis pathway. Essential genes are in green, non-essential genes are in yellow. Genes without homologs in *C. burnetii* are in grey. GTase – glycosyltransferase. TPase – transpeptidase.

Most Gram negative bacterial species source isoprenoids and isopentenyl diphosphate through the glyceraldehyde-3-phosphate pyruvate pathway[6]. However, the *C. burnetii* genome does not encode the components of the gyceraldehyde-3-phosphate pyruvate pathway, and instead utilises the mevalonate pathway, which was probably gained upon transfer from eukaryotic cells [291,292].

The majority of components of the mevalonate pathway were predicted to be essential in this study (Figure 5.14). In chapter 3, RNA-seq data showed significant upregulation in mevalonate pathway genes during infection of *G. mellonella* with *C. burnetii* , and this also correlates with infection of mice or BGM cells[293]. In *S. aureus,* downregulation of the mevalonate pathway components results in the widespread downregulation of metabolism associated genes, and the upregulation of virulence factors and cell wall biosynthesis genes[294]. In addition, the mevalonate pathway has been shown to have a vital virulence functions in *Listeria monocytogenes*[295], *M. tuberculosis* and *K. pneuomoniae* [296–300].
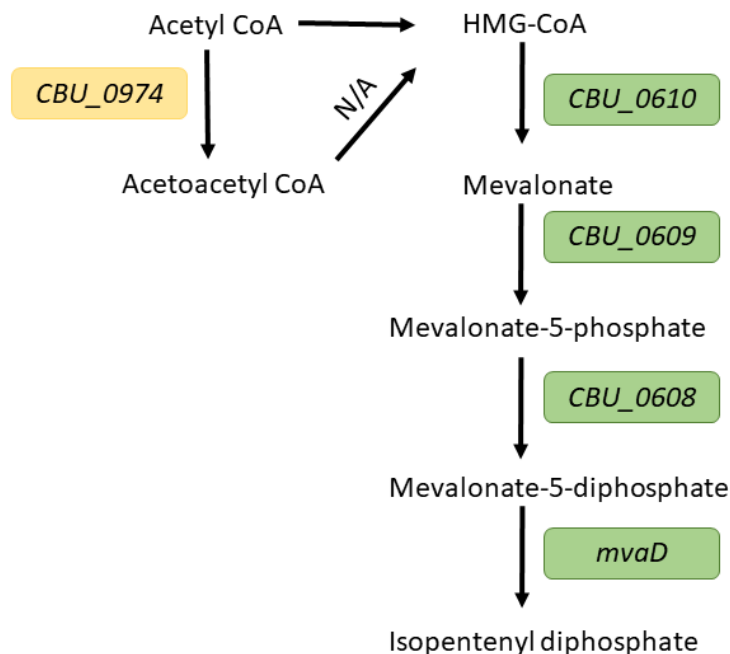
Figure 5.14 The mevalonate pathway of *C. burnetii.* Essential genes are in green, non-essential genes are in yellow

The identification of genes typically associated with virulence in this essential gene screen may be due to the media used. In general, TraDIS studies are carried out in a rich media to ensure all nutritional requirements have been met and environmental stresses have not been caused. Whereas ACCM-2 growth medium has been developed to mimic the acidic *Coxiella*-containing vacuole that *C. burnetii* resides in, in host cells[212]. It therefore may not be surprising that some virulence associated genes have been identified.

The majority of components of the biotin synthesis pathway have also been classified as essential (Figure 5.15), as well as the transcriptional repressor of the biotin operon *birA*. It is interesting that *bioA* is the only gene in this pathway that has been classified as non-essential. *bioA* has been designated as contributing to the left hand 'reduced' peak by mClust, however the Padj and uncertainty values are > 0.2, indicating that this is a true result. However, as noted in section 5.2.3 the *C. burnetii* genome contains natural TGTTA sites which may result in the incorrect mapping of sequencing reads. Further investigation revealed that the *bioA* gene contains two natural TGTTA sites, and two insertions in this gene have been identified, represented by only 319 sequencing reads. Indicating that the classification of *bioA* as non-essential is likely a false result.
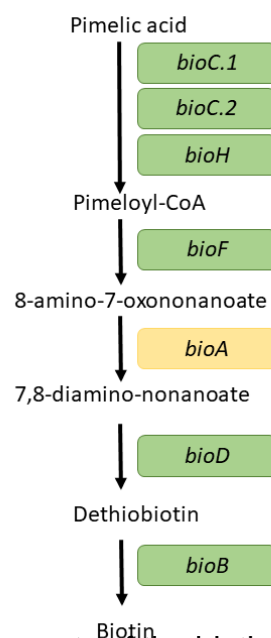
Figure 5.15 Essential components of the biotin synthesis pathway. Essential genes in green, non essential genes in yellow.

Biotin biosynthesis has previously be discussed as a promising target for the development of new antimicrobials[301,302] and has been associated with the virulence of *C. burnetii* [257]. In agreement with this, significant upregulation of biotin synthesis genes *bioC.2, bioF, bioB and bioA* was seen during RNA-seq in chapter 3. As biotin synthesis has been shown to be critical to the virulence of other intracellular pathogens *Francisella tularensis*[256,303,304] and *M. tuberculosis*[255,305] the targeting of these genes be an effective broad-spectrum treatment against intracellular pathogens. The essentiality of biotin synthesis in these species has been attributed to the absence of *bioP* and/or *bioY* in their genomes, high-affinity biotin transporters which *C. burnetii* is also lacking. As a result these pathogens require high levels of exogenous biotin, compared to species which possess *bioP* and/or *bioY* [306].

The compound MAC13772 has been shown to inhibit 7,8-diaminopelargonic acid synthase, conferred by *bioA*[301]. Although *bioA* was not predicted essential as in the current study, for some species such as *Acinitobacter baumannii,* MAC137772 shows inhibiting effects on all components on the biotin synthesis pathway[306]. Indeed incubation of *C. burnetii* in ACCM-2 supplemented with MAC13772 showed significantly reduced growth in a study by Moses *et al.*[257]. Recently, a murine model mimicking human biotin levels has been developed[306] which revealed that MAC13772 has poor bioavailability, with a half-life of 0.3 hours. This may hamper the preclinical success of MAC13772, unless improvements to its pharmacokinetic properties can be made. Nonetheless, there are an array of biotin synthesis inhibitors that have historically been overlooked as possible antimicrobials, which could be effective against *C. burnetii.*

5.2.12. Other notable essential genes

C. burnetii requires microaerobic conditions for optimal growth, demonstrated by the expression of cytochrome *bd* (encoded by *cydAB*)[212]. Although *cydB*, encoding subunit II of cytochrome D was classified as essential in this screen, *cydA.1* and *cydA.2* encoding subunit I were not. It may be that *cydB* encodes an essential subunit of cytochrome D. Browsing the database of essential genes[201] it can be seen that for some strains of *M. tuberculosis,* only the *cydB* subunit were classified as essential. However, although *M. tuberculosis* can occupy low oxygen environments [307] where *C. burnetii* is also found such as tissue granulomas[148], it is not a strictly microaerobic

bacteria. It is also possible that *cydB* has an essential role in protection against oxidative agents in the phagolysosome, as *cydB* mutants in *E. coli* and *Brucella abortus* show hypersensitivity to hydrogen peroxide[308,309].

It is well known that *C. burnetii* requires exceptionally high levels of L-cysteine for axenic growth[212], and *csdB* (also known as *sufS;* the gene conferring a group II cysteine desulfurase) was predicted to be essential in this study. Cysteine desulferases catalyse the decomposition of L-cysteine to L-alanine and sulfane sulphur, with the aid of pyridoxal 5'phosphate as a cofactor. This process provides precursors to many biosynthetic pathways such as iron-sulphur (FE-S) cluster assembly and the synthesis of biotin, lipocic acid, thiamine and nitrogenase[310]. Generally, *csdB* is co-expressed with five additional genes, *sufA, sufB, sufC, sufD* and *sufE*[311,312].

sufBCD were classified as essential in this study. The proteins encoded by these genes form a complex for Fe-S biosynthesis[313], which has been shows to be essential under oxidative stress and iron limitation[314]. The *C. burnetii* genome does not appear to contain *sufA* (or its homologoue *iscA*) or *sufE*, which is known to increase the activity of *csdB* 50-fold[312].

The proline requirements for *C. burnetii* have also been studied. Omsland *et* al. reported that *C. burnetii* was able to oxidatise proline under microaerobic conditions[212]. Bacteria utilise proline for protein synthesis and stablilty[315,316] and protection against osmotic stress[317]. *C. burnetii* has been show to actively transport glucose, glutamate and proline from the host cell intracellular environment in a pH dependent manner[318,319], and early work suggested that proline could be important for survival in the acidic CCV[318]. Later studies showed that *C. burnetii* uses a PmrA/B two-component system to sense the lysosomal environment, and induce a transcriptional shift that mediates virulence through the up-regulation the T4SS and effector proteins[320,321], thus driving the formation of the CCV. A study by Newton *et al.*[322] has shown that the presence of proline (as well as phenylalanine and serine) is sensed by PmrB, and specifically induces the expression of PmrA regulated genes, subsequently inducing virulence of *C. burnetii.* Genes involved both in proline synthesis (*arcB)* and metabolism (*putA)* were predicted to be essential in this study. *arcB* confers ornithine cyclodeaminase, an enzyme capable of synthesising proline in a single step through

the deamination of ornithine[323–325]. *arcB* did not have hits against the database of essential genes in section 5.2.7. and to date, nobody has investigated *arcB* in *C. burnetii* . *putA* encodes a bi-functional enzyme with both proline dehydrogenase and Δ^1-pyrroline-5-carboxylate dehydrogenase activities responsible for the metabolism of proline to glutamate.

sodB and *sodC* encode superoxide dismutase enzymes known to protect bacteria from reactive oxygen species such as superoxide and hydrogen peroxide and have been identified as a potentially important virulence factor for *C. burnetii* [326]. The finding of these genes as essential in this study underpin the importance of superoxide dismutase enzymes in the protection of *C. burnetii* in the harsh intracellular environment.

5.2.13.   T4SS and effector protein essentiality

None of the core components of the T4SS were classified as essential, this is to be expected as transposon mutants in almost all of these genes have previously been made[219]. Twelve predicted T4SS effector proteins were classified as essential (Table 5.4). Ten are designated to confer hypothetical proteins of unknown function. A search against the Pfam database using HMMER[327] did not reveal any significant hits for the proteins encoded by these genes, their function remains elusive.

Table 5.4 Predicted essential genes encoding T4SS effector proteins.

Locus tag	Gene name	Function	Reference
CBU_0773	phnB	PhnB	Larson et al
CBU_0794	CBU_0794	hypothetical protein	Larson et al
CBU_0881	CBU_0881	hypothetical cytosolic protein	Larson et al
CBU_1213	CBU_1213	ankyrin repeat protein	Larson et al
CBU_1314	CBU_1314	hypothetical cytosolic protein	Larson et al
CBU_1349	CBU_1349	hypothetical cytosolic protein	Larson et al
CBU_1370	CBU_1370	hypothetical membrane associated protein	Larson et al
CBU_1607	CBU_1607	hypothetical protein	Larson et al
CBU_1614	CBU_1614	hypothetical protein	Larson et al
CBU_1686	CBU_1686	hypothetical protein	Larson et al
CBU_1819	CBU_1819	hypothetical membrane associated protein	Larson et al
CBUA0023	CBUA0023	hypothetical protein	Larson et al

5.2.14.   Drugability investigation

Antibiotics work by either inducing bacterial cell death (bactericidal antibiotics) or by inhibiting bacterial growth (bacteriostatic antibiotics)[328]. The most commonly used antibiotics generally target one or more essential biochemical processes in bacteria, such as peptidoglycan synthesis (e.g. beta lactams, glycopeptides), protein synthesis (e.g. tetracyclines, macrolides), DNA replication (e.g. quinolones) or RNA transcription (e.g. rifamycins)[329]. Due to the ever increasing emergence of antibiotic resistance, there is a need for new antibiotic drug targets.

Due to the requirement of essential gene products for bacterial survival, the identification of essential genes is a starting point for the identification of unexploited drug targets. However, they do not all have the same drugability potential. There are many criteria for a gene product to be considered a good drug target, these include (but are not limited to), the target being required for survival in the host environment, for all pathogenic strains of the species. The fact that ACCM-2 was developed to imitate the conditions in a host cell suggests that some of the essential genes identified in this study may also prove to be essential during human infection. In addition, the product must be able to be purified to enable the development of biochemical assays to assess drug binding and efficacy i.e. no transmembrane domains, and the target product must be accessible for the drug in the context of the entire bacterial cell. For the case of intracellular pathogens like *C. burnetii,* this is further complicated as the drug must be able to penetrate and be retained in the infected host cell.

To make progress towards the identification of potential drug targets, the products of essential genes identified in this study were used in a BlastP against both the human genome, and human gut microbiome catalogue[232], followed by the identification of genes conserved within the core genome, and finally transmembrane domain prediction. A pipeline of this workflow can be seen in figure 5.16.
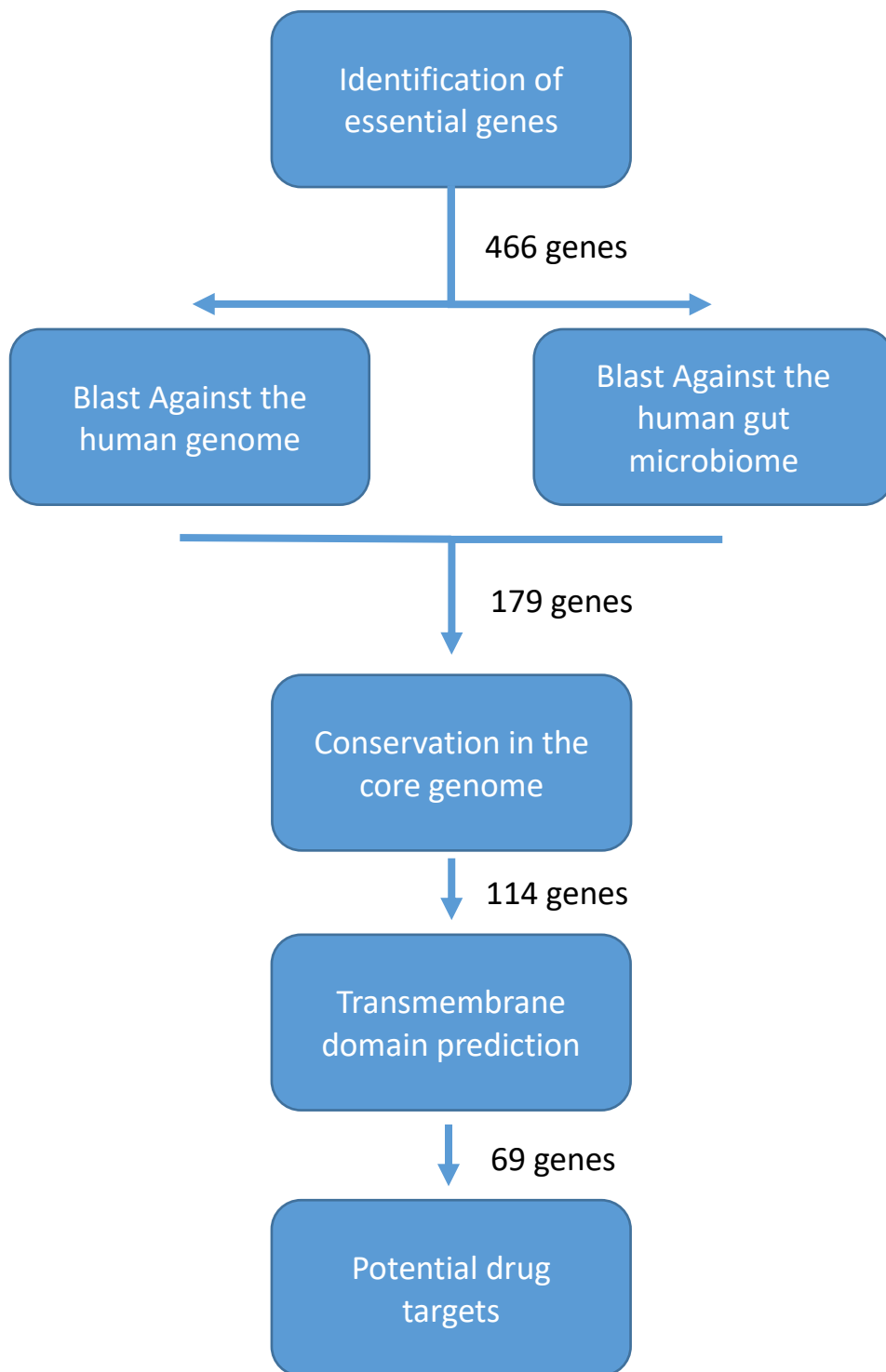
Figure 5.16. Criteria applied to identify potential drug targets from the list of essential genes identified in this study.

As an initial screen to determine whether any of the proteins encoded by the 466 predicted essential genes identified could theoretically make suitable novel drug targets a BlastP was performed against both the human genome, and the human gut microbial gene catalogue[232] using cut off a of E-value $< 1 \times 10^{-5}$ and percentage identity > 40%. For the BlastP against the human gut microbial gene catalogue only proteins encoded by essential genes with greater than 10 hits were excluded, as it has been hypothesized that targets with less than 10 hits are unlikely to disrupt the gut microbiome[265]. All encoded proteins with hits against the human genome were excluded, with the aim to avoid potential toxicity. A total of 87 and 255 hits were obtained for the two databases respectively. 179 encoded proteins did not get hits in either database.

As a key characteristic of novel antimicrobial targets is the conservation of targets across the majority of pathogenic strains of the given species, 114 genes which are conserved across the *C. burnetii* core genome were taken forwards. Additionally, drug targets must also be amenable to the development of biochemical assays on the protein of interest, the presence of transmembrane domains makes this extremely difficult. The transmembrane predictor TMHMM[234] was used to assess transmembrane domains in the candidate potential drug targets, and 45 transmembrane proteins were removed from the analysis, leaving 69 potential drug targets (Table 5.5).

Table 5.5. Potential drug targets identified in this study

Locus Tag	Gene Name	Function
CBU_0168	CBU_0168	acyl carrier protein
CBU_0182	CBU_0182	homing endonuclease
CBU_0221	CBU_0221	4'-phosphopantetheinyl transferase
CBU_0307	CBU_0307	outer membrane protein
CBU_0323	CBU_0323	acyl carrier protein
CBU_0415	CBU_0415	guanine deaminase
CBU_0467	bioC1	biotin synthesis protein
CBU_0500	holB	DNA polymerase III
CBU_0540	smc	chromosome partition protein
CBU_0557	holA	DNA polymerase III
CBU_0562	CBU_0562	hypothetical ATPase
CBU_0586	CBU_0586	pyridine nucleotide-disulfide oxidoreductase family
CBU_0596	CBU_0596	metal-dependent hydrolase
CBU_0609	CBU_0609	mevalonate kinase
CBU_0616	CBU_0616	hydrolase family protein
CBU_0620	lpxB	lipid-A-disaccharide synthase

CBU_0621	CBU_0621	NAD-dependent oxidoreductase
CBU_0640	CBU_0640	pyruvate dehydrogenase E1 component alpha subunit
CBU_0641	CBU_0641	leucine dehydrogenase
CBU_0643	ribD	Diamino-hydroxyphosphoribosylaminopyrimidine deaminase
CBU_0678	CBU_0678	D-glycero-D-manno-heptose-1-phosphate adenylyltransferase
CBU_0706	CBU_0706	hypothetical protein
CBU_0722	CBU_0722	ornithine decarboxylase
CBU_0773	phnB	PhnB
CBU_0793	CBU_0793	hypothetical protein
CBU_0794	CBU_0794	hypothetical protein
CBU_0818	CBU_0818	transcriptional regulator
CBU_0822	CBU_0822	Fic family protein
CBU_0834	CBU_0834	methyltransferase
CBU_0836	CBU_0836	radical SAM superfamily protein
CBU_0840	asnB2	asparagine synthetase family protein
CBU_0842	wecB	UDP-N-acetylglucosamine 2-epimerase
CBU_0858	nadE	glutamine-dependent NAD( ) synthetase
CBU_0860	CBU_0860	hypothetical protein
CBU_0949	CBU_0949	hypothetical cytosolic protein
CBU_0976	CBU_0976	methylglutaconyl-CoA hydratase
CBU_1002	birA	biotin operon repressor
CBU_1004	bioC2	biotin synthesis protein
CBU_1005	bioH	carboxylesterase
CBU_1010	CBU_1010	hypothetical protein
CBU_1015	CBU_1015	hypothetical cytosolic protein
CBU_1028	CBU_1028	hypothetical protein
CBU_1084	CBU_1084	two component system histidine kinase
CBU_1086	CBU_1086	transposase
CBU_1104	CBU_1104	transposase
CBU_1136	CBU_1136	enhanced entry protein enhC
CBU_1213	CBU_1213	ankyrin repeat protein
CBU_1226	CBU_1226	NAD-specific glutamate dehydrogenase
CBU_1293	grpE	GrpE
CBU_1314	CBU_1314	hypothetical cytosolic protein
CBU_1349	CBU_1349	hypothetical cytosolic protein
CBU_1442	nuoG	NADH-quinone oxidoreductase chain G
CBU_1512	CBU_1512	rhodanese-related sulfurtransferase
CBU_1614	CBU_1614	hypothetical protein
CBU_1685	CBU_1685	hypothetical protein
CBU_1686	CBU_1686	hypothetical protein
CBU_1688	CBU_1688	deoxycytidine triphosphate deaminase
CBU_1709	dapB	dihydrodipicolinate reductase
CBU_1727	arcB	ornithine cyclodeaminase
CBU_1799	CBU_1799	acetyltransferase
CBU_1805	CBU_1805	bacterial regulatory protein
CBU_1812	CBU_1812	erythronate-4-phosphate dehydrogenase
CBU_1820	CBU_1820	hypothetical protein
CBU_1821	CBU_1821	hypothetical protein
CBU_1825	CBU_1825	hypothetical protein
CBU_1828	CBU_1828	hypothetical protein
CBU_1942	atpH	ATP synthase delta chain

CBU_2008	argS	arginyl-tRNA synthetase	
CBU_2096	CBU_2096	hypothetical protein	

Potential drug targets were used for a BlastP analysis against targets in the Drugbank database, using a cut-off Evalue of 10^{-25} in line with other studies. The search showed nine of the potential drug targets may be targeted by 18 small molecule drugs in the database (Table 5.6), across the categories of approved, experimental, investigational and nutraceutical. One of the drugs is classified as withdrawn.

Table 5.6. Potential drug targets with BlastP hits against the Drugbank database using a cutoff evalue of 10^{-25}

Gene	Drug	Type	Accession
CBU_0640	NADH	Approved, nutraceutical	DB00157
CBU_0641	(s)-3-phenyllactic acid	Experimental	DB02494
	Phenylpyruvic acid	Experimental	DB03884
	Pyridoxal phosphate	Approved, investigational, nutraceutical	DB00114
	Putrescine	Experimental	DB01917
	Pyridoxine phosphate	Experimental	DB02209
	N-Pyridoxyl-Glycine-5-Monophosphate	Experimental	DB02824
CBU_0722	L-Eflornithine	Experimental, investigational	DB03856
	N(6)-(pyridoxal phosphate)-L-lysine	Experimental	DB04083
	Geneticin	Experimental	DB04263
	Spermine	Experimental, nutraceutical	DB00127
	Eflornithine	Approved, withdrawn	DB06243
CBU_0842 (wecB)	Uridine-Diphosphate-N-Acetylgalactosamine	Experimental	DB02196
	Uridine-5'-Diphosphate	Experimental	DB03435
CBU_0858 (nadE)	Deamido-Nad+	Experimental	DB04099
CBU_1002 (birA)	BIOTINOL-5-AMP	Experimental	DB04651
CBU_1442 (nuoG)	NADH	Approved, nutraceutical	DB00157
CBU_1709 (dapB)	Dipicolinic acid	Experimental	DB04267
CBU_1727 (arcB)	2-(N-morpholino)ethanesulfonic acid	Experimental	DB03814

5.2.15. Determination of a population bottleneck in *G. mellonella*

To identify virulence-associated genes in *G. mellonella* it was first necessary to assess whether there was a population bottleneck during infection. In TraDIS studies, the presence of a population bottleneck can result in the stochastic loss of mutants, rather than because the gene is important for virulence. To identify whether a population bottleneck was apparent in *G. mellonella, C. burnetii* NMII was spiked at a 1:1000 ratio with two NMII mutants: a Tn-*intergenic* mutant which should behave as the wild type, and a Δ*dotA* known attenuated mutant. *G. mellonella* were infected at a dose of 10^6

GE/larvae and the haemocytes were harvested immediately after infection (T0) or at 3 days post-infection (T3) (Figure 5.17). Although no significant difference was seen between *C. burnetii* NMII::Tn-*intergenic* and *C. burnetii* NMIIΔ*dotA* at 3 days post-infection ($p = 0.13$, unpaired t-test) a degree of separation between the two mutants was apparent, which should allow the identification of mutants with reduced fitness in the TraDIS study.
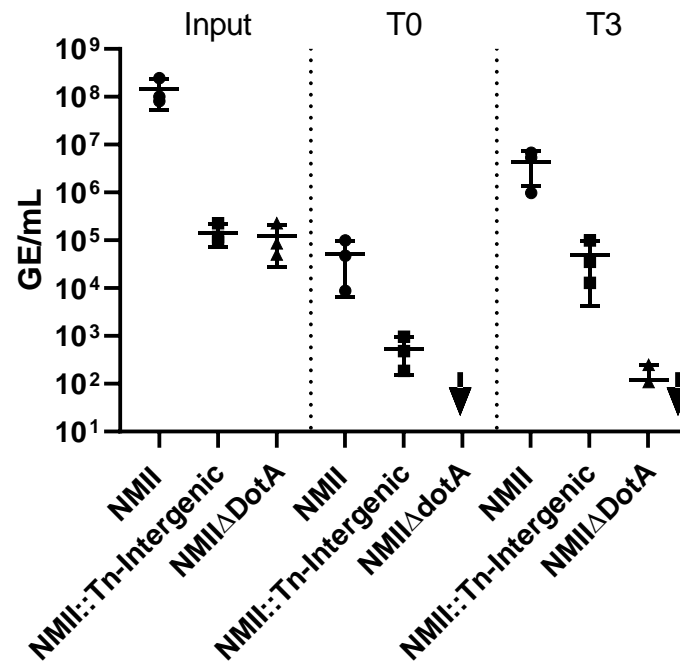
Figure 5.17. Population bottleneck determination in *G. mellonella*. *C. burnetii* NMII was spiked with *C. burnetii* NMII::Tn-*intergenic* and *C. burnetii* NMIIΔ*dotA* at a ratio of 1:1000 mutants: wildtype. Larvae were injected at a dose of 10^6 GE/larvae and haemocytes were harvested immediately after infection (T0) and 3 days post-infection (T3). Each point represents the mean of 3 larvae, error bars show standard deviation. The experiment was repeated on 3 occasions. No significant different was seen between *C. burnetii* NMII::Tn-*intergenic* and *C. burnetii* NMIIΔ*dotA* at T3 ($p = 0.13$, unpaired t-test) however a degree of separation is apparent. Downwards arrows indicate GE/mL less than the limit of detection.

5.2.16.　　　Input of transposon mutant pools into *G. mellonella*

To identify virulence-associated genes in *G. mellonella*, the transposon mutant pools created in section 5.2.1 were plated out at a dilution to obtain approximately 500 colonies per plate. After 14 days of incubation at 37°C in microaerobic plates were pooled in groups of 2 to obtain sub pools of approximately 1,000 colonies. Groups of 10 *G. mellonella* were injected at a dose of 10^6 GE/larvae (i.e. each colony theoretically represented 1,000 times in the inoculum), and larvae were incubated at 37°C for 3 days to allow for competition between mutants. The remaining inoculum was used for gDNA extractions of the input pool. On day 3 post-infection any dead larvae were discarded, and haemocytes were extracted from all survivors. Approximately 100 µl of haemolymph was obtained per group. Haemocytes were washed 3 times in PBS, lysed by three freeze-thaw cycles and diluted 1 in 50 to obtain approximately 500 colonies/plate (calculated using growth in haemocyte data from chapter 4.2.2). One hundred microlitre aliquots were plated onto ACCM-2-agarose plates containing chloramphenicol to select for mutants, and amphotericin B to prevent contamination from larvae flora. 60 plates were used per replicate. After 14 days of incubation at 37°C in microaerobic conditions *C. burnetii* colonies were washed from the plates and expanded in 25ml ACCM-2 containing chloramphenicol to prevent wild-type breakthrough. Cultures were incubated for 7 days at 37°C in microaerobic conditions. No colonies were obtained from plates inoculated with haemocytes from PBS inoculated larvae. Unfortunately, due to time constraints and difficulty with contaminants only one of the sub-pools of 1,000 mutants could be inputted to *G. mellonella*. This is therefore treated as a pilot study.

5.2.17.　　　TraDIS library preparation

After 7 days of expansion gDNA was extracted from the cultures and library preparation was performed on the input and output pools as described in section 5.2.2. Upon fragmentation bioanalyzer traces showed the three replicates of the input pool had mean fragment sizes of 509, 562 and 448 bp and concentrations of 19.88, 24.06 and 20.12 ng/µl respectively (Figure 5.18 A top row, Figure 5.19 B). The three replicates of the output pool had mean fragment size of 446, 470 and 451 and concentrations of 18.08, 18.74 and 36.83 ng/µl respectively (Figure 5.18 A bottom row, Figure 5.18 B).

A

B
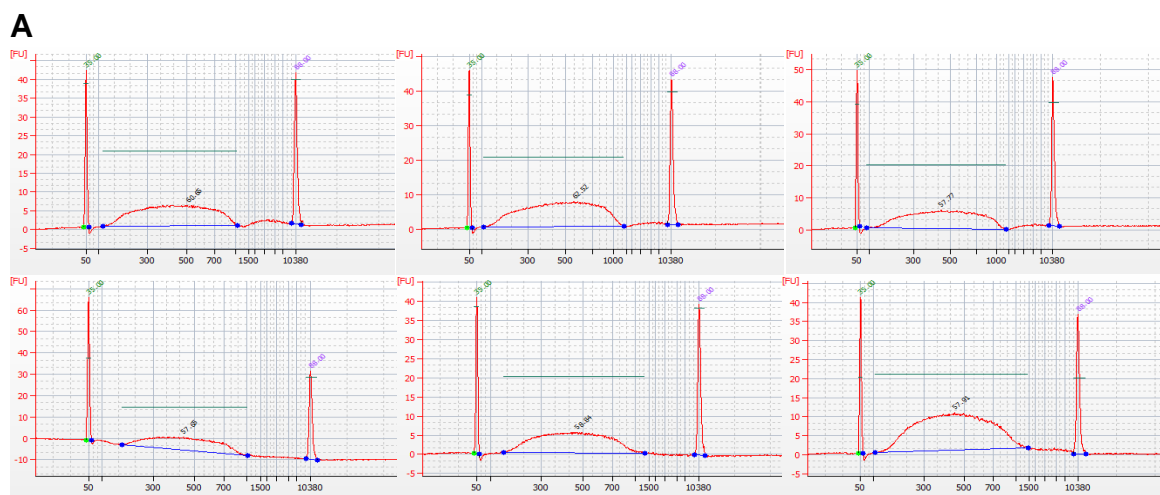
Sample ID	Input 1	Input 2	Input 3	Output 1	Output 2	Output 3
Mean gDNA fragment size (bp)	509	562	448	446	470	451
Concentration of fragmented gDNA (ng/ul)	19.88	24.06	20.12	18.08	18.74	36.83
Molarity of fragmented gDNA (nmol/l)	59.2	64.9	68	61.4	60.4	123.7

Figure 5.18. Bioanalyzer results of gDNA from three replicates of the input pool and three replicates of the output pool after fragmentation by sonication. A) Bioanalyzer traces. Top row – input pool bottom row – output pool B) Sample concentration, molarity and mean fragment size

Size selected, adapter ligated and PCR amplified libraries were size selected by electrophoresis on a 2% agarose gel (Figure 5.19) 300 – 500 bp fragments were excised and gel extracted for sequencing.
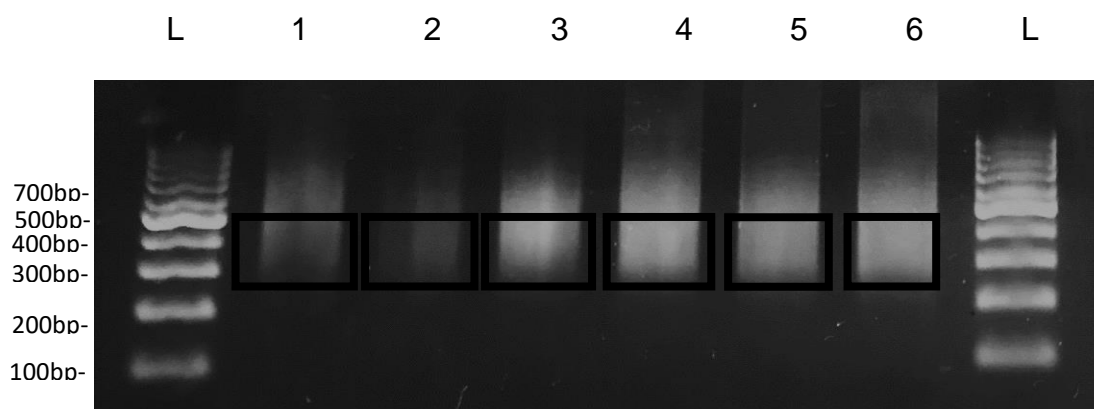
Figure 5.19. 2% Agarose gel electrophoresis of size selected, adapter ligated and PCR amplified libraries. L – 100 bp ladder. 1, 2 and 3 – input pools 4, 5 and 6 – output pools. 300 - 500 bp fragments (black boxes) were excised and gel extracted.

Bioanalyzer traces of final size selected libraries can be seen in figure 5.20. The three replicates of the input pool had mean fragment sizes of 398, 346 and 387 bp and concentrations of 1.81, 0.91 and 3.49 ng/µl respectively (Figure 5.20 A top row, Figure 5.20 B). The three replicates of the output pool had mean fragment size of 377, 384 and 371 and concentrations of 5.38, 3.76 and 4.88 ng/µl respectively (Figure 5.20 A bottom row, Figure 5.20 B).

A

B
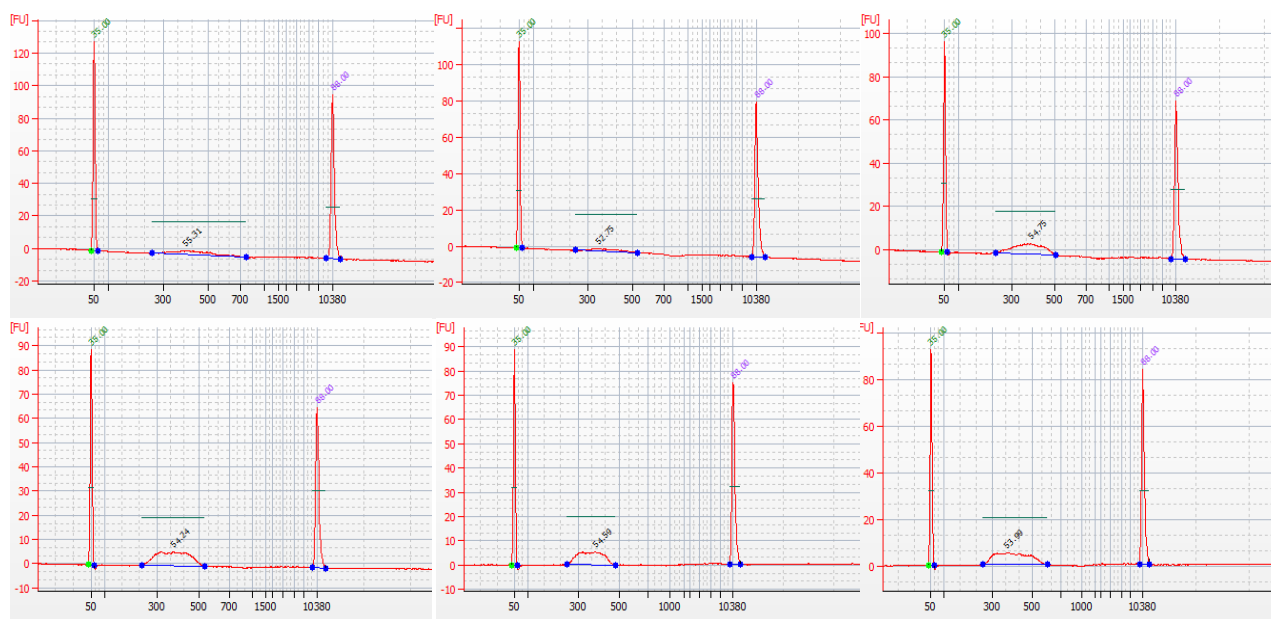
Sample ID	Input 1	Input 2	Input 3	Output 1	Output 2	Output 3
Mean library fragment size (bp)	398	346	387	377	384	371
Library concentration (ng/ul)	1.81	0.91	3.49	5.38	3.76	4.88
Library molarity (nmol/l)	6.9	4	13.7	21.7	14.9	19.9

Figure 5.20. Bioanalyzer results of final size selected libraries. A) Bioanalyzer traces. Top row – input pool bottom row – output pool B) Sample concentration, molarity and mean fragment size

5.2.18.   Analysis of sequencing data

Samples were sequenced as 150 bp single-end reads using an Illumina MiSeq platform. Quality control was performed using FastQC[222]. Per base sequence quality

showed that all resulting reads had a quality score greater than 30, confirming that the data was suitable for further analysis.

The Whiteley lab pipeline script TnSeqDESeq2_DifferentialsAnalysis.R was used to map the obtained reads to the *C. burnetii* RSA439 genome and similar to in the essentials analysis, uses DESeq2 to calculate the Log2 fold change between input and output conditions. For mapping statistics see table 5.7. Input pool replicates yielded approximately 1 million sequencing reads, corresponding to 1,331, 1,498 and 1,729 unique insertion sites for replicates 1, 2 or 3 respectively. Output pool replicates yielded approximately 2.75 million sequencing reads, corresponding to 3,895, 3,679 or 3,534 unique insertion sites for replicates 1, 2 or 3 respectively.

Table 5.7. Mapping statistics of input and output pools

	Input 1	*Input 2*	*Input 3*	*Output 1*	*Output 2*	*Output 3*
Total reads	617,010	1,031,043	1,212,135	3,007,069	2,748,251	2,580,372
Reads matched	567,331	988,845	1,132,621	2,936,264	2,681,298	2,507,585
% matched	91.95	95.91	93.44	97.64	97.56	97.17
Reads mapped	536,845	949,436	1,071,648	2,823,138	2,583,203	2,408,971
% mapped	94.63	96.01	94.62	96.15	96.34	96.07
Unique insertion sites	1331	1498	1729	3895	3679	3534

Correlation of read counts between replicates can be seen in figure 5.21. Spearman correlation coefficients ranged from R = 0.7561 – 0.7844 for the input pools, and R = 0.6591 – 0.6760 for the output pools. Ideally, this would be higher and these findings suggest there is some optimisation to be made for screens of further mutant pools.
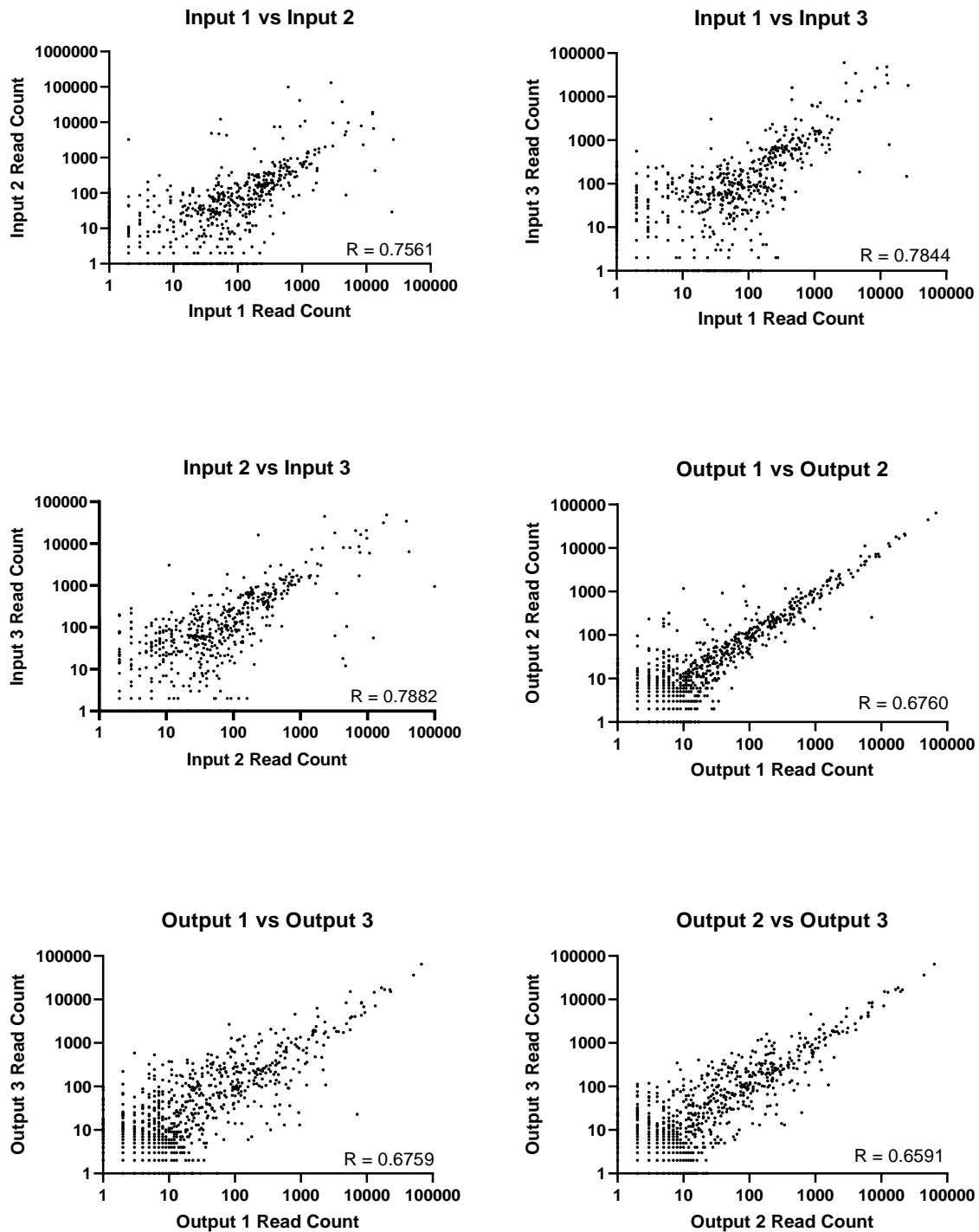
Figure 5.21. Scatter plots showing correlation of read counts between replicates. Spearman correlation coefficient (R) showed correlation between replicates between 0.7561 – 0.7844 for the input pools, and 0.6591 – 0.6760 for the output pools.

Data was obtained for 779 genes, 198 genes which were represented by an average of less than 10 reads in the input pool were removed from analysis due to the potential the reads mapped to them represented sequencing noise, this left data for 581 genes. Genes were classed as potentially virulence-associated if they at least a 2 fold reduction in the output pool compared to the input pool (fold change < 0.5) and Padj < 0.05. According to this classification 55 potentially virulence-associated genes were identified after the removal of 5 pseudogenes (Table 5.8).

Six of the genes identified have been previously predicted to confer T4SS effector proteins[28], a further eight genes have been previously predicted to be virulence associated based on homology to genes associated with detoxification, stress response or enhances cell entry phenotypes[6], or the presence of eukaryotic-like domains[260,261]. Considering only a small number of mutants were inputted in this pilot study, and so little is known about *C. burnetii* virulence, it is not surprising that only a small number of genes have been identified that have previously been discussed. This might reflect the low number of mutants screened in this pilot study

Nine of the genes identified as virulence associated were significantly upregulated at one of more time-points post infection of *G. mellonella* during RNA-Seq in chapter 4, four of these (*CBU_0077, CBU_1697, CBU_1719* and *CBU_1740*) were significantly upregulated at all time-points post infection and could prove to be important virulence determinants. Although it may be expected that the TraDIS data would positively correlate with the RNA-Seq data, many studies have shown this not to be the case[330–332].

Table 5.8. Fifty-five genes potentially important for *C. burnetii* virulence in *G. mellonella* as determined by the Whiteley lab pipeline. Effector = designated as a putative T4SS effector. Virulence = previously identified as a potential virulence-associated gene. Upregulated = Significantly upregulated at one or more time-points post infection in *G. mellonella* during RNA-Seq in chapter 4.

Locus Tag	Gene	Function	Effector	Virulence	Upregulated
CBU_0007		hypothetical protein			
CBU_0053	*enhA.1*	enhanced entry protein		Yes[6]	
CBU_0077		hypothetical membrane spanning protein	Yes[28]		Yes
CBU_0086		putative lactonase			
CBU_0095		sodium-calcium exchanger			
CBU_0098b		hypothetical protein			
CBU_0110		hypothetical exported protein			
CBU_0200		aldose 1-epimerase family protein			
CBU_0282		transcriptional regulator			Yes
CBU_0297	*xth*	exodeoxyribonuclease III			
CBU_0311		outer membrane porin P1			
CBU_0389	*rpsT*	SSU ribosomal protein S20P			
CBU_0488		bis(5'-nucleosyl)-tetraphosphatase (symmetrical)		Yes[260]	
CBU_0668		hypothetical protein			
CBU_0700		sulfate adenylyltransferase			
CBU_0747		LPS ABC transporter periplasmic component			
CBU_0803		acriflavin resistance periplasmic protein			
CBU_0813		hypothetical protein			Yes
CBU_0913		Thioesterase			
CBU_0915	*enhB.1*	enhanced entry protein		Yes[6]	
CBU_0931	*glpD*	glycerol-3-phosphate dehydrogenase			
CBU_0963	*bcp*	thioredoxin peroxidase		Yes[6,260]	
CBU_0982		3-deoxy-7-phosphoheptulonate synthase			
CBU_1039	*cyoB*	cytochrome c oxidase polypeptide I			Yes
CBU_1059		ribosomal large subunit pseudouridine synthase B			
CBU_1064		hypothetical cytosolic protein			
CBU_1177		hypothetical cytosolic protein			
CBU_1259	*nhaP.1*	Na+/H+ antiporter		Yes[260,261]	
CBU_1346		Trehalase			
CBU_1485		cyclin protein			
CBU_1501	*recO*	DNA repair protein			Yes
CBU_1520	*grxC*	Glutaredoxin		Yes[260]	
CBU_1538		carboxy-terminal processing protease precursor			
CBU_1542		hypothetical membrane associated protein			
CBU_1636		hypothetical protein	Yes[28]		
CBU_1670		peptidoglycan-specific endopeptidase			
CBU_1697	*nth*	endonuclease III			Yes
CBU_1719	*groES*	10 kDa chaperonin GROES			Yes
CBU_1740		hypothetical protein			Yes
CBU_1752		hypothetical protein	Yes[28]		
CBU_1756		multidrug resistance transporter			
CBU_1763		hypothetical ATPase			
CBU_1879		peptide deformylase			
CBU_1893	*aroB*	3-dehydroquinate synthase			
CBU_1907		ribosomal-protein-serine acetyltransferase			
CBU_1909	*rpoH*	RNA polymerase sigma-32 factor			
CBU_1916		universal stress protein A		Yes[6]	
CBU_1925	*gidB*	methyltransferase			
CBU_1953		hypothetical membrane spanning protein			
CBU_2048	*metE*	5-methyltetrahydropteroyltriglutamate--homocysteine methyltransferase			Yes
CBU_2056		hypothetical protein	Yes[28]		

CBU_2078		Fic family protein	Yes[28]	Yes[261]	
CBU_2081	*hemY*	HemY			
CBUA0021		hypothetical protein			
CBUA0025		hypothetical protein	Yes[28]		

5.3. Conclusion

In conclusion, in this chapter the saturation of an existing transposon mutant library has been increased five-fold from 2, 415 to 10,129 unique insertion sites. This is, to my knowledge, the first time a whole genome TraDIS study has been conducted for *C. burnetii.* Analysis using a pipeline that has been shown to be successful in other studies with a similar level of saturation revealed 511 genes which may be essential for the growth and survival of *C. burnetii* NMII. Interestingly, some of the essential genes identified are typically considered to be virulence-associated. This is most likely a consequence of the use of ACCM-2 media, which mimics the conditions *C. burnetii* would reside in, in host cells. Essential routes were identified for the mevalonate pathway, as well as peptidoglycan and biotin synthesis. In addition, further evidence of the requirement of L-cysteine and proline for axenic growth was shown.By investigating predicted essential genes *in silico*, 69 genes were identified which could be considered potential drug targets subsequent to further validation For future work the development of methodology to prove essential genes in *C. burnetii* should be prioritised.

Progress has been made in method development for the screening of transposon mutant pools in *G. mellonella* for the identification of virulence-associated genes, although this requires further optimisation which the time constraints of this study did not allow. Nonetheless 55 potential virulence-associated genes were identified, some of which have previously been discussed in other studies.

Chapter 6 Characterisation of attenuated *C. burnetii* mutant NMII::Tn-*CBU_1468*

6.1.   Introduction:

Virulence-associated genes can be identified by screening transposon mutants in relevant infection models and looking for mutants that confer an attenuated phenotype (i.e., increased survival compared to wild type). In *C. burnetii,* the T4SS effector protein CvpB, and the invasin OmpA were identified by screening transposon mutants in *G. mellonella*[117,219] and the SCID mouse model[120]. In chapter five, a pool of ~10,000 *C. burnetii* transposon mutants were created, some of which were picked individually and expanded in ACCM-2. In this chapter, an individual transposon mutant, was further characterised after it was found to be attenuated in a *G. mellonella* model. First the transposon insertion site was identified by arbitrary PCR. In addition, the *G. mellonella* infection model was further characterised to confirm the attenuation seen, as well as to investigate the growth rate of the mutant in *G. mellonella* and ACCM-2 medium. Both fluorescent and transmission electron microscopy of haemocytes isolated from infected *G. mellonella* were performed to look at haemocyte infection. In addition, the transposon mutant was assessed for the ability to grow in the presence of a variety of compounds *in vitro*. Finally, RNA-seq was performed on the transposon mutant and wild-type *C. burnetii* NMII to look at differential gene expression.

6.2. Results and discussion

6.2.1. Transposon insertion site identification by arbitrary PCR

During transposon mutagenesis performed for chapter 4, some individual transposon mutants were picked at random from the pool and expanded in ACCM-2. During a screen of a subset of ten randomly picked individual mutants in *G. mellonella*, a transposon mutant that was attenuated in *G. mellonella* was identified. To determine the transposon insertion site, arbitrary PCR was performed. Arbitrary PCR is a technique using two PCR reactions (Figure 6.1). The first PCR reaction utilised a primer that recognises the transposon insertion, and one of four degenerate primers that contain multiple 'N' bases (that permit primer binding to random DNA sequences) and a conserved region. This initial reaction resulted in PCR products of different lengths. The second PCR reaction was performed on the PCR product from the first reaction, and used one primer which recognises part of the transposon, and another primer which recognises a conserved region in the arbitrary primers used in reaction one.
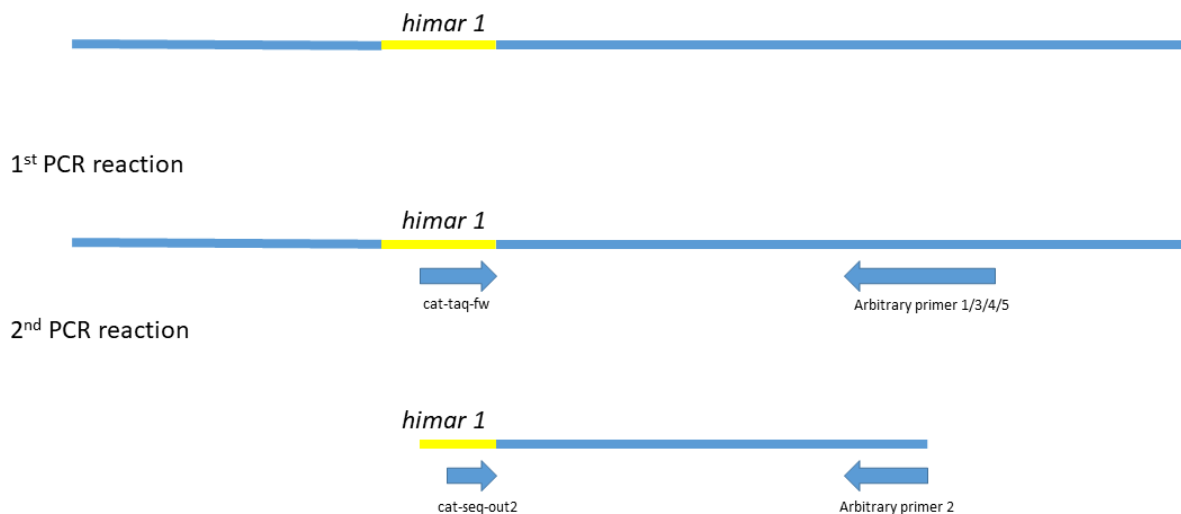
Figure 6.1. Arbitrary PCR overview. In the 1st PCR reaction the forward primer (cat-taq-fw) recognises the transposable element, and arbitrary primers (arb1, 3, 4 or 5) bind to random sequences of the flanking DNA. In the second PCR reaction, using the PCR product from reaction 1, primers recognises conserved regions from the primers used in reaction 1.

PCR products from the second arbitrary PCR reaction were resolved by electrophoresis on a 1.5% agarose gel (Figure 6.2) and bands were excised, gel extracted and sent for Sanger sequencing by Eurofins genomics.
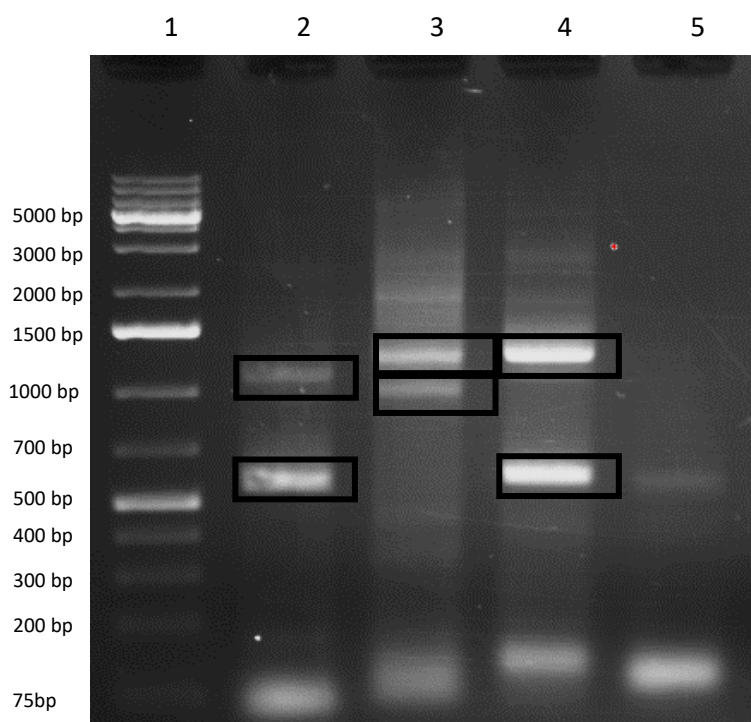
Figure 6.2 Arbitrary PCR gel image. Lane 1 shows a 1000kb+ ladder, Lanes 2-5 show results of arbitrary PCR for NMII::Tn-*CBU_1468,* boxed bands were excised and gel extracted prior to Sanger sequencing to identify the transposon insertion site.

The transposon sequence was present in all 6 PCR products indicating that the method had been successful. The transposon sequence was trimmed, and the resulting DNA sequence was aligned to the *C. burnetii* NMI RSA493 reference genome using BlastN, the corresponding insertion site was found in Artemis. The transposon was found to insert into the gene *CBU_1468* (Figure 6.3), which encodes a hypothetical protein of unknown function. Although arbitrary PCR methodology has been regularly used to identify transposon insertion sites in a variety of species[333–336], this finding should be confirmed by performing whole genome sequencing, to ensure that transposon insertion in *CBU_1468* is the only identified difference between the mutant and wild type *C. burnetii* NMII.
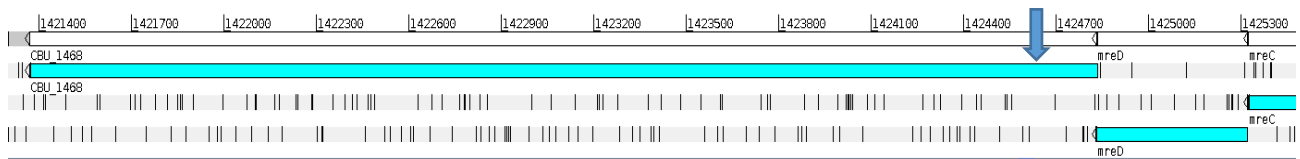
Figure 6.3. Identification of the transposon insertion site in *CBU_1468.* Blue arrow indicates the site disrupted.

6.2.2. Infection of *G. mellonella* with *C. burnetii* NMII::Tn-*CBU_1468*

6.2.2.1. Survival assay

To screen for attenuation, *G. mellonella* were infected with 10^6 GE/larvae NMII, NMII::Tn-*CBU_1468* and known attenuated mutant NMIIΔ*dotA.* Larvae were incubated at 37°C and inspected for survival at daily timepoints. NMIIΔ*DotA* was used as a positive control, as it has a defect in the formation of the T4SS that has been shown to be vital for *C. burnetii* infection in *G. mellonella*[115]. NMII::Tn-*CBU_1468* and NMIIΔ*dotA* showed 97% larval survival at day 7 post infection, compared to 100% larval death of NMII. (Figure 6.4, significant, $p = <0.0001$, Log-rank test).
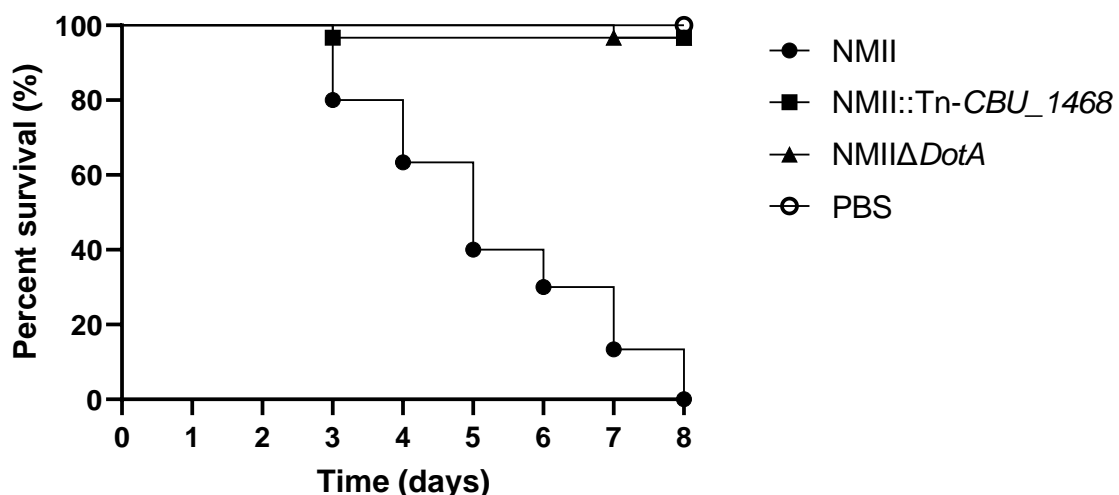
Figure 6.4. Survival of *G. mellonella* post infection with 10^6 GE/larvae NMII, NMII::Tn-*CBU_1468* and NMIIΔ*dotA.* After 7 days of infection 100% of larvae infected with *C. burnetii* NMII succumbed to infection. 100% of larvae infected with *C. burnetii* NMIIΔ*dotA* and *C. burnetii* NMII::Tn-*CBU_1468* were alive ($p = < 0.0001$, log-rank

test). Results show the mean of three independent replicates. Ten larvae were used per strain for each replicate.

In addition to assessing *G. mellonella* on survival alone, a health index scoring system has been proposed by Loh *et al.*[145] which looks at numerous factors including cocoon formation, melanisation and motility. When using this system, NMII::Tn-*CBU_1468* infected larvae showed reduced melanisation, and increased mobility compared to larvae infected with wild type NMII, and appeared more similar to larvae infected NMIIΔ*dot*A (Table 6.1`)

Table 6.1. Average scores of larvae assessed by the larvae scoring system proposed by Loh *et al.*[145]. Scores shown are the average from 10 larvae per group. Mobility scores were between 0 and 3, melanisation scores were between 0 and 4.

	Mobility						Melanisation					
	Days post-infection											
	1	2	4	5	6	7	1	2	4	5	6	7
PBS	3.0	3.0	3.0	3.0	3.0	3.0	4.0	4.0	4.0	4.0	4.0	4.0
NMII	3.0	3.0	1.1	0.3	0.1	0.0	4.0	4.0	2.5	2.5	2.1	1.9
NMII::Tn-*CBU_1468*	3.0	3.0	2.4	2.4	1.8	1.6	4.0	4.0	3.5	3.3	3.0	2.8
NMIIΔ*dotA*	3.0	3.0	2.9	2.8	2.4	1.4	4.0	4.0	3.8	3.8	3.7	2.8

6.2.2.2. Growth of NMII::Tn-*CBU_1468* in ACCM-2 and *G. mellonella*

To identify if transposon insertion in *CBU_1468* confers a growth defect *in vitro*, growth in ACCM-2 was assessed (Figure 6.5). No significant difference was seen between wild type *C. burnetii* NMII and NMII::Tn-*CBU_1468* ($p = 0.77$, unpaired t-test).
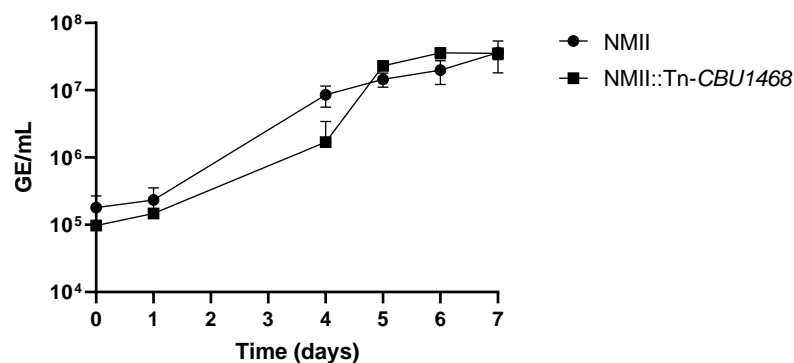
Figure 6.5 Growth curve of NMII and NMII::Tn-*CBU_1468* in ACCM-2. X axis shows time post inoculation, Y axis shows genome equivalents per ml. NMII::Tn-*CBU_1468* does not have a growth defect in ACCM-2 ($p = 0.77$, unpaired t-test).

To assess growth of NMII::Tn-*CBU_1468* in *G. mellonella*, larvae were injected with 10^6 GE/larvae of *C. burnetii* NMII and NMII::Tn-*CBU_1468* and incubated at 37°C. At daily timepoints haemocytes were harvested from three larvae, and qPCR was used to determine the bacterial burden within the haemocytes. This showed that whilst lacking a growth defect *in vitro, in vivo* the mutant has significantly reduced growth on day 3 post infection when compared with the wild type (Figure 6.6, $p = 0.0009$, 2 way ANOVA, multiple comparisons). No significant difference was seen at any other time point.
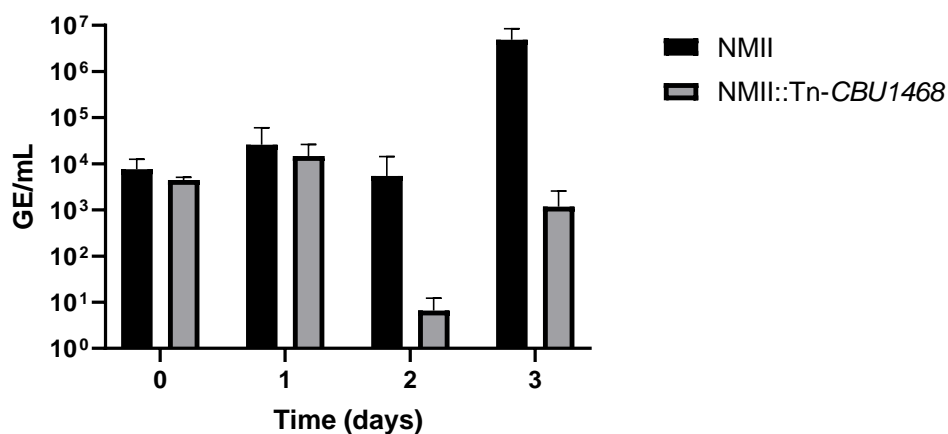
Figure 6.6. Growth of NMII and NMII::Tn-*CBU_1468* in *G. mellonella.* At each time point haemocytes were harvested from three infected larvae, and qPCR was performed to determine GE/ml. A significant difference was seen on day 3 post infection ($p = 0.0009$, two way ANOVA with multiple comparisons), no significant difference was seen at any other time point. Results show the mean of three independent replicates. Three larvae were used per strain for each replicate.

6.2.2.3. Fluorescence microscopy of infected haemocytes

To look at intracellular infection, haemocytes from larvae infected with a fluorescent wild type strain (NMII-*mCherry*) and NMII::Tn-*CBU_1468* were harvested and fixed for imaging. In mammalian cells, after internalisation by cells, *C. burnetii* resides in a fusogenic CCV that upon replication expands to fill the entire cell cytoplasm[29]. By 96 hours post-infection, haemocytes from larvae infected with NMII-*mCherry* showed fluorescence in every field of view observed, as expected (Figure 6.7). Conversely, in haemocytes from larvae infected with NMII::Tn-*CBU_1468*, bacteria could not be seen (Figure 6.7). These findings are similar to those reported after the imaging of haemocytes from larvae infected with a deletion in one of the T4SS genes, *C. burnetii* NMIIΔ*dot*A by Norville *et al*[115]. It has been previously reported by Newton *et al.* that transposon insertion in *CBU_1468* showed a moderate intracellular replication defect [51] rather than the severe defect identified in this study. This may reflect differences in the cell types infected, as Newton *et al.* used the mammalian cell line HeLa 224.
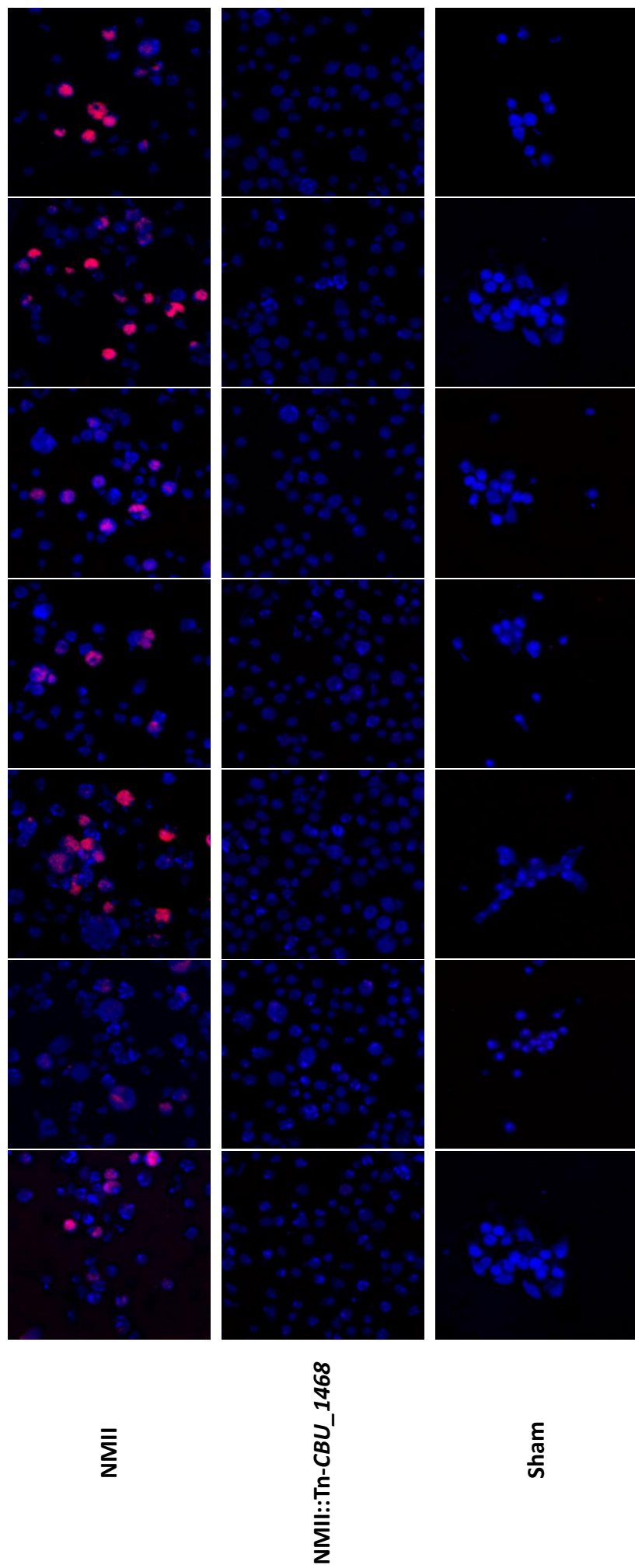
Figure 6.7. Fluorescence microscopy of haemocytes from *G. mellonella* infected with *C. burnetii* NMII-mCherry or NMII::Tn-*CBU_1468* at 96 hours post infection. Sham infections show haemocytes from *G. mellonella* injected with sterile PBS. In haemocytes from larvae infected with NMII-mCherry, bacteria could be seen in every field of view. No bacteria could be seen in haemocytes from NMII::Tn-*CBU_1468* or sham infected larvae. 20 fields of view were imaged per slide. Three slides were viewed from three independent replicates.

6.2.2.4. Transmission electron microscopy of infected haemocytes

Transmission electron microscopy of haemocytes harvested from *G. mellonella* infected with NMII or NMII::Tn-*CBU_1468* was performed to assess internalisation and localisation of NMII::Tn-*CBU_1468* (Figure 6.8). As seen in Chapter four, NMII infected haemocytes are inundated with bacteria (Figure 6.8 A and D). Conversely, haemocytes from *G. mellonella* infected with NMII::Tn-*CBU_1468* appear to be completely lacking visible bacteria (Figure 6.8 B and E), with the haemocytes being more comparable to sham infected controls (Figure 6.8 C and F), confirming what was seen during fluorescent microscopy in the previous section.
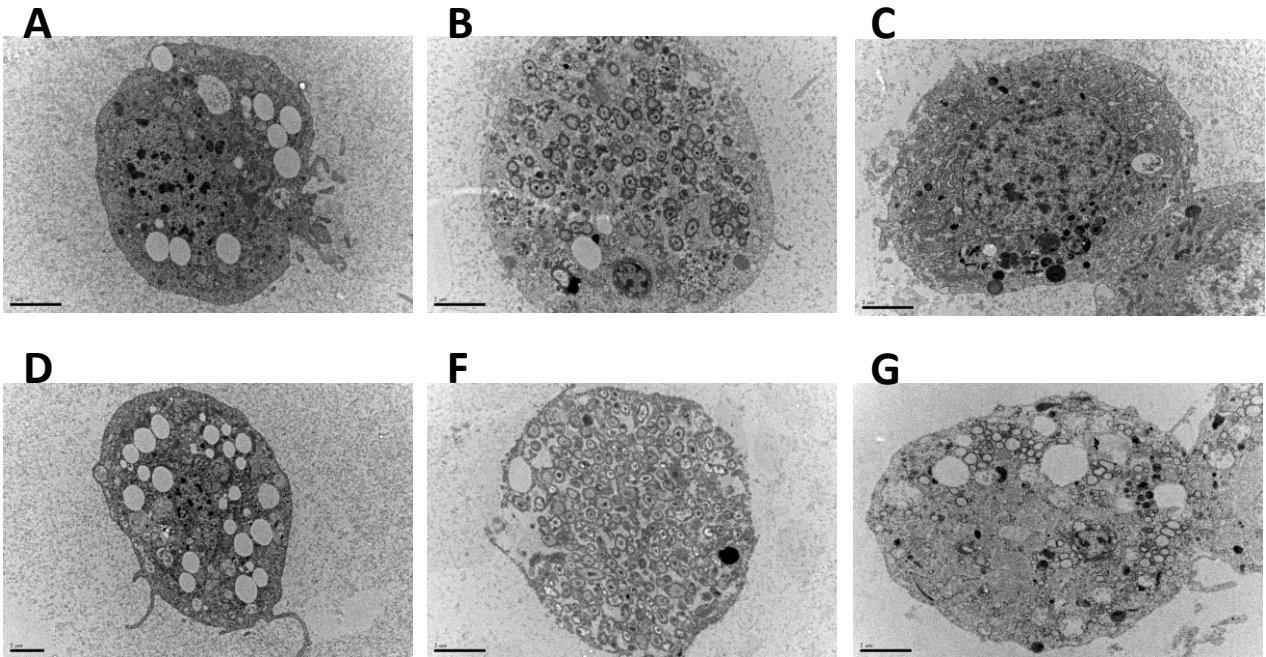
Figure 6.8. Transmission electron microscopy of infected haemocytes. Panels A and D show PBS injected controls. Panels B and F show haemocytes from larvae infected with *C. burnetii* NMII and 48 and 72 hours post infection respectively. Panels C and G show haemocytes from larvae infected with *C. burnetii* NMII::Tn-*CBU_1468* at 48 and 72 hours post infection respectively. Haemocytes from larvae infected with *C. burnetii* NMII show an abundance of bacteria, which fills almost the entire cell cytoplasm. Haemocytes from larvae infected with *C. burnetii* NMII::Tn-*CBU_1468* are more similar to haemocytes from PBS injected control larvae, with no infection seen.

6.2.3. Growth of NMII::Tn-*CBU_1468* in the presence various compounds

In order to gain an insight into a possible function for CBU_1468, *C. burnetii* NMII and *C. burnetii* NMII::Tn-*CBU_1468* were incubated in the presence of sodium chloride (NaCl), polymyxin B, and hydrogen peroxide (H_2O_2) at various concentrations.

H_2O_2 has been used by others to assess *C. burnetii* mutants for involvement in response to oxidative stress[252]. However, in this study no significant differences in growth were seen between the wild type and mutant at any concentration (Figure 6.9, $p = > 0.05$, 2-way ANOVA with multiple comparisons) indicating that CBU_1468 is not involved in the oxidative stress response.

Incubation of bacterial mutants in the presence of sodium chloride can identify a bacterial mutants ability for salt tolerance. Interestingly, *C. burnetii* NMII and NMII::Tn-*CBU_1468* were able to grow in reasonably high concentrations of NaCl. This was unexpected as the addition of up to 16 mM NaCl changes the composition of ACCM-2, a media which is not amenable to large changes in its composition[212]. Again, no significant difference were seen between the wild type and mutant at any concentration (Figure 6.9, $p = >0.05$, 2-way ANOVA with multiple comparisons) indicating that CBU_1468 is not involved in salt tolerance.

Finally, polymyxin B, an outer membrane stressor can be used to assess a mutant for involvement in outer membrane integrity[52]. However, no significant difference were seen between the wild type and mutant at any concentration (Figure 6.9, $p = > 0.05$, 2-way ANOVA with multiple comparisons) suggesting that CBU_1468 is not involved in outer membrane integrity.
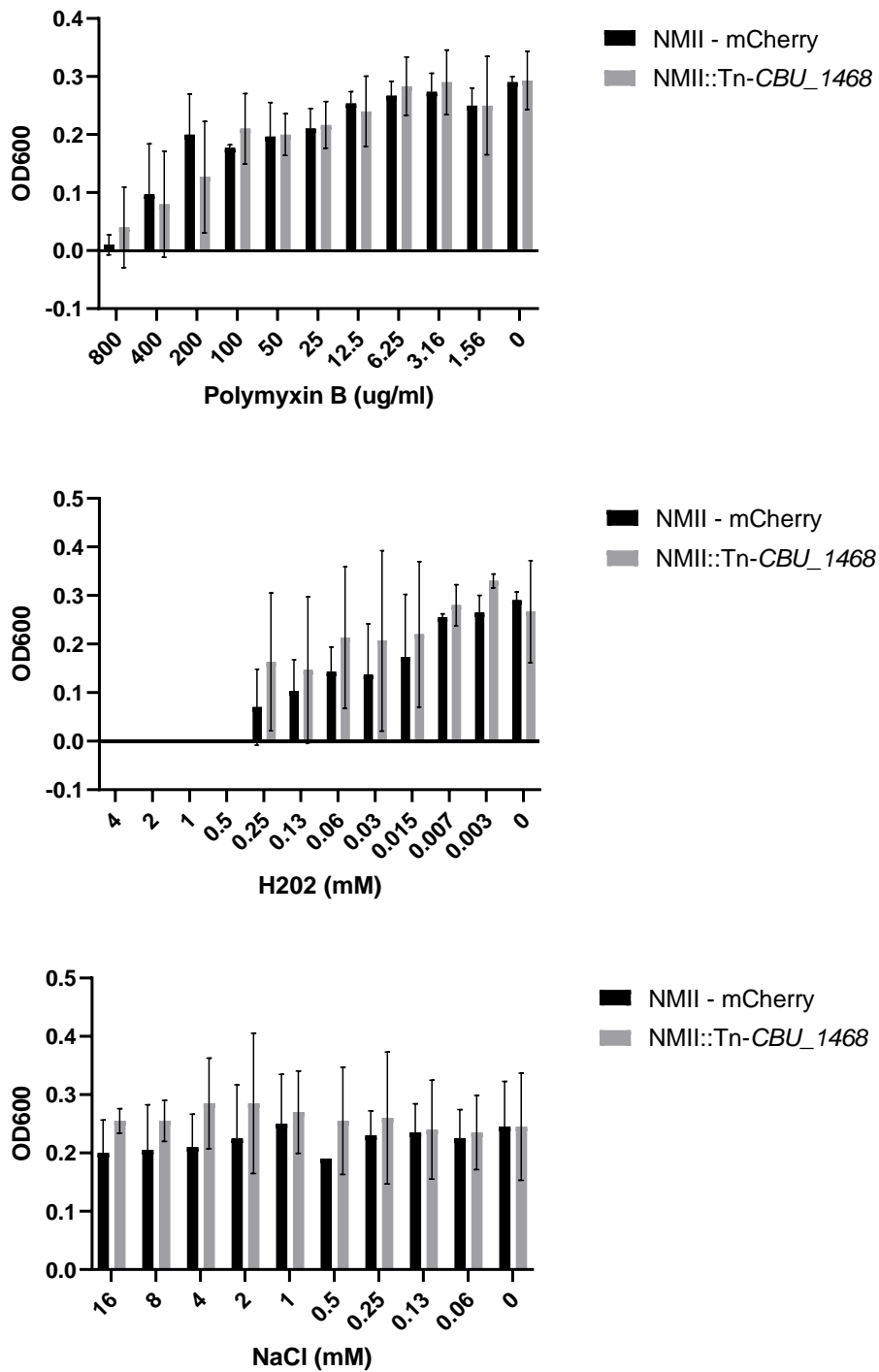
Figure 6.9. Incubation of *C. burnetii* NMII or NMII::Tn-*CBU_1468* in the presence of various concentrations of Polymyxin B, H202 and NaCl. No significant difference was seen between the wild type and the mutant for any compound at any concentration ($p = >0.05$, Two-way ANOVA with multiple comparisons)

6.2.4. Bioinformatic investigation of *CBU_1468*

CBU_1468 spans positions 1,421,564 to 1,425,025 in the *C. burnetii* reference genome and encodes a protein that is 1,153 amino acids in length. The encoded protein, CBU_1468, has a predicted molecular weight of 128,569 and its theoretical isoelectric point is 9.67.

To predict whether *CBU_1468* is contained within an operon, the online database BioCyc was used. BioCyc contains information from a variety of computational inferences and manually curated data. It was predicted by BioCyc that *CBU_1468* is contained within an operon with cell shape determining genes *mreB, mreC* and *mreD* (www.biocyc.org, Figure 6.10) indicating that there is a possibility that it could share a similar function. *mreB, mreC* and *mreD* are rod-shape determining proteins that are critical for cell wall synthesis and cell shape determination in many bacterial species.

Figure 6.10 *CBU_1468* is predicted to share an operon with *mreB, mreC and mreD.* Image from www.biocyc.org

The importance of MreBCD and CBU_1468 in cell morphology of *C. burnetii* has not been confirmed [249]. Although TEM showed little difference between *C. burnetii* NMII and NMII::Tn-*CBU_1468* cell shape (figure 6.11), a possible role in cell wall synthesis and cell shape cannot be completely discounted. In *E. coli mre* deletion mutants grown in unfavourable conditions (inducing those that impart a slow growth rate) resulted in stable, spherical cells, but favourable growth conditions resulted in large cells with an inability to replicate[337]. If CBU_1468 is linked to the function of these proteins, transposon insertion could be having a similar effect. As *C. burnetii* grows more rapidly in *G. mellonella* than in ACCM-2 medium (Chapter 3, Chapter 4 and [293]), ACCM-2 medium could be inducing the production of stable, replicating cells which are unable to replicate during the faster growth conditions in the *G. mellonella* model. However, caution should be taken when comparing *C. burnetii* to *E. coli*, as there are a multitude of differences between the two species.
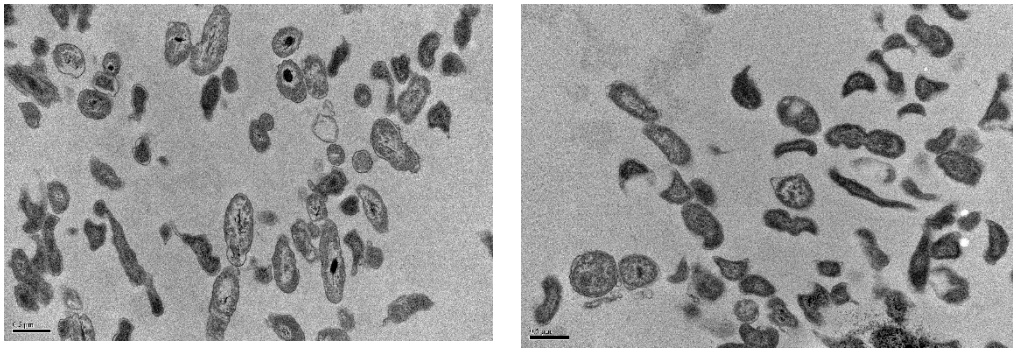
Figure 6.11 TEM imaging of *C. burnetii* NMII (left) and *C. burnetii* NMII::Tn-*CBU_1468* (right). No obvious difference in cell shape between the two strains was seen. Images representative of 10 images per strain. Scale bar 0.5 µm.

CBU_1468 has a conserved TIGR02099 domain, TIGR02099 family proteins are long (>1250 amino acids) proteins found in Proteobacteria. There is low sequence similarity between proteins in this family between different genera. However it is suggested that proteins in this family are insert into, or exported through the membrane. Using the UniProt Knowledgebase it was found that CBU_1468 shares sequence similarity with YhdP from *E. coli,* a protein involved in outer membrane biogenesis[338,339] Comparing the sequences with Clustal Omega shows low identity (19.5 %) but a higher level of similarity (38.6%) (Figure 6.12)


```
TR|Q83BN5|Q83BN    1  MIKILLRSCLKWGMMTAASVIILFAVLISGVRYTVPLLNHQRDFFEHWASHALHQPVHIG
SP|P46474|YHDP_    1  -----MRRLPGILLLTGAALVVIAAILVSGLRIALPHLDAWRPEILNKIESATGMPVEAS

TR|Q83BN5|Q83BN   61  QIAKSWYGFNEALTFQKVIVTDPTQHKSLLRVSQLSISVNLFQSLLHWR--LFPGHVWLS
SP|P46474|YHDP_   56  QLSASWQNFGPTLEAHDIRAEL--KDGGEFSVKRVTLALDVWQSLLHMRWQFRDLTFWQL

TR|Q83BN5|Q83BN  119  GARFNVFE---GKDGKLNVEGMIAQKKQVFTDIGEVKKVFLGLLNQSNITLKNIDIYYHT
SP|P46474|YHDP_  114  RFRTNTPITSGGSDDSLEA-------------SHISDLFLRQFD--HFDLRDSEVSELT

TR|Q83BN5|Q83BN  176  AEGQLIPLTHLRLKVTNGLLHQQIAGVGSLSQTVP----TRFRFL---LQGSSKNAELYL
SP|P46474|YHDP_  158  PSGQRAELAIPQLTWLNDPRRHRAEGLVSLSSLTGQHGVMQVRMDLRDDEGLLSNCRVWL

TR|Q83BN5|Q83BN  229  DIKNLVFSQWESSYFLQKYFKRVSLTDGRGNVQLWAKFKNDELESVQSVVKSDQIRLSVA
SP|P46474|YHDP_  218  QADDIDLKPWLGKWMQDNI----ALETAQFSLEGWMTIDKGDVTGGDVWLKQGGASWLGE

TR|Q83BN5|Q83BN  289  KSHSPLFIDILNANLYWQRYANGWGLIADHVNLQMNGRQWPEHTFGVRVTHSQS-G----
SP|P46474|YHDP_  274  KQTHTLSVDILTA--HITRENPGWQFSIPDTRITVMDGKPWPSGALTAWIPEQDVGGKDN

TR|Q83BN5|Q83BN  344  ---MRLLLKSDYFNLSDVQTITAEICYQPKRIQTLPQQLKPSGILRHFTLLYSQRAQTPY
SP|P46474|YHDP_  332  KRSDELRIRASNLELAGLEGIRPLAAKLSPAIGDVWRSTQPSGKINTLAIDIPLQAAD-K

TR|Q83BN5|Q83BN  401  YHIITDFEDLNEQPQEGWPGCAHLMGAIDAIAQH-------------------------
SP|P46474|YHDP_  391  TRFQASWSDLAWKQWKLLPGAEHFSGTLSGSVENGLLTASMKQAKMPYETVFRAPLEIAD

TR|Q83BN5|Q83BN  435  ---------PASGWRFQVSQSDIQNNNLHWHGEGFLSLPAKGSPFVNLKGKIGLKNINAI
SP|P46474|YHDP_  451  GQATISWLNNNKGFQLDGRNIDVKAKAVHARGGFRYLQPANDEPWLGLLAGISTDDGSQA

TR|Q83BN5|Q83BN  486  KNYLPSRGLSPHLRAWLNQAFSTGEITSGTVNLKGPLDRFPFLHIEGSEDAIANVDRVTL
SP|P46474|YHDP_  511  WRYFPENLVGKDLVDYLSGAIQGGEADNATLVLGGNPQLFPYKHNEGQFEVLVPLRNAKF

TR|Q83BN5|Q83BN  546  NYHSGWPALQNIKAKVMFHNNQLRIVASHANISGNPLDHIKAVIPDLKDPVLSVSCHSTS
SP|P46474|YHDP_  571  AEQPDWPALTNLDIELDFINDGLWWKTDGVNLGGVRASNLTAVIPDYSKEKLLIDADIKG

TR|Q83BN5|Q83BN  606  NLANGFKELKAAPIS--VAKRVQSTTAQGPVNLNLKIRIPLDHSNQEVRAEGQLAVKDGQ
```

167

```
SP|P46474|YHDP_    631  PGKAVGPYFDETPIKDSLGATLQELQLDGDVNARLFLDIPLNG--ELVTAKGEVTLRNNS

TR|Q83BN5|Q83BN    664  FSTNNWGIMLDHINGNFHFINEDFSADPVFAKWLGLPIAFHIATLNPSSQSPVLQFEYSG
SP|P46474|YHDP_    689  LFIKPLDSTLKNISGKFSFINSDLQSEPLTASWFNQPINVDFSTKEGAKAYQV-AVNING

TR|Q83BN5|Q83BN    724  E-----------LAMQALQKKFKWSI-----LNYLNGATTYRALLNLHGKDSQQDSLSLA
SP|P46474|YHDP_    748  NWQPAKTGVLPEAVNEALSGSVAWDGKVGIDLPYHAGA--------------TYNIEIN

TR|Q83BN5|Q83BN    768  TDLSGIQSTLEAEYNKLSKEVSLITSHL----------------------SFYGNKLSKI
SP|P46474|YHDP_    793  GDLKNVSSHLPSPLAKPAGEPLAVNVKVDGNLNSFELTGQAGADNHFNSRWLLGQKLNLD
```

Figure 6.12. Clustal omega sequence alignment between *C. burnetii* CBU_1468 (top) and *E. coli* YhdP (bottom). Black boxes indicate identical amino acids, grey boxes indicate highly similar amino acids.

To predict the subcellular location of CBU_1468 the program PSortB was used. Both CBU_1468 and YhdP are predicted to be localised to the inner membrane, with a proportion of the structure residing in the periplasm (Figure 6.13), suggesting further that there is a high degree of similarity between the two proteins.

```
SeqID: NP_820451.2 hypothetical protein CBU_1468 [Coxiella burnetii RSA 493]
  Localization Scores:
    Cytoplasmic            0.04
    CytoplasmicMembrane     9.82
    Periplasmic            0.12
    OuterMembrane          0.01
    Extracellular          0.01
  Final Prediction:
    CytoplasmicMembrane     9.82
--------------------------------------------------------------------------
SeqID: CAD5995550.1 yhdP [Escherichia coli]
  Localization Scores:
    Cytoplasmic            0.00
    CytoplasmicMembrane     9.86
    Periplasmic            0.12
    OuterMembrane          0.01
    Extracellular          0.01
  Final Prediction:
    CytoplasmicMembrane     9.86
```

Figure 6.13. Subcellular location predictions for CBU_1468 (top) and YhdP (bottom) as determined by PSortB.

Using TMpred, it was predicted that CBU_1468 has three transmembrane regions with the N-terminus on the outer membrane. On the other hand, YhdP is predicted to have two transmembrane regions, with the N-terminus on the inner membrane (Figure 6.14). The presence of three transmembrane domains in CBU_1468 may make purification of the protein for further assessment difficult.

```
SeqID: NP_820451.2 hypothetical protein CBU_1468 [Coxiella burnetii RSA 493]
-----> STRONGLY prefered model: N-terminus outside
 3 strong transmembrane helices, total score : 4772
 # from   to length score orientation
 1   14   31 (18)    2175 o-i
 2   92  111 (20)     626 i-o
 3 1095 1114 (20)    1971 o-i


SeqID: CAD5995550.1 yhdP [Escherichia coli]

-----> STRONGLY prefered model: N-terminus inside
 2 strong transmembrane helices, total score : 4255
 # from   to length score orientation
 1    4   22 (19)    2355 i-o
 2 1203 1226 (24)    1900 o-i
```

Figure 6.14. TMpred transmembrane domain prediction for CBU_1468 (top) and YhdP (bottom)

Finally, the program SignalP was used to predict the presence of a signal peptide, CBU_1468 is not predicted to have a signal sequence, indicating that it is not exported via a Sec-dependent system. Conversely, YhdP is predicted to have a signal sequence suggesting that it is likely to be an exported protein.

Together these results show that there is not a high degree of similarity between CBU_1468 and YhdP. However, this does not rule out the possibility that they may have a related function. YhdP has been shown to have involvement in the enhancement of outer membrane permeability during stationary phase growth of *E. coli*[338], and possibly a role in the transport of phospholipids across the periplasm, from the inner membrane to the outer membrane[340]. In addition, Δ*yhdP* mutants show SDS/EDTA and vancomycin sensitivity during all growth stages, suggesting a further role in outer membrane integrity[339]. To gain an insight into whether these functions are shared, *C. burnetii* NMII::Tn-*CBU_1468* should be assessed for SDS and vancomycin susceptibility. In addition, as it was predicted above that the protein is membrane located, this could be experimentally confirmed by, for example, fluorescently tagging the protein and imaging.

6.2.5. RNA-seq

In order to determine the effect of transposon insertion into *CBU_1468* on the transcriptome of *C. burnetii* NMII, RNA-seq was performed on mRNA extracted from a 7 day stationary phase culture grown in ACCM-2. First, a principle component analysis (PCA) was undertaken to compare the datasets obtained from three biological replicates (Figure 6.15). The *CBU_1468* samples clustered

together well, indicating good reproducibility between the datasets. The wild type samples showed more variability, which could lead to the identification of false negatives however there remains a clear distinction between the mutant and wild-type samples.
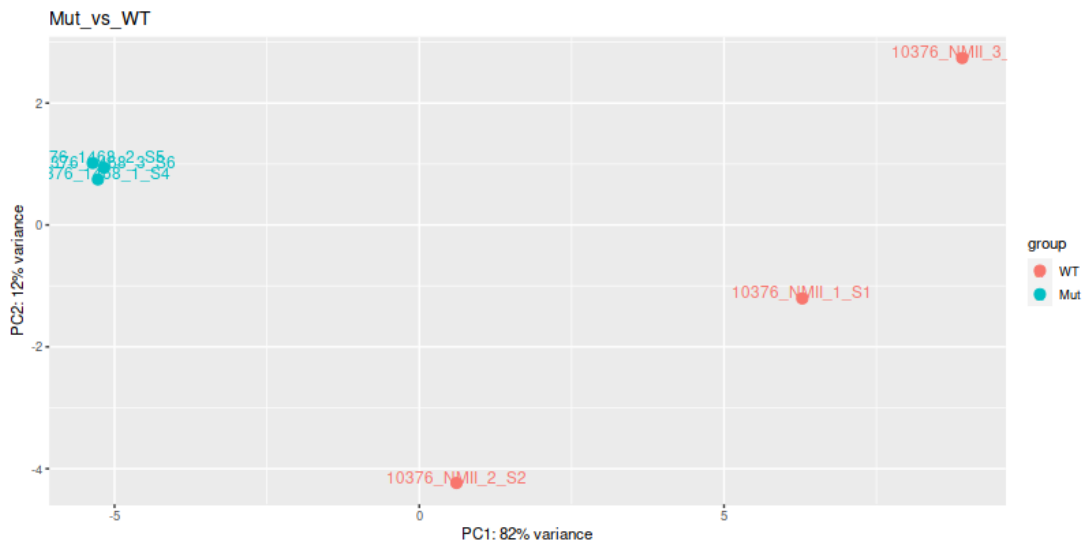
Figure 6.15. Principle component analysis. Datasets for NMII::Tn-*CBU_1468* (blue) clustered well, with little variance between the samples. Datasets for *C. burnetii* NMII (red) clustered less well. However, there remains a clear distinction between the two datasets

Overall the transcriptomes of NMII and NMII::Tn-*CBU_1468* were similar. Using a cut-off criteria of a two-fold change in expression 40 significantly downregulated genes were identified (Table 6.2). Forty percent (16/40) significantly downregulated genes are annotated as hypothetical proteins and therefore will not aid in assigning a function to *CBU_1468.* In addition, neither up-stream or down-stream genes showed differential expression, suggesting that the transposon insertion is not having a polar effect. This could be confirmed by *in trans* complementation. Interestingly, operon sharing genes *mreC* and *mreD* were not identified as significantly downregulated. Overall the RNA-seq analysis has not aided in functional assignment to *CBU_1468,* however, as this analysis was performed in ACCM-2, rather than from *C. burnetii* recovered from *G. mellonella* this may not be surprising. *CBU_1468* was not identified as being significantly upregulated during *G. mellonella* in the RNA-seq from chapter 4, this suggests that the attenuation seen is not as a result of a stress response and is

possibly associated with the core cell biology of *C. burnetii* in the *G. mellonella* model. Unfortunately, due to the lack of growth of *C. burnetii* NMII::Tn-*CBU_1468* in *G. mellonella,* it would not be possibly to recover enough bacteria to perform the RNA-seq analysis in this condition, which could aid in assignment of a function. It should be noted that as the NMII::Tn-*CBU_1468* has not been whole genome sequenced, the possibility that the down regulation of these genes could be as a result of point mutations cannot be discounted.

Table.6.2 Forty genes identified as significantly downregulated in *C. burnetii* NMII::Tn-*CBU_1468* using a cut off criteria of a two-fold change in expression (Fold change = < 0.5, Padj < 0.05)

Locus Tag	Gene	Function	Fold Change	Padj
CBU_0008a	CBU_0008a	hypothetical protein	0.493442	1.49E-09
CBU_0016	visC	xanthosine phosphorylase	0.462604	2.42E-08
CBU_0215	CBU_0215	peptidase, C40 family	0.456862	6.48E-12
CBU_0400a	CBU_0400a	hypothetical protein	0.47962	2.79E-06
CBU_0661	CBU_0661	hypothetical protein	0.414995	0.002718
CBU_0691	CBU_0691	methyltransferase	0.029933	0.041535
CBU_0700	CBU_0700	sulfate adenylyltransferase	0.467416	4.72E-05
CBU_0703	CBU_0703	O-antigen export system permease protein	0.482982	0.000883
CBU_0819	CBU_0819	glutathione S-transferase	0.422296	4.19E-19
CBU_0822	CBU_0822	Fic family protein	0.351133	5.00E-18
CBU_0869	Alr	alanine racemase, biosynthetic	0.483085	4.36E-10
CBU_0888	CBU_0888	disulfide bond formation protein B	0.387216	1.71E-05
CBU_0896	dedE	colicin V production protein	0.416641	3.08E-10
CBU_0898	CBU_0898	thyroglobulin type-1 repeat domain protein	0.465973	8.33E-07
CBU_0906	CBU_0906	transporter, MFS superfamily	0.486575	0.000435
CBU_0959	CBU_0959	multidrug resistance transporter, Bcr family	0.450467	4.71E-13
CBU_1042	CBU_1042	hypothetical membrane spanning protein	0.359212	4.19E-19
CBU_1132	CBU_1132	hypothetical protein	0.224266	0.03174
CBU_1220	purC	phosphoribosylaminoimidazole-succinocarboxamide synthase	0.492787	1.21E-05
CBU_1244	CBU_1244	multidrug resistance protein B	0.401407	1.09E-07
CBU_1346	CBU_1346	trehalase	0.443981	3.16E-13
CBU_1413	CBU_1413	hypothetical exported membrane spanning protein	0.428618	4.52E-18
CBU_1468	CBU_1468	hypothetical protein	0.314741	1.16E-31
CBU_1485	CBU_1485	cyclin protein	0.449534	3.37E-11
CBU_1553	nrdA	ribonucleoside-diphosphate reductase alpha chain	0.493216	4.68E-10
CBU_1573	CBU_1573	transporter, MFS superfamily	0.450393	1.99E-10
CBU_1574	tolQ	TolQ	0.401232	1.65E-12
CBU_1588	shaA	sodium/proton antiporter protein	0.42057	3.03E-08
CBU_1589	CBU_1589	hypothetical membrane associated protein	0.426224	1.67E-09
CBU_1800	CBU_1800	hypothetical membrane spanning protein	0.372364	4.52E-18
CBU_1865	CBU_1865	hypothetical membrane associated protein	0.490085	1.42E-07
CBU_1880	CBU_1880	hypothetical membrane spanning protein	0.475201	3.05E-05
CBU_1884	CBU_1884	hypothetical exported membrane spanning protein	0.470652	9.23E-07
CBU_1886	CBU_1886	hypothetical protein	0.426799	0.007248
CBU_1895	CBU_1895	hypothetical protein	0.399956	3.59E-17
CBU_1904	ftsE	cell division ATP-binding protein	0.476188	1.18E-06
CBU_1928	CBU_1928	acyl-CoA synthetase	0.473154	1.06E-09
CBU_1987	apaH	bis(5'-nucleosyl)-tetraphosphatase, symmetrical	0.497642	0.000265
CBUA0011	CBUA0011	hypothetical protein	0.457184	5.43E-05
CBUA0024	CBUA0024	hypothetical protein	0.471509	1.81E-10

6.3. Conclusion

In this chapter it was found that transposon insertion into *CBU_1468* results in an attenuated phenotype in the *C. burnetii G. mellonella* model, and further investigation of haemocytes from infected larvae show a complete absence of infection. This suggests that the mutant could possibly have defect in internalisation into, or survival and replication within haemocytes, or otherwise is eliminated from the larvae by the innate immune system before it is able to infect haemocytes (i.e by antimicrobial peptides). Future work should first subject *C. burnetii* NMII::Tn-*CBU_1468* to whole genome sequencing, to confirm the attenuation seen is not as a result of other differences between the mutant and the wild-type. In addition, the phenotype of *C. burnetii* NMII::Tn-*CBU_1468* should be assessed *ex vivo* in a primary culture of *G. mellonella* haemocytes or in a mammalian cell line, to see if the same phenotype is seen.

As *CBU_1468* confers a hypothetical protein of unknown function, an attempt was made to build a picture of what could be causing the attenuation seen through RNA-seq, incubation with various compounds, and bioinformatic investigation. Both RNA-seq and incubation studies were inconclusive. Bioinformatic investigations suggested a potential role involving the outer membrane, possibly similar to the role of YhdP in *E. coli.* To further investigate this possibility the mutant could be assessed in the presence of SDS/EDTA and vancomycin, to see whether a similar increase in susceptibility is seen which would suggest a role in outer membrane integrity. Protein localisation studies would also confirm the computational prediction that the protein is located to the inner membrane with a significant portion residing in the periplasm.

In addition to the above, a deletion mutant of *CBU_1468* should be created to confirm that what it is seen in this chapter is truly reflective of CBU_1468 disruption, which should then be complemented to confirm restoration of the wild-type phenotype. This is required to fulfil molecular Koch's postulates. Although it should be noted that targeted gene deletion and subsequent complementation is not easy to perform in *C. burnetii.*

Should CBU_1468 be found to have a similar role to YhdP, it could make an attractive drug target. As Δ*yhdP* mutant's show increased susceptibility to vancomycin, it is possible that targeting CBU_1468 could increase susceptibility

to certain antibiotics, allowing for combined treatment with antibiotics to reduce the currently very lengthy antibiotic treatment regime for chronic Q-fever.

Chapter 7: Final conclusions and future perspectives

In conclusion, the early work in this project optimised the growth of *C. burnetii* NMII in our laboratory by utilising homemade ACCM-2 (rather than pre formulated) and using a specialist anaerobic gas mix (2.5% O_2, 5% CO_2). Together the use of these conditions ensured reliable growth of *C. burnetii.* The sequence of the *C. burnetii* NMII strain held in our laboratory was determined and no obvious difference were found between the strain used in this project and those with available published data. These experiments were required to underpin the studies performed in this project.

The *G. mellonella* model of *C. burnetii* infection was further characterised. It was shown that *in vivo* growth of *C. burnetii* in *G. mellonella* haemocytes is faster than axenic growth in ACCM-2. In haemocytes, *C. burnetii* formed a CCV that is similar to the CCV seen in mammalian cells that appeared to contain bacteria in both LCV and SCV forms. It would be interesting to see if the CCV seen contains CCV markers that are seen during infection of mammalian cells. For example, the early CCV is known to be decorated with LC3, the maturing CCV is known to be decorated with LAMP1 and RAB7, and the mature CCV is decorated with RAB1B[29]. *G. mellonella* possess five different types of haemocytes: prohaemocytes, plasmatocytes, granulocytes, oenocytoids and spherulocytes, and in this study *C. burnetii* was not found in all cells. Future work looking total and differential haemocyte counts would aid in further characterisation of this model. In addition, only haemocytes were looked at. It is possible that *C. burnetii* also resides in other *G. mellonella* tissues such as the fat body, which could be assessed with further experiments by dissecting and homogenising different *G. mellonella* compartments. RNA-seq of *C. burnetii* RNA extracted from *G. mellonella* haemocytes at different time-points post infection showed a progressive decrease in expression of LCV associated genes in parallel to a progressive increase of SCV associated genes. It would be interesting to see if at time-points later that 3 days post infection (the longest time point analysed in this study), CCVs contained a larger population of *C. burnetii* in SCV form. Unfortunately, when infected *in vivo*, it would be difficult to extract haemolymph from *G. mellonella* at later time-points. However, recently a method has been developed to sustain *G. mellonella* haemocytes *ex vivo* in Graces insect medium[341], which would permit this experiment. RNA-seq also revealed a wide

174

range of *C. burnetii* genes that are upregulated during *G. mellonella* infection, many encoding hypothetical proteins of unknown function. The creation of deletion mutants in these genes would permit future studies into *C. burnetii* virulence.

The utility of immunocompromising *G. mellonella* via pre-treatment of *G. mellonella* with Dex.P, a phosphorylated pro-drug of Dex. was also assessed. Survival studies showed that Dex.P increased *G. mellonella* susceptibility to *C. burnetii* in a dose-dependent manner, and that this pre-treatment permitted the identification of attenuated phenotypes. However, conversion of the pro-drug was not observed during HPLC analysis. This aspect of the project was not continued due to time constraints, however it is possible that further investigation into the effect of Dex.P on *G. mellonella* could prove pre-treatment to be a useful model for *C. burnetii* infection.

A transposon mutant pool was generated that contained 10, 129 unique transposon insertion sites, allowing the first whole genome TraDIS study in *C. burnetii.* By utilising a data analysis pipeline that has been used in other studies with a similar level of saturation permitted the identification of 511 genes which may be essential for *C. burnetii* NMII growth and survival in ACCM-2 media. It was noted that some of the essential genes identified, such as predicted T4SS effectors, are typically considered to be virulence-associated. It was concluded that this is most likely as a result of ACCM-2, which mimics the acidic CCV. Essential routes of synthesis were identified for the mevalonate pathway, as well as peptidoglycan and biotin synthesis. In addition, further evidence of the requirement of L-cysteine and proline for axenic growth was shown. By investigating predicted essential genes *in silico* to look at transmembrane domains, human genes, common genes to human gut commensals and conserved genes among *C. burnetii* strains , 69 genes were identified which could be considered potential drug targets subsequent to further validation. To date, methodology to prove essential genes in *C. burnetii* has not been developed. This should be considered a matter of priority. In other species, this has been achieved by putting essential genes under the control of an inducible promoter. By doing this the gene is only expressed in the presence of the inducing compound, for example L-rhamnose[203]. In addition, it is important to note that *C. burnetii* NMII is

a derogated surrogate for the fully virulent *C. burnetii* NMI, it would be valuable to carry out a TraDIS screen in this more clinically relevant strain.

Progress has been made in method development for the screening of transposon mutant pools in *G. mellonella* for the identification of virulence-associated genes, and a sub-pool of 1,000 colonies from the transposon mutant pool were analysed. Fifty-five potential virulence-associated genes were identified, some of which have previously been discussed in other studies. Future work in screening the other sub-pools of transposon mutants in *G. mellonella* should be carried out. In addition, the transposon pool could be studied in other infection relevant conditions. As a common symptom of chronic Q fever, and a rarer symptom of acute Q fever is endocarditis[342], screening the mutant pool in a cardiac cell line such as H9c2 cardiac myoblast-like cells[343] could provide useful information on this complication. In addition, a mammalian model of infection such as the SCID mouse could be used as a screen in a higher order animal.

Finally, it was found that transposon insertion into *CBU_1468* results in an attenuated phenotype when screened in the *C. burnetii G. mellonella* model. Further investigation of haemocytes from infected larvae showed a complete absence of infection. Suggesting that the mutant could possibly have defect in internalisation into, or survival and replication within haemocytes, or otherwise is eliminated from the larvae by the innate immune system before it is able to infect haemocytes (i.e. by antimicrobial peptides). It should be noted that the *G. mellonella* model has its limitations, such as a lack of an adaptive immune response. Therefore, findings in this model may not correlate with what is seen in a mammalian model of infection (such as mammalian cell culture, mice or guinea pigs). Future work should first subject *C. burnetii* NMII::Tn-*CBU_1468* to whole genome sequencing, to confirm the attenuation seen is not as a result of other differences between the mutant and the wild-type that have not been found during arbitrary PCR. In addition, the phenotype of *C. burnetii* NMII::Tn-*CBU_1468* should be assessed *ex vivo* in a mammalian cell line to see if the same phenotype is seen, before screening for attenuation in a higher order model such as the SCID mouse, and effective model for screening *C. burnetii* NMII[120].

RNA-seq and incubation of *C. burnetii* NMII::Tn-*CBU_1468* with various compounds was inconclusive in finding the cause behind the attenuation seen. Bioinformatic investigations look at conserved domains, predicted signal

peptides, predicted transmembrane domains and predicted subcellular location suggested a potential role involving the outer membrane, possibly similar to the role of YhdP in *E. coli.* To further investigate this possibility the mutant could be assessed in the presence of SDS/EDTA and vancomycin, to see whether a similar increase in susceptibility is seen[339] which would suggest a role in outer membrane integrity. Protein localisation studies would also confirm the computational prediction that the protein is located to the inner membrane with a significant portion residing in the periplasm.

In addition to the above, a deletion mutant of *CBU_1468* should be created in the *C. burnetii* NMI strain to confirm that what it is seen in this chapter is truly reflective of CBU_1468 disruption, which should then be complemented to confirm restoration of the wild-type phenotype. This is required to fulfil molecular Koch's postulates. Should CBU_1468 be found to have a similar role to YhdP, it could make an attractive drug target. As Δ*YhdP* mutant's show increased susceptibility to vancomycin, it is possible that targeting CBU_1468 could increase susceptibility to certain antibiotics, allowing for combined treatment with antibiotics to reduce the currently very lengthy antibiotic treatment regime for chronic Q-fever.

Appendices

Appendix 4.1. RNA-seq of *C. burnetii* during *in vitro* growth and at different time-points post infection of *G. mellonella*

Locus tag	SCV/LCV	*in vitro* Detected	1 day post infection Detected	Fold change	2 days post infection Detected	Fold change	3 days post infection Detected	Fold change	4 days post infection Detected	Fold change
CBU_0001		D	D	0.37	D	0.48	D	0.64	D	0.73
CBU_0002		D	D	0.56	D	0.76	D	0.94	D	0.89
CBU_0003		D	D	0.70	D	0.82	D	0.78	D	0.70
CBU_0004	SCV	D	D	0.49	D	0.56	D	0.52	D	0.59
CBU_0006		D	D	2.68	D	3.86	D	3.28	D	4.25
CBU_0006a		D	D	153.19	D	243.49	D	284.12	D	86.19
CBU_0007	SCV	D	D	0.25	D	0.74	D	0.39	D	0.72
CBU_0007a	SCV	D	D	0.42	D	1.31	D	0.65	D	0.79
CBU_0008		D	D	54.16	D	9.95	D	6.43	ND	0.48
CBU_0008a		D	D	0.54	D	0.80	D	0.81	D	0.96
CBU_0009		D	D	0.33	D	0.90	D	1.37	D	1.52
CBU_0010	LCV	D	D	1.27	D	0.92	D	1.13	D	1.03
CBU_0011		ND	ND	#VALUE!	ND	#VALUE!	ND	#VALUE!	ND	#VALUE!
CBU_0014		D	D	0.88	D	1.05	D	0.94	D	0.75
CBU_0015		D	D	0.61	D	0.95	D	0.87	D	0.89
CBU_0016		D	D	0.73	D	1.09	D	1.07	D	1.06
CBU_0017		D	D	0.54	D	0.89	D	0.93	D	0.82
CBU_0018		D	D	1.11	D	0.74	D	0.43	D	0.40
CBU_0019	SCV	D	D	0.10	D	0.06	D	0.07	D	0.06
CBU_0020	SCV	D	D	0.01	D	0.03	D	0.05	D	0.20
CBU_0021	SCV	D	D	0.24	D	0.33	D	0.37	D	0.34
CBU_0022		D	D	0.48	D	0.53	D	0.34	D	0.33
CBU_0023		D	D	0.11	D	0.23	D	0.20	D	0.26
CBU_0024	LCV	D	D	2.61	D	1.82	D	0.94	D	1.20
CBU_0025	LCV	D	D	3.36	D	1.75	D	0.72	D	0.88
CBU_0026		D	D	0.29	D	0.71	D	0.43	D	0.57
CBU_0027		D	D	2.19	D	0.94	D	0.85	D	0.77
CBU_0029	LCV	D	D	2.35	D	3.13	D	3.44	D	2.51
CBU_0030	LCV	D	D	1.26	D	1.82	D	1.45	D	1.83
CBU_0031		D	D	3.61	D	3.12	D	2.85	D	2.61
CBU_0032		D	D	3.36	D	2.63	D	1.99	D	1.28
CBU_0033		D	D	2.47	D	2.86	D	2.02	D	1.84
CBU_0034		D	D	2.58	D	2.60	D	2.54	D	2.09
CBU_0035		D	D	4.54	D	4.12	D	3.42	D	2.52
CBU_0036		D	D	2.75	D	3.35	D	2.87	D	2.31
CBU_0037		D	D	10.16	D	7.89	D	6.12	D	4.68
CBU_0037a		ND	D	127.76	D	196.36	D	63.48	D	42.35
CBU_0038		D	D	3.82	D	2.95	D	3.06	D	2.45
CBU_0039		D	D	1.78	D	1.82	D	1.98	D	1.88
CBU_0040		ND	ND		ND		ND		ND	
CBU_0040a		ND	ND		ND		ND		ND	
CBU_0041		D	D	1.64	D	0.62	D	0.54	D	0.18
CBU_0042	LCV	D	D	3.11	D	2.06	D	1.64	D	1.46
CBU_0043		D	D	0.85	D	1.52	D	1.18	D	1.06
CBU_0044		D	D	0.13	D	0.19	D	0.18	D	0.18
CBU_0045		D	D	0.16	D	0.22	D	0.24	D	0.33
CBU_0048	SCV	D	D	0.40	D	0.51	D	0.64	D	0.64
CBU_0049	LCV	D	D	7.36	D	3.14	D	2.74	D	2.68
CBU_0050		D	D	0.52	D	0.36	D	0.28	D	0.34
CBU_0051		D	D	0.45	D	0.65	D	0.39	D	0.40
CBU_0053	SCV	D	D	0.03	D	0.06	D	0.24	D	0.57
CBU_0054		D	D	1.25	D	0.80	D	0.63	D	0.66
CBU_0055		D	D	2.01	D	1.25	D	0.87	D	0.89
CBU_0056		D	D	0.20	D	0.33	D	0.37	D	0.36
CBU_0057		D	ND	0.60	ND	0.29	ND	0.31	D	0.18
CBU_0058	SCV	D	D	2.53	D	1.22	ND	0.34	D	0.37
CBU_0062		D	D	0.18	D	0.18	D	0.25	D	0.16
CBU_0063	LCV	D	D	2.48	D	1.48	D	1.74	D	1.88
CBU_0064		D	D	0.78	D	0.67	D	0.71	D	0.72
CBU_0065		D	D	0.58	D	0.96	D	0.83	D	0.86

CBU_0065a		D	D	0.48	D	0.46	D	0.33	D	0.47
CBU_0066	SCV	D	D	0.51	D	0.46	D	0.42	D	0.38
CBU_0067		D	D	1.25	D	0.63	D	0.58	D	1.57
CBU_0068	LCV	D	D	1.01	D	0.52	D	0.29	D	0.44
CBU_0068a		D	ND	2.20	D	4.55	D	2.20	D	2.12
CBU_0072		D	D	0.62	D	0.64	D	0.56	D	0.36
CBU_0073		D	D	0.88	D	0.92	D	0.86	D	0.81
CBU_0074		D	D	39.64	D	90.28	D	39.66	D	14.59
CBU_0075		D	D	2.09	D	2.15	D	1.43	D	1.39
CBU_0076		D	D	1.11	D	1.28	D	1.16	D	1.08
CBU_0077		D	D	2.31	D	2.19	D	2.37	D	2.53
CBU_0081		D	D	4.03	D	3.06	D	3.20	D	2.68
CBU_0083		D	D	2.84	D	6.25	D	12.22	D	5.26
CBU_0084		D	D	0.56	D	0.32	D	0.59	D	0.54
CBU_0085		D	D	0.41	D	0.87	D	0.73	D	1.06
CBU_0086		D	D	1.01	D	1.28	D	1.74	D	1.88
CBU_0087	SCV	D	D	0.03	D	0.06	D	0.13	D	0.28
CBU_0089		D	ND	0.07	D	0.35	D	1.03	D	0.57
CBU_0089a		D	D	0.02	D	0.07	D	0.16	D	0.28
CBU_0090	SCV	D	D	0.17	D	0.20	D	0.23	D	0.33
CBU_0091		D	D	0.06	D	0.10	D	0.10	D	0.14
CBU_0092		D	D	0.24	D	0.17	D	0.18	D	0.25
CBU_0093		D	D	1.49	D	1.14	D	1.70	D	1.16
CBU_0094		D	D	0.89	D	1.20	D	1.53	D	2.09
CBU_0095		D	D	0.88	D	0.63	D	0.88	D	1.07
CBU_0095a		D	D	0.40	D	0.35	D	0.23	D	0.27
CBU_0096		D	D	0.67	D	0.48	D	0.52	D	0.54
CBU_0097		D	D	0.63	D	0.57	D	0.65	D	0.71
CBU_0098		D	D	0.39	D	0.19	D	0.23	D	0.28
CBU_0098a		D	D	3.05	D	1.72	D	1.04	D	0.71
CBU_0098b		D	ND	0.41	D	1.28	ND	0.21	D	0.98
CBU_0099	LCV	D	D	0.98	D	0.75	D	0.49	D	0.62
CBU_0100		D	D	2.66	D	2.98	D	2.18	D	1.37
CBU_0101		D	D	4.28	D	2.59	D	1.78	D	1.71
CBU_0102		D	D	2.04	D	1.30	D	2.14	D	1.20
CBU_0103	LCV	D	D	1.52	D	1.38	D	1.32	D	1.20
CBU_0106		D	ND	0.82	D	1.45	ND	0.42	D	1.45
CBU_0107		D	D	0.99	D	1.23	D	1.03	D	1.35
CBU_0108		D	D	0.47	D	0.79	D	1.03	D	0.84
CBU_0109		D	D	1.34	D	1.50	D	2.10	D	1.57
CBU_0110		D	D	0.04	D	0.13	D	0.28	D	0.60
CBU_0110a		D	D	20.99	D	14.45	D	8.59	D	2.80
CBU_0111		D	D	0.87	D	0.86	D	0.97	D	1.11
CBU_0112		D	D	1.66	D	1.47	D	1.57	D	1.38
CBU_0113		D	D	0.33	D	0.65	D	0.63	D	0.73
CBU_0114		D	D	2.56	D	0.95	D	0.99	D	0.71
CBU_0115	SCV	D	D	0.47	D	0.75	D	0.67	D	0.75
CBU_0116	SCV	D	D	0.21	D	0.43	D	0.49	D	0.63
CBU_0117		D	D	0.17	D	0.39	D	0.53	D	0.77
CBU_0118		D	D	0.11	D	0.18	D	0.21	D	0.20
CBU_0119		D	D	0.98	D	0.90	D	0.96	D	0.50
CBU_0121		D	ND	18.67	ND	9.09	ND	9.59	ND	2.70
CBU_0122		D	D	0.97	D	2.24	D	2.44	D	3.47
CBU_0123		D	D	1.11	D	1.39	D	1.74	D	1.47
CBU_0124	LCV	D	D	1.72	D	1.43	D	1.48	D	1.37
CBU_0125	LCV	D	D	1.92	D	1.37	D	1.25	D	1.22
CBU_0127		D	D	19.43	D	2.97	D	4.77	D	2.89
CBU_0130		D	D	0.22	D	0.40	D	0.42	D	0.22
CBU_0131		D	D	0.43	D	0.35	D	0.60	D	0.69
CBU_0132		D	D	0.47	D	0.35	D	0.54	D	0.52
CBU_0135		D	D	0.89	D	1.04	D	0.94	D	0.80
CBU_0136		D	D	0.81	D	0.99	D	1.27	D	1.29
CBU_0137		D	D	0.60	D	0.77	D	0.78	D	0.87
CBU_0138		D	D	0.37	D	0.42	D	0.46	D	0.44
CBU_0139		D	D	0.38	D	0.84	D	0.81	D	0.87
CBU_0140		D	D	0.92	D	1.13	D	1.10	D	1.07
CBU_0141	LCV	D	D	0.82	D	1.16	D	1.20	D	1.26
CBU_0142		D	D	1.04	D	0.91	D	0.65	D	0.90
CBU_0143		D	D	0.76	D	0.55	D	0.38	D	0.61
CBU_0146	LCV	D	D	0.96	D	1.28	D	0.85	D	0.99

CBU_0147	LCV	D	D	1.47	D	1.05	D	1.08	D	1.12
CBU_0148	LCV	D	D	2.48	D	1.82	D	2.03	D	1.87
CBU_0149		D	D	7.01	D	2.64	D	3.02	D	1.65
CBU_0150		D	D	0.35	D	0.28	D	0.25	D	0.18
CBU_0151		D	D	0.28	D	0.49	D	0.52	D	0.49
CBU_0152		D	D	2.16	D	0.92	D	0.49	D	1.56
CBU_0153		D	D	0.88	D	0.50	D	0.53	D	0.60
CBU_0154		D	D	1.36	D	1.56	D	0.71	D	0.68
CBU_0155	LCV	D	D	2.28	D	0.65	D	0.79	D	1.01
CBU_0156		D	D	1.80	D	0.80	D	0.94	D	0.66
CBU_0156a	LCV	D	D	1.93	D	2.28	D	1.94	D	1.37
CBU_0157		D	ND	3.13	D	8.87	ND	1.61	D	1.77
CBU_0158		D	D	1.03	D	0.25	D	0.53	D	0.59
CBU_0159		D	D	0.45	D	0.22	D	0.87	D	0.78
CBU_0165		D	D	1.18	D	1.67	D	1.28	D	0.82
CBU_0166		D	D	4.73	D	2.53	D	2.76	D	0.75
CBU_0167	SCV	D	ND	0.14	D	0.73	D	0.14	D	0.19
CBU_0168		D	D	17.70	ND	4.40	ND	4.64	D	2.60
CBU_0173	SCV	D	D	0.03	D	0.09	ND	0.01	D	0.14
CBU_0175		D	D	3.79	D	3.35	D	2.08	D	2.34
CBU_0176	SCV	D	D	0.03	D	0.05	D	0.14	D	0.36
CBU_0177		D	D	0.22	D	0.26	D	0.27	D	0.21
CBU_0178		D	D	0.23	D	0.25	D	0.14	D	0.18
CBU_0179		D	D	1.51	D	2.39	D	2.69	D	1.83
CBU_0180		D	D	0.31	D	0.50	D	0.40	D	0.49
CBU_0181		D	D	0.62	D	1.03	D	0.96	D	0.88
CBU_0181a	SCV	D	D	0.01	D	0.01	D	0.01	D	0.02
CBU_0182		D	D	1.31	D	0.91	D	0.93	D	1.19
CBU_0183		D	D	7.25	D	4.46	D	9.11	D	5.31
CBU_0184		D	D	1.54	D	0.58	D	0.64	D	0.33
CBU_0193	SCV	D	D	0.04	D	0.03	D	0.05	D	0.10
CBU_0194		D	D	0.27	D	0.33	D	0.31	D	0.29
CBU_0195		D	D	1.36	D	1.04	D	0.87	D	1.05
CBU_0196		D	D	0.39	D	0.41	D	0.68	D	0.56
CBU_0197		D	D	0.53	D	0.63	D	0.74	D	0.60
CBU_0198		D	D	0.28	D	0.36	D	0.46	D	0.48
CBU_0199		D	D	0.31	D	0.44	D	0.32	D	0.43
CBU_0200		D	D	0.37	D	0.48	D	0.54	D	0.50
CBU_0201		D	D	1.74	D	1.23	D	0.94	D	1.02
CBU_0205	LCV	D	D	2.67	D	1.45	D	1.61	D	1.55
CBU_0206	SCV	D	D	0.01	D	0.03	D	0.14	D	0.41
CBU_0207		D	D	0.26	D	0.26	D	0.29	D	0.35
CBU_0209		D	D	1.33	D	1.06	D	0.65	D	0.81
CBU_0210		D	D	3.81	D	1.91	D	4.14	D	1.66
CBU_0213		D	D	40.32	ND	9.96	D	22.13	ND	2.96
CBU_0214		D	D	0.67	D	0.59	D	0.42	D	0.60
CBU_0215		D	D	0.09	D	0.19	D	0.25	D	0.28
CBU_0217a	SCV	D	ND	4.72	D	4.82	D	4.87	D	1.43
CBU_0218		D	D	1.15	D	1.66	D	1.49	D	1.37
CBU_0220		D	D	0.54	D	0.86	D	0.71	D	0.79
CBU_0221		D	D	0.97	D	0.97	D	1.13	D	1.09
CBU_0221a		D	D	9.40	D	7.73	D	6.75	D	6.49
CBU_0221b		D	D	12.76	D	8.39	D	8.85	D	9.74
CBU_0224		D	D	5.65	D	4.19	ND	5.05	D	5.01
CBU_0225		D	D	5.57	D	5.15	D	6.22	D	6.27
CBU_0226		D	D	9.58	D	8.32	D	9.25	D	9.95
CBU_0227		D	D	7.08	D	6.96	D	8.89	D	9.29
CBU_0228		D	D	13.03	D	10.00	D	11.76	D	11.44
CBU_0229		D	D	10.64	D	8.43	D	10.98	D	10.82
CBU_0230		D	D	6.34	D	9.44	D	14.54	D	13.74
CBU_0231		D	D	7.37	D	5.97	D	8.24	D	7.31
CBU_0232		D	D	5.50	D	4.38	D	5.22	D	4.77
CBU_0233		D	D	11.63	D	8.09	D	5.94	D	6.61
CBU_0234		D	D	7.77	D	5.18	D	4.25	D	5.66
CBU_0235		D	D	7.34	D	4.23	D	4.90	D	4.48
CBU_0236	LCV	ND	ND		ND		ND		ND	
CBU_0237		D	D	17.23	D	9.37	D	9.87	D	8.87
CBU_0238		D	D	5.64	D	3.16	D	3.92	D	4.04
CBU_0239		D	D	11.70	D	7.95	D	9.68	D	10.29
CBU_0240		D	D	8.04	D	6.43	D	5.43	D	5.93

CBU_0241		D	D	8.84	D	6.37	D	7.30	D	7.08
CBU_0242		D	D	7.49	D	5.06	D	5.46	D	4.62
CBU_0243		D	D	6.32	D	3.79	D	5.93	D	4.72
CBU_0244		D	D	4.59	D	2.92	D	3.03	D	3.49
CBU_0245		D	D	5.30	D	3.50	D	4.18	D	4.66
CBU_0246		D	D	5.58	D	7.19	D	6.53	D	5.03
CBU_0247		D	D	5.69	D	4.62	D	5.75	D	4.79
CBU_0248		D	D	6.77	D	5.73	D	6.34	D	5.69
CBU_0249		D	D	7.86	D	6.53	D	8.11	D	7.10
CBU_0250		D	D	1.60	D	1.81	D	1.65	D	1.66
CBU_0251		D	D	3.77	D	3.74	D	3.74	D	4.95
CBU_0252		D	D	2.46	D	2.59	D	2.88	D	2.55
CBU_0253		D	D	6.22	D	4.20	D	4.24	D	3.82
CBU_0254		D	D	3.55	D	2.77	D	2.10	D	2.54
CBU_0255		D	D	5.98	D	4.74	D	5.09	D	5.28
CBU_0256		D	D	7.63	D	6.10	D	7.88	D	6.35
CBU_0257		D	D	8.28	D	6.83	D	7.50	D	6.90
CBU_0258		D	D	7.19	D	4.54	D	4.90	D	4.60
CBU_0259		D	D	9.18	D	9.41	D	7.14	D	7.12
CBU_0260		D	D	4.08	D	4.46	D	3.44	D	3.31
CBU_0261		D	D	5.10	D	6.15	D	5.20	D	5.35
CBU_0262		D	D	4.16	D	4.20	D	4.37	D	4.37
CBU_0263		D	D	4.01	D	3.40	D	3.69	D	3.73
CBU_0264		D	D	6.70	D	5.68	D	6.61	D	5.94
CBU_0265		D	D	7.56	D	4.73	D	4.63	D	4.69
CBU_0270	LCV	D	D	1.33	D	1.03	D	0.91	D	1.12
CBU_0271		D	D	0.26	D	0.38	D	0.35	D	0.38
CBU_0272		D	D	1.07	D	1.39	D	1.24	D	1.24
CBU_0273		D	D	0.89	D	1.16	D	1.87	D	1.57
CBU_0274	SCV	D	D	0.22	D	0.38	D	0.30	D	0.28
CBU_0274a	SCV	D	D	4.10	D	6.41	D	9.20	D	5.10
CBU_0275	SCV	D	D	0.18	D	0.47	D	0.44	D	0.59
CBU_0276		D	D	0.18	D	0.43	D	0.41	D	0.46
CBU_0277		D	ND	0.98	D	3.91	D	3.98	D	0.83
CBU_0278		D	D	0.39	D	0.48	D	0.29	D	0.31
CBU_0279		D	D	1.02	D	0.90	D	1.13	D	1.07
CBU_0280		D	D	0.63	D	1.19	D	0.96	D	1.41
CBU_0282		D	D	3.21	D	2.03	D	2.07	D	1.62
CBU_0283		D	D	5.33	D	5.27	D	2.59	D	2.25
CBU_0284		D	D	5.12	D	5.56	D	3.38	D	2.60
CBU_0285		D	D	3.23	D	3.39	D	1.31	D	2.00
CBU_0286	LCV	D	D	0.92	D	0.58	D	0.62	D	0.66
CBU_0287	LCV	D	D	1.76	D	1.40	D	2.10	D	1.65
CBU_0288		D	D	0.78	D	0.83	D	0.86	D	1.21
CBU_0289		D	D	1.18	D	1.72	D	1.12	D	1.35
CBU_0290	LCV	D	D	2.38	D	1.58	D	0.74	D	1.46
CBU_0291	LCV	D	D	3.43	D	1.95	D	1.13	D	1.21
CBU_0291b		D	ND	0.63	D	0.62	ND	0.32	D	0.51
CBU_0293	LCV	D	D	0.80	D	0.48	D	0.43	D	0.65
CBU_0294	LCV	D	D	2.01	D	1.65	D	1.63	D	1.92
CBU_0295		D	D	0.33	D	0.47	D	0.53	D	0.41
CBU_0296		D	D	0.11	D	0.17	D	0.13	D	0.16
CBU_0297		D	D	0.22	D	0.43	D	0.30	D	0.41
CBU_0298		D	D	2.02	D	1.46	D	1.54	D	1.39
CBU_0299		D	D	1.16	D	0.74	D	0.61	D	0.74
CBU_0300		D	D	1.46	D	1.20	D	0.92	D	0.98
CBU_0301		D	D	2.86	D	2.29	D	2.51	D	2.30
CBU_0302	SCV	D	D	0.20	D	0.47	D	0.56	D	0.64
CBU_0303	SCV	D	D	0.31	D	0.58	D	0.58	D	0.56
CBU_0304		D	D	0.49	D	0.69	D	0.76	D	0.83
CBU_0305		D	D	0.35	D	0.57	D	0.69	D	0.70
CBU_0306		D	D	0.39	D	0.40	D	0.46	D	0.33
CBU_0307		D	D	0.89	D	0.80	D	0.79	D	0.85
CBU_0307a		D	D	13.65	D	1.91	D	1.95	D	0.91
CBU_0309	LCV	D	D	1.54	D	1.35	D	1.22	D	1.79
CBU_0311	SCV	D	D	0.20	D	0.59	D	1.09	D	1.38
CBU_0312	LCV	D	D	5.98	D	5.20	D	5.13	D	3.99
CBU_0312a		D	D	1.47	D	1.01	D	0.50	D	0.25
CBU_0313		D	D	1.33	D	1.00	D	0.76	D	0.81
CBU_0314		D	D	0.10	D	0.07	D	0.16	D	0.32

181

ID	Type									
CBU_0315		D	D	0.44	D	0.38	D	0.27	D	0.33
CBU_0316		D	D	0.67	D	0.58	D	0.51	D	0.56
CBU_0316a	SCV	D	D	9.44	D	4.75	D	2.57	D	0.90
CBU_0317		D	D	1.64	D	1.79	D	1.91	D	1.59
CBU_0318	SCV	D	D	0.01	D	0.02	D	0.16	D	0.47
CBU_0319		D	D	6.42	ND	1.50	ND	1.58	ND	0.45
CBU_0321		D	D	0.10	D	0.11	D	0.14	D	0.15
CBU_0322		D	D	0.90	D	1.10	D	1.06	D	0.77
CBU_0323		D	D	0.35	D	1.03	D	0.87	D	0.36
CBU_0324		D	D	0.58	D	0.73	D	0.88	D	0.63
CBU_0326		D	D	0.55	D	0.78	D	0.62	D	0.58
CBU_0330		D	D	2.67	D	1.82	D	1.15	D	0.85
CBU_0331		D	D	2.32	D	2.03	D	0.71	D	1.67
CBU_0332		D	D	8.55	D	1.10	D	5.43	D	2.84
CBU_0333		D	D	1.85	D	2.37	D	1.92	D	1.61
CBU_0334		D	D	1.85	D	1.40	D	1.60	D	1.80
CBU_0335		D	D	1.60	D	1.30	D	1.29	D	1.53
CBU_0336	LCV	D	D	1.58	D	1.06	D	1.20	D	1.18
CBU_0337		D	D	2.20	D	1.72	D	1.66	D	1.95
CBU_0338	LCV	D	D	2.83	D	2.43	D	2.82	D	2.82
CBU_0339		D	D	2.46	D	1.40	D	1.20	D	1.29
CBU_0340		D	D	0.88	D	0.66	D	0.89	D	0.77
CBU_0341		D	D	0.80	D	1.04	D	0.81	D	1.27
CBU_0342		ND	D	70.82	ND	1.00	ND	1.00	ND	1.00
CBU_0343		D	D	0.93	D	0.69	D	1.12	D	0.93
CBU_0346		D	D	1.31	D	1.16	D	0.98	D	0.72
CBU_0347	LCV	D	D	0.89	D	0.54	D	0.44	D	0.48
CBU_0349		D	D	0.99	D	0.68	D	1.08	D	0.77
CBU_0350		D	D	0.24	D	0.35	D	0.43	D	0.46
CBU_0351		D	D	0.04	D	0.09	D	0.05	D	0.11
CBU_0352		D	D	0.08	D	0.09	D	0.08	D	0.09
CBU_0353		D	D	0.33	D	0.66	D	0.35	D	0.46
CBU_0354	SCV	D	D	0.40	D	0.66	D	0.57	D	0.55
CBU_0357		D	D	7.02	D	2.58	D	2.41	D	2.41
CBU_0362		D	D	0.45	D	0.84	D	0.95	D	0.85
CBU_0364	LCV	D	D	5.41	D	2.49	D	2.59	D	2.64
CBU_0365		D	D	22.42	D	10.58	ND	5.73	ND	1.61
CBU_0366		D	D	1.24	D	0.90	D	1.32	D	1.24
CBU_0367		D	D	0.30	D	0.40	D	0.33	D	0.63
CBU_0368		D	D	0.47	D	0.61	D	0.72	D	0.85
CBU_0369		D	D	0.39	D	0.88	D	0.81	D	0.70
CBU_0370		D	D	0.09	D	0.38	D	0.36	D	0.88
CBU_0371		D	D	0.26	D	0.54	D	0.42	D	0.53
CBU_0372		D	D	0.34	D	0.34	D	0.46	D	0.50
CBU_0373		D	D	0.37	D	0.56	ND	0.05	D	0.06
CBU_0377		D	D	3.53	D	1.84	D	1.25	D	0.47
CBU_0378	LCV	D	D	7.14	D	3.85	D	3.61	D	3.78
CBU_0379		D	D	0.25	D	0.31	D	0.48	D	0.40
CBU_0380		D	ND	0.12	D	0.22	ND	0.06	D	0.11
CBU_0381		D	D	0.42	D	0.46	D	0.44	D	0.48
CBU_0382	LCV	D	D	0.94	D	0.82	D	0.60	D	0.73
CBU_0383	LCV	D	D	0.50	D	0.63	D	0.70	D	1.18
CBU_0384		ND	ND		ND		ND		ND	
CBU_0384a		ND	ND		ND		ND		ND	
CBU_0384b		D	D	0.21	D	0.28	D	0.20	D	0.33
CBU_0385		D	D	4.89	D	3.40	D	2.01	D	2.42
CBU_0386		D	D	5.80	D	4.20	D	3.55	D	4.65
CBU_0387		D	D	4.86	D	2.87	D	2.63	D	2.71
CBU_0388		D	D	4.14	D	1.50	D	1.75	D	1.32
CBU_0389	LCV	D	D	2.98	D	1.48	D	1.10	D	1.32
CBU_0390		D	D	0.29	D	0.29	D	0.23	D	0.27
CBU_0391		D	D	1.61	D	0.83	D	0.75	D	0.94
CBU_0394	SCV	D	ND	0.39	D	0.39	ND	0.20	D	0.32
CBU_0395		D	D	0.48	D	0.76	D	1.41	D	1.27
CBU_0396	LCV	D	D	0.90	D	0.64	D	0.81	D	0.79
CBU_0397		D	D	0.82	D	0.99	D	0.78	D	0.58
CBU_0398		D	D	0.22	D	0.31	D	0.31	D	0.30
CBU_0400	SCV	D	D	0.29	D	0.37	D	0.47	D	0.36
CBU_0400a		D	D	0.80	D	0.54	D	0.94	D	0.65
CBU_0402		D	D	0.42	ND	0.10	D	0.22	ND	0.03

182

CBU_0403		D	D	0.70	D	0.54	D	0.71	D	0.55
CBU_0407		D	ND	19.66	ND	9.58	ND	10.09	D	5.83
CBU_0409	SCV	D	D	12.60	D	6.42	ND	3.21	D	3.88
CBU_0410		D	D	0.65	D	0.72	D	0.84	D	1.00
CBU_0411		D	D	2.54	D	2.30	D	1.39	D	2.34
CBU_0412		D	D	1.05	D	1.57	D	0.72	D	1.32
CBU_0415		D	D	3.58	D	1.75	D	5.18	D	1.94
CBU_0416		D	D	0.52	D	1.61	D	0.27	D	1.17
CBU_0417		D	D	2.41	D	1.21	D	0.32	D	1.21
CBU_0418	SCV	D	D	0.72	D	0.57	D	0.51	D	0.55
CBU_0419	SCV	D	D	0.03	D	0.02	D	0.08	D	0.28
CBU_0422	LCV	D	D	0.92	D	0.80	D	1.16	D	0.91
CBU_0423	LCV	D	D	4.53	D	2.21	D	1.08	D	1.90
CBU_0424	LCV	D	D	2.27	D	1.33	D	1.29	D	1.15
CBU_0425	SCV	D	D	0.74	D	0.39	D	0.27	D	0.19
CBU_0426	LCV	D	D	1.39	D	0.97	D	1.09	D	0.97
CBU_0426a		D	ND	5.97	ND	2.91	ND	3.06	ND	0.86
CBU_0429		D	D	0.47	D	0.83	D	0.59	D	0.65
CBU_0430	LCV	D	D	1.37	D	1.03	D	1.14	D	1.07
CBU_0431		D	D	0.31	D	0.29	D	0.30	D	0.33
CBU_0432		D	D	5.57	D	1.37	D	1.54	D	1.45
CBU_0433		D	D	0.71	D	0.78	D	0.97	D	1.08
CBU_0434		D	D	38.58	D	15.16	D	19.76	D	6.08
CBU_0434a		D	D	2.32	D	2.45	D	2.45	D	1.36
CBU_0436	LCV	D	D	2.34	D	0.56	D	0.33	D	0.95
CBU_0439	LCV	D	D	1.12	D	4.42	D	0.61	D	1.80
CBU_0440		D	D	1.45	D	1.44	D	1.83	D	1.87
CBU_0441	LCV	D	D	3.63	D	1.77	D	1.69	D	1.32
CBU_0442	LCV	D	D	5.30	D	3.05	D	2.82	D	3.06
CBU_0443		D	D	2.74	D	1.27	D	0.96	D	0.87
CBU_0444		D	D	0.53	D	0.44	D	0.39	D	0.46
CBU_0445	LCV	D	D	1.44	D	1.20	D	1.02	D	1.05
CBU_0446		D	D	0.66	D	0.49	D	0.28	D	0.26
CBU_0447	LCV	D	D	0.77	D	0.82	D	0.60	D	0.80
CBU_0448		D	ND	1.34	ND	0.65	ND	0.69	ND	0.19
CBU_0450	LCV	D	D	6.74	D	3.11	D	2.19	D	2.47
CBU_0451		D	D	0.64	D	0.49	D	0.42	D	0.33
CBU_0452		D	D	1.23	D	1.38	D	1.22	D	0.91
CBU_0453		D	D	2.74	D	2.71	D	1.94	D	1.53
CBU_0454		D	D	2.23	D	2.54	D	2.30	D	2.00
CBU_0455		D	D	1.19	D	1.47	D	1.53	D	1.38
CBU_0456	SCV	D	D	0.12	D	0.64	D	1.30	D	2.12
CBU_0457		ND	ND	#VALUE!	ND	#VALUE!	ND	#VALUE!	ND	#VALUE!
CBU_0458		D	D	2.39	D	1.63	D	1.92	D	2.10
CBU_0459	LCV	D	D	1.60	D	1.13	D	1.43	D	1.57
CBU_0460		D	D	1.13	D	0.83	D	0.64	D	0.71
CBU_0461	LCV	D	D	2.09	D	1.83	D	1.86	D	1.87
CBU_0462		D	D	4.10	D	3.56	D	4.72	D	4.67
CBU_0463		D	D	2.45	D	1.95	D	3.10	D	2.94
CBU_0465	LCV	D	D	21.75	D	8.72	D	2.44	D	4.59
CBU_0467		D	D	3.24	D	1.90	D	1.49	D	1.55
CBU_0468		D	D	0.04	D	0.04	D	0.03	D	0.04
CBU_0469	SCV	D	D	0.05	D	0.03	D	0.07	D	0.15
CBU_0470	SCV	D	D	0.02	D	0.05	D	0.06	D	0.15
CBU_0472		D	D	0.57	D	0.91	D	1.12	D	1.37
CBU_0473		D	D	1.90	D	3.56	D	2.51	D	4.95
CBU_0474		D	D	1.22	D	2.61	D	2.86	D	4.19
CBU_0476		D	D	0.73	D	1.03	D	1.11	D	1.09
CBU_0477	SCV	D	ND	0.15	D	0.84	D	0.83	D	0.40
CBU_0478		D	ND	0.95	ND	0.47	D	1.00	ND	0.14
CBU_0478a		D	D	0.87	D	2.33	D	2.29	D	2.20
CBU_0479	LCV	D	D	0.84	D	1.63	D	2.01	D	2.03
CBU_0480	SCV	D	D	0.58	D	0.66	D	0.71	D	0.99
CBU_0481	SCV	D	D	0.46	D	0.50	D	0.86	D	1.66
CBU_0482	SCV	D	D	0.33	D	0.55	D	0.88	D	1.60
CBU_0483	SCV	D	D	1.02	D	0.91	D	1.01	D	1.70
CBU_0484		D	D	1.80	D	1.05	D	1.06	D	1.22
CBU_0485		D	D	1.04	D	1.25	D	1.16	D	1.09
CBU_0486	LCV	D	D	4.36	D	3.04	D	2.08	D	2.54
CBU_0487		D	D	3.45	D	2.70	D	2.83	D	2.34

CBU_0488	SCV	D	D	0.12	D	0.25	D	0.30	D	0.44
CBU_0489	LCV	D	D	0.78	D	0.79	D	0.67	D	0.56
CBU_0490	SCV	D	D	0.10	D	0.27	D	0.30	D	0.38
CBU_0491	LCV	D	D	2.26	D	1.51	D	0.89	D	0.92
CBU_0492	LCV	D	D	4.70	D	2.68	D	2.23	D	2.37
CBU_0493	LCV	D	D	9.49	D	6.25	D	5.88	D	5.13
CBU_0494		D	D	16.51	D	9.79	D	9.97	D	8.21
CBU_0495		D	D	5.27	D	4.00	D	4.73	D	4.11
CBU_0496		D	D	1.98	D	1.90	D	1.36	D	1.34
CBU_0497	LCV	D	D	2.44	D	2.08	D	1.80	D	1.72
CBU_0498	SCV	D	D	0.55	D	0.33	D	0.34	D	0.45
CBU_0499		D	D	0.50	D	0.31	D	0.39	D	0.37
CBU_0500		D	D	0.52	D	0.50	D	0.49	D	0.57
CBU_0501		D	D	1.77	D	2.31	D	1.29	D	1.28
CBU_0502		D	D	0.72	D	0.73	D	0.75	D	0.91
CBU_0503		D	D	0.77	D	0.87	D	0.89	D	1.10
CBU_0504		D	D	1.44	D	1.04	D	1.38	D	1.34
CBU_0505	SCV	D	D	0.60	D	0.60	D	1.11	D	0.84
CBU_0505a		D	D	0.46	D	0.78	D	0.36	D	0.49
CBU_0506		D	D	0.35	D	0.63	D	0.76	D	0.80
CBU_0507		D	D	0.61	D	0.52	D	0.57	D	0.56
CBU_0508	SCV	D	D	0.35	D	0.35	D	0.59	D	0.49
CBU_0509		D	D	0.46	D	0.68	D	0.81	D	0.75
CBU_0510		D	D	0.26	D	0.28	D	0.29	D	0.37
CBU_0510a		D	D	1.27	D	0.99	D	0.73	D	0.56
CBU_0513		D	D	0.09	D	0.10	D	0.18	D	0.24
CBU_0514		D	D	0.29	D	0.55	D	0.52	D	0.41
CBU_0514a	SCV	D	D	0.67	D	1.13	D	2.56	D	1.09
CBU_0515	SCV	D	D	0.58	D	0.76	D	0.51	D	0.42
CBU_0516	SCV	D	D	8.10	D	10.24	D	14.38	D	5.83
CBU_0516a		D	D	0.48	D	0.70	D	0.72	D	0.91
CBU_0517	LCV	D	D	2.53	D	1.42	D	1.59	D	1.55
CBU_0518		D	D	0.82	D	0.58	D	0.64	D	0.82
CBU_0519	LCV	D	D	2.23	D	1.31	D	1.35	D	1.46
CBU_0520	LCV	D	D	1.48	D	1.10	D	1.11	D	1.30
CBU_0521	LCV	D	D	2.20	D	1.62	D	1.33	D	1.77
CBU_0522		D	ND	1.44	D	1.53	ND	0.74	ND	0.21
CBU_0522a		ND	ND		ND		ND		ND	
CBU_0523		ND	ND		ND		ND		ND	
CBU_0524		D	D	0.28	D	0.39	D	0.32	D	0.40
CBU_0525		D	D	0.38	D	0.46	D	0.57	D	0.61
CBU_0526		D	D	1.35	D	1.29	D	1.70	D	1.38
CBU_0527		D	D	2.52	D	1.98	D	1.76	D	1.77
CBU_0528	LCV	D	D	2.03	D	1.42	D	1.65	D	1.74
CBU_0529		D	D	0.36	D	0.33	D	0.23	D	0.41
CBU_0530		D	D	0.56	D	0.54	D	0.53	D	0.69
CBU_0531		D	D	0.90	D	0.81	D	0.77	D	0.88
CBU_0532	LCV	D	D	0.91	D	1.46	D	1.75	D	1.60
CBU_0533		D	D	0.72	D	0.58	D	0.67	D	0.74
CBU_0534		D	D	0.45	D	0.54	D	0.49	D	0.42
CBU_0535		D	D	0.33	D	0.29	D	0.25	D	0.34
CBU_0536	SCV	D	D	0.07	D	0.16	D	0.09	D	0.24
CBU_0537	SCV	D	D	85.67	D	29.74	D	38.32	D	8.88
CBU_0538	SCV	D	D	0.94	D	1.24	D	0.73	D	1.68
CBU_0539		D	D	0.33	D	0.43	D	0.49	D	0.53
CBU_0540		D	D	0.60	D	0.71	D	0.80	D	0.79
CBU_0541		D	D	1.35	D	1.26	D	1.34	D	1.02
CBU_0542		D	D	1.27	D	1.51	D	1.63	D	1.39
CBU_0543		D	D	0.59	D	0.77	D	0.64	D	0.48
CBU_0544		D	D	0.18	D	0.32	D	0.23	D	0.30
CBU_0545	SCV	D	D	0.01	D	0.05	D	0.07	D	0.15
CBU_0546	SCV	D	D	0.03	D	0.07	D	0.13	D	0.25
CBU_0547		D	D	0.18	D	0.22	D	0.27	D	0.19
CBU_0548		D	D	0.23	D	0.35	D	0.41	D	0.47
CBU_0549		D	D	0.35	D	0.46	D	0.56	D	0.57
CBU_0550		D	D	0.21	D	0.34	D	0.45	D	0.45
CBU_0552		D	D	1.76	D	1.17	D	0.83	D	0.86
CBU_0554		ND	ND		ND		ND		ND	
CBU_0554a		ND	ND		ND		ND		ND	
CBU_0555	SCV	D	D	0.02	D	0.01	D	0.05	D	0.20

184

Gene	Type								
CBU_0556		D	D	8.64	D	5.66	D	6.74	D	4.66
CBU_0557		D	D	4.17	D	3.07	D	2.72	D	2.19
CBU_0558		D	D	8.43	D	3.99	D	4.13	D	3.66
CBU_0559	LCV	D	D	1.79	D	1.44	D	1.41	D	1.33
CBU_0560		D	D	0.78	D	1.02	D	1.17	D	1.29
CBU_0562		D	D	0.29	D	0.40	D	0.42	D	0.33
CBU_0562a	SCV	D	D	0.06	D	0.16	D	0.21	D	0.32
CBU_0563		ND	ND			ND		ND		ND	
CBU_0564		D	D	1.42	D	0.86	D	0.58	D	0.58
CBU_0565		D	D	0.48	D	0.48	D	0.24	D	0.30
CBU_0566		D	D	0.77	D	0.59	D	0.62	D	0.51
CBU_0567		D	D	0.52	D	0.49	D	0.73	D	0.56
CBU_0568		D	D	0.46	D	0.51	D	0.77	D	0.90
CBU_0569		D	D	4.20	D	2.95	D	3.68	D	3.46
CBU_0570	LCV	D	D	2.05	D	1.24	D	1.00	D	1.06
CBU_0571	SCV	D	ND	0.01	D	0.07	D	0.02	D	0.07
CBU_0572		D	D	0.47	D	0.61	D	0.62	D	0.58
CBU_0573		D	D	1.18	D	1.25	D	1.37	D	1.07
CBU_0574		D	D	0.47	D	0.62	D	0.73	D	0.81
CBU_0576		D	D	0.54	D	0.96	D	1.33	D	1.25
CBU_0577		D	D	0.60	D	0.94	D	1.04	D	1.18
CBU_0578		D	D	1.39	D	1.66	D	1.73	D	1.42
CBU_0579		D	D	0.37	D	0.69	D	0.42	D	0.41
CBU_0580		D	D	1.03	D	1.60	D	1.77	D	1.43
CBU_0581		D	D	0.80	D	1.32	D	1.35	D	1.32
CBU_0582		D	D	0.25	D	0.51	D	0.45	D	0.45
CBU_0583		D	D	0.10	D	0.31	D	0.37	D	0.50
CBU_0584		D	D	0.04	D	0.08	D	0.06	D	0.09
CBU_0585		D	D	0.41	D	0.82	D	0.88	D	1.14
CBU_0586		D	D	0.28	D	0.42	D	0.51	D	0.57
CBU_0587		D	D	0.23	D	0.40	D	0.36	D	0.44
CBU_0588		D	D	0.41	D	0.49	D	0.53	D	0.52
CBU_0589		D	D	0.59	D	1.00	D	1.19	D	0.99
CBU_0590		D	D	0.39	D	0.60	D	0.45	D	0.90
CBU_0591		D	D	0.48	D	0.72	D	0.74	D	0.61
CBU_0592		D	D	0.69	D	0.48	D	0.49	D	0.33
CBU_0596		D	D	0.25	D	0.40	D	0.33	D	0.16
CBU_0596a		D	D	0.55	D	1.49	D	2.84	D	1.58
CBU_0597		D	D	1.93	D	0.96	D	0.71	D	0.52
CBU_0598		D	D	0.26	D	0.32	D	0.33	D	0.40
CBU_0599		D	D	0.42	D	0.75	D	0.69	D	0.66
CBU_0607	LCV	D	D	7.76	D	3.40	D	3.74	D	3.31
CBU_0608		D	D	5.61	D	2.46	D	3.04	D	2.32
CBU_0609	LCV	D	D	6.14	D	3.56	D	4.05	D	3.85
CBU_0610	LCV	D	D	1.92	D	1.56	D	1.14	D	1.37
CBU_0611	LCV	D	D	3.22	D	1.99	D	1.88	D	1.92
CBU_0612		D	D	0.88	D	0.86	D	1.31	D	1.56
CBU_0613		D	D	2.51	D	2.18	D	2.27	D	2.30
CBU_0614		D	D	2.13	D	1.53	D	2.27	D	1.82
CBU_0615		D	D	1.73	D	1.53	D	1.96	ND	1.71
CBU_0616	LCV	D	D	5.40	D	4.22	D	4.61	D	3.03
CBU_0617	LCV	D	D	1.20	D	0.46	D	0.99	D	0.87
CBU_0618		D	D	1.05	D	0.30	D	0.36	D	0.39
CBU_0619		D	D	0.29	D	0.47	D	0.56	D	0.45
CBU_0620		D	D	1.08	D	1.13	D	1.51	D	1.22
CBU_0621		D	D	0.93	D	1.28	D	1.70	D	1.74
CBU_0622		D	D	0.88	D	0.84	D	0.76	D	0.89
CBU_0623		D	ND	0.51	D	2.37	ND	0.26	D	0.75
CBU_0624		D	D	1.06	D	1.40	D	1.01	D	1.08
CBU_0625		D	D	0.28	D	0.52	D	0.45	D	0.44
CBU_0626		D	D	0.34	D	0.36	D	0.30	D	0.27
CBU_0627		D	D	126.17	D	68.34	D	61.22	D	12.67
CBU_0628		D	D	1.70	D	2.14	D	2.08	D	2.09
CBU_0629		D	D	2.01	D	2.07	D	2.20	D	2.49
CBU_0630		D	D	1.19	D	1.24	D	1.36	D	1.61
CBU_0631		D	D	5.59	D	5.39	D	5.18	D	4.54
CBU_0632		D	D	0.32	D	0.85	D	0.79	D	0.63
CBU_0634		D	D	0.53	D	0.73	D	0.56	D	0.57
CBU_0635		D	D	0.30	D	0.36	D	0.48	D	0.42
CBU_0636		D	D	0.39	D	0.71	D	0.80	D	0.73

CBU_0637		D	D	0.32	D	0.50	D	0.74	D	1.01
CBU_0638		D	D	3.56	D	2.63	D	4.21	D	3.45
CBU_0639		D	D	4.66	D	2.87	D	2.72	D	2.53
CBU_0640	LCV	D	D	3.76	D	3.37	D	3.95	D	3.65
CBU_0641	LCV	D	D	1.21	D	0.78	D	0.65	D	0.80
CBU_0642		D	D	0.21	D	0.41	D	0.39	D	0.39
CBU_0643		D	D	0.22	D	0.58	D	0.64	D	0.65
CBU_0644	SCV	D	D	0.24	ND	0.01	D	0.12	D	0.07
CBU_0645	SCV	D	D	0.15	D	0.11	D	0.19	D	0.27
CBU_0646		D	D	0.42	D	0.24	D	0.20	D	0.27
CBU_0647		D	D	0.32	D	0.26	D	0.33	D	0.44
CBU_0648	LCV	D	D	0.66	D	0.49	D	0.58	D	0.76
CBU_0649		D	D	0.60	D	0.38	D	0.43	D	0.59
CBU_0656		D	D	0.69	D	0.93	D	0.95	D	1.03
CBU_0657		D	D	0.87	D	1.00	D	1.48	D	1.31
CBU_0658	LCV	D	D	0.89	D	1.31	D	1.44	D	1.70
CBU_0659		D	D	0.62	D	0.57	D	0.75	D	0.72
CBU_0660		D	D	0.68	D	0.46	D	0.26	D	0.39
CBU_0661		D	D	0.30	D	0.86	D	1.17	D	0.49
CBU_0662		D	ND	18.67	ND	9.09	ND	9.59	ND	2.70
CBU_0663		D	ND	18.67	ND	9.09	ND	9.59	ND	2.70
CBU_0664		D	D	1.48	D	1.21	D	0.62	D	0.52
CBU_0665		D	D	0.97	D	1.95	D	1.51	D	2.02
CBU_0666		D	D	0.31	D	0.40	D	0.38	D	0.30
CBU_0667		D	D	0.23	D	0.39	D	0.33	D	0.25
CBU_0668		D	D	0.44	D	0.54	D	0.35	D	0.24
CBU_0669		D	D	1.16	D	0.57	D	0.61	D	1.06
CBU_0670		D	D	3.90	D	2.40	D	1.22	D	0.72
CBU_0671	LCV	D	D	2.69	D	2.47	D	2.29	D	2.34
CBU_0672		D	D	10.58	D	9.09	D	7.08	D	4.88
CBU_0673	LCV	D	D	2.15	D	2.49	D	2.12	D	2.53
CBU_0674		D	D	1.55	D	2.20	D	2.75	D	2.61
CBU_0675	LCV	D	D	3.90	D	3.35	D	2.60	D	2.55
CBU_0676	LCV	D	D	8.56	D	8.07	D	8.59	D	10.02
CBU_0677	LCV	D	D	9.28	D	10.05	D	12.56	D	12.69
CBU_0678		D	D	10.93	D	11.58	D	16.71	D	14.70
CBU_0679		ND	ND	#VALUE!	ND	#VALUE!	ND	#VALUE!	ND	#VALUE!
CBU_0680		ND	ND	#VALUE!	ND	#VALUE!	ND	#VALUE!	ND	#VALUE!
CBU_0681	SCV	ND	ND	#VALUE!	ND	#VALUE!	ND	#VALUE!	ND	#VALUE!
CBU_0682		ND	ND	#VALUE!	ND	#VALUE!	ND	#VALUE!	ND	#VALUE!
CBU_0683	SCV	ND	ND	#VALUE!	ND	#VALUE!	ND	#VALUE!	ND	#VALUE!
CBU_0684		ND	ND	#VALUE!	ND	#VALUE!	ND	#VALUE!	ND	#VALUE!
CBU_0685		ND	ND	#VALUE!	ND	#VALUE!	ND	#VALUE!	ND	#VALUE!
CBU_0686		ND	ND	#VALUE!	ND	#VALUE!	ND	#VALUE!	ND	#VALUE!
CBU_0687		ND	ND	#VALUE!	ND	#VALUE!	ND	#VALUE!	ND	#VALUE!
CBU_0688		ND	ND	#VALUE!	ND	#VALUE!	ND	#VALUE!	ND	#VALUE!
CBU_0689		ND	ND	#VALUE!	ND	#VALUE!	ND	#VALUE!	ND	#VALUE!
CBU_0690	SCV	ND	ND	#VALUE!	ND	#VALUE!	ND	#VALUE!	ND	#VALUE!
CBU_0691		ND	ND	#VALUE!	ND	#VALUE!	ND	#VALUE!	ND	#VALUE!
CBU_0692	SCV	ND	ND	#VALUE!	ND	#VALUE!	ND	#VALUE!	ND	#VALUE!
CBU_0693	SCV	ND	ND	#VALUE!	ND	#VALUE!	ND	#VALUE!	ND	#VALUE!
CBU_0694	SCV	ND	ND	#VALUE!	ND	#VALUE!	ND	#VALUE!	ND	#VALUE!
CBU_0695	LCV	ND	ND	#VALUE!	ND	#VALUE!	ND	#VALUE!	ND	#VALUE!
CBU_0696	SCV	ND	ND	#VALUE!	ND	#VALUE!	ND	#VALUE!	ND	#VALUE!
CBU_0697		ND	ND	#VALUE!	ND	#VALUE!	ND	#VALUE!	ND	#VALUE!
CBU_0698		D	D	0.25	D	0.48	D	0.42	D	0.36
CBU_0699		D	D	1.07	D	1.87	D	2.46	D	2.15
CBU_0700		D	D	0.68	D	0.93	D	1.30	D	1.32
CBU_0701	LCV	D	D	0.71	D	1.53	D	1.43	D	1.23
CBU_0702		D	D	3.94	D	3.92	D	3.32	D	3.37
CBU_0703	LCV	D	D	2.32	D	3.57	D	4.37	D	3.60
CBU_0704		D	D	5.85	D	6.31	D	6.21	D	5.49
CBU_0705		D	D	1.87	D	1.39	D	0.98	D	1.14
CBU_0706		D	D	2.97	D	3.09	D	2.92	D	2.40
CBU_0707	SCV	D	D	0.71	D	1.82	D	0.97	D	1.56
CBU_0711	SCV	D	D	0.04	D	0.22	D	0.18	D	0.17
CBU_0712		D	D	0.17	D	0.36	D	0.32	D	0.40
CBU_0713		D	D	0.36	D	0.58	D	0.55	D	0.64
CBU_0714		D	D	0.53	D	0.82	D	0.93	D	0.90
CBU_0715		D	D	0.69	D	0.68	D	0.52	D	0.40

CBU_0716		D	D	0.11	D	0.25	D	0.21	D	0.46
CBU_0718	SCV	D	D	0.00	D	0.02	D	0.08	D	0.21
CBU_0719	SCV	D	D	0.00	D	0.03	D	0.07	D	0.19
CBU_0720	LCV	D	D	5.95	D	3.25	D	4.67	D	4.59
CBU_0721	LCV	D	D	6.72	D	3.43	D	5.13	D	5.42
CBU_0722	LCV	D	D	5.89	D	4.24	D	3.04	D	5.19
CBU_0724		ND	ND		ND		ND		ND	
CBU_0724c	LCV	ND	ND		ND		ND		ND	
CBU_0727		D	D	0.75	D	0.93	D	1.01	D	0.85
CBU_0728		D	D	1.13	D	1.57	D	1.59	D	1.48
CBU_0729		D	D	0.20	D	0.38	D	0.37	D	0.38
CBU_0730		D	D	0.27	D	0.53	D	0.46	D	0.49
CBU_0731	SCV	D	D	0.04	D	0.06	D	0.17	D	0.52
CBU_0734		D	ND	4.76	ND	2.32	ND	2.44	ND	0.69
CBU_0735		D	D	2.86	D	1.66	D	1.46	D	1.45
CBU_0736		D	D	0.14	D	0.11	D	0.13	D	0.14
CBU_0737	LCV	D	D	1.07	D	1.00	D	0.95	D	0.98
CBU_0738		D	D	0.44	D	0.88	D	0.83	D	0.83
CBU_0739		D	D	0.49	D	0.56	D	0.56	D	0.85
CBU_0740		D	D	0.67	D	0.72	D	1.00	D	1.20
CBU_0741		D	D	0.61	D	0.59	D	0.77	D	0.61
CBU_0742	SCV	D	D	2.96	ND	0.71	ND	0.75	D	0.46
CBU_0743	SCV	D	D	0.40	D	0.38	D	0.09	D	0.07
CBU_0744		D	D	0.39	D	0.42	D	0.34	D	0.26
CBU_0745	SCV	D	D	0.13	D	0.33	D	0.25	D	0.26
CBU_0746		D	D	0.11	D	0.17	D	0.16	D	0.16
CBU_0747	LCV	D	D	1.78	D	1.49	D	1.74	D	0.63
CBU_0748		D	D	0.27	D	0.34	D	0.31	D	0.20
CBU_0749	LCV	D	D	1.92	D	1.48	D	1.84	D	1.87
CBU_0750		D	D	0.86	D	0.80	D	0.78	D	0.86
CBU_0751	SCV	D	D	0.12	D	0.12	D	0.21	D	0.38
CBU_0752		D	D	0.20	D	0.20	D	0.19	D	0.24
CBU_0752a		D	D	1.47	D	1.32	D	0.77	D	0.69
CBU_0753		D	D	1.37	D	1.27	D	0.89	D	0.70
CBU_0754		D	D	0.49	D	0.59	D	0.57	D	0.54
CBU_0755		D	D	0.24	D	0.34	D	0.33	D	0.41
CBU_0756		D	D	0.90	D	0.71	D	0.59	D	0.40
CBU_0757		D	D	0.28	D	0.47	D	0.45	D	0.32
CBU_0758	LCV	D	D	0.95	D	0.83	D	0.72	D	0.76
CBU_0760		D	ND	0.26	D	0.49	D	0.51	D	0.63
CBU_0761		D	D	0.82	D	1.54	D	1.03	D	0.81
CBU_0762		D	D	0.53	D	1.11	D	1.00	D	0.76
CBU_0763		D	D	0.63	D	0.90	D	1.03	D	0.85
CBU_0766		D	D	1.86	D	1.65	D	1.51	D	1.28
CBU_0767	LCV	D	D	7.81	D	4.88	D	2.98	D	2.14
CBU_0768		D	D	2.87	D	2.79	D	1.47	D	1.31
CBU_0769		D	D	0.37	D	1.88	D	1.34	D	1.19
CBU_0770		D	D	0.95	D	1.28	D	1.24	D	1.22
CBU_0771		D	D	1.66	D	2.27	D	2.18	D	2.78
CBU_0772		D	D	0.52	D	1.38	D	1.82	D	2.09
CBU_0773		D	D	0.47	D	1.01	D	1.02	D	1.10
CBU_0774	SCV	D	D	0.74	D	1.22	D	0.66	D	0.43
CBU_0775	SCV	D	D	1.24	D	1.30	D	0.50	D	0.42
CBU_0776	SCV	D	D	0.20	D	0.53	D	0.53	D	0.39
CBU_0777		D	D	0.35	D	0.72	D	0.74	D	0.83
CBU_0777c		D	D	1.77	D	0.73	D	0.76	D	0.75
CBU_0780		D	D	1.49	D	1.79	D	1.74	D	1.78
CBU_0781		D	D	0.78	D	1.15	D	1.90	D	1.63
CBU_0782		D	D	0.66	D	1.01	D	1.79	D	1.56
CBU_0784	SCV	D	D	0.65	D	0.57	ND	0.17	D	0.31
CBU_0786		D	D	0.24	D	0.33	D	0.30	D	0.23
CBU_0787		D	D	0.36	D	0.44	D	0.65	D	0.46
CBU_0788		D	D	1.00	D	1.12	D	1.07	D	0.89
CBU_0789	SCV	D	D	0.25	D	0.77	D	0.76	D	0.78
CBU_0792		D	D	1.20	D	1.75	D	1.59	D	1.35
CBU_0793		D	D	17.25	D	5.93	D	1.37	D	1.92
CBU_0794		D	D	2.89	D	2.00	D	2.78	D	1.65
CBU_0795		D	D	0.68	D	1.32	D	0.62	D	1.03
CBU_0796	LCV	D	D	1.86	D	2.90	D	2.38	D	2.89
CBU_0797		D	D	0.70	D	0.59	D	0.48	D	0.41

187

CBU_0798		D	D	0.33	D	0.33	D	0.26	D	0.25
CBU_0799	LCV	D	D	6.94	D	3.38	D	10.58	D	1.00
CBU_0800	LCV	D	D	0.94	D	1.01	D	1.88	D	1.40
CBU_0801	LCV	D	D	0.71	D	2.10	D	1.55	D	1.54
CBU_0802		D	D	0.16	D	0.22	D	0.20	D	0.20
CBU_0803		D	D	0.48	D	0.67	D	0.48	D	0.60
CBU_0804		D	D	1.46	D	1.52	D	1.62	D	1.48
CBU_0805		D	D	20.73	D	19.07	D	29.41	D	11.11
CBU_0806		D	D	11.17	D	16.99	D	15.27	D	2.46
CBU_0807		D	D	2.30	D	1.65	D	1.48	D	1.38
CBU_0808	LCV	D	D	0.79	D	0.49	D	0.58	D	0.58
CBU_0809		D	D	2.78	D	2.10	D	2.17	D	1.69
CBU_0810		D	D	1.75	D	1.38	D	1.28	D	1.41
CBU_0811		D	D	8.69	D	5.24	D	3.41	D	3.50
CBU_0812	LCV	D	D	6.85	D	4.43	D	1.88	D	2.31
CBU_0813		D	D	1.63	D	2.93	D	1.38	D	1.70
CBU_0817		D	D	2.85	D	3.88	D	1.63	D	0.97
CBU_0818		D	D	0.50	D	1.41	D	0.76	D	0.88
CBU_0819	SCV	D	D	0.12	D	1.83	D	0.75	D	1.20
CBU_0822		D	D	0.63	D	0.81	D	0.51	D	0.41
CBU_0823		D	D	1.08	D	1.10	D	0.91	D	1.03
CBU_0824		D	D	0.38	D	0.63	D	0.67	D	0.68
CBU_0825	LCV	D	D	13.04	D	7.19	D	5.49	D	5.80
CBU_0826	LCV	D	D	15.33	D	9.74	D	10.12	D	8.67
CBU_0827	LCV	D	D	0.69	D	0.91	D	0.86	D	0.82
CBU_0828	LCV	D	D	1.18	D	1.24	D	1.48	D	1.40
CBU_0829		D	D	1.54	D	2.15	D	1.74	D	1.63
CBU_0830		D	D	0.85	D	1.63	D	1.73	D	1.54
CBU_0831		D	D	0.71	D	0.96	D	1.04	D	0.77
CBU_0832		D	D	1.17	D	2.48	D	2.32	D	1.92
CBU_0833	LCV	D	D	1.27	D	1.57	D	1.26	D	1.13
CBU_0834		D	D	1.09	D	1.25	D	0.59	D	0.75
CBU_0835		D	D	3.73	D	2.57	D	2.27	D	1.44
CBU_0836		D	D	1.14	D	2.44	D	1.82	D	1.52
CBU_0837		D	D	1.90	D	2.13	D	1.41	D	1.17
CBU_0838		D	D	3.00	D	3.21	D	2.57	D	2.16
CBU_0839		D	D	2.01	D	2.59	D	1.79	D	1.82
CBU_0840		D	D	1.83	D	2.01	D	1.48	D	1.31
CBU_0841	LCV	D	D	2.09	D	2.57	D	2.14	D	1.73
CBU_0842		D	D	3.25	D	2.97	D	2.43	D	1.97
CBU_0843		D	D	2.60	D	2.49	D	2.43	D	1.61
CBU_0844	LCV	D	D	3.13	D	2.58	D	2.93	D	3.43
CBU_0845	LCV	D	D	2.35	D	1.57	D	1.45	D	2.02
CBU_0846		D	D	2.67	D	2.59	D	2.50	D	2.35
CBU_0847	LCV	D	D	1.69	D	1.85	D	1.90	D	2.19
CBU_0848		D	D	1.61	D	1.37	D	1.78	D	1.63
CBU_0849		D	D	5.09	D	4.39	D	5.49	D	4.53
CBU_0850		D	D	0.09	D	0.12	D	0.16	D	0.29
CBU_0851	LCV	D	D	2.67	D	1.69	D	1.50	D	1.58
CBU_0852		D	D	6.54	D	3.99	D	4.13	D	4.21
CBU_0853		D	D	1.63	D	0.62	D	0.65	D	0.48
CBU_0854		D	D	15.99	D	3.98	ND	2.06	D	1.18
CBU_0856		D	D	0.44	D	0.44	D	0.53	D	0.56
CBU_0857		D	D	0.92	D	1.36	D	1.99	D	1.26
CBU_0858		D	D	0.64	D	0.68	D	0.62	D	0.72
CBU_0859		D	D	0.27	D	0.45	D	0.33	D	0.46
CBU_0860		D	ND	0.11	D	0.29	D	0.41	D	0.45
CBU_0863		D	D	1.15	ND	0.10	D	0.57	D	0.18
CBU_0864	LCV	D	D	1.36	D	1.20	D	0.98	D	1.06
CBU_0865	LCV	D	D	1.81	D	1.35	D	1.48	D	1.61
CBU_0866		D	D	1.32	D	0.80	D	0.78	D	0.87
CBU_0867	LCV	D	D	3.73	D	2.53	D	3.23	D	3.48
CBU_0868		D	D	0.82	D	0.76	D	0.89	D	1.03
CBU_0869		D	D	0.55	D	0.92	D	1.20	D	0.95
CBU_0870		D	D	1.27	D	1.09	D	0.72	D	0.85
CBU_0872	LCV	D	D	1.44	D	1.45	D	1.67	D	1.56
CBU_0873	LCV	D	D	0.69	D	0.45	D	0.49	D	0.40
CBU_0874		D	D	0.88	D	1.04	D	1.13	D	1.24
CBU_0875		D	D	0.37	D	0.64	D	0.74	D	0.73
CBU_0876		D	D	0.94	D	1.51	D	1.98	D	1.99

CBU_0877	SCV	ND	ND	1.00	D	34.49	ND	1.00	ND	1.00
CBU_0880		D	D	1.84	D	2.90	D	1.76	D	1.12
CBU_0881		D	D	1.16	D	0.28	D	0.51	D	0.44
CBU_0883		D	D	0.18	D	0.89	D	1.14	D	1.10
CBU_0884	LCV	D	D	8.08	D	4.03	D	3.38	D	3.59
CBU_0885	LCV	D	D	2.52	D	2.04	D	1.79	D	1.97
CBU_0886	LCV	D	D	6.18	D	2.86	D	3.86	D	2.75
CBU_0888	LCV	D	D	0.34	D	0.37	D	0.35	D	0.31
CBU_0889		D	D	0.63	D	0.58	D	0.64	D	0.63
CBU_0890	LCV	D	D	0.96	D	1.25	D	1.18	D	1.24
CBU_0891		D	D	0.92	D	0.98	D	1.01	D	0.94
CBU_0892		D	D	1.29	D	1.42	D	1.49	D	1.33
CBU_0893	SCV	D	D	1.34	D	1.49	D	1.86	D	1.80
CBU_0894	LCV	D	D	2.81	D	1.84	D	1.42	D	1.54
CBU_0895		D	D	0.55	D	0.46	D	0.32	D	0.35
CBU_0896		D	D	0.41	D	0.36	D	0.27	D	0.28
CBU_0897		D	D	1.10	D	0.84	D	0.81	D	0.80
CBU_0898		D	D	0.53	D	1.25	D	1.04	D	1.46
CBU_0900		D	ND	0.90	D	0.95	D	0.95	ND	0.13
CBU_0904		D	D	0.21	D	0.31	D	0.37	D	0.36
CBU_0905	LCV	D	D	1.78	D	0.94	D	0.62	D	0.77
CBU_0906		D	D	0.60	D	0.64	D	0.79	D	0.83
CBU_0907		D	D	1.27	D	1.00	D	1.09	D	0.60
CBU_0908	LCV	D	D	0.39	D	0.27	D	0.12	D	0.25
CBU_0909	SCV	D	D	0.38	D	0.61	D	0.70	D	0.74
CBU_0910		D	D	0.49	D	0.47	D	0.40	D	0.43
CBU_0911		D	D	25.22	D	10.34	D	9.57	D	1.75
CBU_0912	LCV	D	D	1.42	D	1.22	D	1.46	D	1.60
CBU_0913	LCV	D	D	1.88	D	1.44	D	1.75	D	1.81
CBU_0914	SCV	D	D	0.13	D	0.21	D	0.21	D	0.26
CBU_0915		D	D	0.05	D	0.11	D	0.11	D	0.14
CBU_0916		D	D	0.07	D	0.15	D	0.18	D	0.26
CBU_0918		D	D	1.13	D	0.63	D	0.43	D	0.42
CBU_0920	SCV	D	D	0.17	D	0.22	D	0.20	D	0.22
CBU_0921	SCV	D	D	0.04	D	0.08	D	0.10	D	0.13
CBU_0922		D	D	0.36	D	0.74	D	0.88	D	1.20
CBU_0923		D	D	0.47	D	0.44	D	0.35	D	0.39
CBU_0924	SCV	D	D	0.04	D	0.04	D	0.08	D	0.14
CBU_0925	SCV	D	D	0.00	D	0.01	D	0.05	D	0.14
CBU_0926		D	D	0.40	D	0.45	D	0.40	D	0.37
CBU_0927		D	D	0.57	D	0.55	D	0.46	D	0.46
CBU_0928		D	D	0.30	D	0.33	D	0.35	D	0.39
CBU_0929		D	D	1.18	D	1.26	D	1.21	D	1.21
CBU_0930		D	D	0.44	D	0.46	D	0.39	D	0.51
CBU_0931		D	D	0.52	D	0.63	D	0.63	D	0.59
CBU_0932		D	D	0.24	D	0.36	D	0.48	D	0.58
CBU_0933		D	D	0.87	D	0.59	D	0.45	D	0.41
CBU_0934		D	D	0.86	D	0.78	D	0.74	D	0.70
CBU_0935		D	D	0.86	D	0.73	D	0.67	D	0.62
CBU_0936		D	D	0.97	D	1.67	D	1.91	D	1.94
CBU_0937		D	D	0.56	D	0.54	D	0.74	D	0.84
CBU_0939	LCV	D	D	1.17	D	0.94	D	0.61	D	0.68
CBU_0940		D	D	2.05	D	1.74	D	1.33	D	1.05
CBU_0941	LCV	D	D	0.43	D	0.22	D	0.31	D	0.21
CBU_0942		D	D	0.30	D	0.70	D	0.37	D	0.38
CBU_0943	SCV	D	D	0.02	D	0.07	D	0.15	D	0.41
CBU_0944		D	D	1.85	D	0.47	D	0.90	D	0.71
CBU_0945		D	D	0.24	D	0.51	D	0.52	D	0.48
CBU_0946	LCV	D	D	0.61	D	0.60	D	0.67	D	0.75
CBU_0948		D	D	0.28	D	0.52	D	0.77	D	0.44
CBU_0949		D	D	5.70	D	1.53	D	1.60	ND	2.32
CBU_0952	LCV	D	D	0.23	D	0.43	D	0.45	D	0.56
CBU_0953		D	D	1.20	D	0.92	D	0.71	D	0.65
CBU_0954		D	D	1.02	D	1.06	D	0.60	D	0.54
CBU_0955		D	D	1.09	D	0.89	D	0.76	D	0.79
CBU_0956	SCV	D	D	0.04	D	0.08	D	0.23	D	0.42
CBU_0957	SCV	D	D	0.06	D	0.04	D	0.10	D	0.17
CBU_0959		D	D	0.06	D	0.11	D	0.13	D	0.18
CBU_0960	SCV	D	D	0.02	D	0.08	D	0.05	D	0.10
CBU_0961	SCV	D	D	0.12	D	0.18	D	0.22	D	0.29

CBU_0962		D	D	0.72	D	0.71	D	1.17	D	1.12
CBU_0963	LCV	D	D	0.38	D	0.63	D	0.79	D	0.92
CBU_0964		D	D	0.53	D	0.50	D	0.29	D	0.31
CBU_0964a	LCV	D	D	2.15	D	2.15	D	1.91	D	1.57
CBU_0965		D	D	2.06	D	1.65	D	2.02	D	2.14
CBU_0966		D	D	3.29	D	3.48	D	4.10	D	4.52
CBU_0967		D	D	4.24	D	1.62	D	2.53	D	2.24
CBU_0968		D	D	1.11	D	2.16	D	2.16	D	2.61
CBU_0970	LCV	D	D	6.25	D	4.00	D	5.37	D	5.66
CBU_0971		D	D	0.80	D	1.70	D	1.77	D	1.39
CBU_0972		D	D	0.48	D	1.00	D	0.85	D	0.90
CBU_0973		D	D	0.72	D	0.86	D	1.03	D	1.12
CBU_0974		D	D	0.63	D	1.16	D	1.37	D	1.65
CBU_0975		D	D	1.00	D	1.48	D	2.06	D	1.81
CBU_0976		D	D	0.98	D	1.54	D	2.06	D	1.52
CBU_0977		D	D	0.98	D	1.17	D	1.34	D	1.39
CBU_0978		D	D	0.24	D	0.45	D	0.46	D	0.36
CBU_0979	SCV	D	D	0.05	D	0.15	D	0.26	D	0.36
CBU_0980		D	D	0.00	D	0.03	D	0.22	D	0.62
CBU_0981		D	D	43.61	D	34.14	D	33.94	ND	1.65
CBU_0982		D	D	0.23	D	0.29	D	0.27	D	0.26
CBU_0984		D	D	0.70	D	0.56	D	0.66	D	0.50
CBU_0985		D	D	3.50	D	1.86	D	1.61	D	0.50
CBU_0986		D	D	0.73	D	0.94	D	1.33	D	1.36
CBU_0987		D	D	0.11	D	0.14	D	0.21	D	0.43
CBU_0988		D	D	0.27	D	0.26	D	0.25	D	0.30
CBU_0993	LCV	D	D	5.57	D	3.51	D	3.18	D	4.10
CBU_0994	SCV	D	D	27.61	ND	2.44	D	5.32	D	2.72
CBU_0995	LCV	D	D	1.45	D	1.32	D	0.80	D	0.82
CBU_0996	LCV	D	D	0.78	D	0.65	D	0.61	D	0.80
CBU_0997	LCV	D	D	0.93	D	1.09	D	1.37	D	1.71
CBU_0998		D	D	4.43	D	4.61	D	3.10	D	2.39
CBU_0999	LCV	D	D	2.69	D	2.67	D	2.41	D	1.68
CBU_1000		D	D	1.62	D	1.86	D	1.86	D	1.63
CBU_1001		D	D	1.52	D	1.35	D	1.17	D	0.95
CBU_1002	LCV	D	D	0.73	D	0.73	D	1.12	D	0.75
CBU_1003		D	D	5.74	D	3.90	D	3.73	D	2.03
CBU_1004		D	D	41.31	D	30.94	D	25.58	D	11.76
CBU_1005		D	D	12.62	D	12.52	D	12.69	D	7.63
CBU_1006		D	D	17.08	D	19.35	D	21.16	D	9.64
CBU_1007		D	D	8.34	D	18.66	D	14.75	D	9.82
CBU_1008		D	D	34.55	D	30.43	D	28.60	D	15.91
CBU_1010		D	D	5.70	D	4.08	D	2.75	D	2.35
CBU_1011	SCV	D	D	1.41	D	2.94	D	1.37	D	1.24
CBU_1014		D	D	2.21	D	6.78	D	3.26	D	1.84
CBU_1015		D	D	1.70	D	1.08	D	0.51	D	0.49
CBU_1016		D	ND	4.06	D	4.21	ND	2.08	ND	0.59
CBU_1017		D	D	0.65	D	2.00	D	2.05	D	2.00
CBU_1018	LCV	D	D	0.47	D	0.50	D	0.57	D	0.50
CBU_1019	LCV	D	D	0.20	D	1.56	D	0.82	D	0.83
CBU_1020		D	D	17.53	D	8.82	ND	4.56	ND	1.28
CBU_1021		D	D	0.49	D	0.49	D	0.52	D	0.62
CBU_1022		D	D	0.43	D	0.39	D	0.31	D	0.47
CBU_1023		D	D	0.41	D	0.71	D	1.18	D	1.15
CBU_1023a		D	D	0.82	D	0.54	D	1.11	D	0.22
CBU_1027		D	D	0.67	D	1.51	D	1.41	D	1.51
CBU_1028		D	D	0.87	D	1.93	D	0.98	D	0.91
CBU_1031	SCV	D	D	0.16	D	0.63	D	0.46	D	0.39
CBU_1034	LCV	D	D	0.86	D	0.92	D	0.73	D	0.69
CBU_1035		D	D	0.67	D	0.82	D	0.89	D	0.89
CBU_1035d		D	D	3.70	D	2.37	D	4.08	D	3.44
CBU_1038		D	D	4.75	D	3.14	D	5.01	ND	4.28
CBU_1039	LCV	D	D	3.35	D	1.80	D	2.66	D	2.73
CBU_1040	LCV	D	D	0.96	D	0.62	D	0.63	D	0.75
CBU_1041		D	ND	0.50	D	1.01	D	0.51	D	0.44
CBU_1042		D	D	0.14	D	0.27	D	0.31	D	0.43
CBU_1043		D	D	0.77	D	0.73	D	0.82	D	0.63
CBU_1045a		ND	ND	1.00	ND	1.00	ND	1.00	D	29.02
CBU_1050	SCV	D	D	0.14	D	0.23	D	0.36	D	0.65
CBU_1051		D	D	0.86	D	1.19	D	1.33	D	1.07

CBU_1052		D	D	0.47	D	0.66	D	0.65	D	0.64
CBU_1053		D	D	0.38	D	0.60	D	0.49	D	0.44
CBU_1054		D	D	0.56	D	0.90	D	0.87	D	0.90
CBU_1055		D	D	1.14	D	1.47	D	1.37	D	1.18
CBU_1056		D	D	0.52	D	0.76	D	0.72	D	0.80
CBU_1057		D	D	0.31	D	0.26	D	0.34	D	0.34
CBU_1058		D	D	0.52	D	0.64	D	0.77	D	0.77
CBU_1059		D	D	0.34	D	0.52	D	0.50	D	0.48
CBU_1060	LCV	D	D	0.25	D	0.39	D	0.48	D	0.55
CBU_1061		D	D	0.79	D	1.04	D	0.91	D	0.80
CBU_1061a		D	D	5.81	D	2.87	D	3.00	D	1.23
CBU_1063		D	D	1.20	D	0.98	D	1.45	D	0.56
CBU_1064		D	D	0.78	D	1.04	D	1.09	D	0.74
CBU_1065		D	D	0.11	D	0.31	D	0.27	D	0.27
CBU_1066	LCV	D	D	0.27	D	0.33	D	0.43	D	0.54
CBU_1067	LCV	D	D	2.91	D	2.16	D	1.84	D	1.91
CBU_1067a		D	D	0.13	D	0.36	D	0.38	D	0.33
CBU_1071		D	D	0.57	D	0.89	D	0.92	D	1.02
CBU_1072	LCV	D	D	1.37	D	1.28	D	1.23	D	1.35
CBU_1073		D	D	0.57	D	0.82	D	0.66	D	0.87
CBU_1074		D	D	0.84	D	1.54	D	1.62	D	1.54
CBU_1075		D	D	0.47	D	0.52	D	0.58	D	0.53
CBU_1075a		ND	ND		ND		ND		ND	
CBU_1076		D	D	1.83	D	1.27	D	1.59	D	1.71
CBU_1077		D	D	10.05	D	4.82	D	4.51	D	4.15
CBU_1078		D	D	1.45	D	0.69	D	0.54	D	0.70
CBU_1079		D	D	2.57	D	1.18	D	0.92	D	0.94
CBU_1080		D	D	2.69	D	1.49	D	1.57	D	1.33
CBU_1081	LCV	D	D	2.77	D	3.20	D	2.86	D	2.82
CBU_1082		D	D	0.97	D	0.89	D	0.87	D	0.60
CBU_1083		D	D	0.73	D	1.04	D	1.10	D	1.00
CBU_1084		D	D	0.24	D	0.64	D	0.70	D	0.63
CBU_1085		D	D	0.26	D	0.38	D	0.48	D	0.41
CBU_1086		ND	ND		ND		ND		ND	
CBU_1087		D	D	0.73	D	0.53	D	0.44	D	0.19
CBU_1088		D	D	1.01	D	0.85	D	0.79	D	0.78
CBU_1089	SCV	D	D	0.83	D	0.39	D	0.28	D	0.18
CBU_1090		ND	ND		ND		ND		ND	
CBU_1090a		ND	ND		ND		ND		ND	
CBU_1091		D	D	1.51	D	1.35	D	1.54	D	1.39
CBU_1092	SCV	D	D	0.13	D	0.14	D	0.08	D	0.09
CBU_1093		D	D	0.41	D	0.74	D	0.79	D	0.76
CBU_1094		D	D	0.26	D	0.41	D	0.48	D	0.49
CBU_1095	SCV	D	D	0.04	D	0.08	D	0.11	D	0.21
CBU_1096	SCV	D	D	0.04	D	0.10	D	0.18	D	0.29
CBU_1097		D	D	0.15	D	0.22	D	0.19	D	0.14
CBU_1098		D	D	1.14	D	1.31	D	1.63	D	2.00
CBU_1099		D	D	1.36	D	1.43	D	1.40	D	1.76
CBU_1100		D	D	3.70	D	2.61	D	2.64	D	2.42
CBU_1100a	SCV	D	D	5.44	D	2.70	D	2.78	D	1.26
CBU_1103		D	D	0.90	D	0.91	D	1.21	D	1.16
CBU_1104		ND	ND		ND		ND		ND	
CBU_1111		D	D	0.71	D	1.05	D	0.90	D	0.78
CBU_1112	LCV	D	D	0.58	D	0.88	D	0.64	D	0.55
CBU_1115		D	D	0.81	D	1.33	D	1.22	D	1.09
CBU_1116		D	D	6.11	D	4.28	D	5.04	D	4.00
CBU_1117	LCV	D	D	3.31	D	2.88	D	3.27	D	3.02
CBU_1118	LCV	D	D	1.88	D	1.21	D	1.42	D	1.41
CBU_1119	LCV	D	D	2.19	D	1.33	D	1.29	D	1.20
CBU_1120		D	D	1.17	D	1.12	D	1.28	D	1.26
CBU_1121		D	D	0.72	D	0.58	D	0.54	D	0.16
CBU_1122	LCV	D	D	1.38	D	1.10	D	0.94	D	1.11
CBU_1123		D	D	0.73	D	0.64	D	0.90	D	0.90
CBU_1124	LCV	D	D	2.64	D	1.66	D	1.52	D	1.13
CBU_1127	LCV	D	D	0.64	D	0.72	D	0.70	D	0.71
CBU_1128		D	D	0.90	D	1.24	D	1.49	D	1.01
CBU_1129		D	D	0.91	D	0.90	D	0.98	D	0.95
CBU_1130		D	D	0.47	D	0.65	D	0.57	D	0.56
CBU_1131		D	D	1.09	D	1.08	D	0.96	D	0.96
CBU_1132		ND	ND	#VALUE!	ND	#VALUE!	ND	#VALUE!	ND	#VALUE!

191

CBU_1133	LCV	D	D	4.78	D	1.98	D	1.77	D	1.79
CBU_1134		D	D	0.41	D	0.43	D	0.45	D	0.42
CBU_1135	SCV	D	D	0.19	D	0.44	D	0.38	D	0.54
CBU_1136	SCV	D	D	0.00	D	0.01	D	0.04	D	0.10
CBU_1137	SCV	D	ND	0.00	D	0.00	D	0.05	D	0.12
CBU_1138	SCV	D	D	0.00	D	0.01	D	0.11	D	0.34
CBU_1138a		D	D	0.19	D	0.47	D	0.48	D	0.24
CBU_1139	SCV	D	ND	0.24	D	0.49	ND	0.12	D	0.07
CBU_1141		D	D	4.16	D	3.00	D	3.12	D	3.06
CBU_1142		D	D	1.57	D	1.40	D	1.56	D	1.59
CBU_1143		D	D	0.36	D	0.40	D	0.28	D	0.36
CBU_1144		D	D	0.37	D	0.71	D	0.78	D	0.81
CBU_1145		D	D	7.87	D	10.97	D	14.80	D	3.17
CBU_1147		D	D	0.40	D	0.50	D	0.43	D	0.54
CBU_1148		D	D	1.00	D	0.72	D	0.73	D	0.79
CBU_1151		D	D	0.91	D	1.28	D	0.90	D	0.91
CBU_1152		D	D	0.01	D	0.00	D	0.00	D	0.00
CBU_1154	SCV	D	D	0.36	D	0.49	D	0.29	D	0.45
CBU_1155	SCV	D	D	0.21	D	0.42	D	0.65	D	0.52
CBU_1156	SCV	D	D	0.55	D	0.25	D	0.39	D	0.36
CBU_1157		D	D	0.69	D	0.46	D	0.39	D	0.57
CBU_1158	SCV	D	D	1.02	D	0.88	D	0.64	D	0.69
CBU_1159	SCV	D	D	0.72	D	0.81	D	0.73	D	0.60
CBU_1160		D	D	0.91	D	1.05	D	0.83	D	0.93
CBU_1161		D	D	3.15	D	1.44	D	1.12	D	0.16
CBU_1162		D	D	2.50	D	2.71	D	2.38	D	2.59
CBU_1169	SCV	D	D	0.11	D	0.21	D	0.44	D	1.14
CBU_1170		D	D	0.01	D	0.03	D	0.11	D	0.39
CBU_1171		D	D	0.13	D	0.08	D	0.16	D	0.17
CBU_1173	SCV	D	D	0.06	D	0.21	D	0.29	D	0.53
CBU_1175	SCV	D	D	1.20	D	1.07	D	1.16	D	1.16
CBU_1176		D	D	0.12	D	0.24	D	0.32	D	0.24
CBU_1177		D	D	2.08	ND	0.48	ND	0.51	ND	0.14
CBU_1178		D	D	7.04	D	4.20	D	4.05	D	1.11
CBU_1179	LCV	D	D	1.47	D	1.22	D	1.23	D	1.64
CBU_1180	SCV	D	D	7.36	ND	1.69	ND	1.78	ND	0.50
CBU_1181		D	D	6.36	D	2.55	D	2.49	D	2.12
CBU_1182		D	D	2.29	D	1.64	D	1.49	D	1.12
CBU_1183		D	D	1.18	D	1.92	D	1.14	D	1.03
CBU_1184	LCV	D	D	1.00	D	0.89	D	1.32	D	1.36
CBU_1185		D	D	0.87	D	0.84	D	1.15	D	1.17
CBU_1186		ND	ND		ND		ND		ND	
CBU_1186a		ND	ND		ND		ND		ND	
CBU_1186b		D	ND	1.88	D	1.94	D	1.97	D	0.57
CBU_1187		D	D	0.32	D	0.26	D	0.27	D	0.34
CBU_1188		D	D	1.01	D	1.10	D	1.50	D	1.21
CBU_1189	LCV	D	D	0.67	D	0.62	D	0.85	D	0.86
CBU_1190		D	D	0.34	D	0.42	D	0.37	D	0.45
CBU_1191		D	D	0.82	D	0.78	D	0.89	D	0.95
CBU_1193	LCV	D	D	2.20	D	1.62	D	1.51	D	1.58
CBU_1194	LCV	D	D	2.37	D	1.52	D	1.91	D	2.10
CBU_1195		D	D	2.52	D	2.03	D	2.08	D	1.75
CBU_1196	SCV	D	D	0.02	D	0.03	D	0.13	D	0.30
CBU_1197		D	ND	0.77	ND	0.38	D	0.83	ND	0.11
CBU_1198		D	D	0.33	D	0.33	D	0.32	D	0.39
CBU_1199		D	D	0.49	D	0.40	D	0.10	D	0.11
CBU_1200	LCV	D	D	3.13	D	1.64	D	1.65	D	1.82
CBU_1201	LCV	D	D	2.72	D	1.61	D	1.18	D	1.52
CBU_1202	SCV	D	D	0.17	D	0.35	D	0.26	D	0.24
CBU_1203		D	D	0.13	D	0.29	D	0.33	D	0.45
CBU_1204		D	D	0.11	D	0.25	D	0.21	D	0.26
CBU_1206	LCV	D	D	3.29	D	2.40	D	1.62	D	1.37
CBU_1207	LCV	D	ND	13.04	ND	6.35	ND	6.69	D	3.96
CBU_1208		D	D	0.91	D	1.03	D	0.61	D	0.40
CBU_1209		D	D	0.59	D	0.68	D	0.54	D	0.81
CBU_1212a		ND	ND	#VALUE!	ND	#VALUE!	ND	#VALUE!	ND	#VALUE!
CBU_1213		D	D	0.25	D	0.66	D	0.42	D	0.50
CBU_1214	SCV	D	D	2.22	D	2.15	ND	0.54	ND	0.15
CBU_1216a		D	ND	8.68	D	8.82	ND	4.45	D	2.58
CBU_1217	SCV	D	D	0.27	D	0.18	D	0.09	D	0.19

CBU_1217a		ND	ND		ND		ND		ND	
CBU_1219		D	D	1.68	D	2.27	D	3.03	D	1.92
CBU_1220		D	D	0.81	D	0.90	D	1.19	D	1.25
CBU_1221		D	D	0.25	D	0.47	D	0.49	D	0.42
CBU_1222		D	D	1.23	D	1.18	D	1.20	D	1.00
CBU_1223		D	D	1.74	D	1.85	D	2.29	D	2.23
CBU_1224		D	D	0.78	D	1.14	D	1.23	D	1.31
CBU_1224a		D	D	0.78	D	2.01	D	2.50	D	2.25
CBU_1225		D	D	0.25	D	0.36	D	0.49	D	0.68
CBU_1226		D	D	0.73	D	0.82	D	1.07	D	1.20
CBU_1227		D	D	0.14	D	0.24	D	0.33	D	0.39
CBU_1228		D	D	0.28	D	0.41	D	0.60	D	0.48
CBU_1229		D	D	2.00	D	1.43	D	0.98	D	0.63
CBU_1230	LCV	D	D	4.91	D	2.90	D	2.19	D	1.28
CBU_1231		D	D	0.65	D	1.17	D	0.93	D	1.14
CBU_1233	SCV	D	D	0.11	D	0.24	D	0.17	D	0.15
CBU_1234	SCV	D	D	0.40	D	0.47	D	0.19	D	0.18
CBU_1235		D	D	0.06	D	0.10	D	0.04	D	0.05
CBU_1236		D	D	0.53	D	0.26	D	0.53	D	0.21
CBU_1237	LCV	D	D	0.63	D	0.87	D	1.02	D	1.29
CBU_1238	LCV	D	D	0.80	D	0.90	D	0.61	D	0.81
CBU_1239		D	D	0.22	D	0.27	D	0.35	D	0.44
CBU_1240	LCV	D	D	6.65	D	5.33	D	5.74	D	5.21
CBU_1241	LCV	D	D	4.01	D	3.11	D	3.36	D	3.68
CBU_1242		D	D	4.22	D	3.12	D	1.82	D	1.17
CBU_1243		D	D	0.64	D	0.62	D	0.74	D	0.78
CBU_1244	LCV	D	D	0.74	D	0.79	D	0.91	D	0.93
CBU_1245		D	D	1.10	D	1.08	D	0.55	D	0.68
CBU_1247		D	D	1.05	D	0.85	D	0.69	D	0.60
CBU_1248		D	D	1.34	D	1.45	D	1.37	D	0.96
CBU_1249		D	D	0.38	D	0.44	D	0.46	D	0.50
CBU_1250		D	ND	3.13	ND	1.52	ND	1.61	ND	0.45
CBU_1252	SCV	D	D	0.15	D	0.29	D	0.31	D	0.39
CBU_1255		D	D	0.34	D	0.54	D	0.47	D	0.53
CBU_1256		D	D	0.38	D	0.34	D	0.29	D	0.24
CBU_1257		D	D	0.47	D	0.58	D	0.72	D	0.63
CBU_1258	LCV	D	D	2.44	D	2.22	D	2.12	D	2.49
CBU_1259		D	D	0.08	D	0.20	D	0.28	D	0.29
CBU_1260		D	D	3.46	D	1.50	D	1.37	D	1.32
CBU_1261	LCV	D	D	1.02	D	1.01	D	1.07	D	1.42
CBU_1262	LCV	D	D	1.28	D	1.28	D	1.25	D	1.65
CBU_1263	LCV	D	D	1.07	D	0.90	D	0.50	D	0.62
CBU_1265	LCV	D	D	0.47	D	0.51	D	0.47	D	0.55
CBU_1266		D	D	0.89	D	0.76	D	0.81	D	0.72
CBU_1267		D	D	0.69	D	0.45	D	0.45	D	0.40
CBU_1267a	SCV	D	D	0.00	D	0.01	D	0.03	D	0.07
CBU_1268		D	D	0.35	D	0.47	D	0.76	D	0.59
CBU_1269		D	D	0.06	D	0.19	D	0.14	D	0.18
CBU_1269a		D	D	5.23	D	4.30	D	4.29	D	2.14
CBU_1270		ND	ND		ND		ND		ND	
CBU_1272	SCV	D	D	0.02	D	0.19	D	0.25	D	0.42
CBU_1273	LCV	D	D	4.92	D	3.07	D	3.03	D	3.29
CBU_1274		D	D	0.18	D	0.12	D	0.09	D	0.08
CBU_1275		D	D	1.78	D	1.45	D	1.48	D	1.53
CBU_1276	LCV	D	D	3.10	D	2.20	D	1.88	D	1.76
CBU_1277		D	D	1.08	D	1.05	D	1.17	D	1.40
CBU_1278	LCV	D	D	1.57	D	1.50	D	1.90	D	1.95
CBU_1279		D	D	1.05	D	1.57	D	1.67	D	1.39
CBU_1279a		D	D	5.97	D	3.94	ND	0.54	D	2.80
CBU_1280		D	D	0.31	D	0.67	D	0.56	D	0.52
CBU_1280a	SCV	D	D	0.02	D	0.06	D	0.22	D	0.49
CBU_1281	LCV	D	D	5.11	D	2.41	D	2.61	D	2.47
CBU_1282	LCV	D	D	3.46	D	2.02	D	1.46	D	1.44
CBU_1284		D	D	3.22	D	4.52	D	2.96	D	1.85
CBU_1285		D	D	8.72	D	7.64	D	3.88	D	2.54
CBU_1286		D	D	1.62	D	1.25	D	0.80	D	0.80
CBU_1289		D	D	3.79	D	2.34	D	3.22	D	3.59
CBU_1290		D	D	2.30	D	1.61	D	1.70	D	2.52
CBU_1291		D	D	0.43	D	0.46	D	0.54	D	0.67
CBU_1292		D	D	0.67	D	0.51	D	0.46	D	0.59

193

CBU_1293		D	D	0.98	D	0.77	D	0.83	D	0.91
CBU_1294	SCV	D	D	0.22	D	0.25	D	0.16	D	0.22
CBU_1295	SCV	D	D	0.09	D	0.14	D	0.13	D	0.12
CBU_1296		D	D	0.15	D	0.19	D	0.14	D	0.15
CBU_1297		D	D	0.45	D	0.68	D	0.67	D	0.64
CBU_1300	SCV	D	D	0.17	D	0.30	D	0.30	D	0.43
CBU_1301		D	D	1.12	D	1.47	D	1.60	D	1.68
CBU_1302		D	D	1.29	D	1.24	D	1.27	D	1.42
CBU_1303		D	D	2.81	D	2.03	D	2.35	D	1.20
CBU_1304		D	D	0.18	D	0.26	D	0.25	D	0.21
CBU_1305	LCV	D	D	1.83	D	1.12	D	0.77	D	1.01
CBU_1306	LCV	D	D	1.15	D	0.93	D	0.88	D	0.98
CBU_1307		D	D	16.65	D	5.21	D	6.55	D	2.29
CBU_1308	LCV	D	D	0.30	D	0.57	D	0.42	D	0.66
CBU_1310	SCV	D	ND	1.11	ND	0.54	D	1.16	D	0.34
CBU_1311		D	D	5.46	D	3.15	D	1.20	D	0.36
CBU_1312		D	ND	4.23	D	4.31	D	4.33	ND	0.61
CBU_1313	LCV	D	D	0.78	D	0.20	D	0.61	D	0.29
CBU_1314	SCV	D	D	0.38	D	0.47	D	0.20	D	0.19
CBU_1316		D	ND	6.98	ND	3.40	D	7.66	ND	1.01
CBU_1316a		D	ND	0.79	ND	0.39	ND	0.41	ND	0.11
CBU_1317		D	D	9.30	ND	0.59	ND	0.63	D	0.70
CBU_1318	LCV	D	D	0.97	D	1.02	D	0.69	D	0.70
CBU_1319		D	D	0.58	D	0.72	D	0.92	D	1.10
CBU_1320		D	D	0.75	D	1.11	D	1.14	D	1.16
CBU_1321		D	D	3.44	D	2.43	D	3.55	D	2.92
CBU_1322		D	D	3.23	D	2.45	D	2.35	D	2.32
CBU_1323		D	D	2.17	D	1.92	D	2.08	D	2.09
CBU_1323a		D	D	50.04	D	16.87	D	18.94	D	4.82
CBU_1324		D	D	4.07	D	4.18	D	3.83	D	3.66
CBU_1325		D	D	3.20	D	2.18	D	2.36	D	2.69
CBU_1326		D	D	2.74	D	2.51	D	2.54	D	2.63
CBU_1328	LCV	D	D	1.63	D	1.44	D	0.75	D	0.89
CBU_1329		D	D	0.36	D	0.41	D	0.63	D	0.67
CBU_1331	SCV	D	D	0.00	D	0.01	D	0.02	D	0.05
CBU_1332	SCV	D	ND	0.02	D	0.02	D	0.02	D	0.07
CBU_1332a		D	ND	0.07	ND	0.04	ND	0.04	D	0.04
CBU_1333		D	D	0.53	D	0.26	D	0.23	D	0.33
CBU_1334		D	D	1.80	D	1.14	D	0.96	D	0.74
CBU_1335		D	D	0.94	D	0.79	D	0.52	D	0.42
CBU_1336		D	D	1.89	D	1.47	D	0.76	D	0.93
CBU_1337	LCV	D	D	1.63	D	1.43	D	1.79	D	1.61
CBU_1338		D	D	0.99	D	0.92	D	0.89	D	0.96
CBU_1339	LCV	D	D	3.37	D	2.14	D	2.52	D	1.71
CBU_1340		D	D	4.92	D	2.60	D	3.27	D	2.60
CBU_1341	LCV	D	D	3.62	D	2.86	D	2.77	D	2.57
CBU_1342	LCV	D	D	2.62	D	1.97	D	1.72	D	1.70
CBU_1345		D	D	1.24	D	1.46	D	1.08	D	0.92
CBU_1346		D	D	0.23	D	0.30	D	0.46	D	0.38
CBU_1347	SCV	D	D	1.07	D	1.03	D	1.03	D	1.75
CBU_1348	SCV	D	ND	10.86	ND	5.29	ND	5.58	ND	1.57
CBU_1349		D	D	1.15	D	1.33	D	1.42	D	1.43
CBU_1350		D	D	0.95	D	0.98	D	1.45	D	1.27
CBU_1351		D	D	1.48	D	1.24	D	1.73	D	1.68
CBU_1352		D	D	1.06	D	1.08	D	1.28	D	1.48
CBU_1353		D	D	2.32	D	2.40	D	1.81	D	1.59
CBU_1354		D	D	2.29	D	2.86	D	3.22	D	2.34
CBU_1355		D	D	1.59	D	2.69	D	2.28	D	1.89
CBU_1356		D	D	1.64	D	2.09	D	2.37	ND	1.81
CBU_1357		D	D	2.63	D	4.10	D	5.12	D	3.84
CBU_1358		D	D	1.83	D	2.44	D	2.88	D	2.80
CBU_1359		D	D	1.62	D	2.07	D	2.16	D	2.31
CBU_1360	SCV	D	D	0.63	D	0.98	D	1.07	D	1.22
CBU_1361		D	D	1.50	D	2.02	D	1.23	D	1.64
CBU_1362		D	D	0.95	D	1.13	D	1.08	D	1.47
CBU_1363		D	D	1.09	D	1.96	D	1.97	D	2.36
CBU_1366		D	D	0.60	D	1.32	D	1.13	D	1.82
CBU_1369		D	D	2.22	D	1.61	D	1.37	D	1.02
CBU_1370		D	D	0.47	D	0.84	D	0.91	D	1.16
CBU_1371		D	D	0.17	D	0.10	D	0.11	D	0.16

CBU_1372		D	D	1.23	D	1.04	D	1.06	D	1.16
CBU_1373	LCV	D	D	0.78	D	0.98	D	0.68	D	1.05
CBU_1374	LCV	D	D	0.86	D	1.68	D	2.37	D	2.69
CBU_1375		D	D	0.49	D	0.70	D	0.98	D	0.84
CBU_1376		D	D	1.32	D	0.97	D	0.34	D	0.50
CBU_1376a		ND	ND	#VALUE!	ND	#VALUE!	ND	#VALUE!	ND	#VALUE!
CBU_1378	LCV	D	ND	0.96	D	0.98	D	1.03	ND	0.14
CBU_1379a	LCV	D	D	1.89	D	1.09	D	1.18	D	0.95
CBU_1380		D	D	0.20	D	0.28	D	0.26	D	0.25
CBU_1381		D	D	3.60	D	2.16	D	2.23	D	1.80
CBU_1382		D	D	1.95	D	1.31	D	1.52	D	1.30
CBU_1383		D	D	3.97	D	2.59	D	3.16	D	2.48
CBU_1384		D	D	3.86	D	2.18	D	2.97	D	3.01
CBU_1385		D	D	3.65	D	2.27	D	2.67	D	3.09
CBU_1386	LCV	D	D	0.91	D	0.60	D	0.44	D	0.62
CBU_1387	SCV	D	D	0.22	D	0.50	D	0.65	D	0.59
CBU_1388	LCV	D	D	1.06	D	0.77	D	0.55	D	0.75
CBU_1388d		D	D	15.93	ND	3.73	ND	3.93	D	6.26
CBU_1394	SCV	D	D	0.01	D	0.01	D	0.14	D	0.52
CBU_1395		D	D	4.31	D	2.79	D	3.69	D	2.59
CBU_1396		D	D	6.45	D	4.37	D	5.16	D	4.48
CBU_1397	LCV	ND	D	3.95	D	3.13	D	3.70	D	3.24
CBU_1398		D	D	4.07	D	2.96	D	3.36	D	3.44
CBU_1399	LCV	D	D	5.51	D	3.80	D	4.79	D	3.90
CBU_1400	LCV	D	D	2.40	D	1.91	D	2.31	D	2.38
CBU_1401	LCV	D	D	5.14	D	3.26	D	3.40	D	3.72
CBU_1402	LCV	D	D	1.04	D	0.68	D	0.67	D	0.66
CBU_1403	LCV	D	D	0.98	D	0.73	D	0.47	D	0.54
CBU_1404	SCV	D	D	0.04	D	0.26	D	0.26	D	0.45
CBU_1405		D	D	0.12	D	0.34	D	0.52	D	0.32
CBU_1408		D	D	6.31	ND	1.51	ND	1.60	ND	0.45
CBU_1409		D	D	1.06	D	0.69	D	0.61	D	0.80
CBU_1410		D	D	0.21	D	0.20	D	0.19	D	0.29
CBU_1411		D	D	0.60	D	0.16	D	0.20	D	0.14
CBU_1412	LCV	D	D	0.10	D	0.36	D	0.79	D	0.97
CBU_1413		D	D	0.09	D	0.35	D	0.56	D	0.89
CBU_1414	LCV	D	D	0.30	D	0.44	D	0.76	D	0.89
CBU_1415		D	D	0.25	D	0.45	D	0.50	D	0.61
CBU_1416	LCV	D	D	0.07	D	0.16	D	0.23	D	0.26
CBU_1417	LCV	D	D	3.01	D	2.29	D	3.41	D	2.31
CBU_1418		D	D	1.89	D	1.59	D	2.04	D	2.17
CBU_1419		D	D	3.31	D	2.48	D	2.42	D	2.12
CBU_1422	LCV	D	D	0.70	D	0.58	D	0.62	D	0.63
CBU_1422a		D	ND	2.16	D	2.22	D	2.24	D	0.65
CBU_1424		D	D	0.55	D	0.56	D	0.85	D	0.78
CBU_1425		D	D	0.46	D	0.65	D	0.87	D	0.85
CBU_1426		D	D	29.00	D	8.74	D	9.21	D	4.55
CBU_1427a	SCV	D	ND	10.99	ND	5.35	ND	5.64	ND	1.59
CBU_1429		D	D	0.04	D	0.06	D	0.06	D	0.16
CBU_1429a	SCV	D	D	0.08	D	0.19	D	0.29	D	0.59
CBU_1430		D	D	6.53	D	4.47	D	5.05	D	3.82
CBU_1431	LCV	D	D	4.91	D	3.24	D	3.50	D	2.40
CBU_1432		D	D	6.06	D	3.80	D	4.41	D	4.03
CBU_1433	LCV	D	D	3.35	D	2.41	D	2.00	D	1.94
CBU_1434		D	D	6.09	D	4.98	D	3.95	D	4.64
CBU_1435	LCV	D	D	4.33	D	2.60	D	2.37	D	2.39
CBU_1436	LCV	D	D	3.23	D	1.84	D	1.63	D	1.61
CBU_1437		D	D	4.00	D	2.47	D	2.34	D	2.02
CBU_1438		D	D	4.75	D	3.18	D	2.01	D	1.99
CBU_1439		D	D	3.88	D	2.38	D	3.18	D	2.24
CBU_1440		D	D	2.70	D	2.06	D	1.44	D	1.85
CBU_1441	LCV	D	D	1.40	D	0.92	D	0.57	D	0.85
CBU_1442		D	D	2.26	D	1.63	D	1.76	D	1.76
CBU_1443		D	D	2.70	D	1.69	D	2.48	D	2.33
CBU_1444		D	D	2.12	D	1.78	D	2.79	D	2.39
CBU_1445	LCV	D	D	2.11	D	1.24	D	1.71	D	1.72
CBU_1446	LCV	D	D	1.15	D	0.96	D	1.27	D	1.19
CBU_1447		D	D	1.32	D	1.07	D	1.52	D	1.65
CBU_1448		D	D	1.09	D	0.43	D	0.68	D	0.71
CBU_1449		D	D	3.33	D	1.96	D	1.12	D	1.60

CBU_1450		D	D	3.18	D	1.81	D	1.04	D	1.45
CBU_1451	LCV	D	D	3.19	D	1.87	D	1.00	D	1.14
CBU_1457		D	D	0.90	D	0.74	D	0.53	D	0.76
CBU_1458	LCV	D	D	1.09	D	0.93	D	0.72	D	0.86
CBU_1458a		D	D	0.56	D	0.56	ND	0.14	D	0.22
CBU_1459		D	D	0.69	D	2.58	D	0.66	D	0.48
CBU_1460	SCV	D	D	0.51	D	0.88	D	1.19	D	1.31
CBU_1462a		D	ND	3.71	ND	1.81	ND	1.91	ND	0.54
CBU_1463		D	D	23.77	D	11.72	D	9.33	D	8.98
CBU_1464		D	D	5.13	D	3.99	D	4.32	D	4.64
CBU_1465		D	D	0.29	D	0.31	D	0.35	D	0.41
CBU_1466		D	D	0.20	D	0.25	D	0.33	D	0.31
CBU_1467		D	D	4.30	D	3.38	D	2.60	D	2.79
CBU_1468		D	D	0.67	D	0.68	D	0.63	D	0.52
CBU_1469		D	D	0.20	D	0.29	D	0.40	D	0.35
CBU_1470		D	D	0.70	D	0.80	D	0.71	D	0.79
CBU_1471		D	D	2.34	D	2.23	D	2.16	D	2.11
CBU_1472		D	D	94.08	D	34.57	D	21.01	D	6.35
CBU_1473	LCV	D	D	3.77	D	2.45	D	1.22	D	1.47
CBU_1474		D	D	4.66	D	2.99	D	3.26	D	3.48
CBU_1475		D	D	4.23	D	2.24	D	2.71	D	2.63
CBU_1476	SCV	D	D	0.67	D	6.89	D	2.76	D	3.83
CBU_1477	SCV	D	D	5.78	D	250.54	D	206.04	D	359.22
CBU_1478	SCV	D	D	6.31	D	84.59	D	77.78	D	113.82
CBU_1479		D	D	1.78	D	2.06	D	0.93	D	1.28
CBU_1480		D	D	0.70	D	1.09	D	0.90	D	0.65
CBU_1481		D	D	0.56	D	0.82	D	0.40	D	0.32
CBU_1482		D	D	0.15	D	0.26	D	0.33	D	0.39
CBU_1483		D	D	0.14	D	0.26	D	0.29	D	0.38
CBU_1484		D	D	0.49	D	0.53	D	0.47	D	0.47
CBU_1485		D	D	0.33	D	0.64	D	0.70	D	0.59
CBU_1486		D	ND	9.42	ND	4.59	ND	4.83	ND	1.36
CBU_1487		D	D	2.10	D	1.48	D	2.12	D	2.17
CBU_1488	LCV	D	D	1.72	D	1.54	D	1.72	D	1.95
CBU_1489		D	D	0.63	D	0.97	D	0.65	D	0.77
CBU_1490		D	D	0.16	D	0.37	D	0.32	D	0.46
CBU_1491		D	D	0.32	D	0.79	D	0.57	D	0.54
CBU_1492		ND	ND		ND		ND		ND	
CBU_1493		D	D	0.43	D	0.69	D	0.59	D	0.38
CBU_1494	SCV	D	D	0.16	D	0.16	D	0.19	D	0.37
CBU_1497		D	D	2.78	D	1.37	D	1.12	D	0.91
CBU_1501		D	D	2.19	D	1.37	D	1.08	D	0.62
CBU_1502	SCV	D	D	0.75	D	0.45	D	0.62	D	0.34
CBU_1503		D	D	1.14	D	0.94	D	1.05	D	0.96
CBU_1504		D	D	0.38	D	0.32	D	0.24	D	0.33
CBU_1505	LCV	D	D	1.58	D	0.89	D	0.67	D	0.72
CBU_1506		D	D	1.60	D	1.95	D	1.94	D	1.63
CBU_1507		D	D	1.07	D	0.96	D	0.68	D	0.77
CBU_1508		D	D	1.07	D	1.39	D	1.13	D	0.91
CBU_1509	LCV	D	D	0.86	D	0.94	D	0.85	ND	0.75
CBU_1510		D	D	0.57	D	0.84	D	0.90	D	0.96
CBU_1511		D	D	0.91	D	0.63	D	0.58	D	0.68
CBU_1512	SCV	D	D	0.25	D	0.40	D	0.43	D	0.46
CBU_1513	SCV	D	D	0.41	D	0.50	D	0.40	D	0.47
CBU_1514		D	D	0.38	D	0.28	D	0.20	D	0.34
CBU_1515		D	D	0.23	D	0.11	D	0.22	D	0.50
CBU_1516	SCV	D	D	0.01	D	0.10	D	0.12	D	0.26
CBU_1517	SCV	D	D	0.19	D	0.14	D	0.14	D	0.12
CBU_1518		D	D	1.03	D	0.95	D	0.88	D	0.83
CBU_1519		D	D	0.86	D	1.22	D	1.09	D	1.15
CBU_1520		D	D	0.64	D	0.50	D	0.43	D	0.65
CBU_1521		D	D	0.65	D	0.79	D	0.71	D	0.70
CBU_1522		D	D	1.15	D	2.09	ND	0.29	ND	0.08
CBU_1526a		ND	ND	#VALUE!	ND	#VALUE!	ND	#VALUE!	ND	#VALUE!
CBU_1529		D	D	0.75	D	1.02	D	1.27	D	1.40
CBU_1530	SCV	D	D	0.48	D	1.04	D	1.05	D	1.08
CBU_1530a		D	ND	2.28	ND	1.11	ND	1.17	ND	0.33
CBU_1536		D	D	1.21	D	0.97	D	1.08	D	1.14
CBU_1537		D	D	0.46	D	0.76	D	0.58	D	0.39
CBU_1538		D	D	0.52	D	0.71	D	0.65	D	0.62

Gene	Type									
CBU_1539		D	D	1.12	D	0.96	D	0.71	D	0.65
CBU_1540		D	D	3.62	D	2.40	D	3.08	D	1.24
CBU_1541		D	D	1.40	D	0.87	D	0.77	D	0.39
CBU_1542		D	D	0.40	D	0.53	D	0.37	D	0.66
CBU_1543		D	D	1.90	D	1.41	D	1.13	D	0.96
CBU_1544		ND	ND		ND		ND		ND	
CBU_1547		D	D	1.29	D	1.12	D	1.22	D	1.54
CBU_1548		D	D	0.73	D	0.65	D	0.46	D	0.63
CBU_1549	LCV	D	D	1.26	D	0.77	D	0.52	D	0.54
CBU_1550		D	D	1.08	D	1.13	D	1.01	D	0.95
CBU_1551		D	D	2.27	D	3.32	D	2.23	D	1.94
CBU_1552		D	D	2.55	D	2.33	D	1.30	D	0.47
CBU_1552a		D	D	0.10	D	0.09	ND	0.03	D	0.01
CBU_1553		D	D	0.38	D	0.40	D	0.39	D	0.51
CBU_1554		D	D	0.65	D	0.83	D	1.12	D	1.12
CBU_1555		ND	ND		ND		ND		ND	
CBU_1556	LCV	D	D	5.76	D	2.06	D	1.88	D	1.81
CBU_1558		D	D	0.75	D	0.62	D	0.87	D	0.99
CBU_1559		D	D	0.31	D	0.45	D	0.62	D	0.69
CBU_1559a		D	ND	2.17	ND	1.06	ND	1.11	D	1.78
CBU_1560	SCV	D	D	0.15	D	0.22	D	0.21	D	0.27
CBU_1561	SCV	D	D	0.01	D	0.01	D	0.02	D	0.07
CBU_1565		D	D	3.64	D	1.95	D	1.94	D	1.85
CBU_1566		D	D	4.54	D	2.65	D	2.86	D	2.65
CBU_1567		D	D	2.80	D	0.94	D	0.62	D	0.48
CBU_1568		D	D	0.08	D	0.12	D	0.18	D	0.17
CBU_1569		D	D	0.96	D	0.54	D	0.42	D	0.50
CBU_1570		D	D	1.31	D	1.00	D	0.93	D	1.06
CBU_1570a		ND	ND		ND		ND		ND	
CBU_1570b		ND	ND		ND		ND		ND	
CBU_1573		D	D	0.10	D	0.19	D	0.14	D	0.21
CBU_1574		D	D	0.19	D	0.26	D	0.21	D	0.29
CBU_1575		D	D	0.37	D	0.37	D	0.35	D	0.42
CBU_1576		D	D	0.48	D	0.26	D	0.49	D	0.48
CBU_1577		D	D	2.29	D	1.74	D	1.69	D	1.43
CBU_1578		D	D	1.44	D	1.38	D	1.27	D	1.09
CBU_1579	LCV	D	D	1.33	D	1.01	D	0.66	D	0.97
CBU_1580		D	D	6.59	D	3.19	D	2.75	D	2.06
CBU_1581		D	D	87.80	D	54.71	D	12.06	D	38.61
CBU_1582		D	D	5.91	D	3.99	D	3.80	D	3.22
CBU_1583		D	D	6.45	D	5.56	D	3.78	D	3.89
CBU_1584		D	D	4.55	D	3.91	D	3.54	D	3.29
CBU_1585		D	D	3.76	D	3.41	D	3.75	D	2.23
CBU_1586		D	D	3.46	D	2.53	D	2.72	D	1.99
CBU_1587		D	D	3.94	D	2.49	D	2.56	D	2.03
CBU_1588		D	D	1.29	D	1.04	D	0.76	D	0.88
CBU_1589		D	D	0.16	D	0.32	D	0.46	D	0.75
CBU_1590		D	D	0.61	D	0.48	D	0.45	D	0.49
CBU_1590a		ND	ND		ND		ND		ND	
CBU_1590b		ND	ND		ND		ND		ND	
CBU_1593		D	D	1.39	D	1.13	D	0.56	D	0.62
CBU_1594	LCV	D	D	2.72	D	2.04	D	1.85	D	1.89
CBU_1595		D	D	1.47	D	1.04	D	0.97	D	0.77
CBU_1596	SCV	D	D	0.35	D	0.55	D	0.63	D	0.69
CBU_1597	LCV	D	D	2.57	D	0.83	D	2.06	D	1.45
CBU_1600		D	D	1.49	D	1.17	D	1.28	D	1.29
CBU_1601		D	D	0.59	D	0.69	D	0.95	D	0.85
CBU_1602		D	D	0.85	D	0.68	D	1.02	D	1.64
CBU_1603	LCV	D	D	0.41	D	0.45	D	1.02	D	1.24
CBU_1607		D	D	0.72	D	1.04	D	1.03	D	1.28
CBU_1612		ND	ND	1.00	ND	1.00	ND	1.00	D	10.24
CBU_1613		D	ND	3.46	ND	1.69	ND	1.78	ND	0.50
CBU_1614		D	D	35.90	ND	4.99	ND	5.26	ND	1.48
CBU_1618		D	D	7.56	D	3.55	D	2.56	D	2.36
CBU_1621		D	D	9.50	D	5.50	D	3.43	D	2.29
CBU_1622		D	D	0.35	D	0.28	D	0.32	D	0.27
CBU_1623	SCV	D	D	0.37	D	0.53	D	0.78	D	0.76
CBU_1624		D	D	0.32	D	0.35	D	0.46	D	0.54
CBU_1625		D	D	1.75	D	1.41	D	1.42	D	1.13
CBU_1626	SCV	D	D	0.84	D	0.97	D	1.15	D	0.91

197

ID	Type									
CBU_1627	SCV	D	D	0.93	D	0.97	D	1.18	D	1.06
CBU_1628	SCV	D	D	0.66	D	0.52	D	0.76	D	0.61
CBU_1629		D	D	0.25	D	0.16	D	0.32	D	0.26
CBU_1630		D	D	0.31	D	0.24	D	0.52	D	0.43
CBU_1631		D	D	0.66	D	0.51	D	1.13	D	0.98
CBU_1632	SCV	D	D	0.41	D	0.41	D	0.78	D	0.72
CBU_1633		D	D	0.14	D	0.18	D	0.31	D	0.31
CBU_1634	SCV	D	D	0.14	D	0.16	D	0.22	D	0.28
CBU_1634a		D	D	0.15	D	0.22	D	0.31	D	0.26
CBU_1635		D	D	9.43	D	9.37	D	8.73	ND	0.66
CBU_1636		D	D	0.84	D	0.85	D	1.08	D	0.92
CBU_1638		D	D	1.45	D	1.33	D	1.18	D	1.10
CBU_1639		D	D	0.66	D	0.62	D	0.61	D	0.58
CBU_1639c		ND	ND		ND		ND		ND	
CBU_1641		D	D	0.24	D	0.27	D	0.27	D	0.32
CBU_1642		D	D	0.38	D	0.41	D	0.45	D	0.49
CBU_1643		D	D	0.14	D	0.12	D	0.10	D	0.12
CBU_1644	SCV	D	D	0.18	D	0.13	D	0.19	D	0.20
CBU_1645		D	D	0.48	D	0.58	D	0.84	D	0.75
CBU_1646		D	D	0.73	D	0.61	D	0.68	D	0.55
CBU_1647		D	D	0.24	D	0.39	D	0.54	D	0.35
CBU_1648	SCV	D	D	0.20	D	0.26	D	0.58	D	0.54
CBU_1649	SCV	D	D	0.23	D	0.17	D	0.32	D	0.38
CBU_1650		D	D	0.66	D	0.82	D	1.16	D	1.42
CBU_1651		D	D	0.32	D	0.55	D	0.74	D	1.01
CBU_1652		D	D	0.27	D	0.23	D	0.45	D	0.54
CBU_1653a	LCV	D	D	2.96	D	0.73	ND	0.18	ND	0.05
CBU_1655	LCV	D	D	2.68	D	2.18	D	2.26	D	2.42
CBU_1656	LCV	D	ND	0.45	D	1.21	ND	0.23	D	0.25
CBU_1657		D	D	0.79	D	0.66	D	0.65	D	0.58
CBU_1658	LCV	D	D	1.00	D	1.26	D	1.04	D	0.93
CBU_1659	LCV	D	D	1.37	D	0.81	D	0.69	D	0.73
CBU_1660		D	D	8.56	D	3.71	D	4.19	D	1.54
CBU_1661		D	D	1.29	D	1.08	D	1.04	D	1.00
CBU_1662		D	D	0.84	D	0.88	D	0.66	D	0.62
CBU_1663		D	ND	4.98	D	4.99	D	5.09	D	1.48
CBU_1664		D	D	0.49	D	0.63	D	0.58	D	0.68
CBU_1665		D	D	1.52	D	2.38	D	2.37	D	1.34
CBU_1669	SCV	D	D	0.18	D	0.37	D	0.34	D	0.40
CBU_1670		D	D	0.42	D	0.51	D	0.47	D	0.32
CBU_1671		D	D	1.82	D	1.43	D	0.94	D	1.08
CBU_1673		D	D	0.59	D	0.42	D	0.28	D	0.23
CBU_1674		D	D	0.73	D	0.67	D	0.53	D	0.75
CBU_1675	LCV	D	D	2.86	D	1.56	D	1.18	D	1.26
CBU_1675a		D	D	6.67	D	6.65	D	3.93	D	0.79
CBU_1676		D	D	0.28	D	0.53	D	0.72	D	0.79
CBU_1677	SCV	D	D	0.02	D	0.06	D	0.10	D	0.29
CBU_1678	SCV	D	D	0.39	D	0.85	D	0.57	D	0.73
CBU_1681	SCV	D	D	0.01	D	0.07	D	0.13	D	0.36
CBU_1682		D	D	0.45	D	0.62	D	0.57	D	0.52
CBU_1683		D	ND	1.87	D	1.90	ND	0.96	ND	0.27
CBU_1684		ND	ND	#VALUE!	ND	#VALUE!	ND	#VALUE!	ND	#VALUE!
CBU_1685		D	D	14.41	D	12.38	D	7.88	D	6.90
CBU_1686		D	D	4.06	D	3.36	D	2.28	D	1.83
CBU_1688		D	D	3.29	D	1.87	D	1.99	D	2.26
CBU_1689		D	ND	1.21	D	1.53	D	1.02	D	1.22
CBU_1690		D	D	3.59	D	4.38	D	0.97	D	1.36
CBU_1691		D	D	0.34	D	1.06	D	0.65	D	0.94
CBU_1692		D	ND	0.08	D	0.32	D	0.15	D	0.27
CBU_1692a		D	ND	2.37	ND	1.16	ND	1.22	ND	0.34
CBU_1695		D	D	2.12	D	1.10	D	0.83	D	0.77
CBU_1696		D	D	5.45	D	2.68	D	2.47	D	2.01
CBU_1697		D	D	8.06	D	4.79	D	3.90	D	2.98
CBU_1698		D	D	0.95	D	1.18	D	1.13	D	0.97
CBU_1699	LCV	D	D	2.32	D	1.61	D	1.27	D	1.13
CBU_1699a		D	D	0.50	D	0.70	D	1.12	D	1.48
CBU_1699b		D	D	2.20	D	0.97	D	0.24	D	0.53
CBU_1701	LCV	D	D	1.25	D	1.20	D	1.00	D	1.10
CBU_1702		D	ND	1.02	ND	0.50	ND	0.53	ND	0.15
CBU_1703		D	D	0.64	D	0.72	D	0.47	D	0.60

198

CBU_1704	LCV	D	D	3.28	D	2.51	D	3.74	D	2.73
CBU_1705		D	D	1.25	D	1.31	D	0.68	D	1.19
CBU_1706		D	D	1.36	D	2.04	D	1.85	D	2.29
CBU_1707	LCV	D	D	2.96	D	3.63	D	5.11	D	4.09
CBU_1708		D	D	0.25	D	0.38	D	0.41	D	0.54
CBU_1709		D	D	1.27	D	1.14	D	1.06	D	1.27
CBU_1710	LCV	D	D	0.80	D	1.76	D	3.17	D	1.67
CBU_1711	LCV	D	D	2.19	D	2.38	D	2.39	D	2.31
CBU_1712	LCV	D	D	0.80	D	0.94	D	0.55	D	0.51
CBU_1713	LCV	D	D	4.55	D	2.92	D	3.42	D	2.82
CBU_1714	LCV	D	D	2.73	D	2.53	D	2.52	D	2.55
CBU_1715	LCV	D	D	2.99	D	1.76	D	1.79	D	1.63
CBU_1716	LCV	D	D	5.65	D	2.67	D	1.68	D	1.92
CBU_1716a		ND	ND		ND		ND		ND	
CBU_1716b		D	D	4.90	D	4.74	D	14.13	D	3.91
CBU_1718	LCV	D	D	2.53	D	1.92	D	2.50	D	3.13
CBU_1719		D	D	4.14	D	3.85	D	3.20	D	3.67
CBU_1720	LCV	D	D	5.45	D	3.42	D	2.61	D	2.71
CBU_1721		D	D	5.83	D	3.52	D	3.53	D	2.72
CBU_1723		D	D	0.50	D	0.64	D	0.58	D	0.60
CBU_1724	SCV	D	D	0.09	D	0.10	D	0.07	D	0.09
CBU_1724a		ND	ND		ND		ND		ND	
CBU_1725		D	D	1.71	D	1.66	D	1.52	D	1.66
CBU_1726		D	D	2.38	D	2.00	D	2.49	D	2.33
CBU_1727	LCV	D	D	3.45	D	1.81	D	1.68	D	1.79
CBU_1728	LCV	D	D	2.83	D	1.24	D	0.82	D	1.05
CBU_1729		D	D	1.55	D	1.86	D	2.12	D	2.01
CBU_1730	LCV	D	D	1.71	D	1.16	D	1.01	D	1.19
CBU_1732	LCV	D	D	3.56	D	2.08	D	0.75	D	1.77
CBU_1733		D	D	6.17	D	3.18	D	4.22	D	3.31
CBU_1734		D	D	0.11	D	0.15	D	0.17	D	0.20
CBU_1735		D	D	0.07	D	0.12	D	0.13	D	0.18
CBU_1736	LCV	D	D	1.74	D	0.76	D	0.64	D	0.71
CBU_1737		D	D	1.72	D	0.73	D	0.66	D	0.58
CBU_1738		D	D	0.13	D	0.31	D	0.29	D	0.34
CBU_1739		D	D	1.90	D	1.71	D	1.18	D	1.23
CBU_1740		D	D	4.33	D	6.54	D	4.62	D	2.76
CBU_1741		D	D	0.97	D	0.75	D	0.62	D	0.51
CBU_1742	LCV	D	ND	0.12	D	1.08	D	1.38	D	0.49
CBU_1743		D	D	1.15	D	1.01	D	0.82	D	0.82
CBU_1744		D	D	1.35	D	1.17	D	0.85	D	1.07
CBU_1745		D	D	0.31	D	0.32	D	0.25	D	0.27
CBU_1746		D	D	4.05	D	2.45	D	2.33	D	2.43
CBU_1747	LCV	D	D	3.74	D	2.64	D	2.12	D	2.55
CBU_1748		D	D	1.69	D	1.18	D	0.75	D	1.03
CBU_1749		D	D	2.10	D	1.50	D	0.88	D	1.17
CBU_1749a		D	D	0.63	D	1.67	D	2.96	D	5.59
CBU_1751		D	D	0.40	D	0.57	D	0.84	D	0.79
CBU_1752		D	D	0.59	D	0.43	D	0.80	D	0.66
CBU_1753		D	D	0.47	D	0.63	D	0.60	D	0.76
CBU_1754	LCV	D	D	0.25	D	0.33	D	0.38	D	0.34
CBU_1755	SCV	D	D	2.48	D	1.19	D	1.23	D	0.36
CBU_1756		D	D	0.69	D	0.84	D	1.13	D	1.03
CBU_1758a		D	ND	0.00	D	0.06	D	0.49	D	0.50
CBU_1758b		D	D	2.61	D	2.08	D	2.03	D	0.68
CBU_1760		D	ND	0.94	ND	0.46	ND	0.48	ND	0.14
CBU_1761		D	D	0.32	D	0.29	D	0.41	D	0.45
CBU_1762		D	D	0.04	D	0.14	D	0.11	D	0.16
CBU_1763	LCV	D	D	0.31	D	0.36	D	0.16	D	0.18
CBU_1764		D	D	2.01	D	5.42	D	4.04	D	0.59
CBU_1764a		D	D	0.14	D	0.32	D	0.35	D	0.56
CBU_1765	SCV	D	D	0.66	D	1.22	D	1.50	D	1.33
CBU_1766		D	D	0.38	D	0.77	D	1.27	D	1.29
CBU_1767		D	D	0.56	D	1.19	D	1.38	D	1.41
CBU_1768	SCV	D	D	0.04	D	0.06	D	0.08	D	0.11
CBU_1769		D	D	6.55	D	4.75	D	5.17	D	4.09
CBU_1770		D	D	1.46	D	1.67	D	2.35	D	2.53
CBU_1771		D	D	0.54	D	0.59	D	0.43	D	0.48
CBU_1772	LCV	D	D	2.59	D	1.34	D	0.78	D	0.94
CBU_1777	LCV	D	D	4.59	D	2.92	D	2.74	D	2.16

199

CBU_1778	LCV	D	D	0.86	D	0.77	D	0.81	D	0.83
CBU_1780		D	D	1.38	D	0.74	D	1.03	D	0.52
CBU_1781		D	D	2.00	D	1.84	D	2.57	D	2.42
CBU_1782		D	D	2.30	D	2.23	D	3.00	D	2.56
CBU_1783		D	D	3.42	D	2.85	D	4.04	D	4.66
CBU_1784	LCV	D	D	4.72	D	2.80	D	3.01	D	3.19
CBU_1785		ND	ND		ND		ND		ND	
CBU_1785a		ND	ND		ND		ND		ND	
CBU_1786		D	D	0.55	D	0.35	D	0.28	D	0.24
CBU_1787	LCV	D	D	2.04	D	1.68	D	1.16	D	1.02
CBU_1788	LCV	D	D	4.12	D	3.61	D	2.30	D	1.94
CBU_1789	SCV	D	D	0.14	D	0.38	D	0.35	D	0.43
CBU_1790	LCV	D	D	0.77	D	0.92	D	0.67	D	0.35
CBU_1794	SCV	D	D	2.01	D	1.20	D	1.17	D	0.64
CBU_1795		D	D	0.79	D	0.68	D	0.51	D	0.48
CBU_1796		D	D	0.90	D	0.80	D	0.70	D	0.52
CBU_1797		D	D	2.57	D	3.71	D	3.14	D	1.72
CBU_1798	LCV	D	D	1.62	D	0.87	D	0.86	D	0.90
CBU_1799		D	D	0.40	D	0.73	D	0.92	D	0.82
CBU_1799a		D	D	1.84	D	1.82	D	1.23	D	1.10
CBU_1800		D	D	0.09	D	0.13	D	0.17	D	0.20
CBU_1801		D	D	1.06	D	0.60	D	0.24	D	0.17
CBU_1802		D	D	0.58	D	0.71	D	0.59	D	0.66
CBU_1803		D	D	0.44	ND	0.11	D	0.24	D	0.31
CBU_1804		D	D	1.07	D	0.42	D	0.21	D	0.13
CBU_1805		D	D	0.16	D	0.11	D	0.22	D	0.18
CBU_1806		D	D	3.92	D	7.08	D	1.98	D	0.81
CBU_1808		D	D	1.68	D	1.11	D	1.41	D	1.21
CBU_1809	LCV	D	D	0.66	D	1.61	D	2.76	D	2.27
CBU_1810		D	D	0.85	D	0.84	D	1.12	D	1.25
CBU_1811		D	D	1.67	D	0.98	D	0.65	D	0.52
CBU_1812		D	D	0.36	D	0.48	D	0.30	D	0.89
CBU_1813		D	D	0.19	ND	0.04	D	0.27	D	0.17
CBU_1814	LCV	D	D	1.43	D	1.65	D	1.81	D	2.14
CBU_1815		D	D	0.94	D	1.15	D	0.95	D	0.92
CBU_1816		D	D	2.63	D	2.30	D	2.34	D	2.40
CBU_1817		D	D	4.92	D	3.44	D	4.02	D	2.62
CBU_1818		D	D	2.94	D	1.05	D	0.94	D	0.62
CBU_1819		D	D	10.95	D	2.76	D	1.85	D	1.66
CBU_1820		D	D	2.59	D	2.31	D	2.15	D	2.10
CBU_1821		D	D	1.14	D	0.98	D	0.67	D	0.78
CBU_1822	SCV	D	D	0.19	D	0.28	D	0.27	D	0.45
CBU_1823		D	D	2.94	D	1.49	D	1.32	D	0.97
CBU_1824		D	D	9.80	D	13.71	D	5.01	ND	0.69
CBU_1825		D	D	19.91	D	6.65	D	4.66	D	1.60
CBU_1826	LCV	D	D	3.92	D	2.25	D	1.50	D	1.35
CBU_1827	LCV	D	D	3.18	D	3.03	D	1.93	D	2.30
CBU_1828	LCV	D	D	3.17	D	2.39	D	2.07	D	1.59
CBU_1829		D	D	0.26	D	0.35	D	0.42	ND	0.42
CBU_1830	LCV	D	D	1.18	D	0.72	D	0.67	ND	0.82
CBU_1831	LCV	D	D	1.32	D	0.75	D	0.85	D	0.95
CBU_1831a		D	ND	3.78	D	3.78	ND	1.94	D	1.15
CBU_1833		D	ND	0.82	ND	0.40	D	1.59	D	1.75
CBU_1834	LCV	D	D	3.49	D	2.15	D	2.15	D	1.77
CBU_1835	LCV	D	D	3.83	D	3.52	D	3.51	D	3.03
CBU_1836	LCV	D	D	2.48	D	1.86	D	2.08	D	2.01
CBU_1837	LCV	D	D	2.03	D	1.58	D	1.58	D	1.59
CBU_1838	LCV	D	D	2.44	D	1.40	D	1.39	D	1.26
CBU_1839	LCV	D	D	3.99	D	2.22	D	2.03	D	2.22
CBU_1840	LCV	D	D	8.18	D	4.45	D	3.80	D	4.56
CBU_1841	LCV	D	D	24.39	D	13.98	D	13.86	D	14.66
CBU_1842	LCV	D	D	9.93	D	7.08	D	8.37	D	6.95
CBU_1843	LCV	D	D	1.18	D	2.18	D	2.05	D	2.23
CBU_1843a		D	D	5.83	D	4.34	D	4.53	D	2.12
CBU_1845		D	D	0.69	D	0.83	D	1.23	D	0.88
CBU_1847		D	D	0.61	D	0.48	D	0.98	D	1.78
CBU_1847b	SCV	D	D	0.04	D	0.22	D	0.43	D	0.56
CBU_1849		D	D	6.57	D	6.87	D	3.33	D	2.44
CBU_1850		D	D	1.64	D	2.07	D	1.12	D	1.12
CBU_1851		D	D	2.06	D	1.30	D	0.94	D	0.84

CBU_1852		D	D	2.57	D	1.42	D	1.86	D	1.66
CBU_1853		D	D	0.76	D	0.92	D	1.52	D	1.47
CBU_1854		D	D	0.69	D	0.54	D	0.67	D	1.05
CBU_1855		D	ND	0.22	D	1.18	D	0.42	D	0.36
CBU_1856		D	D	0.63	D	1.02	D	1.02	D	0.95
CBU_1857		D	D	2.24	D	1.10	D	3.54	D	2.14
CBU_1858		D	D	3.52	D	2.58	D	1.59	D	1.94
CBU_1859		D	D	1.55	D	2.31	D	0.29	D	1.67
CBU_1862		D	D	2.13	D	1.42	D	1.48	D	1.34
CBU_1863	LCV	D	D	4.22	D	3.38	D	5.36	D	4.84
CBU_1864		D	D	0.30	D	0.21	D	0.68	D	0.33
CBU_1865		D	D	0.32	D	0.31	D	0.38	D	0.43
CBU_1866		D	D	0.36	D	0.47	D	0.49	D	0.55
CBU_1867		D	D	2.61	D	1.27	D	1.37	D	1.47
CBU_1867a		D	D	1.33	D	1.68	D	1.14	D	0.84
CBU_1869		D	D	0.36	D	0.58	D	0.77	D	0.75
CBU_1870		D	D	0.33	D	0.71	D	0.75	D	0.79
CBU_1871		D	D	1.58	D	1.79	D	1.42	D	1.20
CBU_1872	LCV	D	D	2.06	D	1.72	D	2.18	D	1.65
CBU_1873		D	D	2.25	D	1.22	D	1.01	D	0.91
CBU_1874	SCV	D	D	0.38	D	0.42	D	0.59	D	0.60
CBU_1875		D	D	0.52	D	0.65	D	0.77	D	0.71
CBU_1876		D	D	1.50	D	0.59	D	0.38	D	0.31
CBU_1877		D	D	1.04	D	1.13	D	1.07	D	0.65
CBU_1878		D	D	0.06	D	0.18	D	0.10	D	0.15
CBU_1879		D	D	0.45	D	0.50	D	0.65	D	0.59
CBU_1880		D	D	0.44	D	0.38	D	0.38	D	0.41
CBU_1881	LCV	D	D	1.68	D	2.32	D	1.16	D	1.21
CBU_1882		D	D	0.66	D	0.68	D	0.63	D	0.80
CBU_1883		D	D	0.40	D	1.00	D	0.96	D	1.28
CBU_1884		D	D	0.49	D	0.43	D	0.55	D	0.49
CBU_1886		D	D	0.82	D	1.26	D	1.23	D	0.85
CBU_1887		D	D	1.10	D	0.64	D	0.54	D	0.56
CBU_1888	LCV	D	D	5.08	D	1.86	D	2.18	D	1.28
CBU_1890		D	ND	5.03	D	4.73	D	4.97	ND	0.73
CBU_1891		D	D	0.40	D	0.30	D	0.23	D	0.27
CBU_1892		D	D	0.31	D	0.58	D	0.55	D	0.73
CBU_1893		D	D	1.65	D	1.51	D	1.73	D	1.65
CBU_1894		D	D	21.43	D	14.75	D	13.45	D	3.58
CBU_1894a		D	D	19.33	D	12.24	D	8.17	D	2.29
CBU_1895		D	D	1.21	D	1.10	D	0.68	D	0.64
CBU_1896		D	D	3.61	D	1.45	D	1.08	D	1.16
CBU_1896a		ND	ND		ND		ND		ND	
CBU_1896b		ND	ND		ND		ND		ND	
CBU_1899		D	D	2.13	D	1.61	D	2.02	D	1.31
CBU_1901		D	D	1.88	D	1.46	D	2.06	D	1.98
CBU_1902		D	D	0.73	D	0.70	D	0.67	D	0.86
CBU_1903		D	D	0.22	D	0.56	D	0.37	D	0.37
CBU_1904		D	D	0.77	D	1.10	D	1.19	D	0.86
CBU_1905		D	D	1.13	D	1.52	D	1.10	D	0.67
CBU_1906		D	D	4.77	D	2.29	D	9.52	D	2.03
CBU_1907		D	D	0.46	D	0.72	D	0.74	D	0.85
CBU_1908		D	ND	4.43	ND	2.16	ND	2.27	ND	0.64
CBU_1909		D	D	0.28	D	0.27	D	0.20	D	0.27
CBU_1910		D	D	1.24	D	1.12	D	1.17	D	1.69
CBU_1911	SCV	D	D	8.01	D	2.03	D	1.63	D	0.81
CBU_1913	LCV	D	D	1.70	D	1.07	D	0.88	D	0.94
CBU_1914		D	D	1.15	D	0.91	D	0.97	D	0.81
CBU_1915		D	D	7.73	D	3.94	D	5.29	D	1.87
CBU_1916	LCV	D	D	0.71	D	1.26	D	1.68	D	1.68
CBU_1917		D	D	1.83	D	1.87	D	1.58	D	1.34
CBU_1918		D	D	2.75	D	2.93	D	2.26	D	2.09
CBU_1919		D	D	5.72	D	6.88	D	5.56	D	5.04
CBU_1920		D	D	5.66	D	4.25	D	3.99	D	3.81
CBU_1921	LCV	D	D	15.30	D	4.09	D	5.90	D	8.07
CBU_1922		D	D	4.08	D	2.34	D	1.87	D	1.90
CBU_1924		D	D	1.52	D	1.06	D	0.67	D	0.95
CBU_1925		D	D	1.18	D	0.58	D	0.72	D	0.61
CBU_1926		D	D	1.27	D	1.40	D	1.27	D	1.22
CBU_1927	LCV	D	D	0.83	D	1.11	D	1.02	D	0.89

201

CBU_1928	LCV	D	D	0.52	D	0.77	D	1.02	D	0.80
CBU_1929	LCV	D	D	1.86	D	1.83	D	2.36	D	1.84
CBU_1930		D	D	0.40	D	1.08	D	1.06	D	2.32
CBU_1930a		D	D	0.15	D	0.30	D	0.34	D	0.52
CBU_1931	LCV	D	D	0.38	D	0.48	D	0.84	D	0.66
CBU_1932	SCV	D	D	0.00	D	0.03	D	0.20	D	0.52
CBU_1933	SCV	D	D	0.01	D	0.03	D	0.09	D	0.23
CBU_1934	SCV	D	D	0.06	D	0.04	D	0.15	D	0.21
CBU_1934a		D	D	0.35	ND	0.09	D	0.34	D	0.10
CBU_1936		D	D	4.25	D	2.15	D	0.29	D	1.19
CBU_1938		D	D	5.26	D	3.25	D	2.12	D	2.34
CBU_1939	LCV	D	D	5.50	D	3.01	D	1.73	D	2.22
CBU_1940	LCV	D	D	9.21	D	4.68	D	4.73	D	5.15
CBU_1941		D	D	7.94	D	4.11	D	4.04	D	4.70
CBU_1942		D	D	5.90	D	3.35	D	4.14	D	3.93
CBU_1943	LCV	D	D	7.26	D	4.93	D	7.57	D	6.97
CBU_1944	LCV	D	D	7.53	D	4.76	D	5.58	D	4.94
CBU_1945		D	D	5.19	D	3.32	D	3.85	D	3.64
CBU_1946		D	D	2.39	D	1.89	D	1.82	D	1.83
CBU_1947		D	D	1.73	D	1.51	D	1.60	D	1.53
CBU_1947a		D	D	1.36	D	0.93	D	0.66	D	0.90
CBU_1948		D	D	0.57	D	0.32	D	0.40	D	0.52
CBU_1950	SCV	D	D	0.03	D	0.07	D	0.16	D	0.42
CBU_1951	LCV	D	ND	0.04	D	0.21	D	0.11	D	0.09
CBU_1952		D	D	0.80	D	0.44	D	0.46	D	0.43
CBU_1953	LCV	D	D	0.35	D	0.62	D	0.90	D	1.25
CBU_1954	LCV	D	D	0.38	D	0.54	D	0.46	D	0.63
CBU_1955	LCV	D	D	4.46	D	3.27	D	3.54	D	3.21
CBU_1956	LCV	D	D	8.60	D	5.70	D	4.86	D	3.30
CBU_1957		D	D	5.89	D	5.43	D	4.86	D	4.34
CBU_1959a		ND	ND		ND		ND		ND	
CBU_1959b		ND	ND		ND		ND		ND	
CBU_1960	LCV	D	D	2.84	D	1.41	D	1.10	D	1.00
CBU_1964		D	D	2.76	D	1.43	D	1.26	D	1.73
CBU_1965		D	D	1.22	D	0.85	D	1.23	D	0.99
CBU_1966	LCV	D	D	3.02	D	1.91	D	1.47	D	1.78
CBU_1967		D	D	0.70	D	0.67	D	0.59	D	0.58
CBU_1968	LCV	D	D	2.04	D	1.92	D	2.16	D	1.43
CBU_1969	LCV	D	D	0.78	D	0.70	D	0.53	D	0.96
CBU_1970		D	D	1.08	D	1.31	D	1.00	D	1.13
CBU_1971		D	D	2.13	D	6.77	D	3.53	D	3.70
CBU_1972		D	ND	1.17	ND	0.57	D	3.75	D	0.64
CBU_1973	LCV	D	D	0.77	ND	0.18	D	0.72	D	0.43
CBU_1974		ND	ND	#VALUE!	ND	#VALUE!	ND	#VALUE!	ND	#VALUE!
CBU_1975		D	D	0.45	D	0.49	D	0.49	D	0.55
CBU_1976		D	D	2.19	D	1.58	D	2.08	D	1.90
CBU_1977	LCV	D	D	1.22	D	1.12	D	1.10	D	1.19
CBU_1978	LCV	D	D	0.46	D	0.45	D	0.45	D	0.35
CBU_1980		D	D	0.37	D	0.32	D	0.35	D	0.36
CBU_1981		D	D	0.43	D	0.50	D	0.45	D	0.42
CBU_1982		D	D	0.85	D	0.82	D	0.74	D	0.74
CBU_1983	LCV	D	D	0.29	D	0.30	D	0.28	D	0.35
CBU_1984		D	D	0.12	D	0.87	D	0.62	D	0.87
CBU_1985	LCV	D	D	1.33	D	1.91	D	1.99	D	1.42
CBU_1986		D	D	0.70	D	1.02	D	0.91	D	0.88
CBU_1987		D	D	0.49	D	0.59	D	0.43	D	0.45
CBU_1987a		D	D	0.91	D	0.98	D	0.82	D	0.59
CBU_1987b		ND	ND		ND		ND		ND	
CBU_1987c		ND	ND		ND		ND		ND	
CBU_1991		D	D	0.88	D	1.55	D	1.33	D	1.43
CBU_1992		D	D	1.22	D	0.57	D	0.31	D	0.60
CBU_1993		D	D	0.25	D	0.45	D	0.56	D	0.44
CBU_1994		D	D	0.22	D	0.50	D	0.54	D	0.55
CBU_1995	SCV	D	D	0.33	D	0.73	D	0.65	D	0.69
CBU_1996		D	D	1.49	D	1.77	D	2.05	D	1.53
CBU_1997		D	D	0.73	D	0.81	D	0.85	D	0.78
CBU_1998		D	D	2.27	D	2.69	D	1.66	D	1.28
CBU_1999		D	D	1.41	D	1.48	D	1.90	D	1.66
CBU_2000		D	D	1.10	D	1.39	D	1.29	D	1.07
CBU_2001		D	D	43.94	D	27.24	D	8.50	D	3.88

ID	Type									
CBU_2002		D	D	2.39	D	1.81	D	0.98	D	0.77
CBU_2003		D	D	2.20	D	1.01	D	0.83	D	0.52
CBU_2003a		D	D	432.69	D	68.63	D	84.39	D	7.01
CBU_2004		D	D	5.77	D	3.56	D	2.77	D	2.00
CBU_2005	LCV	D	D	5.87	D	3.02	D	3.67	D	2.44
CBU_2006		D	D	9.64	D	4.83	D	4.87	D	3.92
CBU_2007		D	D	13.10	D	12.78	D	18.51	D	13.78
CBU_2008	LCV	D	D	1.25	D	1.27	D	0.86	D	0.86
CBU_2009		D	D	0.40	D	0.54	D	0.35	D	0.44
CBU_2010		D	D	2.13	D	1.72	D	0.24	D	0.79
CBU_2011		D	D	15.53	D	9.69	D	6.15	D	7.68
CBU_2012	LCV	D	D	7.19	D	4.17	D	3.94	D	5.12
CBU_2013		D	D	1.05	D	0.83	D	1.08	D	0.92
CBU_2014		D	D	1.01	D	2.34	D	2.29	D	1.45
CBU_2016	SCV	D	D	0.14	D	0.42	D	0.23	D	0.23
CBU_2017		D	D	0.84	D	1.09	D	0.86	D	1.04
CBU_2018		D	D	0.60	D	0.96	D	0.86	D	0.88
CBU_2019		D	D	1.55	D	1.55	D	1.50	D	1.30
CBU_2020		D	D	1.47	D	0.96	D	0.80	D	0.83
CBU_2021		D	D	0.57	D	0.46	D	0.70	D	0.80
CBU_2023	SCV	D	D	0.23	D	0.45	D	0.53	D	0.67
CBU_2024	LCV	D	D	1.60	D	0.94	D	0.83	D	0.78
CBU_2025	LCV	D	D	1.51	D	0.97	D	0.90	D	0.81
CBU_2027		D	D	0.57	D	0.45	D	0.34	D	0.43
CBU_2028		D	D	0.49	D	0.72	D	0.82	D	0.38
CBU_2029		D	D	0.47	D	0.55	D	0.51	D	0.70
CBU_2030	LCV	D	D	2.43	D	1.85	D	1.16	D	1.70
CBU_2031	LCV	D	D	3.48	D	3.31	D	4.37	D	4.31
CBU_2032		D	D	3.61	D	3.23	D	3.72	D	2.77
CBU_2033		D	D	3.31	D	2.22	D	0.90	D	0.27
CBU_2036		D	D	6.88	D	6.05	D	3.97	D	1.65
CBU_2040		D	D	1.47	D	2.19	D	1.33	D	0.47
CBU_2041		D	D	0.75	D	1.43	D	0.57	D	0.70
CBU_2046		D	ND	11.94	ND	5.82	D	29.07	ND	1.73
CBU_2047		D	D	1.73	D	1.62	D	2.10	D	2.30
CBU_2048		D	D	1.18	D	1.23	D	1.77	D	2.19
CBU_2049	LCV	D	D	2.12	D	1.02	D	0.99	D	1.04
CBU_2051a		D	D	0.72	D	1.15	D	0.76	D	0.79
CBU_2052		D	D	0.50	D	0.46	D	0.47	D	0.49
CBU_2054	LCV	D	D	3.59	D	1.88	D	1.94	D	2.09
CBU_2055	LCV	D	D	7.58	D	4.31	D	4.91	D	4.42
CBU_2056		D	D	1.13	D	1.15	D	1.25	D	0.97
CBU_2057		D	D	0.85	D	1.07	D	0.68	D	1.13
CBU_2058		D	D	0.08	D	0.07	D	0.08	D	0.12
CBU_2061		D	ND	1.20	ND	0.59	ND	0.62	D	0.70
CBU_2065		D	D	0.35	D	0.27	D	0.33	D	0.22
CBU_2067		D	D	4.50	D	4.13	D	4.41	D	3.18
CBU_2068	LCV	D	D	2.56	D	1.92	D	1.52	D	1.31
CBU_2069		D	D	0.46	D	0.90	D	0.94	D	0.84
CBU_2070	LCV	D	D	0.35	D	0.96	D	0.54	D	0.75
CBU_2071	SCV	D	D	0.01	D	0.03	D	0.07	D	0.30
CBU_2072		D	D	0.13	D	0.20	D	0.24	D	0.26
CBU_2073		D	D	0.13	D	0.24	D	0.24	D	0.29
CBU_2074		D	D	0.33	D	0.44	D	0.47	D	0.39
CBU_2075		D	D	0.28	D	0.66	D	0.51	D	0.41
CBU_2076		D	D	0.16	D	0.50	D	0.46	D	0.51
CBU_2077		D	D	0.87	D	1.05	D	1.07	D	0.58
CBU_2078		D	D	0.18	D	0.42	D	0.34	D	0.38
CBU_2079	SCV	D	D	0.04	D	0.12	D	0.29	D	0.41
CBU_2080		D	D	0.18	D	0.21	D	0.17	D	0.19
CBU_2081		D	D	0.28	D	0.40	D	0.50	D	0.51
CBU_2082		D	D	1.61	D	1.48	D	1.49	D	1.12
CBU_2083	LCV	D	D	1.59	D	2.03	D	2.36	D	1.48
CBU_2084		D	D	0.91	D	2.40	D	1.65	D	1.48
CBU_2085		D	D	0.21	D	0.79	D	0.60	D	0.67
CBU_2086		D	D	1.38	D	0.97	D	0.87	D	0.92
CBU_2087		D	D	0.89	D	1.15	D	1.15	D	1.33
CBU_2088	LCV	D	D	2.00	D	1.06	D	1.08	D	1.22
CBU_2089		D	D	3.30	D	2.70	D	2.31	D	1.83
CBU_2090		D	D	2.38	D	2.44	D	2.41	D	1.75

ID									
CBU_2091		D	D	1.65	D	1.44	D	1.43	D	1.27
CBU_2092		D	D	3.19	D	2.92	D	2.63	D	2.35
CBU_2093		D	D	1.59	D	1.33	D	0.97	D	0.89
CBU_2094		D	D	0.86	D	1.05	D	0.89	D	0.92
CBU_2095		D	D	2.56	D	1.53	D	1.34	D	1.38
CBU_2095a		D	D	5.39	ND	0.69	D	1.45	D	0.75
CBU_2096		D	D	2.22	D	2.02	D	2.64	D	3.15
CBU_2097		D	D	4.69	D	4.92	D	6.60	D	5.19
CBUA0001		D	D	0.56	D	1.22	D	0.81	D	0.87
CBUA0003		D	D	0.29	D	0.32	D	0.33	D	0.43
CBUA0003b		D	ND	6.03	ND	2.94	ND	3.10	ND	0.87
CBUA0006		D	D	0.23	D	0.46	D	0.29	D	0.33
CBUA0007	SCV	D	D	0.19	D	0.58	D	0.32	D	0.42
CBUA0007a		ND	ND	#VALUE!	ND	#VALUE!	ND	#VALUE!	ND	#VALUE!
CBUA0010		D	D	0.14	D	0.32	D	0.24	D	0.27
CBUA0011		D	D	3.08	D	1.58	D	1.70	D	2.11
CBUA0012		D	D	0.41	D	0.98	D	0.84	D	0.86
CBUA0013		D	D	1.09	D	1.78	D	2.12	D	1.73
CBUA0013a		D	ND	8.39	ND	4.09	D	8.90	D	2.46
CBUA0014		D	D	3.84	D	0.98	D	3.05	D	1.42
CBUA0015		D	D	2.86	D	1.88	D	3.45	D	2.57
CBUA0016		D	D	5.17	D	2.19	D	2.36	D	2.29
CBUA0017		D	D	97.78	D	12.06	ND	6.19	ND	1.74
CBUA0020		D	D	0.54	D	0.58	D	0.44	D	0.80
CBUA0021		D	ND	0.38	D	2.42	D	1.80	D	0.69
CBUA0022		D	D	32.67	D	10.60	D	11.18	D	4.70
CBUA0023		D	D	1.38	D	1.83	D	2.13	D	2.26
CBUA0023a		D	ND	2.70	ND	1.32	D	2.82	D	0.79
CBUA0024		D	D	0.99	D	1.49	D	0.76	D	1.41
CBUA0025		D	D	0.22	D	0.34	D	0.27	D	0.26
CBUA0026		D	D	1.91	D	0.90	D	0.54	D	1.42
CBUA0027		D	D	0.21	D	1.19	D	0.53	D	0.92
CBUA0028	SCV	D	D	3.64	D	4.22	D	3.02	D	1.71
CBUA0031	SCV	D	D	5.59	D	5.34	D	2.62	D	0.97
CBUA0032		D	D	2.52	D	1.75	D	1.32	D	1.40
CBUA0033	SCV	D	D	0.49	D	1.15	D	0.17	D	0.39
CBUA0034		D	ND	0.22	D	1.69	D	0.43	D	0.58
CBUA0036		D	D	0.23	D	0.30	D	0.13	D	0.11
CBUA0036a		ND	ND	#VALUE!	ND	#VALUE!	ND	#VALUE!	ND	#VALUE!
CBUA0037		D	D	0.29	D	0.57	D	0.34	D	0.41
CBUA0038		D	D	0.16	D	0.29	D	0.26	D	0.42
CBUA0039		D	D	0.17	D	0.35	D	0.32	D	0.30
CBUA0039a		D	D	0.23	D	0.26	D	0.10	D	0.15

Appendix 5.1. Essential genes as determined by the BioTraDIS pipeline

Locus tag	Gene	Function	
CBU_1488	gltX2	glutamyl-tRNA synthetase	
CBU_2003	CBU_2003	sua5/YciO/YrdC/YwlC family protein	
CBU_1052	alaS	alanyl-tRNA synthetase	
CBU_0824	purB	adenylosuccinate lyase TetR family	
CBU_1322	pheS	phenylalanyl-tRNA synthetase alpha chain	
CBU_2008	argS	arginyl-tRNA synthetase	
CBU_0722	CBU_0722	ornithine decarboxylase	
CBU_0639	CBU_0639	pyruvate dehydrogenase E1 component beta subunit	
CBU_0692	CBU_0692	pyruvate dehydrogenase E1 component beta subunit	
CBU_0897	purF	amidophosphoribosyltransferase	
CBU_1509	tilS	tRNA(Ile)-lysidine synthetase	
CBU_1241	mdh	malate dehydrogenase	
CBU_2002	purE	phosphoribosylaminoimidazole carboxylase carboxyltransferase subunit	
CBU_1397	sucC	succinyl-CoA synthetase beta chain	
CBU_0631	purL	phosphoribosylformylglycinamidine synthase	
CBU_0233	rpsL	SSU ribosomal protein S12P	
CBU_0234	rpsG	SSU ribosomal protein S7P	
CBU_0237	rpsJ	SSU ribosomal protein S10P	
CBU_1386	rpsB	SSU ribosomal protein S2P	
CBU_0648	ribH		6
CBU_0396	ileS	isoleucyl-tRNA synthetase	
CBU_1475	gatB	aspartyl/glutamyl-tRNA(Asn/Gln) amidotransferase subunit B	
CBU_1396	sucD	succinyl-CoA synthetase alpha chain	
CBU_0226	rplK	LSU ribosomal protein L11P	
CBU_0231	rpoB	DNA-directed RNA polymerase beta chain	
CBU_0232	rpoC	DNA-directed RNA polymerase beta' chain	
CBU_0238	rplC	LSU ribosomal protein L3P	
CBU_0239	rplD	LSU ribosomal protein L1E (= L4P)	
CBU_0243	rplV	LSU ribosomal protein L22P	
CBU_0244	rpsC	SSU ribosomal protein S3P	
CBU_0250	rplE	LSU ribosomal protein L5P	
CBU_0252	rpsH	SSU ribosomal protein S8P	
CBU_0253	rplF	LSU ribosomal protein L6P	
CBU_0260	CBU_0260	SSU ribosomal protein S13P	
CBU_0261	rpsK	SSU ribosomal protein S11P	
CBU_1749	rplM	LSU ribosomal protein L13P	
CBU_1748	rpsI	SSU ribosomal protein S9P	
CBU_1258	ndk	nucleoside diphosphate kinase	
CBU_0647	ribA	GTP cyclohydrolase II	
CBU_1096	fumC	fumarate hydratase	
CBU_0643	ribD	diaminohydroxyphosphoribosylaminopyrimidine deaminase	
CBU_0026	rpiA	ribose 5-phosphate isomerase	
CBU_0499	tmk	thymidylate kinase	
CBU_1003	bioD	dethiobiotin synthetase	
CBU_1154	trpC	indole-3-glycerol phosphate synthase	
CBU_0382	ispB	farnesyl pyrophosphate synthetase	
CBU_1695	metG	methionyl-tRNA synthetase	
CBU_0326	purD	phosphoribosylamine--glycine ligase	
CBU_1220	purC	phosphoribosylaminoimidazole-succinocarboxamide synthase	
CBU_1006	bioF	8-amino-7-oxononanoate synthase	
CBU_0181	tyrS	tyrosyl-tRNA synthetase	
CBU_0971	pyrD	dihydroorotate dehydrogenase	
CBU_0858	nadE	glutamine-dependent NAD( ) synthetase	
CBU_1188	serS	seryl-tRNA synthetase	
CBU_2049	trpS	tryptophanyl-tRNA synthetase	
CBU_0242	rpsS	SSU ribosomal protein S19P	
CBU_0247	rpsQ	SSU ribosomal protein S17P	
CBU_0064	parE	topoisomerase IV subunit B	
CBU_0312	folD	methylenetetrahydrofolate dehydrogenase (NADP)	
CBU_1841	pth	peptidyl-tRNA hydrolase	
CBU_0301	gmk	guanylate kinase	
CBU_1433	nusA	N utilization substance protein A	
CBU_0245	rplP	LSU ribosomal protein L16P	
CBU_0251	rpsN	SSU ribosomal protein S14P	
CBU_0258	secY	protein translocase subunit	
CBU_0263	rpoA	DNA-directed RNA polymerase alpha chain	
CBU_2073	CBU_2073	acyltransferase family protein	
CBU_1554	nrdB	ribonucleoside-diphosphate reductase beta chain	
CBU_1553	nrdA	ribonucleoside-diphosphate reductase alpha chain	
CBU_0386	rpmA	LSU ribosomal protein L27P	

CBU_1487	cysS	cysteinyl-tRNA synthetase
CBU_1965	prfA	bacterial peptide chain release factor 1 (RF-1)
CBU_0628	ppa	inorganic pyrophosphatase
CBU_1997	fmt	methionyl-tRNA formyltransferase
CBU_1944	atpG	ATP synthase gamma chain
CBU_0445	rpsP	SSU ribosomal protein S16P
CBU_1816	efp	protein translation elongation factor P (EF-P) luxR family
CBU_0323	CBU_0323	acyl carrier protein
CBU_0496	acpP	acyl carrier protein
CBU_0152	coaE	dephospho-CoA kinase
CBU_0865	rpsR	SSU ribosomal protein S18P
CBU_0673	CBU_0673	histidinol-phosphatase
CBU_1970	dapF	diaminopimelate epimerase
CBU_0246	rpmC	LSU ribosomal protein L29P
CBU_0254	rplR	LSU ribosomal protein L18P
CBU_0928	pdxH	pyridoxamine 5'-phosphate oxidase
CBU_1993	folA	dihydrofolate reductase
CBU_1385	tsf	protein translation elongation factor Ts (EF-Ts) peptidase family M22
CBU_0176	degP1	endopeptidase
CBU_0894	folC	folylpolyglutamate synthase
CBU_1709	dapB	dihydrodipicolinate reductase
CBU_1323	rplT	LSU ribosomal protein L20P
CBU_0795	folE	GTP cyclohydrolase I
CBU_0497	fabF	3-oxoacyl-[acyl-carrier-protein] synthase
CBU_0868	dnaB	replicative DNA helicase
CBU_0646	ribE	riboflavin synthase alpha chain
CBU_1355	CBU_1355	HesB protein family
CBU_1878	CBU_1878	HesB protein family
CBU_0567	CBU_0567	hypothetical metal-binding protein
CBU_1266	lipA	lipoic acid synthetase
CBU_0493	fabH	3-oxoacyl-[acyl-carrier-protein] synthase III
CBU_0442	rplS	LSU ribosomal protein L19P
CBU_1002	birA	biotin operon repressor
CBU_1142	secD	protein translocase subunit
CBU_1239	CBU_1239	hypothetical membrane spanning protein
CBU_0431	CBU_0431	aminomethyltransferase family protein
CBU_1946	atpC	ATP synthase epsilon chain
CBU_1939	atpB	ATP synthase A chain
CBU_0864	rpsF	SSU ribosomal protein S6P
CBU_1195	infA	bacterial protein translation initiation factor 1 (IF-1)
CBU_0840	asnB2	asparagine synthetase family protein
CBU_1447	nuoB	NADH-quinone oxidoreductase chain B
CBU_0842	wecB	UDP-N-acetylglucosamine 2-epimerase
CBU_0055	ubiA	4-hydroxybenzoate polyprenyltransferase
CBU_0696	CBU_0696	nucleotide-sugar aminotransferase
CBU_0697	CBU_0697	dTDP-4-dehydro-6-deoxy-D-glucose 4-aminotransferase
CBU_0825	CBU_0825	nucleotide-sugar aminotransferase
CBU_0423	panC	pantoate--beta-alanine ligase
CBU_0492	plsX	fatty acid/phospholipid synthesis protein
CBU_1703	pyrC	dihydroorotase
CBU_1511	CBU_1511	ZIP family zinc transporter
CBU_1027	CBU_1027	ATPase
CBU_1726	accC	biotin carboxylase
CBU_1326	thrS	threonyl-tRNA synthetase
CBU_1290	dnaK	chaperone protein
CBU_1787	glmS	glucosamine--fructose-6-phosphate aminotransferase (isomerizing)
CBU_1477	CBU_1477	peroxiredoxin
CBU_0681	CBU_0681	NAD dependent epimerase/dehydratase family
CBU_0688	wcaG	GDP-L-fucose synthase
CBU_0844	CBU_0844	UDP-N-acetylglucosamine 4-epimerase
CBU_0886	coaBC	phosphopantothenoylcysteine decarboxylase
CBU_1799	CBU_1799	acetyltransferase
CBU_1281	carB	carbamoyl-phosphate synthase large chain
CBU_1830	prsA	ribose-phosphate pyrophosphokinase
CBU_0690	CBU_0690	polyprenyl-phosphate beta-D-mannosyltransferase
CBU_1352	ftsH	cell division protein
CBU_1781	pyk	pyruvate kinase
CBU_0500	holB	DNA polymerase III
CBU_0125	mraY	phospho-N-acetylmuramoyl-pentapeptide-transferase
CBU_0235	fusA	protein translation elongation factor G (EF-G)
CBU_1147	trmU	tRNA (5-methylaminomethyl-2-thiouridylate)-methyltransferase
CBU_1689	apbC	iron-sulfur cluster assembly/repair protein
CBU_0586	CBU_0586	pyridine nucleotide-disulfide oxidoreductase family
CBU_0559	leuS	leucyl-tRNA synthetase

CBU_1007	bioB	biotin synthase
CBU_1682	pyrG	CTP synthase
CBU_1282	carA	carbamoyl-phosphate synthase small chain
CBU_0462	pdhC	dihydrolipoamide acetyltransferase component of pyruvate dehydrogenase complex
CBU_0638	CBU_0638	dihydrolipoamide acetyltransferase component of pyruvate dehydrogenase complex
CBU_1398	sucB	dihydrolipoamide succinyltransferase component (E2) of 2-oxoglutarate dehydrogenase complex
CBU_1725	accB	biotin carboxyl carrier protein of acetyl-CoA carboxylase
CBU_0769	CBU_0769	GMP synthase (glutamine-hydrolyzing)
CBU_1341	guaA	GMP synthase (glutamine-hydrolyzing)
CBU_1357	csdB	cysteine desulfurase
CBU_0262	rpsD	SSU ribosomal protein S4P
CBU_0808	valS	valyl-tRNA synthetase
CBU_1384	pyrH	uridylate kinase
CBU_1798	CBU_1798	lysine-specific permease
CBU_1432	infB	bacterial protein translation initiation factor 2 (IF-2)
CBU_0836	CBU_0836	radical SAM superfamily protein
CBU_0387	cgtA	GTP-binding protein (probably involved in DNA repair)
CBU_0796	CBU_0796	adenosine 5'-monophosphoramidase
CBU_2095	pyrB	aspartate carbamoyltransferase
CBU_1903	ftsY	cell division protein
CBU_1034	pgsA	CDP-diacylglycerol--glycerol-3-phosphate 3-phosphatidyltransferase
CBU_1399	sucA	2-oxoglutarate dehydrogenase E1 component
CBU_1596	rpoD	RNA polymerase sigma factor
CBU_1503	CBU_1503	ribonuclease III
CBU_1293	grpE	GrpE
CBU_1337	dnaE	DNA polymerase III alpha subunit
CBU_0415	CBU_0415	guanine deaminase
CBU_0002	dnaN	DNA polymerase III, beta chain
CBU_1918	rnpA	ribonuclease P protein component
CBU_1005	bioH	carboxylesterase
CBU_1859	oppB	oligopeptide transport system permease protein
CBU_1708	sodB	superoxide dismutase
CBU_1415	thiL	thiamine-monophosphate kinase
CBU_1827	CBU_1827	tRNA nucleotidyltransferase
CBU_0666	dapE	succinyl-diaminopimelate desuccinylase
CBU_0819	CBU_0819	glutathione S-transferase
CBU_1445	nuoD	NADH-quinone oxidoreductase chain D
CBU_0076	visC	monooxygenase
CBU_2019	ubiB	2-polyprenylphenol 6-hydroxylase accessory protein
CBU_0288	coaD	phosphopantetheine adenylyltransferase
CBU_0621	CBU_0621	NAD-dependent oxidoreductase
CBU_0679	CBU_0679	NADH-dependent dehydrogenase
CBU_1549	lgt	prolipoprotein diacylglyceryl transferase
CBU_1826	psd	phosphatidylserine decarboxylase
CBU_0224	secE	protein translocase subunit
CBU_1305	smpB	SsrA-binding protein
CBU_0135	murG	UDP-N-acetylglucosamine--N-acetylmuramyl-(pentape ptide) pyrophosphoryl-undecaprenol N-acetylglucosamine transferase
CBU_1438	nuoK	NADH-quinone oxidoreductase chain K
CBU_1688	CBU_1688	deoxycytidine triphosphate deaminase
CBU_0656	CBU_0656	hypothetical transcriptional regulatory protein
CBU_1358	sufD	SufD
CBU_1360	sufB	ABC transporter-associated protein
CBU_1473	gatC	aspartyl/glutamyl-tRNA(Asn/Gln) amidotransferase subunit C
CBU_0419	CBU_0419	polysaccharide deacetylase family
CBU_0367	phoB	phosphate regulon transcriptional regulatory protein
CBU_1914	glyS	glycyl-tRNA synthetase beta chain
CBU_1913	glyQ	glycyl-tRNA synthetase alpha chain
CBU_0620	lpxB	lipid-A-disaccharide synthase
CBU_0614	fabZ	(3R)-hydroxymyristoyl-[acyl carrier protein] dehydratase
CBU_0751	murA	UDP-N-acetylglucosamine 1-carboxyvinyltransferase
CBU_0123	murE	UDP-N-acetylmuramoylalanyl-D-glutamate--2
CBU_0124	murF	UDP-N-acetylmuramoyl-tripeptide--D-alanyl-D-alani ne ligase 6-diami nopimelate ligase
CBU_0131	murD	UDP-N-acetylmuramoylalanine--D-glutamate ligase
CBU_0132	ftsW	cell division protein
CBU_0136	murC	UDP-N-acetylmuramate--alanine ligase
CBU_0142	lpxC	UDP-3-O-[3-hydroxymyristoyl] N-acetylglucosamine deacetylase
CBU_0473	CBU_0473	bacterial DNA-binding protein
CBU_1320	ihfA	integration host factor alpha-subunit
CBU_1738	hipB	integration host factor beta-subunit
CBU_0893	accD	acetyl-coenzyme A carboxylase carboxyl transferase subunit beta
CBU_0809	CBU_0809	hypothetical membrane spanning protein
CBU_0810	CBU_0810	hypothetical membrane spanning protein

CBU_0298	murI	glutamate racemase
CBU_0287	folK2	2-amino-4-hydroxy-6-hydroxymethyldihydropteridine pyrophosphokinase
CBU_0444	rimM	16S rRNA processing protein
CBU_0137	murB	UDP-N-acetylenolpyruvoylglucosamine reductase
CBU_2094	CBU_2094	hypothetical cytosolic protein
CBU_1567	ruvC	crossover junction endodeoxyribonuclease
CBU_1510	accA	acetyl-coenzyme A carboxylase carboxyl transferase subunit alpha
CBU_1593	rpsU	SSU ribosomal protein S21P
CBU_0482	CBU_0482	arginine-binding protein
CBU_1448	nuoA	NADH-quinone oxidoreductase chain A
CBU_1439	nuoJ	NADH-quinone oxidoreductase chain J
CBU_1704	rnt	ribonuclease T
CBU_0422	panD	aspartate 1-decarboxylase
CBU_0680	CBU_0680	UDP-glucose 6-dehydrogenase
CBU_1586	CBU_1586	hypothetical protein
CBU_1435	nuoN	NADH-quinone oxidoreductase chain N
CBU_1436	nuoM	NADH-quinone oxidoreductase chain M
CBU_0976	CBU_0976	methylglutaconyl-CoA hydratase
CBU_1442	nuoG	NADH-quinone oxidoreductase chain G
CBU_0615	lpxA	acyl-[acyl-carrier-protein]--UDP-N-acetylglucosam ine O-acyltransferase
CBU_1401	sdhA	succinate dehydrogenase flavoprotein subunit
CBU_0693	CBU_0693	pyruvate dehydrogenase E1 component alpha subunit 6 dehydratase
CBU_0689	gmd	GDP-mannose 4
CBU_1350	glmM	phosphoglucosamine mutase
CBU_0481	artP	arginine transport ATP-binding protein
CBU_0776	CBU_0776	ABC transporter ATP-binding protein
CBU_0856	CBU_0856	phospholipid-lipopolysaccharide ABC transporter
CBU_1000	lolD	lipoprotein releasing system ATP-binding protein
CBU_1809	CBU_1809	ABC transporter ATP-binding protein
CBU_0746	CBU_0746	LPS ABC transporter ATP-binding protein
CBU_1440	nuoI	NADH-quinone oxidoreductase chain I
CBU_1245	CBU_1245	GTP-binding protein
CBU_1338	CBU_1338	D-alanine--D-alanine ligase
CBU_0430	lysS	lysyl-tRNA synthetase
CBU_0540	smc	chromosome partition protein
CBU_1815	priA	primosomal protein N' luxR family
CBU_1947	glmU	glucosamine-1-phosphate acetyltransferase
CBU_1371	CBU_1371	non-proteolytic protein
CBU_0463	lpdA	dihydrolipoamide dehydrogenase
CBU_0610	CBU_0610	3-hydroxy-3-methylglutaryl-coenzyme A reductase
CBU_0818	CBU_0818	transcriptional regulator
CBU_0770	CBU_0770	hypothetical ATPase
CBU_1060	scpB	segregation and condensation protein
CBU_1978	ostA	organic solvent tolerance protein
CBU_0557	holA	DNA polymerase III
CBUA0038	parB2	DNA-binding protein
CBU_0096	clS	cardiolipin synthetase
CBU_1968	folB	dihydroneopterin aldolase
CBU_0745	CBU_0745	ribosome-associated factor Y
CBU_1828	CBU_1828	hypothetical protein
CBU_0608	CBU_0608	phosphomevalonate kinase 2Fe-2s
CBU_0609	CBU_0609	mevalonate kinase
CBU_2077	hemD	uroporphyrinogen-III synthase
CBU_0138	ftsQ	cell division protein
CBU_0857	lpxK	tetraacyldisaccharide 4'-kinase
CBU_1678	speG	spermidine N1-acetyltransferase
CBU_0775	CBU_0775	transcriptional regulator
CBU_0279	CBU_0279	amidinotransferase family protein
CBU_1584	shaE	sodium/proton antiporter protein
CBU_1443	nuoF	NADH-quinone oxidoreductase chain F
CBU_0721	CBU_0721	deoxyhypusine synthase
CBU_1444	nuoE	NADH-quinone oxidoreductase chain E
CBU_1361	CBU_1361	rrf2 family protein
CBU_0774	pspC	stress-responsive transcriptional regulator
CBU_1010	CBU_1010	hypothetical protein
CBU_1403	sdhC	succinate dehydrogenase cytochrome b556 subunit
CBU_0333	thiG	thiazole biosynthesis protein
CBU_0373	CBU_0373	dehydrogenase with MaoC-like domain
CBU_1822	sodC	superoxide dismutase (Cu-Zn)
CBU_0221	CBU_0221	4'-phosphopantetheinyl transferase
CBU_0332	thiS	ThiS
CBU_1402	sdhD	succinate dehydrogenase membrane anchor subunit
CBU_1354	CBU_1354	hypothetical cytosolic protein
CBU_0616	CBU_0616	hydrolase family protein

CBU_0780	gacA2	response regulator GntR family
CBU_1583	shaF	sodium/proton antiporter protein
CBU_1004	bioC2	biotin synthesis protein
CBU_2017	ubiE	ubiquinone/menaquinone biosynthesis methyltransferase
CBU_0350	ubiG	3-demethylubiquinone 3-methyltransferase
CBU_1817	CBU_1817	lysyl-tRNA synthetase
CBU_0833	CBU_0833	phospholipid-lipopolysaccharide ABC transporter
CBU_0461	pdhA	pyruvate dehydrogenase E1 component
CBU_0773	phnB	PhnB
CBU_1804	CBU_1804	bacterial regulatory protein
CBU_0659	dnaZX	DNA polymerase III subunit gamma/tau
CBU_1208	CBU_1208	multidrug transporter
CBU_1304	CBU_1304	oligoketide cyclase/lipid transport protein
CBU_0337	fis	DNA-binding protein fis
CBU_1303	CBU_1303	hypothetical cytosolic protein
CBU_1673	ftsB	cell division protein
CBUA0027	CBUA0027	putative DNA-binding protein
CBU_1465	CBU_1465	hypothetical protein
CBU_0270	CBU_0270	short-chain alcohol dehydrogenase
CBU_1490	higA	virulence-associated protein I
CBU_0117	ftsL	cell division protein
CBU_0822	CBU_0822	Fic family protein
CBU_1938	atpI	ATP synthase protein I
CBU_0607	mvaD	diphosphomevalonate decarboxylase
CBU_0589	CBU_0589	ferredoxin
CBU_1603	CBU_1603	succinylglutamate desuccinylase/aspartoacylase family protein
CBU_0483	artQ	arginine transport system permease protein
CBU_0629	putA	proline dehydrogenase
CBU_1662	CBU_1662	hypothetical protein
CBU_1001	lolC	lipoprotein releasing system transmembrane protein
CBU_1018	CBU_1018	hypothetical protein
CBU_0089	CBU_0089	hypothetical protein
CBU_0106	CBU_0106	hypothetical protein
CBU_0110a	CBU_0110a	hypothetical protein
CBU_0127	CBU_0127	hypothetical protein
CBU_0156a	CBU_0156a	phage integrase family protein
CBU_0166	CBU_0166	hypothetical protein
CBU_0167	pksH	enoyl-CoA hydratase
CBU_0168	CBU_0168	acyl carrier protein
CBU_0173	CBU_0173	hypothetical membrane spanning protein
CBU_0182	CBU_0182	homing endonuclease
CBU_0183	CBU_0183	hypothetical protein 23S rRNA intron
CBU_0210	CBU_0210	hypothetical protein
CBU_0213	CBU_0213	hypothetical protein
CBU_0217a	CBU_0217a	hypothetical protein
CBU_0221a	CBU_0221a	hypothetical protein
CBU_0259	CBU_0259	hypothetical protein
CBU_0290	rpmG	LSU ribosomal protein L33P
CBU_0306	CBU_0306	hypothetical protein
CBU_0307	CBU_0307	outer membrane protein
CBU_0319	CBU_0319	hypothetical protein
CBU_0339	CBU_0339	hypothetical membrane associated protein
CBU_0357	CBU_0357	hypothetical protein
CBU_0369	CBU_0369	hypothetical protein
CBU_0372	CBU_0372	Fic family protein
CBU_0378	CBU_0378	hypothetical membrane associated protein
CBU_0380	CBU_0380	hypothetical protein
CBU_0400a	CBU_0400a	hypothetical protein
CBU_0403	CBU_0403	acetyltransferase family protein
CBU_0407	CBU_0407	hypothetical protein
CBU_0409	CBU_0409	hypothetical protein
CBU_0411	CBU_0411	hypothetical protein
CBU_0416	CBU_0416	hypothetical protein
CBU_0417	CBU_0417	hypothetical protein
CBU_0440	CBU_0440	hypothetical protein
CBU_0455	CBU_0455	thioredoxin
CBU_0456	CBU_0456	histone H1 homolog
CBU_0474	CBU_0474	hypothetical protein
CBU_0478	CBU_0478	hypothetical protein
CBU_0501	CBU_0501	hypothetical protein
CBU_0516	CBU_0516	hypothetical protein
CBU_0541	zipA	cell division protein
CBU_0585	CBU_0585	hypothetical protein delta subunit
CBU_0592	CBU_0592	hypothetical membrane spanning protein

CBU_0627	CBU_0627	hypothetical protein
CBU_0644	CBU_0644	plasmid stabilization system toxin protein
CBU_0662	CBU_0662	hypothetical protein 7-dimethyl-8-ribityllumazine synthase
CBU_0663	CBU_0663	hypothetical protein
CBU_0669	CBU_0669	hypothetical protein
CBU_0682	CBU_0682	methyltransferase
CBU_0683	CBU_0683	hypothetical protein
CBU_0684	CBU_0684	sulfotransferase
CBU_0685	CBU_0685	hypothetical protein
CBU_0686	CBU_0686	pyruvate dehydrogenase E1 component beta subunit
CBU_0687	CBU_0687	hypothetical exported membrane spanning protein
CBU_0691	CBU_0691	methyltransferase
CBU_0694	CBU_0694	glycosyltransferase
CBU_0695	CBU_0695	hypothetical protein
CBU_0705	CBU_0705	hypothetical protein
CBU_0706	CBU_0706	hypothetical protein
CBU_0707	CBU_0707	permease
CBU_0719	CBU_0719	hypothetical protein
CBU_0742	CBU_0742	hypothetical protein
CBU_0761	CBU_0761	hypothetical protein
CBU_0763	CBU_0763	hypothetical membrane spanning protein
CBU_0767	CBU_0767	hypothetical protein
CBU_0777c	CBU_0777c	hypothetical protein
CBU_0784	CBU_0784	hypothetical protein
CBU_0793	CBU_0793	hypothetical protein
CBU_0794	CBU_0794	hypothetical protein
CBU_0805	CBU_0805	hypothetical protein
CBU_0817	aacA4	aminoglycoside N6'-acetyltransferase
CBU_0835	CBU_0835	hypothetical protein
CBU_0854	CBU_0854	hypothetical protein
CBU_0860	CBU_0860	hypothetical protein
CBU_0877	CBU_0877	hypothetical protein
CBU_0880	CBU_0880	hypothetical cytosolic protein
CBU_0881	CBU_0881	hypothetical cytosolic protein
CBU_0883	CBU_0883	hypothetical protein
CBU_0900	CBU_0900	hypothetical protein
CBU_0944	CBU_0944	hypothetical protein
CBU_0948	CBU_0948	hypothetical protein
CBU_0949	CBU_0949	hypothetical cytosolic protein
CBU_0956	CBU_0956	hypothetical membrane associated protein
CBU_0961	CBU_0961	hypothetical protein
CBU_0964a	CBU_0964a	hypothetical protein
CBU_0967	ybgT	YbgT protein
CBU_0994	CBU_0994	hypothetical protein
CBU_0997	CBU_0997	hypothetical protein
CBU_1014	CBU_1014	hypothetical membrane associated protein, beta-dioxygenase
CBU_1015	CBU_1015	hypothetical cytosolic protein
CBU_1016	CBU_1016	hypothetical protein
CBU_1019	CBU_1019	hypothetical protein
CBU_1020	CBU_1020	hypothetical protein
CBU_1021	CBU_1021	nucleotidyltransferase
CBU_1022	CBU_1022	nucleotidyltransferase
CBU_1023a	CBU_1023a	hypothetical protein
CBU_1028	CBU_1028	hypothetical protein
CBU_1045a	CBU_1045a	hypothetical protein
CBU_1099	lepB1	signal peptidase I
CBU_1121	CBU_1121	hypothetical protein
CBU_1138a	CBU_1138a	hypothetical protein
CBU_1159	CBU_1159	hypothetical cytosolic protein
CBU_1161	CBU_1161	hypothetical protein
CBU_1180	CBU_1180	hypothetical protein
CBU_1199	CBU_1199	hypothetical protein
CBU_1206	CBU_1206	delta(24(24(1)))-sterol reductase
CBU_1207	CBU_1207	hypothetical protein
CBU_1214	CBU_1214	hypothetical cytosolic protein
CBU_1256	CBU_1256	hypothetical protein
CBU_1267a	scvA	ScvA
CBU_1307	CBU_1307	hypothetical membrane associated protein
CBU_1310	CBU_1310	hypothetical protein
CBU_1312	CBU_1312	hypothetical protein
CBU_1314	CBU_1314	hypothetical cytosolic protein
CBU_1316	CBU_1316	hypothetical cytosolic protein
CBU_1316a	CBU_1316a	hypothetical protein
CBU_1317	CBU_1317	hypothetical protein

CBU_1340	CBU_1340	hypothetical protein
CBU_1348	CBU_1348	hypothetical protein
CBU_1366	CBU_1366	hypothetical exported protein
CBU_1411	CBU_1411	hypothetical protein
CBU_1426	CBU_1426	hypothetical protein
CBU_1427a	CBU_1427a	hypothetical protein
CBU_1458a	CBU_1458a	hypothetical protein
CBU_1459	CBU_1459	hypothetical exported protein
CBU_1460	CBU_1460	hypothetical protein
CBU_1463	CBU_1463	hypothetical protein
CBU_1479	CBU_1479	hypothetical protein
CBU_1481	CBU_1481	hypothetical protein
CBU_1486	CBU_1486	hypothetical protein
CBU_1497	CBU_1497	hypothetical protein
CBU_1515	CBU_1515	hypothetical protein
CBU_1526a	CBU_1526a	hypothetical protein
CBU_1530a	CBU_1530a	hypothetical protein
CBU_1541	CBU_1541	hypothetical protein
CBU_1552a	CBU_1552a	hypothetical protein
CBU_1559a	CBU_1559a	hypothetical protein
CBU_1560	CBU_1560	hypothetical protein
CBU_1587	shaB	sodium/proton antiporter protein
CBU_1589	CBU_1589	hypothetical membrane associated protein
CBU_1607	CBU_1607	hypothetical protein
CBU_1612	CBU_1612	hypothetical protein
CBU_1613	CBU_1613	hypothetical protein
CBU_1614	CBU_1614	hypothetical protein
CBU_1621	CBU_1621	hypothetical protein
CBU_1635	CBU_1635	hypothetical protein
CBU_1677	CBU_1677	hypothetical cytosolic protein
CBU_1681	CBU_1681	hypothetical exported protein
CBU_1683	CBU_1683	hypothetical protein
CBU_1684	CBU_1684	hypothetical protein
CBU_1685	CBU_1685	hypothetical protein
CBU_1686	CBU_1686	hypothetical protein
CBU_1690	CBU_1690	hypothetical protein
CBU_1691	CBU_1691	transcriptional regulator
CBU_1692	CBU_1692	hypothetical cytosolic protein
CBU_1692a	CBU_1692a	hypothetical protein
CBU_1755	CBU_1755	hypothetical protein
CBU_1764	CBU_1764	hypothetical protein
CBU_1777	CBU_1777	hypothetical protein
CBU_1805	CBU_1805	bacterial regulatory protein
CBU_1806	CBU_1806	hypothetical protein
CBU_1813	CBU_1813	hypothetical protein
CBU_1818	CBU_1818	hypothetical membrane spanning protein
CBU_1819	CBU_1819	hypothetical membrane associated protein
CBU_1820	CBU_1820	hypothetical protein
CBU_1821	CBU_1821	hypothetical protein
CBU_1825	CBU_1825	hypothetical protein
CBU_1833	CBU_1833	hypothetical protein
CBU_1849	CBU_1849	hypothetical protein
CBU_1852	CBU_1852	hypothetical protein
CBU_1853	CBU_1853	GtrA family protein
CBU_1854	CBU_1854	hypothetical cytosolic protein
CBU_1864	CBU_1864	hypothetical protein
CBU_1917	rpmH	LSU ribosomal protein L34P
CBU_1919	CBU_1919	hypothetical cytosolic protein
CBU_1930	CBU_1930	hypothetical protein
CBU_1934a	CBU_1934a	hypothetical cytosolic protein
CBU_1940	atpE	ATP synthase C chain
CBU_1971	CBU_1971	hypothetical protein
CBU_2001	CBU_2001	hypothetical protein
CBU_2036	CBU_2036	hypothetical protein
CBU_2046	CBU_2046	hypothetical protein
CBU_2096	CBU_2096	hypothetical protein
CBUA0003b	CBUA0003b	hypothetical protein
CBUA0007	CBUA0007	hypothetical protein
CBUA0007a	CBUA0007a	hypothetical protein
CBUA0011	CBUA0011	hypothetical protein
CBUA0017	CBUA0017	hypothetical protein
CBUA0023a	CBUA0023a	hypothetical protein
CBUA0034	CBUA0034	hypothetical protein
CBUA0036a	CBUA0036a	hypothetical protein

Appendix 5.2. Essential genes as determined by the Whiteley lab pipeline

Locus tag	Gene	Function
CBU_0001	dnaA	chromosomal replication initiator protein
CBU_0002	dnaN	DNA polymerase III
CBU_0004	gyrB	DNA gyrase subunit B
CBU_0026	rpiA	ribose 5-phosphate isomerase
CBU_0040	CBU_0040	transposase
CBU_0042	hemH	ferrochelatase
CBU_0055	ubiA	4-hydroxybenzoate polyprenyltransferase
CBU_0064	parE	topoisomerase IV subunit B
CBU_0076	visC	monooxygenase
CBU_0081	proS	prolyl-tRNA synthetase
CBU_0097	pssA	CDP-diacylglycerol--serine O-phosphatidyltransferase
CBU_0118	ftsI	division specific D
CBU_0123	murE	UDP-N-acetylmuramoylalanyl-D-glutamate--2
CBU_0124	murF	UDP-N-acetylmuramoyl-tripeptide--D-alanyl-D-alani ne ligase
CBU_0125	mraY	phospho-N-acetylmuramoyl-pentapeptide-transferase
CBU_0131	murD	UDP-N-acetylmuramoylalanine--D-glutamate ligase
CBU_0132	ftsW	cell division protein
CBU_0135	murG	UDP-N-acetylglucosamine--N-acetylmuramyl-(pentape ptide) pyrophosphoryl-undecaprenol N-acetylglucosamine transferase
CBU_0136	murC	UDP-N-acetylmuramate--alanine ligase
CBU_0137	murB	UDP-N-acetylenolpyruvoylglucosamine reductase
CBU_0138	ftsQ	cell division protein
CBU_0141	ftsZ	cell division protein
CBU_0142	lpxC	UDP-3-O-[3-hydroxymyristoyl] N-acetylglucosamine deacetylase
CBU_0147	secA	protein translocase subunit
CBU_0152	coaE	dephospho-CoA kinase
CBU_0153	pilD	type 4 prepilin peptidase
CBU_0154	pilC	type 4 pili biogenesis protein (plasma membrane protein)
CBU_0155	pilB	type 4 pili biogenesis protein (nuleotide-binding protein)
CBU_0167	pksH	enoyl-CoA hydratase
CBU_0168	CBU_0168	acyl carrier protein
CBU_0173	CBU_0173	hypothetical membrane spanning protein
CBU_0176	degP1	endopeptidase
CBU_0177	CBU_0177	glycine betaine transport system permease protein
CBU_0181	tyrS	tyrosyl-tRNA synthetase
CBU_0182	CBU_0182	homing endonuclease
CBU_0199	coaA	pantothenate kinase
CBU_0205	gltX1	glutamyl-tRNA synthetase
CBU_0221	CBU_0221	4'-phosphopantetheinyl transferase
CBU_0221b	CBU_0221b	protein translation elongation factor Tu (EF-TU)
CBU_0224	secE	protein translocase subunit
CBU_0225	nusG	transcription antitermination protein
CBU_0226	rplK	LSU ribosomal protein L11P
CBU_0231	rpoB	DNA-directed RNA polymerase beta chain
CBU_0232	rpoC	DNA-directed RNA polymerase beta' chain
CBU_0235	fusA	protein translation elongation factor G (EF-G)
CBU_0236	tuf2	protein translation elongation factor Tu (EF-TU)
CBU_0237	rpsJ	SSU ribosomal protein S10P
CBU_0238	rplC	LSU ribosomal protein L3P
CBU_0239	rplD	LSU ribosomal protein L1E (= L4P)
CBU_0241	rplB	LSU ribosomal protein L2P
CBU_0244	rpsC	SSU ribosomal protein S3P
CBU_0248	rplN	LSU ribosomal protein L14P
CBU_0250	rplE	LSU ribosomal protein L5P
CBU_0253	rplF	LSU ribosomal protein L6P
CBU_0255	rpsE	SSU ribosomal protein S5P
CBU_0258	secY	protein translocase subunit
CBU_0262	rpsD	SSU ribosomal protein S4P
CBU_0263	rpoA	DNA-directed RNA polymerase alpha chain
CBU_0270	CBU_0270	short-chain alcohol dehydrogenase
CBU_0271	ssb	single-strand DNA binding protein
CBU_0275	hemE	uroporphyrinogen decarboxylase
CBU_0279	CBU_0279	amidinotransferase family protein
CBU_0287	folK2	2-amino-4-hydroxy-6-hydroxymethyldihydropteridine pyrophosphokinase
CBU_0288	coaD	phosphopantetheine adenylyltransferase
CBU_0296	pyrE	orotate phosphoribosyltransferase
CBU_0298	murI	glutamate racemase
CBU_0301	gmk	guanylate kinase
CBU_0303	spoT	GTP pyrophosphokinase

CBU_0307	CBU_0307	outer membrane protein
CBU_0312	folD	methylenetetrahydrofolate dehydrogenase (NADP)
CBU_0316	CBU_0316	ribonuclease HI
CBU_0323	CBU_0323	acyl carrier protein
CBU_0326	purD	phosphoribosylamine--glycine ligase
CBU_0333	thiG	thiazole biosynthesis protein
CBU_0336	purH	phosphoribosylaminoimidazolecarboxamide formyltransferase
CBU_0350	ubiG	3-demethylubiquinone 3-methyltransferase
CBU_0367	phoB	phosphate regulon transcriptional regulatory protein
CBU_0371	CBU_0371	multidrug resistance transporter
CBU_0378	CBU_0378	hypothetical membrane associated protein
CBU_0382	ispB	farnesyl pyrophosphate synthetase
CBU_0384	CBU_0384	transposase
CBU_0387	cgtA	GTP-binding protein (probably involved in DNA repair)
CBU_0390	mviN	virulence factor
CBU_0396	ileS	isoleucyl-tRNA synthetase
CBU_0397	lspA	lipoprotein signal peptidase
CBU_0415	CBU_0415	guanine deaminase
CBU_0422	panD	aspartate 1-decarboxylase
CBU_0423	panC	pantoate--beta-alanine ligase
CBU_0430	lysS	lysyl-tRNA synthetase
CBU_0441	ogt	O6-methylguanine-DNA methyltransferase
CBU_0450	ffh	signal recognition particle
CBU_0454	adk	adenylate kinase
CBU_0461	pdhA	pyruvate dehydrogenase E1 component
CBU_0462	pdhC	dihydrolipoamide acetyltransferase component of pyruvate dehydrogenase complex
CBU_0463	lpdA	dihydrolipoamide dehydrogenase
CBU_0467	bioC1	biotin synthesis protein
CBU_0479	kdsB	3-deoxy-manno-octulosonate cytidylyltransferase
CBU_0481	artP	arginine transport ATP-binding protein
CBU_0482	CBU_0482	arginine-binding protein
CBU_0483	artQ	arginine transport system permease protein
CBU_0484	artM	arginine transport system permease protein
CBU_0492	plsX	fatty acid/phospholipid synthesis protein
CBU_0493	fabH	3-oxoacyl-[acyl-carrier-protein] synthase III
CBU_0494	fabD	malonyl-CoA-[acyl-carrier-protein] transacylase
CBU_0495	fabG	3-oxoacyl-[acyl-carrier protein] reductase
CBU_0497	fabF	3-oxoacyl-[acyl-carrier-protein] synthase
CBU_0499	tmk	thymidylate kinase
CBU_0500	holB	DNA polymerase III
CBU_0503	glnA	glutamine synthetase
CBU_0524	gyrA	DNA gyrase subunit A
CBU_0525	serC	phosphoserine aminotransferase
CBU_0531	pyrF	orotidine 5'-phosphate decarboxylase
CBU_0540	smc	chromosome partition protein
CBU_0541	zipA	cell division protein
CBU_0542	ligA	NAD-dependent DNA ligase
CBU_0549	rodA	rod shape-determining protein
CBU_0556	nadD	nicotinate-nucleotide adenylyltransferase
CBU_0557	holA	DNA polymerase III
CBU_0559	leuS	leucyl-tRNA synthetase
CBU_0562	CBU_0562	hypothetical ATPase
CBU_0564	cutE	apolipoprotein N-acyltransferase
CBU_0567	CBU_0567	hypothetical metal-binding protein
CBU_0586	CBU_0586	pyridine nucleotide-disulfide oxidoreductase family
CBU_0589	CBU_0589	ferredoxin
CBU_0592	CBU_0592	hypothetical membrane spanning protein
CBU_0596	CBU_0596	metal-dependent hydrolase
CBU_0607	mvaD	diphosphomevalonate decarboxylase
CBU_0608	CBU_0608	phosphomevalonate kinase
CBU_0609	CBU_0609	mevalonate kinase
CBU_0610	CBU_0610	3-hydroxy-3-methylglutaryl-coenzyme A reductase
CBU_0611	yaeT	outer membrane protein assembly factor
CBU_0613	lpxD	UDP-3-O-[3-hydroxymyristoyl] glucosamine N-acyltransferase
CBU_0614	fabZ	(3R)-hydroxymyristoyl-[acyl carrier protein] dehydratase
CBU_0615	lpxA	acyl-[acyl-carrier-protein]--UDP-N-acetylglucosam ine O-acyltransferase
CBU_0616	CBU_0616	hydrolase family protein
CBU_0617	CBU_0617	hypothetical membrane spanning protein
CBU_0620	lpxB	lipid-A-disaccharide synthase
CBU_0621	CBU_0621	NAD-dependent oxidoreductase
CBU_0628	ppa	inorganic pyrophosphatase
CBU_0629	putA	proline dehydrogenase
CBU_0631	purL	phosphoribosylformylglycinamidine synthase
CBU_0638	CBU_0638	dihydrolipoamide acetyltransferase component of pyruvate dehydrogenase complex

CBU_0639	CBU_0639	pyruvate dehydrogenase E1 component beta subunit
CBU_0640	CBU_0640	pyruvate dehydrogenase E1 component alpha subunit
CBU_0641	CBU_0641	leucine dehydrogenase
CBU_0643	ribD	diaminohydroxyphosphoribosylaminopyrimidine deaminase
CBU_0646	ribE	riboflavin synthase alpha chain
CBU_0647	ribA	GTP cyclohydrolase II
CBU_0659	dnaZX	DNA polymerase III subunit gamma/tau
CBU_0664	CBU_0664	transposase
CBU_0666	dapE	succinyl-diaminopimelate desuccinylase
CBU_0667	dapD	
CBU_0673	CBU_0673	histidinol-phosphatase
CBU_0678	CBU_0678	D-glycero-D-manno-heptose-1-phosphate adenylyltransferase
CBU_0703	CBU_0703	O-antigen export system permease protein
CBU_0704	rfbI	polysaccharide export ATP-binding protein
CBU_0706	CBU_0706	hypothetical protein
CBU_0719	CBU_0719	hypothetical protein
CBU_0720	CBU_0720	agmatinase
CBU_0721	CBU_0721	deoxyhypusine synthase
CBU_0722	CBU_0722	ornithine decarboxylase
CBU_0746	CBU_0746	LPS ABC transporter ATP-binding protein
CBU_0751	murA	UDP-N-acetylglucosamine 1-carboxyvinyltransferase
CBU_0758	CBU_0758	lipoprotein
CBU_0763	CBU_0763	hypothetical membrane spanning protein
CBU_0766	CBU_0766	acetoacetyl-CoA synthetase
CBU_0768	CBU_0768	multidrug resistance protein B
CBU_0769	CBU_0769	GMP synthase (glutamine-hydrolyzing)
CBU_0770	CBU_0770	hypothetical ATPase
CBU_0771	prpB	methylisocitrate lyase
CBU_0772	prpC	2-methylcitrate synthase
CBU_0773	phnB	PhnB
CBU_0776	CBU_0776	ABC transporter ATP-binding protein
CBU_0777c	CBU_0777c	hypothetical protein
CBU_0780	gacA2	response regulator
CBU_0793	CBU_0793	hypothetical protein
CBU_0794	CBU_0794	hypothetical protein
CBU_0795	folE	GTP cyclohydrolase I
CBU_0797	CBU_0797	multidrug resistance protein B
CBU_0798	CBU_0798	multidrug resistance protein A
CBU_0807	CBU_0807	beta-lactamase family protein
CBU_0808	valS	valyl-tRNA synthetase
CBU_0809	CBU_0809	hypothetical membrane spanning protein
CBU_0810	CBU_0810	hypothetical membrane spanning protein
CBU_0812	CBU_0812	Na driven multidrug efflux pump
CBU_0818	CBU_0818	transcriptional regulator
CBU_0819	CBU_0819	glutathione S-transferase
CBU_0822	CBU_0822	Fic family protein
CBU_0823	sfcA	NAD-dependent malic enzyme
CBU_0825	CBU_0825	nucleotide-sugar aminotransferase
CBU_0828	CBU_0828	NAD-dependent oxidoreductase
CBU_0832	CBU_0832	bacterial transferase family (hexapeptide motif)
CBU_0833	CBU_0833	phospholipid-lipopolysaccharide ABC transporter
CBU_0834	CBU_0834	methyltransferase
CBU_0836	CBU_0836	radical SAM superfamily protein
CBU_0837	CBU_0837	hypothetical membrane spanning protein
CBU_0839	CBU_0839	glycosyltransferase
CBU_0840	asnB2	asparagine synthetase family protein
CBU_0842	wecB	UDP-N-acetylglucosamine 2-epimerase
CBU_0844	CBU_0844	UDP-N-acetylglucosamine 4-epimerase
CBU_0852	pnp	hypothetical protein
CBU_0856	CBU_0856	phospholipid-lipopolysaccharide ABC transporter
CBU_0857	lpxK	tetraacyldisaccharide 4'-kinase
CBU_0858	nadE	glutamine-dependent NAD( ) synthetase
CBU_0860	CBU_0860	hypothetical protein
CBU_0864	rpsF	SSU ribosomal protein S6P
CBU_0868	dnaB	replicative DNA helicase
CBU_0875	asd	aspartate-semialdehyde dehydrogenase
CBU_0880	CBU_0880	hypothetical cytosolic protein
CBU_0881	CBU_0881	hypothetical cytosolic protein
CBU_0886	coaBC	phosphopantothenoylcysteine decarboxylase
CBU_0893	accD	acetyl-coenzyme A carboxylase carboxyl transferase subunit beta
CBU_0894	folC	folylpolyglutamate synthase
CBU_0897	purF	amidophosphoribosyltransferase
CBU_0900	CBU_0900	hypothetical protein
CBU_0904	CBU_0904	NifR3-like protein

CBU_0928	pdxH	pyridoxamine 5'-phosphate oxidase
CBU_0948	CBU_0948	hypothetical protein
CBU_0949	CBU_0949	hypothetical cytosolic protein
CBU_0952	CBU_0952	hypothetical exported protein
CBU_0953	CBU_0953	amino acid permease
CBU_0956	CBU_0956	hypothetical membrane associated protein
CBU_0966	cydB	cytochrome d ubiquinol oxidase subunit II
CBU_0971	pyrD	dihydroorotate dehydrogenase
CBU_0975	CBU_0975	methylcrotonyl-CoA carboxylase carboxyl transferase subunit
CBU_0976	CBU_0976	methylglutaconyl-CoA hydratase
CBU_1000	lolD	lipoprotein releasing system ATP-binding protein
CBU_1001	lolC	lipoprotein releasing system transmembrane protein
CBU_1002	birA	biotin operon repressor
CBU_1003	bioD	dethiobiotin synthetase
CBU_1004	bioC2	biotin synthesis protein
CBU_1005	bioH	carboxylesterase
CBU_1006	bioF	8-amino-7-oxononanoate synthase
CBU_1007	bioB	biotin synthase
CBU_1010	CBU_1010	hypothetical protein
CBU_1015	CBU_1015	hypothetical cytosolic protein
CBU_1018	CBU_1018	hypothetical protein
CBU_1021	CBU_1021	nucleotidyltransferase
CBU_1027	CBU_1027	ATPase
CBU_1028	CBU_1028	hypothetical protein
CBU_1034	pgsA	CDP-diacylglycerol--glycerol-3-phosphate 3-phosphatidyltransferase
CBU_1051	CBU_1051	aspartokinase
CBU_1052	alaS	alanyl-tRNA synthetase
CBU_1060	scpB	segregation and condensation protein
CBU_1061a	CBU_1061a	hypothetical membrane associated protein
CBU_1071	CBU_1071	hypothetical membrane spanning protein
CBU_1076	CBU_1076	transposase
CBU_1084	CBU_1084	two component system histidine kinase
CBU_1086	CBU_1086	transposase
CBU_1087	CBU_1087	ATP/GTP hydrolase
CBU_1096	fumC	fumarate hydratase
CBU_1099	lepB1	signal peptidase I
CBU_1100	CBU_1100	hypothetical exported protein
CBU_1104	CBU_1104	transposase
CBU_1133	suhB	myo-inositol-1(or 4)-monophosphatase
CBU_1136	CBU_1136	enhanced entry protein enhC
CBU_1142	secD	protein translocase subunit
CBU_1147	trmU	tRNA (5-methylaminomethyl-2-thiouridylate)-methyltransferase
CBU_1160	CBU_1160	tetratricopeptide repeat family protein
CBU_1186	CBU_1186	transposase
CBU_1188	serS	seryl-tRNA synthetase
CBU_1191	ftsK	cell division protein
CBU_1193	trxB	thioredoxin reductase
CBU_1208	CBU_1208	multidrug transporter
CBU_1209	CBU_1209	hypothetical membrane spanning protein
CBU_1213	CBU_1213	ankyrin repeat protein
CBU_1217a	CBU_1217a	transposase
CBU_1219	CBU_1219	hypothetical cytosolic protein
CBU_1220	purC	phosphoribosylaminoimidazole-succinocarboxamide synthase
CBU_1226	CBU_1226	NAD-specific glutamate dehydrogenase
CBU_1239	CBU_1239	hypothetical membrane spanning protein
CBU_1240	gcp	O-sialoglycoprotein endopeptidase
CBU_1241	mdh	malate dehydrogenase
CBU_1245	CBU_1245	GTP-binding protein
CBU_1248	hisS	histidyl-tRNA synthetase
CBU_1261	CBU_1261	D-alanyl-D-alanine serine-type carboxypeptidase
CBU_1266	lipA	lipoic acid synthetase
CBU_1270	CBU_1270	transposase
CBU_1275	rspA	starvation sensing protein
CBU_1277	eda	4-Hydroxy-2-oxoglutarate aldolase
CBU_1281	carB	carbamoyl-phosphate synthase large chain
CBU_1282	carA	carbamoyl-phosphate synthase small chain
CBU_1290	dnaK	chaperone protein
CBU_1293	grpE	GrpE
CBU_1296	CBU_1296	ATP-NAD kinase
CBU_1307	CBU_1307	hypothetical membrane associated protein
CBU_1314	CBU_1314	hypothetical cytosolic protein
CBU_1321	pheT	phenylalanyl-tRNA synthetase beta chain
CBU_1322	pheS	phenylalanyl-tRNA synthetase alpha chain
CBU_1323	rplT	LSU ribosomal protein L20P

CBU_1326	thrS	threonyl-tRNA synthetase
CBU_1337	dnaE	DNA polymerase III alpha subunit
CBU_1338	CBU_1338	D-alanine--D-alanine ligase
CBU_1341	guaA	GMP synthase (glutamine-hydrolyzing)
CBU_1342	guaB	inosine-5'-monophosphate dehydrogenase
CBU_1347	CBU_1347	glutamate/gamma-aminobutyrate antiporter
CBU_1349	CBU_1349	hypothetical cytosolic protein
CBU_1350	glmM	phosphoglucosamine mutase
CBU_1351	folP	dihydropteroate synthase
CBU_1352	ftsH	cell division protein
CBU_1354	CBU_1354	hypothetical cytosolic protein
CBU_1357	csdB	cysteine desulfurase
CBU_1358	sufD	SufD
CBU_1359	sufC	ATP-dependent transporter
CBU_1360	sufB	ABC transporter-associated protein
CBU_1370	CBU_1370	hypothetical membrane associated protein
CBU_1371	CBU_1371	non-proteolytic protein
CBU_1373	pabB	para-aminobenzoate synthetase component I
CBU_1384	pyrH	uridylate kinase
CBU_1385	tsf	protein translation elongation factor Ts (EF-Ts)
CBU_1396	sucD	succinyl-CoA synthetase alpha chain
CBU_1397	sucC	succinyl-CoA synthetase beta chain
CBU_1398	sucB	dihydrolipoamide succinyltransferase component (E2) of 2-oxoglutarate dehydrogenase complex
CBU_1399	sucA	2-oxoglutarate dehydrogenase E1 component
CBU_1400	sdhB	succinate dehydrogenase iron-sulfur protein
CBU_1401	sdhA	succinate dehydrogenase flavoprotein subunit
CBU_1402	sdhD	succinate dehydrogenase membrane anchor subunit
CBU_1403	sdhC	succinate dehydrogenase cytochrome b556 subunit
CBU_1415	thiL	thiamine-monophosphate kinase
CBU_1418	CBU_1418	putative regulatory protein
CBU_1432	infB	bacterial protein translation initiation factor 2 (IF-2)
CBU_1433	nusA	N utilization substance protein A
CBU_1435	nuoN	NADH-quinone oxidoreductase chain N
CBU_1436	nuoM	NADH-quinone oxidoreductase chain M
CBU_1437	nuoL	NADH-quinone oxidoreductase chain L
CBU_1438	nuoK	NADH-quinone oxidoreductase chain K
CBU_1439	nuoJ	NADH-quinone oxidoreductase chain J
CBU_1440	nuoI	NADH-quinone oxidoreductase chain I
CBU_1441	nuoH	NADH-quinone oxidoreductase chain H
CBU_1442	nuoG	NADH-quinone oxidoreductase chain G
CBU_1443	nuoF	NADH-quinone oxidoreductase chain F
CBU_1444	nuoE	NADH-quinone oxidoreductase chain E
CBU_1445	nuoD	NADH-quinone oxidoreductase chain D
CBU_1446	nuoC	NADH-quinone oxidoreductase chain C
CBU_1447	nuoB	NADH-quinone oxidoreductase chain B
CBU_1448	nuoA	NADH-quinone oxidoreductase chain A
CBU_1474	gatA	aspartyl/glutamyl-tRNA(Asn/Gln) amidotransferase subunit A
CBU_1475	gatB	aspartyl/glutamyl-tRNA(Asn/Gln) amidotransferase subunit B
CBU_1479	CBU_1479	hypothetical protein
CBU_1481	CBU_1481	hypothetical protein
CBU_1487	cysS	cysteinyl-tRNA synthetase
CBU_1488	gltX2	glutamyl-tRNA synthetase
CBU_1489	lpxH	UDP-2
CBU_1492	CBU_1492	transposase
CBU_1494	pdxJ	pyridoxal phosphate biosynthetic protein
CBU_1502	era	GTP-binding protein
CBU_1503	CBU_1503	ribonuclease III
CBU_1509	tilS	tRNA(Ile)-lysidine synthetase
CBU_1510	accA	acetyl-coenzyme A carboxylase carboxyl transferase subunit alpha
CBU_1511	CBU_1511	ZIP family zinc transporter
CBU_1512	CBU_1512	rhodanese-related sulfurtransferase
CBU_1514	CBU_1514	hypothetical protein
CBU_1530a	CBU_1530a	hypothetical protein
CBU_1547	thyA	thymidylate synthase
CBU_1548	CBU_1548	hypothetical membrane spanning protein
CBU_1553	nrdA	ribonucleoside-diphosphate reductase alpha chain
CBU_1554	nrdB	ribonucleoside-diphosphate reductase beta chain
CBU_1565	aspS	aspartyl-tRNA synthetase
CBU_1570b	CBU_1570b	transposase
CBU_1580	CBU_1580	ATPase
CBU_1583	shaF	sodium/proton antiporter protein
CBU_1584	shaE	sodium/proton antiporter protein
CBU_1586	CBU_1586	hypothetical protein

CBU_1587	shaB	sodium/proton antiporter protein
CBU_1590	nhaP2	Na /H antiporter
CBU_1590b	CBU_1590b	transposase
CBU_1595	dnaG	DNA primase
CBU_1596	rpoD	RNA polymerase sigma factor
CBU_1603	CBU_1603	succinylglutamate desuccinylase/aspartoacylase family protein
CBU_1607	CBU_1607	hypothetical protein
CBU_1614	CBU_1614	hypothetical protein
CBU_1675	kdsA	2-dehydro-3-deoxyphosphooctonate aldolase
CBU_1678	speG	spermidine N1-acetyltransferase
CBU_1682	pyrG	CTP synthase
CBU_1685	CBU_1685	hypothetical protein
CBU_1686	CBU_1686	hypothetical protein
CBU_1688	CBU_1688	deoxycytidine triphosphate deaminase
CBU_1689	apbC	iron-sulfur cluster assembly/repair protein
CBU_1695	metG	methionyl-tRNA synthetase
CBU_1699a	CBU_1699a	transposase
CBU_1703	pyrC	dihydroorotase
CBU_1704	rnt	ribonuclease T
CBU_1708	sodB	superoxide dismutase
CBU_1709	dapB	dihydrodipicolinate reductase
CBU_1726	accC	biotin carboxylase
CBU_1727	arcB	ornithine cyclodeaminase
CBU_1729	hemF	coproporphyrinogen III oxidase
CBU_1738	hipB	integration host factor beta-subunit
CBU_1749	rplM	LSU ribosomal protein L13P
CBU_1758a	CBU_1758a	transposase
CBU_1771	CBU_1771	ABC transporter permease protein
CBU_1772	yihA	GTP-binding protein
CBU_1778	fbaA	fructose-bisphosphate aldolase
CBU_1781	pyk	pyruvate kinase
CBU_1782	pgk	phosphoglycerate kinase
CBU_1783	gap	glyceraldehyde 3-phosphate dehydrogenase
CBU_1784	tkt	transketolase
CBU_1796	CBU_1796	amino acid permease
CBU_1798	CBU_1798	lysine-specific permease
CBU_1799	CBU_1799	acetyltransferase
CBU_1800	CBU_1800	hypothetical membrane spanning protein
CBU_1805	CBU_1805	bacterial regulatory protein
CBU_1809	CBU_1809	ABC transporter ATP-binding protein
CBU_1812	CBU_1812	erythronate-4-phosphate dehydrogenase
CBU_1815	priA	primosomal protein N'
CBU_1817	CBU_1817	lysyl-tRNA synthetase
CBU_1819	CBU_1819	hypothetical membrane associated protein
CBU_1820	CBU_1820	hypothetical protein
CBU_1821	CBU_1821	hypothetical protein
CBU_1822	sodC	superoxide dismutase (Cu-Zn)
CBU_1825	CBU_1825	hypothetical protein
CBU_1826	psd	phosphatidylserine decarboxylase
CBU_1827	CBU_1827	tRNA nucleotidyltransferase
CBU_1828	CBU_1828	hypothetical protein
CBU_1830	prsA	ribose-phosphate pyrophosphokinase
CBU_1841	pth	peptidyl-tRNA hydrolase
CBU_1852	CBU_1852	hypothetical protein
CBU_1853	CBU_1853	GtrA family protein
CBU_1855	pilF	type 4 pili biogenesis protein
CBU_1859	oppB	oligopeptide transport system permease protein
CBU_1866	parC	topoisomerase IV subunit A
CBU_1870	CBU_1870	2-polyprenyl-3-methyl-6-methoxy-1
CBU_1872	rpe	ribulose-phosphate 3-epimerase
CBU_1890	CBU_1890	hypothetical protein
CBU_1903	ftsY	cell division protein
CBU_1913	glyQ	glycyl-tRNA synthetase alpha chain
CBU_1914	glyS	glycyl-tRNA synthetase beta chain
CBU_1918	rnpA	ribonuclease P protein component
CBU_1920	yidC	60 kDa inner membrane protein
CBU_1938	atpI	ATP synthase protein I
CBU_1939	atpB	ATP synthase A chain
CBU_1942	atpH	ATP synthase delta chain
CBU_1944	atpG	ATP synthase gamma chain
CBU_1945	atpD	ATP synthase beta chain
CBU_1947	glmU	glucosamine-1-phosphate acetyltransferase
CBU_1959b	CBU_1959b	transposase
CBU_1965	prfA	bacterial peptide chain release factor 1 (RF-1)

CBU_1966	hemA	glutamyl-tRNA reductase
CBU_1970	dapF	diaminopimelate epimerase
CBU_1976	CBU_1976	mannose-1-phosphate guanyltransferase
CBU_1981	pdxA	4-hydroxythreonine-4-phosphate dehydrogenase
CBU_1987b	CBU_1987b	transposase
CBU_1993	folA	dihydrofolate reductase
CBU_1997	fmt	methionyl-tRNA formyltransferase
CBU_2000	topA	DNA topoisomerase I
CBU_2003	CBU_2003	sua5/YciO/YrdC/YwlC family protein
CBU_2008	argS	arginyl-tRNA synthetase
CBU_2012	hslU	ATP-dependent endopeptidase hsl ATP-binding subunit
CBU_2017	ubiE	ubiquinone/menaquinone biosynthesis methyltransferase
CBU_2019	ubiB	2-polyprenylphenol 6-hydroxylase accessory protein
CBU_2030	metK	S-adenosylmethionine synthetase
CBU_2049	trpS	tryptophanyl-tRNA synthetase
CBU_2073	CBU_2073	acyltransferase family protein
CBU_2077	hemD	uroporphyrinogen-III synthase
CBU_2086	rho	transcription termination factor rho
CBU_2095	pyrB	aspartate carbamoyltransferase
CBU_2096	CBU_2096	hypothetical protein
CBUA0007	CBUA0007	hypothetical protein
CBUA0023	CBUA0023	hypothetical protein
CBUA0033	CBUA0033	hypothetical protein
CBUA0037	CBUA0037	plasmid partition protein A
CBUA0038	parB2	DNA-binding protein
CBUA0039	CBUA0039	plasmid replication initiation protein

References

1. Derrick, E. H. "Q" Fever, A New Fever Entity: Clinical Features, Diagnosis and Laboratory Investigation. *Med. J. Aust.* **2**, 281–299 (1937).

2. Burnet, F. M. & Freeman, M. Experimental Studies on the Virus of "Q" Fever. *Med. J. Aust.* **2**, 299–305 (1937).

3. Davis, G. E., Cox, H. R., Parker, R. R. & Dyer, R. E. A Filter-Passing Infectious Agent Isolated from Ticks. *Public Heal. Reports* **53**, 2259–2282 (1938).

4. Dyer, R. E. Similarity of Australian 'Q' Fever and a Disease Caused by an Infectious Agent Isolated from Ticks in Montana. *Public Heal. Reports* **54**, 1229–1237 (1939).

5. Weisburg, W. G. *et al.* Phylogenetic diversity of the *Rickettsiae. J. Bacteriol.* **171**, 4202–4206 (1989).

6. Seshadri, R. *et al.* Complete genome sequence of the Q-fever pathogen *Coxiella burnetii. Proc. Natl. Acad. Sci. U. S. A.* **100**, 5455–5460 (2003).

7. Madariaga, M. G., Rezai, K., Trenholme, G. M. & Weinstein, R. A. Q fever: A biological weapon in your backyard. *Lancet Infect. Dis.* **3**, 709–721 (2003).

8. McCaul, T. F. & Williams, J. C. Developmental cycle of *Coxiella burnetii*: Structure and morphogenesis of vegetative and sporogenic differentiations. *J. Bacteriol.* **147**, 1063–1076 (1981).

9. STOKER, M. G. & FISET, P. Phase variation of the Nine Mile and other strains of *Rickettsia burneti. Can. J. Microbiol.* **2**, 310–321 (1956).

10. Hotta, A. *et al.* Phase variation analysis of *Coxiella burnetii* during serial passage in cell culture by use of monoclonal antibodies. *Infect. Immun.* **70**, 4747–4749 (2002).

11. Kersh, G. J., Oliver, L. D., Self, J. S., Fitzpatrick, K. A. & Massung, R. F. Virulence of pathogenic *Coxiella burnetii* strains after growth in the absence of host cells. *Vector Borne Zoonotic Dis.* **11**, 1433–1438 (2011).

12. Moos, A. & Hackstadt, T. Comparative virulence of intra- and interstrain lipopolysaccharide variants of *Coxiella burnetii* in the guinea pig model. *Infect. Immun.* **55**, 1144–1150 (1987).

13. Vodkin, M. H. & Williams, J. C. Overlapping deletion in two spontaneous phase variants of *Coxiella burnetii. J. Gen. Microbiol.* **132**, 2587–2594 (1986).

14. Hoover, T. A., Culp, D. W., Vodkin, M. H., Williams, J. C. & Thompson, H. A. Chromosomal DNA deletions explain phenotypic characteristics of two antigenic variants, phase II and RSA 514 (crazy), of the *Coxiella burnetii* nine mile strain. *Infect. Immun.* **70**, 6726–6733 (2002).

15. Beare, P. A. *et al.* Genetic diversity of the Q fever agent, *Coxiella burnetii*, assessed by microarray-based whole-genome comparisons. *J. Bacteriol.* **188**, 2309–2324 (2006).

16. Denison, A. M., Massung, R. F. & Thompson, H. A. Analysis of the O-antigen biosynthesis regions of phase II isolates of *Coxiella burnetii*. *FEMS Microbiol. Lett.* **267**, 102–107 (2007).

17. Beare, P. A., Jeffrey, B. M., Long, C. M., Martens, C. M. & Heinzen, R. A. Genetic mechanisms of *Coxiella burnetii* lipopolysaccharide phase variation. *PLoS Pathogens* vol. 14 (2018).

18. Sandoz, K. M. *et al.* Transcriptional profiling of *Coxiella burnetii* reveals extensive cell wall remodeling in the small cell variant developmental form. *PLoS One* **11**, 1–24 (2016).

19. Sandoz, K. M., Sturdevant, D. E., Hansen, B. & Heinzen, R. A. Developmental transitions of *Coxiella burnetii* grown in axenic media. *J. Microbiol. Methods* **96**, 104–110 (2014).

20. Voth, D. E. & Heinzen, R. A. Lounging in a lysosome: The intracellular lifestyle of *Coxiella burnetii*. *Cell. Microbiol.* **9**, 829–840 (2007).

21. Khavkin, T. & Tabibzadeh, S. S. Histologic, immunofluorescence, and electron microscopic study of infectious process in mouse lung after intranasal challenge with *Coxiella burnetii*. *Infect. Immun.* **56**, 1792–1799 (1988).

22. Russell-Lodrigue, K. E. *et al. Coxiella burnetii* isolates cause genogroup-specific virulence in mouse and guinea pig models of acute Q fever. *Infect. Immun.* **77**, 5640–5650 (2009).

23. Russell-Lodrigue, K. E., Zhang, G. Q., McMurray, D. N. & Samuel, J. E. Clinical and pathologic changes in a guinea pig aerosol challenge model of acute Q fever. *Infect. Immun.* **74**, 6085–6091 (2006).

24. Shannon, J. G. & Heinzen, R. A. Infection of human monocyte-derived macrophages with *Coxiella burnetii*. *Methods Mol. Biol.* **431**, 189–200 (2008).

25. Sobotta, K. *et al.* Coxiella burnetii Infects Primary Bovine Macrophages and Limits Their Host Cell Response. *Infect. Immun.* **84**, 1722–1734 (2016).

26. Baca, O. G., Klassen, D. A. & Aragon, A. S. Entry of *Coxiella burnetii* into host cells. *Acta Virol.* **37**, 143–155 (1993).

27. Tujulin, E., Macellaro, A., Lilliehöök, B. & Norlander, L. Effect of endocytosis inhibitors on *Coxiella burnetii* interaction with host cells. *Acta Virol.* **42**, 125–131 (1998).

28. Larson, C. L. *et al.* Right on Q: genetics begin to unravel *Coxiella burnetii* host cell interactions. *Future Microbiol.* **11**, 919–939 (2016).

29. van Schaik, E. J., Chen, C., Mertens, K., Weber, M. M. & Samuel, J. E. Molecular pathogenesis of the obligate intracellular bacterium *Coxiella burnetii*. *Nat. Rev. Microbiol.* **11**, 561–573 (2013).

30. Newton, H. J., McDonough, J. A. & Roy, C. R. Effector protein translocation by the *Coxiella burnetii* Dot/Icm type IV secretion system requires endocytic maturation of the pathogen-occupied vacuole. *PLoS One* **8**, e54566 (2013).

31. TIGERTT, W. D., BENENSON, A. S. & GOCHENOUR, W. S. Airborne Q fever. *Bacteriol. Rev.* **25**, 285–293 (1961).

32. Valková, D. & Kazár, J. A new plasmid (QpDV) common to *Coxiella burnetii* isolates associated with acute and chronic Q fever. *FEMS Microbiol. Lett.* **125**, 275–280 (1995).

33. Samuel, J. E. *et al.* Isolation and characterization of a plasmid from phase I *Coxiella burnetii. Infect. Immun.* **41**, 488–493 (1983).

34. Hendrix, L. R., Samuel, J. E. & Mallavia, L. P. Differentiation of *Coxiella burnetii* isolates by analysis of restriction-endonuclease-digested DNA separated by SDS-PAGE. *J. Gen. Microbiol.* **137**, 269–276 (1991).

35. SAVINELLI, E. A. & Mallavia, L. P. Comparison of *Coxiella burnetii* Plasmids to Homologous Chromosomal Sequences Present in a Plasmidless Endocarditis-Causing Isolatea. *Ann. N. Y. Acad. Sci.* **590**, 523–533 (1990).

36. Willems, H., Ritter, M., Jäger, C. & Thiele, D. Plasmid-homologous sequences in the chromosome of plasmidless *Coxiella burnetii* Scurry Q217. *J. Bacteriol.* **179**, 3293–3297 (1997).

37. Hornstra, H. M. *et al.* Rapid typing of *Coxiella burnetii. PLoS One* **6**, e26201 (2011).

38. Piñero, A., Barandika, J. F., García-Pérez, A. L. & Hurtado, A. Genetic diversity and variation over time of *Coxiella burnetii* genotypes in dairy cattle and the farm environment. *Infect. Genet. Evol. J. Mol. Epidemiol. Evol. Genet. Infect. Dis.* **31**, 231–235 (2015).

39. Raetz, C. R. H., Reynolds, C. M., Trent, M. S. & Bishop, R. E. Lipid A modification systems in gram-negative bacteria. *Annu. Rev. Biochem.* **76**, 295–329 (2007).

40. Hackstadt, T. The role of lipopolysaccharides in the virulence of *Coxiella burnetii. Ann. N. Y. Acad. Sci.* **590**, 27–32 (1990).

41. Shannon, J. G., Howe, D. & Heinzen, R. A. Virulent *Coxiella burnetii* does not activate human dendritic cells: role of lipopolysaccharide as a shielding molecule. *Proc. Natl. Acad. Sci. U. S. A.* **102**, 8722–8727 (2005).

42. Amano, K. & Williams, J. C. Chemical and immunological characterization of lipopolysaccharides from phase I and phase II *Coxiella burnetii. J. Bacteriol.* **160**, 994–1002 (1984).

43. de la Cruz, F. & Davies, J. Horizontal gene transfer and the origin of species: lessons from bacteria. *Trends Microbiol.* **8**, 128–133 (2000).

44. Finsel, I. & Hilbi, H. Formation of a pathogen vacuole according to *Legionella pneumophila*: how to kill one bird with many stones. *Cell. Microbiol.* **17**, 935–950 (2015).

45. Naumann, M., Sokolova, O., Tegtmeyer, N. & Backert, S. *Helicobacter pylori*: A Paradigm Pathogen for Subverting Host Cell Signal Transmission. *Trends Microbiol.* **25**, 316–328 (2017).

46. Shrivastava, R. & Miller, J. F. Virulence factor secretion and translocation

by *Bordetella* species. *Curr. Opin. Microbiol.* **12**, 88–93 (2009).

47. Carey, K. L., Newton, H. J., Lührmann, A. & Roy, C. R. The *Coxiella burnetii* Dot/Icm system delivers a unique repertoire of type IV effectors into host cells and is required for intracellular replication. *PLoS Pathog.* **7**, e1002056 (2011).

48. Moffatt, J. H., Newton, P. & Newton, H. J. *Coxiella burnetii*: Turning hostility into a home. *Cell. Microbiol.* **17**, 621–631 (2015).

49. Crabill, E., Schofield, W. B., Newton, H. J., Goodman, A. L. & Roy, C. R. Dot/Icm-Translocated Proteins Important for Biogenesis of the *Coxiella burnetii*-Containing Vacuole Identified by Screening of an Effector Mutant Sublibrary. *Infect. Immun.* **86**, (2018).

50. Weber, M. M. & Faris, R. Subversion of the Endocytic and Secretory Pathways by Bacterial Effector Proteins. *Front. cell Dev. Biol.* **6**, 1 (2018).

51. Newton, H. J. *et al.* A screen of *Coxiella burnetii* mutants reveals important roles for Dot/Icm effectors and host autophagy in vacuole biogenesis. *PLoS Pathog.* **10**, e1004286 (2014).

52. Kuba, M. *et al.* EirA Is a Novel Protein Essential for Intracellular Replication of *Coxiella burnetii. Infect. Immun.* **88**, e00913-19 (2020).

53. Pechstein, J. *et al.* The *Coxiella burnetii* T4SS Effector AnkF Is Important for Intracellular Replication . *Frontiers in Cellular and Infection Microbiology* vol. 10 695 (2020).

54. Lührmann, A., Nogueira, C. V, Carey, K. L. & Roy, C. R. Inhibition of pathogen-induced apoptosis by a *Coxiella burnetii* type IV effector protein. *Proc. Natl. Acad. Sci. U. S. A.* **107**, 18997–19001 (2010).

55. Klingenbeck, L., Eckart, R. A., Berens, C. & Lührmann, A. The *Coxiella burnetii* type IV secretion system substrate CaeB inhibits intrinsic apoptosis at the mitochondrial level. *Cell. Microbiol.* **15**, 675–687 (2013).

56. Burette, M. *et al.* Modulation of innate immune signaling by a *Coxiella burnetii* eukaryotic-like effector protein. *Proc. Natl. Acad. Sci.* **117**, 13708 LP – 13718 (2020).

57. Rodolakis, A. Q Fever in dairy animals. *Ann. N. Y. Acad. Sci.* **1166**, 90–93 (2009).

58. Karagiannis, I. *et al.* Investigation of a Q fever outbreak in a rural area of The Netherlands. *Epidemiol. Infect.* **137**, 1283–1294 (2009).

59. Knap, N., Žele, D., Glinšek Biškup, U., Avšič-Županc, T. & Vengušt, G. The prevalence of *Coxiella burnetii* in ticks and animals in Slovenia. *BMC Vet. Res.* **15**, 368 (2019).

60. Izquierdo-Rodríguez, E. *et al.* Rodents as Reservoirs of the Zoonotic Pathogens *Coxiella burnetii* and Toxoplasma gondii in Corsica (France). *Vector Borne Zoonotic Dis.* **19**, 879–883 (2019).

61. González-Barrio, D., Maio, E., Vieira-Pinto, M. & Ruiz-Fons, F. European Rabbits as Reservoir for *Coxiella burnetii. Emerg. Infect. Dis.* **21**, 1055–1058 (2015).

62. Ma, G. C. *et al.* New insights on the epidemiology of *Coxiella burnetii* in pet dogs and cats from New South Wales, Australia. *Acta Trop.* **205**, 105416 (2020).

63. WELSH, H. H., LENNETTE, E. H., ABINANTI, F. R. & WINN, J. F. Q fever in California. IV. Occurrence of *Coxiella burnetii* in the placenta of naturally infected sheep. *Public Heal. reports (Washington, D.C. 1896)* **66**, 1473–1477 (1951).

64. Hansen, M. S. *et al. Coxiella burnetii* associated placental lesions and infection level in parturient cows. *Vet. J.* **190**, e135–e139 (2011).

65. Tissot-Dupont, H., Amadei, M.-A., Nezri, M. & Raoult, D. Wind in November, Q fever in December. *Emerg. Infect. Dis.* **10**, 1264–1269 (2004).

66. Miceli, M. H. *et al.* A case of person-to-person transmission of Q fever from an active duty serviceman to his spouse. *Vector Borne Zoonotic Dis.* **10**, 539–541 (2010).

67. Milazzo, A. *et al.* Sexually transmitted Q fever. *Clin. Infect. Dis. an Off. Publ. Infect. Dis. Soc. Am.* **33**, 399–402 (2001).

68. Angelakis, E. & Raoult, D. Q Fever. *Vet. Microbiol.* **140**, 297–309 (2010).

69. Raoult, D., Marrie, T. & Mege, J. Natural history and pathophysiology of Q fever. *Lancet. Infect. Dis.* **5**, 219–226 (2005).

70. Maurin, M. & Raoult, D. Q fever. *Clin. Microbiol. Rev.* **12**, 518–553 (1999).

71. Budgin, A. M., Abidi, M. Z., Bajrovic, V., Miller, M. A. & Johnson, S. C. Severe acute Q fever pneumonia complicated by presumed persistent localized Q fever endocarditis in a renal transplant recipient: A case report and review of the literature. *Transplant infectious disease : an official journal of the Transplantation Society* vol. 22 e13230 (2020).

72. Fournier, P. E., Etienne, J., Harle, J. R., Habib, G. & Raoult, D. Myocarditis, a rare but severe manifestation of Q fever: report of 8 cases and review of the literature. *Clin. Infect. Dis. an Off. Publ. Infect. Dis. Soc. Am.* **32**, 1440–1447 (2001).

73. Gomes, M. M., Chaves, A., Gouveia, A. & Santos, L. Two rare manifestations of Q fever: splenic and hepatic abscesses and cerebral venous thrombosis, with literature review ma non troppo. *BMJ Case Rep.* **2014**, (2014).

74. Marmion, B. P. *et al.* Q fever: persistence of antigenic non-viable cell residues of *Coxiella burnetii* in the host--implications for post Q fever infection fatigue syndrome and other chronic sequelae. *QJM* **102**, 673–684 (2009).

75. Morroy, G. *et al.* Fatigue following Acute Q-Fever: A Systematic Literature Review. *PLoS One* **11**, e0155884 (2016).

76. Reukers, D. F. M. *et al.* Impact of Q-fever fatigue syndrome on patients' work status. *Occup. Med. (Lond).* **70**, 578–585 (2020).

77. Kampschreur, L. M. *et al.* Chronic Q fever in the Netherlands 5 years after

the start of the Q fever epidemic: results from the Dutch chronic Q fever database. *J. Clin. Microbiol.* **52**, 1637–1643 (2014).

78. Wegdam-Blans, M. C. A. *et al.* Chronic Q fever: review of the literature and a proposal of new diagnostic criteria. *J. Infect.* **64**, 247–259 (2012).

79. Gami, A. S., Antonios, V. S., Thompson, R. L., Chaliki, H. P. & Ammash, N. M. Q fever endocarditis in the United States. *Mayo Clin. Proc.* **79**, 253–257 (2004).

80. Kampschreur, L. M. *et al.* Identification of risk factors for chronic Q fever, the Netherlands. *Emerg. Infect. Dis.* **18**, 563–570 (2012).

81. Fenollar, F. *et al.* Risks factors and prevention of Q fever endocarditis. *Clin. Infect. Dis. an Off. Publ. Infect. Dis. Soc. Am.* **33**, 312–316 (2001).

82. POPPE, K. [Queensland fever, a zoonosis]. *Berl. Tierarztl. Wochenschr.* **4**, 57–59 (1950).

83. Woldehiwet, Z. Q fever (coxiellosis): epidemiology and pathogenesis. *Res. Vet. Sci.* **77**, 93–100 (2004).

84. Halsby, K. D. *et al.* The Epidemiology of Q Fever in England and Wales 2000-2015. *Vet. Sci.* **4**, (2017).

85. Karagiannis, I. *et al.* Q fever outbreak in the Netherlands: a preliminary report. *Euro Surveill. Bull. Eur. sur les Mal. Transm. = Eur. Commun. Dis. Bull.* **12**, E070809.2 (2007).

86. Roest, H. I. J. *et al.* The Q fever epidemic in The Netherlands: history, onset, response and reflection. *Epidemiol. Infect.* **139**, 1–12 (2011).

87. Schneeberger, P. M., Wintenberger, C., van der Hoek, W. & Stahl, J. P. Q fever in the Netherlands - 2007-2010: What we learned from the largest outbreak ever. *Med. Mal. Infect.* **44**, 339–353 (2014).

88. van Asseldonk, M. A. P. M., Prins, J. & Bergevoet, R. H. M. Economic assessment of Q fever in the Netherlands. *Prev. Vet. Med.* **112**, 27–34 (2013).

89. Hawker, J. I. *et al.* A large outbreak of Q fever in the West Midlands: windborne spread into a metropolitan area? *Commun. Dis. public Heal.* **1**, 180–187 (1998).

90. van Woerden, H. C. *et al.* Q fever outbreak in industrial setting. *Emerg. Infect. Dis.* **10**, 1282–1289 (2004).

91. Wilson, L. E. *et al.* Investigation of a Q fever outbreak in a Scottish co-located slaughterhouse and cutting plant. *Zoonoses Public Health* **57**, 493–498 (2010).

92. Huang, M. *et al.* The epidemic of Q fever in 2018 to 2019 in Zhuhai city of China determined by metagenomic next-generation sequencing. *PLoS Negl. Trop. Dis.* **15**, e0009520–e0009520 (2021).

93. Herremans, T. *et al.* Comparison of the performance of IFA, CFA, and ELISA assays for the serodiagnosis of acute Q fever by quality assessment. *Diagn. Microbiol. Infect. Dis.* **75**, 16–21 (2013).

94. Dupont, H. T., Thirion, X. & Raoult, D. Q fever serology: cutoff determination for microimmunofluorescence. *Clin. Diagn. Lab. Immunol.* **1**, 189–196 (1994).

95. Scola, B. La. Current laboratory diagnosis of Q fever. *Semin. Pediatr. Infect. Dis.* **13**, 257–262 (2002).

96. Slabá, K., Skultéty, L. & Toman, R. Efficiency of various serological techniques for diagnosing *Coxiella burnetii* infection. *Acta Virol.* **49**, 123–127 (2005).

97. Sawyer, L. A., Fishbein, D. B. & McDade, J. E. Q fever: current concepts. *Rev. Infect. Dis.* **9**, 935–946 (1987).

98. Cutler, S. J., Bouzid, M. & Cutler, R. R. Q fever. *J. Infect.* **54**, 313–318 (2007).

99. Healy, B. *et al.* Chronic Q fever: different serological results in three countries--results of a follow-up study 6 years after a point source outbreak. *Clin. Infect. Dis. an Off. Publ. Infect. Dis. Soc. Am.* **52**, 1013–1019 (2011).

100. Zhang, P. *et al.* Development and evaluation of an up-converting phosphor technology-based lateral flow assay for rapid and quantitative detection of *Coxiella burnetii* phase I strains. *BMC Microbiol.* **20**, 251 (2020).

101. Klee, S. R. *et al.* Highly sensitive real-time PCR for specific detection and quantification of *Coxiella burnetii*. *BMC Microbiol.* **6**, 2 (2006).

102. Howe, G. B. *et al.* Real-time PCR for the early detection and quantification of *Coxiella burnetii* as an alternative to the murine bioassay. *Mol. Cell. Probes* **23**, 127–131 (2009).

103. Turra, M., Chang, G., Whybrow, D., Higgins, G. & Qiao, M. Diagnosis of acute Q fever by PCR on sera during a recent outbreak in rural south Australia. *Ann. N. Y. Acad. Sci.* **1078**, 566–569 (2006).

104. Cunha, B. A., Domenico, P. & Cunha, C. B. Pharmacodynamics of doxycycline. *Clin. Microbiol. Infect.* **6**, 270–273 (2000).

105. Raoult, D., Drancourt, M. & Vestris, G. Bactericidal effect of doxycycline associated with lysosomotropic agents on *Coxiella burnetii i*n P388D1 cells. *Antimicrob. Agents Chemother.* **34**, 1512–1514 (1990).

106. Raoult, D. *et al.* Treatment of Q fever endocarditis: comparison of 2 regimens containing doxycycline and ofloxacin or hydroxychloroquine. *Arch. Intern. Med.* **159**, 167–173 (1999).

107. Lever, M. S., Bewley, K. R., Dowsett, B. & Lloyd, G. In vitro susceptibility of *Coxiella burnetii* to azithromycin, doxycycline, ciprofloxacin and a range of newer fluoroquinolones. *International journal of antimicrobial agents* vol. 24 194–196 (2004).

108. Spyridaki, I., Psaroulaki, A., Vranakis, I., Tselentis, Y. & Gikas, A. Bacteriostatic and bactericidal activities of tigecycline against *Coxiella burnetii* and comparison with those of six other antibiotics. *Antimicrob. Agents Chemother.* **53**, 2690–2692 (2009).

109. Eldin, C. *et al.* Antibiotic susceptibility determination for six strains of *Coxiella burnetii* MST 17 from Cayenne, French Guiana. *International journal of antimicrobial agents* vol. 46 600–602 (2015).

110. Rouli, L., Rolain, J.-M., El Filali, A., Robert, C. & Raoult, D. Genome sequence of *Coxiella burnetii* 109, a doxycycline-resistant clinical isolate. *J. Bacteriol.* **194**, 6939 (2012).

111. Rolain, J.-M., Lambert, F. & Raoult, D. Activity of telithromycin against thirteen new isolates of *C. burnetii* including three resistant to doxycycline. *Ann. N. Y. Acad. Sci.* **1063**, 252–256 (2005).

112. Marmion, B. P. *et al.* Vaccine prophylaxis of abattoir-associated Q fever: eight years' experience in Australian abattoirs. *Epidemiol. Infect.* **104**, 275–287 (1990).

113. Isken, L. D. *et al.* Implementation of a Q fever vaccination program for high-risk patients in the Netherlands. *Vaccine* **31**, 2617–2622 (2013).

114. Sellens, E. *et al.* Frequency of Adverse Events Following Q Fever Immunisation in Young Adults. *Vaccines* **6**, (2018).

115. Norville, I. H. *et al. Galleria mellonella* as an alternative model of *Coxiella burnetii* infection. *Microbiol. (United Kingdom)* **160**, 1175–1181 (2014).

116. Kohler, L. J. *et al.* Effector Protein Cig2 Decreases Host Tolerance of Infection by Directing Constitutive Fusion of Autophagosomes with the *Coxiella*-Containing Vacuole. *MBio* **7**, (2016).

117. Martinez, E. *et al. Coxiella burnetii* effector CvpB modulates phosphoinositide metabolism for optimal vacuole development. *Proc. Natl. Acad. Sci. U. S. A.* **113**, E3260–E3269 (2016).

118. Weber, M. M. *et al.* The Type IV Secretion System Effector Protein CirA Stimulates the GTPase Activity of RhoA and Is Required for Virulence in a Mouse Model of *Coxiella burnetii* Infection. *Infect. Immun.* **84**, 2524–2533 (2016).

119. Selim, A., Yang, E., Rousset, E., Thiéry, R. & Sidi-Boumedine, K. Characterization of *Coxiella burnetii* strains from ruminants in a *Galleria mellonella* host-based model. *New microbes new Infect.* **24**, 8–13 (2018).

120. van Schaik, E. J., Case, E. D., Martinez, E., Bonazzi, M. & Samuel, J. E. The SCID mouse model for identifying virulence determinants in *Coxiella burnetii. Front. Cell. Infect. Microbiol.* **7**, 1–10 (2017).

121. Norville, I. H. *et al.* Efficacy of liposome-encapsulated ciprofloxacin in a murine model of Q fever. *Antimicrob. Agents Chemother.* **58**, 5510–5518 (2014).

122. Baeten, L. A. *et al.* Standardized guinea pig model for Q fever vaccine reactogenicity. *PLoS One* **13**, e0205882 (2018).

123. Waag, D. M. *et al.* Comparative efficacy and immunogenicity of Q fever chloroform:methanol residue (CMR) and phase I cellular (Q-Vax) vaccines in cynomolgus monkeys challenged by aerosol. *Vaccine* **20**, 2623–2634 (2002).

124. Bastos, R. G., Howard, Z. P., Hiroyasu, A. & Goodman, A. G. Host and bacterial factors control susceptibility of *Drosophila melanogaster* to *Coxiella burnetii* infection. *Infect. Immun.* **85**, (2017).

125. Battisti, J. M. *et al.* Analysis of the *Caenorhabditis elegans* innate immune response to *Coxiella burnetii. Innate Immun.* **23**, 111–127 (2017).

126. Waag, D. M. *et al.* Evaluation of cynomolgus (*Macaca fascicularis*) and rhesus (*Macaca mulatta*) monkeys as experimental models of acute Q fever after aerosol exposure to phase-I *Coxiella burnetii. Lab. Anim. Sci.* **49**, 634–638 (1999).

127. Gonder, J. C., Kishimoto, R. A., Kastello, M. D., Pedersen, C. E. J. & Larson, E. W. Cynomolgus monkey model for experimental Q fever infection. *J. Infect. Dis.* **139**, 191–196 (1979).

128. Hoffmann, J. A. The immune response of *Drosophila. Nature* **426**, 33–38 (2003).

129. Browne, N., Heelan, M. & Kavanagh, K. An analysis of the structural and functional similarities of insect hemocytes and mammalian phagocytes. *Virulence* **4**, 597–603 (2013).

130. Meisel, J. D. & Kim, D. H. Behavioral avoidance of pathogenic bacteria by *Caenorhabditis elegans. Trends Immunol.* **35**, 465–470 (2014).

131. Avery, L. & Thomas, J. H. Feeding and Defecation. in (eds. Riddle, D. L., Blumenthal, T., Meyer, B. J. & Priess, J. R.) (1997).

132. Ermolaeva, M. A. & Schumacher, B. Insights from the worm: The *C. elegans* model for innate immunity. *Semin. Immunol.* **26**, 303–309 (2014).

133. Hellinga, J. R. *et al.* Identification of vacuoles containing extraintestinal differentiated forms of *Legionella pneumophila* in colonized *Caenorhabditis elegans* soil nematodes. *Microbiologyopen* **4**, 660–681 (2015).

134. Zusman, T., Yerushalmi, G. & Segal, G. Functional similarities between the icm/dot pathogenesis systems of *Coxiella burnetii* and *Legionella pneumophila. Infect. Immun.* **71**, 3714–3723 (2003).

135. Brandt, J. P. & Ringstad, N. Toll-like Receptor Signaling Promotes Development and Function of Sensory Neurons Required for a *C. elegans* Pathogen-Avoidance Behavior. *Current Biology* vol. 25 2228–2237 (2015).

136. Ammerdorffer, A. *et al.* Recognition of *Coxiella burnetii* by toll-like receptors and nucleotide-binding oligomerization domain-like receptors. *J. Infect. Dis.* **211**, 978–987 (2015).

137. Ramstead, A. G. *et al.* Roles of Toll-Like Receptor 2 (TLR2), TLR4, and MyD88 during Pulmonary *Coxiella burnetii* Infection. *Infect. Immun.* **84**, 940–949 (2016).

138. Brutkiewicz, R. R. Cell Signaling Pathways That Regulate Antigen Presentation. *J. Immunol.* **197**, 2971 LP – 2979 (2016).

139. H., K. D. *et al.* A Conserved p38 MAP Kinase Pathway in *Caenorhabditis elegans* Innate Immunity. *Science (80-.).* **297**, 623–626 (2002).

140. Evans, E. A., Chen, W. C. & Tan, M.-W. The DAF-2 insulin-like signaling

pathway independently regulates aging and immunity in *C. elegans*. *Aging Cell* **7**, 879–893 (2008).

141. Wangler, M. F., Hu, Y. & Shulman, J. M. Drosophila and genome-wide association studies: a review and resource for the functional dissection of human complex traits. *Dis. Model. Mech.* **10**, 77–88 (2017).

142. Kleino, A. & Silverman, N. The *Drosophila* IMD pathway in the activation of the humoral immune response. *Dev. Comp. Immunol.* **42**, 25–35 (2014).

143. Capo, C. *et al.* Upregulation of tumor necrosis factor alpha and interleukin-1 beta in Q fever endocarditis. *Infect. Immun.* **64**, 1638–1642 (1996).

144. Brandt, S. M. *et al.* Secreted Bacterial Effectors and Host-Produced Eiger/TNF Drive Death in a *Salmonella*-Infected Fruit Fly. *PLOS Biol.* **2**, e418 (2004).

145. Loh, J. M. S., Adenwalla, N., Wiles, S. & Proft, T. *Galleria mellonella* larvae as an infection model for group A streptococcus. *Virulence* **4**, 419–428 (2013).

146. Anna, L. *et al.* Genome Sequence of *Galleria mellonella* (Greater Wax Moth). *Genome Announc.* **6**, e01220-17 (2021).

147. Champion, O. L., Titball, R. W. & Bates, S. Standardization of *G. mellonella* Larvae to Provide Reliable and Reproducible Results in the Study of Fungal Pathogens. *Journal of Fungi* vol. 4 (2018).

148. La Scola, B., Lepidi, H. & Raoult, D. Pathologic changes during acute Q fever: influence of the route of infection and inoculum size in infected guinea pigs. *Infect. Immun.* **65**, 2443–2447 (1997).

149. Marrie, T. J. Q fever pneumonia. *Curr. Opin. Infect. Dis.* **17**, 137–142 (2004).

150. Okimoto, N. *et al.* Clinical features of Q fever pneumonia. *Respirology* **9**, 278–282 (2004).

151. Scott, G. H., Williams, J. C. & Stephenson, E. H. Animal models in Q fever: pathological responses of inbred mice to phase I *Coxiella burnetii*. *J. Gen. Microbiol.* **133**, 691–700 (1987).

152. Andoh, M. *et al.* SCID mouse model for lethal Q fever. *Infect. Immun.* **71**, 4717–4723 (2003).

153. Freylikhman, O., Tokarevich, N., Suvorov, A., Vorobiova, E. & Totolian, A. *Coxiella burnetii* persistence in three generations of mice after application of live attenuated human M-44 vaccine against Q fever. *Ann. N. Y. Acad. Sci.* **990**, 496–499 (2003).

154. Tyczka, J., Eberling, S. & Baljer, G. Immunization experiments with recombinant *Coxiella burnetii* proteins in a murine infection model. *Ann. N. Y. Acad. Sci.* **1063**, 143–148 (2005).

155. Zhang, G. *et al.* Mechanisms of vaccine-induced protective immunity against *Coxiella burnetii* infection in BALB/c mice. *J. Immunol.* **179**, 8372–8380 (2007).

156. Lepidi, H., Houpikian, P., Liang, Z. & Raoult, D. Cardiac valves in patients

with Q fever endocarditis: microbiological, molecular, and histologic studies. *J. Infect. Dis.* **187**, 1097–1106 (2003).

157. Mühlemann, K., Matter, L., Meyer, B. & Schopfer, K. Isolation of *Coxiella burnetii* from heart valves of patients treated for Q fever endocarditis. *J. Clin. Microbiol.* **33**, 428–431 (1995).

158. Stein, A. *et al.* Q fever pneumonia: virulence of *Coxiella burnetii* pathovars in a murine model of aerosol infection. *Infect. Immun.* **73**, 2469–2477 (2005).

159. Elliott, A., Peng, Y. & Zhang, G. *Coxiella burnetii* interaction with neutrophils and macrophages in vitro and in SCID mice following aerosol infection. *Infect. Immun.* **81**, 4604–4614 (2013).

160. Anderson, A. *Operation Whitecoat 1954 - 73: ethical use of human subjects in infectious disease.* (2013).

161. Nelson, M., Salguero, F. J., Hunter, L. & Atkins, T. P. A Novel Marmoset (*Callithrix jacchus)* Model of Human Inhalational Q Fever. *Front. Cell. Infect. Microbiol.* **10**, 621635 (2021).

162. Williams, D. M. Clinical Pharmacology of Corticosteroids. *Respir. Care* **63**, 655 LP – 670 (2018).

163. Ericson-Neilsen, W. & Kaye, A. D. Steroids: Pharmacology, Complications, and Practice Delivery Issues. *Ochsner J.* **14**, 203 LP – 207 (2014).

164. Maggioncalda, E. C. *et al.* A mouse model of pulmonary *Mycobacteroides abscessus* infection. *Sci. Rep.* **10**, 3690 (2020).

165. Satoh, S. *et al.* Dexamethasone impairs pulmonary defence against *Pseudomonas aeruginosa* through suppressing iNOS gene expression and peroxynitrite production in mice. *Clin. Exp. Immunol.* **126**, 266–273 (2001).

166. Garcia, E. S., Castro, D. P., Figueiredo, M. B., Genta, F. A. & Azambuja, P. *Trypanosoma* rangeli: a new perspective for studying the modulation of immune reactions of *Rhodnius prolixus. Parasit. Vectors* **2**, 33 (2009).

167. Stanley, D., Haas, E. & Miller, J. Eicosanoids: Exploiting Insect Immunity to Improve Biological Control Programs. *Insects* **3**, 492–510 (2012).

168. Torres, M. P., Entwistle, F. & Coote, P. J. Effective immunosuppression with dexamethasone phosphate in the *Galleria mellonella* larva infection model resulting in enhanced virulence of *Escherichia coli* and *Klebsiella pneumoniae. Med. Microbiol. Immunol.* **205**, 333–343 (2016).

169. McClintock, B. The origin and behavior of mutable loci in maize. *Proc. Natl. Acad. Sci.* **36**, 344 LP – 355 (1950).

170. Muñoz-López, M. & García-Pérez, J. L. DNA transposons: nature and applications in genomics. *Curr. Genomics* **11**, 115–128 (2010).

171. Finnegan, D. J. Transposable elements. *Curr. Opin. Genet. Dev.* **2**, 861–867 (1992).

172. Kleckner, N., Roth, J. & Botstein, D. Genetic engineering in Vivo using translocatable drug-resistance elements: New methods in bacterial genetics. *J. Mol. Biol.* **116**, 125–159 (1977).

173. Beck, E., Ludwig, G., Auerswald, E. A., Reiss, B. & Schaller, H. Nucleotide sequence and exact localization of the neomycin phosphotransferase gene from transposon Tn5. *Gene* **19**, 327–336 (1982).

174. Lampe, D. J., Grant, T. E. & Robertson, H. M. Factors affecting transposition of the *Himar1* mariner transposon in vitro. *Genetics* **149**, 179–187 (1998).

175. Barquist, L., Boinett, C. J. & Cain, A. K. Approaches to querying bacterial genomes with transposon-insertion sequencing. *RNA Biol.* **10**, 1161–1169 (2013).

176. Caparon, M. G. & Scott, J. R. Genetic Manipulation of Pathogenic *Streptococci*. *Methods Enzymol.* **204**, 556–586 (1991).

177. Burne, R. A. & Quivey, R. G. J. Use of transposons to dissect pathogenic strategies of gram-positive bacteria. *Methods Enzymol.* **235**, 405–426 (1994).

178. Hoover, C. I. & Yoshimura, F. Transposon-induced pigment-deficient mutants of *Porphyromonas gingivalis*. *FEMS Microbiol. Lett.* **124**, 43–48 (1994).

179. Leung, K. Y. & Finlay, B. B. Intracellular replication is essential for the virulence of *Salmonella typhimurium*. *Proc. Natl. Acad. Sci. U. S. A.* **88**, 11470–11474 (1991).

180. Taylor, R. K., Miller, V. L., Furlong, D. B. & Mekalanos, J. J. Use of phoA gene fusions to identify a pilus colonization factor coordinately regulated with cholera toxin. *Proc. Natl. Acad. Sci. U. S. A.* **84**, 2833–2837 (1987).

181. Heather, J. M. & Chain, B. The sequence of sequencers: The history of sequencing DNA. *Genomics* **107**, 1–8 (2016).

182. Smith, V., Botstein, D. & Brown, P. O. Genetic footprinting: A genomic strategy for determining a gene's function given its sequence. *Proc. Natl. Acad. Sci. U. S. A.* **92**, 6479–6483 (1995).

183. Smith, V., Botstein, D. & Brown, P. O. Genetic footprinting: a genomic strategy for determining a gene's function given its sequence. *Proc. Natl. Acad. Sci. U. S. A.* **92**, 6479–6483 (1995).

184. Hare, R. S. *et al.* Genetic footprinting in bacteria. *J. Bacteriol.* **183**, 1694–1706 (2001).

185. Hayes, F. Transposon-Based Strategies for Microbial Functional Genomics and Proteomics. *Annu. Rev. Genet.* **37**, 3–29 (2003).

186. Akerley, B. J. *et al.* Systematic identification of essential genes by *in vitro* mariner mutagenesis. *Proc. Natl. Acad. Sci. U. S. A.* **95**, 8927–8932 (1998).

187. Hensel, M. *et al.* Simultaneous identification of bacterial virulence genes by negative selection. *Science (80-.).* **269**, 400–403 (1995).

188. Cummins, J. & Gahan, C. G. M. Signature tagged mutagenesis in the functional genetic analysis of gastrointestinal pathogens. *Gut Microbes* **3**, 93–103 (2012).

189. Mazurkiewicz, P., Tang, C. M., Boone, C. & Holden, D. W. Signature-

tagged mutagenesis: barcoding mutants for genome-wide screens. *Nat. Rev. Genet.* **7**, 929–939 (2006).

190. Sassetti, C. M., Boyd, D. H. & Rubin, E. J. Comprehensive identification of conditionally essential genes in mycobacteria. *Proc. Natl. Acad. Sci. U. S. A.* **98**, 12712–12717 (2001).

191. Day, W. A., Rasmussen, S. L., Carpenter, B. M., Peterson, S. N. & Friedlander, A. M. Microarray analysis of transposon insertion mutations in *Bacillus anthracis*: Global identification of genes required for sporulation and germination. *J. Bacteriol.* **189**, 3296–3301 (2007).

192. Langridge, G. C. *et al.* Simultaneous assay of every *Salmonella Typhi* gene using one million transposon mutants. *Genome Res.* **19**, 2308–2316 (2009).

193. Goodman, A. L. *et al.* Identifying genetic determinants needed to establish a human gut symbiont in its habitat. *Cell Host Microbe* **6**, 279–289 (2009).

194. van Opijnen, T., Bodi, K. L. & Camilli, A. Tn-seq: high-throughput parallel sequencing for fitness and genetic interaction studies in microorganisms. *Nat. Methods* **6**, 767–772 (2009).

195. Gawronski, J. D., Wong, S. M. S., Giannoukos, G., Ward, D. V. & Akerley, B. J. Tracking insertion mutants within libraries by deep sequencing and a genome-wide screen for *Haemophilus* genes required in the lung. *Proc. Natl. Acad. Sci. U. S. A.* **106**, 16422–16427 (2009).

196. Chao, M. C., Abel, S., Davis, B. M. & Waldor, M. K. The design and analysis of transposon insertion sequencing experiments. *Nature reviews. Microbiology* vol. 14 119–128 (2016).

197. Zomer, A., Burghout, P., Bootsma, H. J., Hermans, P. W. M. & van Hijum, S. A. F. T. Essentials: Software for rapid analysis of high throughput transposon insertion sequencing data. *PLoS One* **7**, 1–9 (2012).

198. Solaimanpour, S., Sarmiento, F. & Mrázek, J. Tn-seq explorer: A tool for analysis of high-throughput sequencing data of transposon mutant libraries. *PLoS One* **10**, 1–15 (2015).

199. Barquist, L. *et al.* The TraDIS toolkit: Sequencing and analysis for dense transposon mutant libraries. *Bioinformatics* **32**, 1109–1111 (2016).

200. Pritchard, J. R. *et al.* ARTIST: High-Resolution Genome-Wide Assessment of Fitness Using Transposon-Insertion Sequencing. *PLoS Genet.* **10**, (2014).

201. Zhang, R. DEG: a database of essential genes. *Nucleic Acids Res.* **32**, 271D – 272 (2004).

202. Chen, W. H., Minguez, P., Lercher, M. J. & Bork, P. OGEE: An online gene essentiality database. *Nucleic Acids Res.* **40**, 901–906 (2012).

203. Moule, M. G. *et al.* Genome-Wide Saturation Mutagenesis of *Burkholderia pseudomallei*. *MBio* **5**, 1–9 (2014).

204. De Vries, S. P. W. *et al.* Genome-wide fitness analyses of the foodborne pathogen *Campylobacter jejuni* in in vitro and in vivo models. *Sci. Rep.* **7**,

1–17 (2017).

205. Lijuan, C., Xing, Y., Minxi, W., Wenkai, L. & Le, D. Development of an aptamer-ampicillin conjugate for treating biofilms. *Biochem. Biophys. Res. Commun.* **483**, 847–854 (2017).

206. Wright, H. T. & Reynolds, K. A. Antibacterial targets in fatty acid biosynthesis. *Curr. Opin. Microbiol.* **10**, 447–453 (2007).

207. Maniloff, J. Commentary The minimal cell " On being the right size ". *Mol. Biol.* **93**, 10004–10006 (1996).

208. Lee, S. A. *et al.* General and condition-specific essential functions of *Pseudomonas aeruginosa. Proc. Natl. Acad. Sci. U. S. A.* **112**, 5189–5194 (2015).

209. Capel, E. *et al.* Comprehensive Identification of Meningococcal Genes and Small Noncoding RNAs Required for Host Cell Colonization. *MBio* **7**, 1–13 (2016).

210. Valentino, M. D. *et al.* Genes Contributing to *Staphylococcus aureus* Fitness in Abscess- and. *MBio* **5**, 1–10 (2014).

211. Cox, H. R. Cultivation of *Rickettsiae* of the Rocky Mountain spotted fever, typhus and Q fever groups in the embryonic tissues of developing chicks. *Science* **94**, 399–403 (1941).

212. Omsland, A. *et al.* Host cell-free growth of the Q fever bacterium *Coxiella burnetii. Proc. Natl. Acad. Sci. U. S. A.* **106**, 4430–4434 (2009).

213. Omsland, A., Cockrell, D. C., Fischer, E. R. & Heinzen, R. A. Sustained axenic metabolic activity by the obligate intracellular bacterium *Coxiella burnetii. J. Bacteriol.* **190**, 3203–3212 (2008).

214. Lockhart, M. G., Islam, A., Fenwick, S. G., Graves, S. R. & Stenos, J. Growth Yields of Four *Coxiella burnetii* Isolates in Four Different Cell Culture Lines. *Adv. Microbiol.* **3**, 88–90 (2013).

215. Tam, J. E., Davis, C. H. & Wyrick, P. B. Expression of recombinant DNA introduced into *Chlamydia trachomatis* by electroporation. *Can. J. Microbiol.* **40**, 583–591 (1994).

216. Suhan, M. L., Chen, S. Y. & Thompson, H. A. Transformation of *Coxiella burnetii* to ampicillin resistance. *J. Bacteriol.* **178**, 2701–2708 (1996).

217. Beare, P. A. *et al.* Characterization of a *Coxiella burnetii* ftsZ mutant generated by *Himar1* transposon mutagenesis. *J. Bacteriol.* **191**, 1369–1381 (2009).

218. Weber, M. M. *et al.* Identification of *Coxiella burnetii* type IV secretion substrates required for intracellular replication and *Coxiella*-containing vacuole formation. *J. Bacteriol.* **195**, 3914–3924 (2013).

219. Martinez, E., Cantet, F., Fava, L., Norville, I. & Bonazzi, M. Identification of OmpA, a *Coxiella burnetii* Protein Involved in Host Cell Invasion, by Multi-Phenotypic High-Content Screening. *PLoS Pathog.* **10**, e1004013 (2014).

220. Li, H. & Durbin, R. Fast and accurate short read alignment with Burrows-Wheeler transform. *Bioinformatics* **25**, 1754–1760 (2009).

221. Li, H. *et al.* The Sequence Alignment/Map format and SAMtools. *Bioinformatics* **25**, 2078–2079 (2009).

222. Andrews, S. Fastqc: a quality control tool for high throughput sequence data. http://www.bioinformatics.babraham.ac.uk/projects/fastqc (2010).

223. García-Alcalde, F. *et al.* Qualimap: evaluating next-generation sequencing alignment data. *Bioinformatics* **28**, 2678–2679 (2012).

224. Trapnell, C., Pachter, L. & Salzberg, S. L. TopHat: discovering splice junctions with RNA-Seq. *Bioinformatics* **25**, 1105–11 (2009).

225. Trapnell, C. *et al.* Differential gene and transcript expression analysis of RNA-seq experiments with TopHat and Cufflinks. *Nat Protoc* **7**, 562–78 (2012).

226. Patro, R., Duggal, G., Love, M. I., Irizarry, R. A. & Kingsford, C. Salmon provides fast and bias-aware quantification of transcript expression. *Nat Methods* **14**, 417–9 (2017).

227. Anders, S. & Huber, W. Differential expression analysis for sequence count data. *Genome Biol* **11**, (2010).

228. Hall, T. BioEdit: A User-Friendly Biological Sequence Alignment Editor and Analysis Program for Windows 95/98/NT. *Nucleic Acids Symp. Ser.* **41**, 95–98 (1999).

229. Rutherford, K. *et al.* Artemis: sequence visualization and annotation . *Bioinformatics* **16**, 944–945 (2000).

230. Morishima, I., Yamano, Y., Inoue, K. & Matsuo, N. Eicosanoids mediate induction of immune genes in the fat body of the silkworm, Bombyx mori. *FEBS Lett.* **419**, 83–86 (1997).

231. Wishart, D. S. *et al.* DrugBank 5.0: a major update to the DrugBank database for 2018. *Nucleic Acids Res.* **46**, D1074–D1082 (2018).

232. Qin, J. *et al.* A human gut microbial gene catalogue established by metagenomic sequencing. *Nature* **464**, 59–65 (2010).

233. Yu, N. Y. *et al.* PSORTb 3.0: improved protein subcellular localization prediction with refined localization subcategories and predictive capabilities for all prokaryotes. *Bioinformatics* **26**, 1608–1615 (2010).

234. Krogh, A., Larsson, B., Von Heijne, G. & Sonnhammer, E. L. L. Predicting transmembrane protein topology with a hidden Markov model: Application to complete genomes. *J. Mol. Biol.* **305**, 567–580 (2001).

235. Almagro Armenteros, J. J. *et al.* SignalP 5.0 improves signal peptide predictions using deep neural networks. *Nat. Biotechnol.* **37**, 420–423 (2019).

236. Sievers, F. *et al.* Fast, scalable generation of high-quality protein multiple sequence alignments using Clustal Omega. *Mol. Syst. Biol.* **7**, 539 (2011).

237. Williams, J. C., Peacock, M. G. & McCaul, T. F. Immunological and biological characterization of *Coxiella burnetii*, phases I and II, separated from host components. *Infect. Immun.* **32**, 840–851 (1981).

238. Cockrell, D. C., Beare, P. A., Fischer, E. R., Howe, D. & Heinzen, R. A. A method for purifying obligate intracellular *Coxiella burnetii* that employs digitonin lysis of host cells. *J. Microbiol. Methods* **72**, 321–325 (2008).

239. Millar, J. A. *et al.* Whole-Genome Sequence of *Coxiella burnetii* Nine Mile RSA439 (Phase II, Clone 4), a Laboratory Workhorse Strain. *Genome Announc.* **5**, (2017).

240. Sanchez, S. E., Vallejo-Esquerra, E. & Omsland, A. Use of Axenic Culture Tools to Study Coxiella burnetii. *Curr. Protoc. Microbiol.* **50**, 1–15 (2018).

241. Kwon, S., Park, S., Lee, B. & Yoon, S. In-depth analysis of interrelation between quality scores and real errors in illumina reads. in *2013 35th Annual International Conference of the IEEE Engineering in Medicine and Biology Society (EMBC)* 635–638 (2013). doi:10.1109/EMBC.2013.6609580.

242. Hackstadt, T., Peacock, M. G., Hitchcock, P. J. & Cole, R. L. Lipopolysaccharide variation in *Coxiella burnetii*: intrastrain heterogeneity in structure and antigenicity. *Infect. Immun.* **48**, 359–365 (1985).

243. Narasaki, C. T. & Toman, R. Lipopolysaccharide of *Coxiella burnetii*. *Adv. Exp. Med. Biol.* **984**, 65–90 (2012).

244. Huang, X., Li, D., Xi, L. & Mylonakis, E. *Galleria mellonella* Larvae as an Infection Model for *Penicillium marneffei*. *Mycopathologia* **180**, 159–164 (2015).

245. Ligeza-Zuber, M. Mechanisms of *Galleria mellonella* cellular immune response after infection with entomopathogenic fungus *Conidiobolus coronatus*. *Ann. Parasitol.* **58**, 227–228 (2012).

246. Arteaga Blanco, L. A. *et al.* Differential cellular immune response of *Galleria mellonella* to *Actinobacillus pleuropneumoniae*. *Cell Tissue Res.* **370**, 153–168 (2017).

247. Mizerska-Dudka, M. & Andrejko, M. *Galleria mellonella* hemocytes destruction after infection with *Pseudomonas aeruginosa*. *J. Basic Microbiol.* **54**, 232–246 (2014).

248. Stanley-Samuelson, D. W. *et al.* Insect immune response to bacterial infection is mediated by eicosanoids. *Proc. Natl. Acad. Sci. U. S. A.* **88**, 1064–1068 (1991).

249. Coleman, S. A., Fischer, E. R., Howe, D., Mead, D. J. & Heinzen, R. A. Temporal analysis of *Coxiella burnetii* morphological differentiation. *J. Bacteriol.* **186**, 7344–7352 (2004).

250. Kohler, L. J. & Roy, C. R. Biogenesis of the lysosome-derived vacuole containing *Coxiella burnetii*. *Microbes Infect.* **17**, 766–771 (2015).

251. Coleman, S. A. *et al.* Proteome and antigen profiling of *Coxiella burnetii* developmental forms. *Infect. Immun.* **75**, 290–298 (2007).

252. Moormeier, D. E. *et al. Coxiella burnetii* RpoS Regulates Genes Involved in Morphological Differentiation and Intracellular Growth. *J. Bacteriol.* **201**, (2019).

253. Kovacs-Simon, A., Hemsley, C. M., Scott, A. E., Prior, J. L. & Titball, R. W. *Burkholderia thailandensis* strain E555 is a surrogate for the investigation of *Burkholderia pseudomallei* replication and survival in macrophages. *BMC Microbiol.* **19**, 97 (2019).

254. Voth, D. E. *et al.* The *Coxiella burnetii* cryptic plasmid is enriched in genes encoding type IV secretion system substrates. *J. Bacteriol.* **193**, 1493–1503 (2011).

255. Woong Park, S. *et al.* Evaluating the sensitivity of *Mycobacterium tuberculosis* to biotin deprivation using regulated gene expression. *PLoS Pathog.* **7**, e1002264–e1002264 (2011).

256. Feng, Y. *et al.* A *Francisella* virulence factor catalyses an essential reaction of biotin synthesis. *Mol. Microbiol.* **91**, 300–314 (2014).

257. Moses, A. S., Millar, J. A., Bonazzi, M., Beare, P. A. & Raghavan, R. Horizontally Acquired Biosynthesis Genes Boost *Coxiella burnetii*'s Physiology. *Front. Cell. Infect. Microbiol.* **7**, 174 (2017).

258. Salaemae, W., Booker, G. W. & Polyak, S. W. The Role of Biotin in Bacterial Physiology and Virulence: a Novel Antibiotic Target for *Mycobacterium tuberculosis. Microbiol. Spectr.* **4**, 1–20 (2016).

259. Feng, J., Paparella, A. S., Booker, G. W., Polyak, S. W. & Abell, A. D. Biotin Protein Ligase Is a Target for New Antibacterials. *Antibiot. (Basel, Switzerland)* **5**, 26 (2016).

260. Beare, P. A. *et al.* Comparative genomics reveal extensive transposon-mediated genomic plasticity and diversity among potential effector proteins within the genus *Coxiella. Infect. Immun.* **77**, 642–656 (2009).

261. Kuley, R. *et al.* Major differential gene regulation in *Coxiella burnetii* between in vivo and in vitro cultivation models. *BMC Genomics* **16**, 953 (2015).

262. Morgan, J. K., Luedtke, B. E., Thompson, H. A. & Shaw, E. I. *Coxiella burnetii* type IVB secretion system region I genes are expressed early during the infection of host cells. *FEMS Microbiol. Lett.* **311**, 61–69 (2010).

263. Shields, R. C. & Jensen, P. A. The bare necessities: Uncovering essential and condition-critical genes with transposon sequencing. *Mol. Oral Microbiol.* **34**, 39–50 (2019).

264. Omsland, A. *et al.* Isolation from animal tissue and genetic transformation of *Coxiella burnetii* are facilitated by an improved axenic growth medium. *Appl. Environ. Microbiol.* **77**, 3720–3725 (2011).

265. Mobegi, F. M. *et al.* From microbial gene essentiality to novel antimicrobial drug targets. *BMC Genomics* **15**, (2014).

266. Dejesus, M. A. *et al.* Comprehensive essentiality analysis of the *Mycobacterium tuberculosis* genome via saturating transposon mutagenesis. *MBio* **8**, 1–17 (2017).

267. Barquist, L. *et al.* A comparison of dense transposon insertion libraries in the *Salmonella* serovars *Typhi* and *Typhimurium. Nucleic Acids Res.* **41**, 4549–4564 (2013).

268. Ruiz, L. *et al.* The essential genomic landscape of the commensal *Bifidobacterium breve* UCC2003. *Sci. Rep.* **7**, 5648 (2017).

269. Dembek, M. *et al.* High-throughput analysis of gene essentiality and sporulation in *Clostridium difficile. MBio* **6**, 1–13 (2015).

270. Le Breton, Y. *et al.* Essential genes in the core genome of the human pathogen *Streptococcus pyogenes. Sci. Rep.* **5**, (2015).

271. Seshadri, R., Hendrix, L. R. & Samuel, J. E. Differential expression of translational elements by life cycle variants of *Coxiella burnetii. Infect. Immun.* **67**, 6026–6033 (1999).

272. Narayanan, A. M., Ramsey, M. M., Stacy, A. & Whiteley, M. Defining Genetic Fitness Determinants and Creating Genomic Resources for an Oral Pathogen. *Appl. Environ. Microbiol.* **83**, (2017).

273. Stacy, A., Fleming, D., Lamont, R. J., Rumbaugh, K. P. & Whiteley, M. A Commensal Bacterium Promotes Virulence of an Opportunistic Pathogen via Cross-Respiration. *MBio* **7**, (2016).

274. Grazziotin, A. L., Vidal, N. M. & Venancio, T. M. Uncovering major genomic features of essential genes in Bacteria and a methanogenic Archaea. *FEBS J.* **282**, 3395–3411 (2015).

275. Larson, C. L., Beare, P. A., Howe, D. & Heinzen, R. A. *Coxiella burnetii* effector protein subverts clathrin-mediated vesicular trafficking for pathogen vacuole biogenesis. *Proc. Natl. Acad. Sci. U. S. A.* **110**, E4770-9 (2013).

276. Hemsley, C. M. *et al.* Extensive genome analysis of *Coxiella burnetii* reveals limited evolution within genomic groups. *BMC Genomics* **20**, 1–17 (2019).

277. Kersh, G. J. *et al.* Genotyping and Axenic Growth of *Coxiella burnetii* Isolates Found in the United States Environment. *Vector Borne Zoonotic Dis.* **16**, 588–594 (2016).

278. Stoenner, H. G. & Lackman, D. B. The biologic properties of *Coxiella burnetii* isolated from rodents collected in Utah. *Am. J. Epidemiol.* **71**, 45–51 (1960).

279. Long, C. M., Beare, P. A., Cockrell, D. C., Larson, C. L. & Heinzen, R. A. Comparative virulence of diverse *Coxiella burnetii* strains. *Virulence* **10**, 133–150 (2019).

280. Tatusov, R. L., Galperin, M. Y., Natale, D. A. & Koonin, E. V. The COG database: A tool for genome-scale analysis of protein functions and evolution. *Nucleic Acids Res.* **28**, 33–36 (2000).

281. Vollmer-Conna, U. *et al.* Cytokine polymorphisms have a synergistic effect on severity of the acute sickness response to infection. *Clin. Infect. Dis. an Off. Publ. Infect. Dis. Soc. Am.* **47**, 1418–1425 (2008).

282. Majiduddin, F. K., Materon, I. C. & Palzkill, T. G. Molecular analysis of beta-lactamase structure and function. *Int. J. Med. Microbiol.* **292**, 127–137 (2002).

283. Lakshmi, R., Nusrin, K., Georgy, S. & Sreelakshmi, K. Role of beta lactamases in antibiotic resistance: A review. *Int. Res. J. Pharm.* **5**, 37–40 (2014).

284. Reygaert, W. Methicillin-resistant *Staphylococcus aureus* (MRSA): molecular aspects of antimicrobial resistance and virulence. *Clin. Lab. Sci.* **22**, 115–119 (2009).

285. Pages, J.-M. *et al.* Efflux pump, the masked side of beta-lactam resistance in *Klebsiella pneumoniae* clinical isolates. *PLoS One* **4**, e4817 (2009).

286. Gikas, A., Kofteridis, D. P., Manios, A., Pediaditis, J. & Tselentis, Y. Newer macrolides as empiric treatment for acute Q fever infection. *Antimicrob. Agents Chemother.* **45**, 3644–3646 (2001).

287. Yeaman, M. R., Mitscher, L. A. & Baca, O. G. In vitro susceptibility of *Coxiella burnetii* to antibiotics, including several quinolones. *Antimicrob. Agents Chemother.* **31**, 1079–1084 (1987).

288. Pérez-del-Molino, A. *et al.* Erythromycin and the treatment of *Coxiella burnetii* pneumonia. *J. Antimicrob. Chemother.* **28**, 455–459 (1991).

289. Limonard, G. J. M. *et al.* One-year follow-up of patients of the ongoing Dutch Q fever outbreak: clinical, serological and echocardiographic findings. *Infection* **38**, 471–477 (2010).

290. Van Bambeke, F., Barcia-Macay, M., Lemaire, S. & Tulkens, P. M. Cellular pharmacodynamics and pharmacokinetics of antibiotics: Current views and perspectives. *Curr. Opin. Drug Discov. Dev.* **9**, 218–230 (2006).

291. Wilding, E. I. *et al.* Identification, Evolution, and Essentiality of the Mevalonate Pathway for Isopentenyl Diphosphate Biosynthesis in Gram-Positive Cocci. *J. Bacteriol.* **182**, 4319 LP – 4327 (2000).

292. Rohdich, F., Bacher, A. & Eisenreich, W. Isoprenoid biosynthetic pathways as anti-infective drug targets. *Biochem. Soc. Trans.* **33**, 785–791 (2005).

293. Kovacs-Simon, A., Metters, G., Norville, I., Hemsley, C. & Titball, R. W. *Coxiella burnetii* replicates in *Galleria mellonella* hemocytes and transcriptome mapping reveals in vivo regulated genes. *Virulence* **11**, 1268–1278 (2020).

294. Balibar, C. J., Shen, X. & Tao, J. The mevalonate pathway of *Staphylococcus aureus*. *J. Bacteriol.* **191**, 851–861 (2009).

295. Wang, S. X. *et al.* (18)F-FDG PET/CT localized valvular infection in chronic Q fever endocarditis. *J. Nucl. Cardiol. Off. Publ. Am. Soc. Nucl. Cardiol.* **22**, 1320–1322 (2015).

296. Shin, S. J., Wu, C.-W., Steinberg, H. & Talaat, A. M. Identification of novel virulence determinants in *Mycobacterium paratuberculosis* by screening a library of insertional mutants. *Infect. Immun.* **74**, 3825–3833 (2006).

297. Lai, Y. C., Peng, H. L. & Chang, H. Y. Identification of genes induced in vivo during *Klebsiella pneumoniae* CG43 infection. *Infect. Immun.* **69**, 7140–7145 (2001).

298. Schauer, K. *et al.* Deciphering the intracellular metabolism of *Listeria*

monocytogenes by mutant screening and modelling. *BMC Genomics* **11**, 573 (2010).

299. Begley, M. *et al.* Analysis of the isoprenoid biosynthesis pathways in *Listeria monocytogenes* reveals a role for the alternative 2-C-methyl-D-erythritol 4-phosphate pathway in murine infection. *Infect. Immun.* **76**, 5392–5401 (2008).

300. Begley, M. *et al.* The interplay between classical and alternative isoprenoid biosynthesis controls gammadelta T cell bioactivity of *Listeria monocytogenes. FEBS Lett.* **561**, 99–104 (2004).

301. Zlitni, S., Ferruccio, L. F. & Brown, E. D. Metabolic suppression identifies new antibacterial inhibitors under nutrient limitation. *Nat. Chem. Biol.* **9**, 796–804 (2013).

302. Shapiro, S. Speculative strategies for new antibacterials: all roads should not lead to Rome. *J. Antibiot. (Tokyo).* **66**, 371–386 (2013).

303. Weiss, D. S. *et al.* In vivo negative selection screen identifies genes required for *Francisella* virulence. *Proc. Natl. Acad. Sci. U. S. A.* **104**, 6037–6042 (2007).

304. Napier, B. A. *et al.* Link between intraphagosomal biotin and rapid phagosomal escape in *Francisella. Proc. Natl. Acad. Sci. U. S. A.* **109**, 18084–18089 (2012).

305. Sassetti, C. M. & Rubin, E. J. Genetic requirements for mycobacterial survival during infection. *Proc. Natl. Acad. Sci. U. S. A.* **100**, 12989–12994 (2003).

306. Carfrae, L. A. *et al.* Mimicking the human environment in mice reveals that inhibiting biotin biosynthesis is effective against antibiotic-resistant pathogens. *Nat. Microbiol.* **5**, 93–101 (2020).

307. Schnappinger, D. *et al.* Transcriptional Adaptation of *Mycobacterium tuberculosis* within Macrophages: Insights into the Phagosomal Environment. *J. Exp. Med.* **198**, 693–704 (2003).

308. Endley, S., McMurray, D. & Ficht, T. A. Interruption of the cydB locus in *Brucella abortus* attenuates intracellular survival and virulence in the mouse model of infection. *J. Bacteriol.* **183**, 2454–2462 (2001).

309. Goldman, B. S., Gabbert, K. K. & Kranz, R. G. The temperature-sensitive growth and survival phenotypes of *Escherichia coli* cydDC and cydAB strains are due to deficiencies in cytochrome bd and are corrected by exogenous catalase and reducing agents. *J. Bacteriol.* **178**, 6348–6351 (1996).

310. Mihara, H. & Esaki, N. Bacterial cysteine desulfurases: their function and mechanisms. *Appl. Microbiol. Biotechnol.* **60**, 12–23 (2002).

311. Nachin, L., El Hassouni, M., Loiseau, L., Expert, D. & Barras, F. SoxR-dependent response to oxidative stress and virulence of *Erwinia chrysanthemi*: the key role of SufC, an orphan ABC ATPase. *Mol. Microbiol.* **39**, 960–972 (2001).

312. Outten, F. W., Wood, M. J., Muñoz, F. M. & Storz, G. The SufE Protein and

the SufBCD Complex Enhance SufS Cysteine Desulfurase Activity as Part of a Sulfur Transfer Pathway for Fe-S Cluster Assembly in *Escherichia coli*. *J. Biol. Chem.* **278**, 45713–45719 (2003).

313. Hidese, R., Mihara, H. & Esaki, N. Bacterial cysteine desulfurases: versatile key players in biosynthetic pathways of sulfur-containing biofactors. *Appl. Microbiol. Biotechnol.* **91**, 47–61 (2011).

314. Takahashi, Y. & Tokumoto, U. A third bacterial system for the assembly of iron-sulfur clusters with homologs in archaea and plastids. *J. Biol. Chem.* **277**, 28380–28383 (2002).

315. Kumar, T. K., Samuel, D., Jayaraman, G., Srimathi, T. & Yu, C. The role of proline in the prevention of aggregation during protein folding in vitro. *Biochem. Mol. Biol. Int.* **46**, 509–517 (1998).

316. Pemberton, T. A. *et al.* Proline: Mother Nature's cryoprotectant applied to protein crystallography. *Acta Crystallogr. D. Biol. Crystallogr.* **68**, 1010–1018 (2012).

317. Culham, D. E. *et al.* Periplasmic loops of osmosensory transporter ProP in *Escherichia coli* are sensitive to osmolality. *Biochemistry* **47**, 13584–13593 (2008).

318. Hendrix, L. & Mallavia, L. P. Active transport of proline by *Coxiella burnetii*. *J. Gen. Microbiol.* **130**, 2857–2863 (1984).

319. Hackstadt, T. & Williams, J. C. Biochemical stratagem for obligate parasitism of eukaryotic cells by *Coxiella burnetii*. *Proc. Natl. Acad. Sci. U. S. A.* **78**, 3240–3244 (1981).

320. Zusman, T. *et al.* The response regulator PmrA is a major regulator of the icm/dot type IV secretion system in *Legionella pneumophila* and *Coxiella burnetii*. *Mol. Microbiol.* **63**, 1508–1523 (2007).

321. Beare, P. A. *et al.* Essential role for the response regulator PmrA in *Coxiella burnetii* type 4B secretion and colonization of mammalian host cells. *J. Bacteriol.* **196**, 1925–1940 (2014).

322. Newton, P. *et al.* Lysosomal degradation products induce Coxiella burnetii virulence. *Proc. Natl. Acad. Sci. U. S. A.* (2020).

323. Trovato, M., Maras, B., Linhares, F. & Costantino, P. The plant oncogene rolD encodes a functional ornithine cyclodeaminase. *Proc. Natl. Acad. Sci. U. S. A.* **98**, 13449–13453 (2001).

324. Schindler, U., Sans, N. & Schröder, J. Ornithine cyclodeaminase from octopine Ti plasmid Ach5: identification, DNA sequence, enzyme properties, and comparison with gene and enzyme from nopaline Ti plasmid C58. *J. Bacteriol.* **171**, 847–854 (1989).

325. Sharma, S., Shinde, S. & Verslues, P. E. Functional characterization of an ornithine cyclodeaminase-like protein of *Arabidopsis thaliana*. *BMC Plant Biol.* **13**, 182 (2013).

326. Brennan, R. E., Kiss, K., Baalman, R. & Samuel, J. E. Cloning, expression, and characterization of a *Coxiella burnetii* Cu/Zn Superoxide dismutase. *BMC Microbiol.* **15**, 99 (2015).

327. Potter, S. C. *et al.* HMMER web server: 2018 update. *Nucleic Acids Res.* **46**, 200–204 (2018).

328. Kohanski, M. A., Dwyer, D. J. & Collins, J. J. How antibiotics kill bacteria: from targets to networks. *Nat. Rev. Microbiol.* **8**, 423–435 (2010).

329. Kapoor, G., Saigal, S. & Elongavan, A. Action and resistance mechanisms of antibiotics: A guide for clinicians. *J. Anaesthesiol. Clin. Pharmacol.* **33**, 300–305 (2017).

330. Bushell, F. *et al.* Mapping the Transcriptional and Fitness Landscapes of a Pathogenic E. coli Strain: The Effects of Organic Acid Stress under Aerobic and Anaerobic Conditions. *Genes* vol. 12 (2021).

331. Price, M. N. *et al.* Indirect and suboptimal control of gene expression is widespread in bacteria. *Mol. Syst. Biol.* **9**, 660 (2013).

332. Keren, L. *et al.* Massively Parallel Interrogation of the Effects of Gene Expression Levels on Fitness. *Cell* **166**, 1282-1294 (2016).

333. Mesarich, C. H. *et al.* Transposon insertion libraries for the characterization of mutants from the kiwifruit pathogen *Pseudomonas syringae* pv. *actinidiae. PLoS One* **12**, e0172790 (2017).

334. Xu, J., Zhao, X. P., Choi, M. H. & Yoon, S. C. Isolation and characterization of a transposon mutant of *Pseudomonas fluorescens* BM07 enhancing the production of polyhydroxyalkanoic acid but deficient in cold-induced exobiopolymer production. *FEMS Microbiol. Lett.* **305**, 91–99 (2010).

335. Saavedra, J. T., Schwartzman, J. A. & Gilmore, M. S. Mapping Transposon Insertions in Bacterial Genomes by Arbitrarily Primed PCR. *Curr. Protoc. Mol. Biol.* **118**, 15.15.1-15.15.15 (2017).

336. Chen, T., Yong, R., Dong, H. & Duncan, M. J. A general method for direct sequencing of transposon mutants by randomly primed PCR. *Technical Tips Online* vol. 4 58–61 (1999).

337. Bendezú, F. O. & De Boer, P. A. J. Conditional lethality, division defects, membrane involution, and endocytosis in mre and mrd shape mutants of *Escherichia coli. J. Bacteriol.* **190**, 1792–1811 (2008).

338. Mitchell, A. M., Wang, W. & Silhavy, T. J. Novel RpoS-Dependent Mechanisms Strengthen the Envelope Permeability Barrier during Stationary Phase. *J. Bacteriol.* **199**, (2017).

339. Mitchell, A. M., Srikumar, T., Silhavy, T. J. & Scott Hultgren, E. J. Cyclic Enterobacterial Common Antigen Maintains the Outer Membrane Permeability Barrier of *Escherichia coli* in a Manner Controlled by YhdP. *mBio.* **9**, 1321–1339 (2018).

340. Grimm, J. *et al.* The inner membrane protein YhdP modulates the rate of anterograde phospholipid flow in *Escherichia coli. Proc. Natl. Acad. Sci. U. S. A.* **117**, 26907–26914 (2020).

341. Senior, N. J. & Titball, R. W. Isolation and primary culture of *Galleria mellonella* hemocytes for infection studies. *F1000Research* **9**, 1392 (2020).

342. Kimbrough, R. C. 3rd *et al.* Q fever endocarditis in the United States. *Ann.*

Intern. Med. **91**, 400–402 (1979).

343. McMullen, P. D. & Freitag, N. E. Assessing bacterial invasion of cardiac cells in culture and heart colonization in infected mice using *Listeria monocytogenes. J. Vis. Exp.* e52497–e52497 (2015) doi:10.3791/52497.